Politecnico di Torino

Degree of Civil Engineering

Master’s Degree Thesis

Effect of Elevated Temperature on Toughness of Concrete Structures

Advisor:
Alessandro Pasquale Fantilli

Student:
Ahmad Raza (s260790)

24th February, 2021

List of Figures

TABLE OF CONTENTS

ACKNOWLEDGEMENT

All the praises for **GOD**, the Most Merciful, the Most Gracious and the Most Knowledgeable to whom one can never thank enough. I gratitude Him Who has bestowed me with knowledge and capability to initiate, carry out and successfully complete my work.

I acknowledge my indebtedness to my diligent research supervisor **Prof. Alessandro Pasquale Fantilli**, for guiding and correcting various documents of mine with attention and care. His guidance during my research was the source of encouragement for me.

Last but not least I pay my thanks to my parents who extended altruistic prayers to make my thesis get completed. I am thankful to my wife **Nida Ahmad** who encouraged me during my research and this thesis would be incomplete without her support. I feel proud to have a family who gave me the freedom to explore on my own and guided me whenever I needed their help. I am also thankful to my friends who supported me during my research.

Ahmad Raza

ABSTRACT

Study of concrete properties at high temperatures remained a focus of many researchers since years. In this research, the impact of heating on concrete specimens was studied while considering the toughness parameter, and then the outcomes were matched with the unheated concrete specimens. For this purpose, experimental data from previous studies was collected, analyzed and functions were proposed for various properties of concrete.

The working was carried out on the after-peak portion of the stress strain curves obtained from the compression testing of concrete specimens in a strain-controlled environment. The stress-strain curves were imported in AutoCAD and scaled as required. Several points were marked on the post-peak portion of each stress-strain curve and the values were imported in an excel spreadsheet. Furthermore, the post-peaks were analyzed by following a methodology and toughness parameter was computed for each available stress-strain curve. After that, the toughness parameter was normalized with respect to room temperature value. The trend of toughness parameter (A_F) was analyzed by plotting normalized A_F versus temperature and a function was proposed for its variation.

Different types of concretes studied in this research include normal strength concrete, concrete with polypropylene fibers, steel fibers, PET, rubber, Meta kaolin etc. The impact of heating on other properties of concrete like compressive strength, elastic modulus and peak strain was also studied at high temperatures and different functions were proposed for these as well after analyzing the collected data. The post-peaks of the tentative stress-strain curves were matched with the ones gained from the models to understand the variation. Two additional post-peaks were also plotted including one using the minimum toughness parameter (A_F) and the second using the maximum toughness parameter (A_F) at a specific temperature. The trends were observed with respect to the maximum temperature attained as well as considering the concrete constituents.

CHAPTER 1: INTRODUCTION

The building industry plays an essential role in the monetary development and social growth and is considered as a backbone of any country (Sohu et al., 2017). Nowadays, concrete is one of the most important construction building material being used in the building industry and due to this, the demand of concrete has been ascended to such a particular level that currently it is perhaps one of the most used construction materials in the world (Lakhiar et al., 2018). The popularity of concrete has increased due to its resilience and accessibility. A wide range of construction projects utilize concrete ranging from residential houses, skyscrapers, bridges, pavements, and dams (Behbahani et al., 2011). Concrete is quite possibly the most adaptable structural materials (Ragavendra et.al., 2017). It is a composite material that comprises of cement, sand, aggregate and water in a specific recommended fraction (Ajagbe et.al., 2018). Concrete can be easily casted into any shape which can be a circular water tank or a structural element like a standard beam or column. (Behbahani et al., 2011).

The most used construction material on earth is concrete (Ragavendra et.al., 2017), still concrete failures occur despite adequate design and mix ratio (Ajagbe et.al., 2018). The upsides of utilizing concrete incorporate high compressive strength, great resistance to fire, low maintenance costs, and longer structure life. While the disadvantages of concrete incorporate poor elasticity, low failure strain and formwork necessity (Ragavendra et.al., 2017). Gollu et al. (2016) mentioned unsuitable materials, and unsound, reactive, and contaminated aggregates as part of the sources of concrete failure in buildings. Concrete will only become a quality material for construction when its constituents are properly sourced. The aggregate quality can vary considerably due to the location from which it was sourced and the ecological conditions (Ajagbe et al., 2018). Fowler and Quiroga (2003) stated that the coarse aggregates in concrete impact the properties of concrete to a great extent. They constitute around 70% to 80% of concrete volume. The characteristics of cement, sand and aggregate used for the concrete are the main components that affect the concrete strength (Shetty, 2005). The aggregate strength significantly affect the resistance and mechanical performance of cement based materials. A low-quality weak gravel used for concrete cannot produce strong concrete (Neville, 2011). However, the aggregate quality is not the only parameter that will impact the strength of concrete and hence a benchmark of concrete performance is used to determine the strength of concrete based on its constituents.

1.1 Compressive and Tensile Strength of Concrete

It's been known by early 1800's that concrete has a very good compressive strength while it is very weak in tension and hence it is not much capable to resist the cracks induced by tensile stresses. (Agarwal et al., 2014). Amongst the concrete's characteristics, its compression strength is the most significant parameter for designing a structural member like a beam or column and calculating its load-bearing capacity. On the other hand, tensile strength can be used as a main parameter to calculate the limiting stress value at which cracking occurs in concrete (Otter et. al., 1988). Nearly complete loss of loading ability can happen once failure is initiated, which eventually bounds its usage and application. To overcome this weakness, usage of steel bars for reinforcing concrete is done thus to improve its tensile strength (Agarwal et al., 2014).

The compressive strength of concrete does not remain constant throughout the life of building due to various effects. This primarily includes curing during the first week after the initial concrete setting. Moreover, the development of cracks in concrete at later stages also impacts the compressive strength. (S. Biondi et. al., 2008). Some of the aspects that effect the concrete strength include gravel quality, sand quality, water to cement ratio, type of cement used etc. (Noorzaei et al., 2007).

1.2 Ductility and Brittleness of Concrete

Ductility is the measure of plastic distortion of a particular material before the final fracture. If a material is ductile then it will have a good energy absorption capacity as compared to a brittle material which usually has higher strength, but the energy absorption capacity is low. The ductile materials are more useful for designing the structural elements and steel is a good example of ductile material. (Mosaberpanah et. al., 2016).

Brittleness is another one of the disadvantages in high strength concretes. Earlier, many researchers have researched on the brittle behavior of concrete structures and proposed different solutions (Mohammad et.al., 2015). The use of ultra-high-performance Concrete in the construction industry is quite common nowadays. It is one of the innovative and progressed composite material with very good mechanical characteristics (Resplendino, 2013). The ultra-high-performance concrete can be obtained by using very fine sand to lower the porosity of concrete. Moreover, proper curing and compaction should be carried out and the water requirement can be lowered by the addition of plasticizers. Finally, fibers can also be added in such concretes to further enhance the tensile strength of concrete. (Park et.al., 2012).

Concrete is a brittle material when compared to other construction materials like metals which include structural steel and hence it has a low tensile strength. Concrete can be reinforced with steel fibers or bars to introduce ductility in its behavior which then allows it to resist cracking caused by tensile stresses. Following are the points that should be considered while reinforcing steel in concrete:

1. The steel fibers when used as reinforcement in concrete significantly reduces its workability. The increase in steel fiber volume fraction will eventually decrease the workability.
2. 3% is the optimum volume of steel fibers at which we can attain the maximum compressive and flexural strength without impacting the workability of concrete (Oad et al., 2018).

1.3 Toughness of Concrete

The toughness of concrete in compression can be obtained by measuring the area below the stress-strain curve obtained by compression testing of concrete (Mindess et al.

1994). Addition of fibers in concrete increase the strain at peak load and at the same time improve the energy absorption capacity of concrete specifically in the post-peak region of the stress-strain curve. The toughness parameter of concrete can be evaluated by calculating the energy required to distort the sample or break it and it can be computed by measuring the area under the stress-strain curve (Mindess et al. 1994). Th obtained value is known as compression toughness of concrete and it has the same units as of work.

Toughness index is a useful parameter that can help in the evaluation of toughness properties of cement-based materials. It is basically a relative term and can be computed by taking a ratio of toughness of fiber reinforced concrete to that of plain cement concrete. (Ahmed et.al., 2014). Based on fracture toughness parameters, the structural steel is dozens of times better than concrete when it comes to resistance to crack development. Concrete is very susceptible to crack development due to tensile stresses and hence it can be fractured easily. These micro-cracks can allow the entrance of harmful agents inside concrete and result in dangerous phenomenon's like steel corrosion, freeze and thaw damages etc. (Ragavendra et.al., 2017).

1.4 Role of Concrete's Tensile Strength in Cracking

The cracking in concrete is a major issue faced in the construction and a number of researches have been carried out to investigate it. Sometimes, concrete only gets micro-cracks and the elements still take all the applicable design loads but there are some other problems associated with the microcracks that need to be taken care of. Fractures in concrete make a way for the harmful chemicals and reagents that causes destruction and reduces the concrete strength. Several underlying reasons can cause cracking in concrete structures and the major one is the increase of tensile stresses. This type of cracking is caused by the shrinkage phenomenon and to avoid this, curing of concrete is carried out during the initial strengthening stage of concrete. However, creep on the other hand is quite related to long time-dependent cracking of concrete under a constant loading. The tensile stresses produced in concrete by the shrinkage and are relieved by creep and this help in limiting the cracking behavior. The magnitudes of corresponding values of shrinkage and creep in concrete determine the amount of tensile stress inside the concrete element. So, it can be deduced that the possibility of cracking in concrete can be determined by comparing the induced tensile stress with the tensile strength or the capacity of concrete. (Jiang, 1997).

It is very important to study the tensile properties and characteristics of concrete to determine the cracking behavior, patterns, and possibilities due to shrinkage phenomenon. Concrete cracking can be best understood by focusing on the nature of tensile stresses which are induced in the concrete due to shrinkage. The existence of creep phenomenon in concrete can greatly help in reducing the tensile stresses due to shrinkage. Moreover, it also allows to determine the methods that can be applied to study the shrinkage behavior cracking in a concrete structure. (Kristiawan, 2006).

1.5 Fibers Reinforced Concrete (FRC)

The addition of steel bars in concrete can enhance its tensile strength and at the same time improves the crack resistance properties. However, this choice is not cost-effective due to high price of reinforing steel. Concrete itself is a cheap material but the addition of reinforcing bars significantly increases the cost of construction. Concrete is a highly dense material because of the presence of coarse aggregates that have high specific weight. The abundant self-weight of concrete elements is a major concern during the design of concrete structures and the addition of heavy steel rebars further increases the self-weight of concrete. This increases the amount of overall deadload on the building and creates certain limitations. So, researchers started focusing on alternatives that can minimize these drawbacks without compromising the tensile properties achieved due to the addition of steel. (Agarwal et al., 2014).

In the past few years, a lot of studies have been carried out in the construction industry to improve the strength of concrete by addition of cheap substitute materials. Addition of plastic flakes, bamboo fibers, rubber crumbs, recycled aggregate and human hairs in the concrete was studied by various researchers in the recent years. However, the addition of plastic fibers (mainly polypropylene) in concrete proved to be the most-effective solution to cater for the low tensile strength. These fibers are usually added in a specific proportion and they are randomly dispersed inside the concrete paste during the mixing. Such concrete is called as Fiber Reinforced Concrete or FRC. Different types of fibers can be added in the concrete mixture to improve its strength and these include steel fibers, plastic fibers, glass and other synthetic fibers. Out of all these additives, the steel fiber addition proved to be the most beneficial in term of strength gain and therefore, frequently used in concrete as well as cement-based mixes like shotcrete. (Malagavelli et.al., 2011).

Once of the major disadvantage of concrete construction is that the elements get microcracks soon after the concrete is poured or casted. If this cracking phenomenon is not controlled with proper curing then these cracks spread-out very fast and become a cause for the low tensile strength of concrete. Therefore, addition of fibers in concrete is the best idea to eliminate this problem up to some extent. Steel or polypropylene fibers addition in concrete increases its overall resistance to shrinkage cracking and imparts greater tensile strength in the element. This is the reason of such a wide popularity of FRC concrete which contains randomly dispersed thousands of fibers thus improving the overall tensile properties of concrete. (Rana, 2013).

Nowadays, a vast variety of synthetic as well as natural fibers are utilized for the preparation of FRC. The use of steel fibers is most common due to the tensile strength benefits achieved by their addition. In the past twenty years, the popularity of SFRC in the construction of concrete pavements, parking lots and runways has increased so much. The SFRC is more effective because of high strength of steel fibers and their diffusion in concrete mix helps in overall mechanical properties improvement. (Sorelli et al., 2006). The steel fibers are introduced in the concrete mixes to improve the response of concrete after cracking. This increases the energy absorbing capability and at the same time imparts ductility to it. In short, steel fibers help in overall integrity and increase in tensile property of concrete element thus improving its crack resistivity and control. (Ragavendra et.al., 2017).

1.6 Applications of Fiber Reinforced Concrete (FRC)

FRC has been used commonly in a number of construction areas including commercial buildings, retaining walls, heavy foundations, pre-stressed concrete and shotcrete. (Malagavelli et.al., 2011). The major advantages of using FRC for construction is cracking control. Moreover, with the use of FRC, the dimensions of concrete beams and columns can be greatly reduced. The results of fiber additions can be enhanced by using a hybrid mix of fibers. This can be a mixture of steel & glass fibers that can contribute to the overall increase in mechanical characteristics. This includes improvement in ductility as well as load bearing capacity of concrete structure. (Wenjun Qu, 2009). Fibers are also being used in the construction of flexible pavements in road construction as investigated by Vasudevan et. al., (2007). The melted plastic fibers coverup the surface of stone aggregates and it also helps in reducing the number of pores, thus improving the overall aggregate soundness. (Malagavelli et.al., 2011).

1.7 Post-peak Behavior of Concrete in Compression

The concrete post-peak behavior under tension has been studied by some researchers but there is only a limited data available regarding the study of after peak concrete behavior in compression testing. Concrete is brittle in nature and it is not easy to get the post-peak curve undress the compression testing using normal procedures. The behavior essentially depends on the test setup used and it is important to carry out the testing in a strain-controlled environment. The post-peak portion of concrete curves can be obtained by performing a compression test in a strain-controlled environment. Various researchers have proposed functions for the computation of pre-peak and post-peak curves of concrete under compression. (Nematzadeh & Mousavimehr, 2019) had suggested models for the complete stress-strain curve of concrete when heated. A single model cannot predict the complete curve because, after the peak, micro-cracking occurs, and this changes the behavior of concrete. Eurocode 2 suggests a model for an initial portion of the curve and recommends a linear or non-linear model for the post-peak portion of the concrete under compression. (Fantilli et al., 2008) also proposed a model for post-peak using stress-inelastic displacement relationship for various types of cement-based materials under compression. This model is used further in this research to analyze the toughness parameter of concrete at high temperatures.

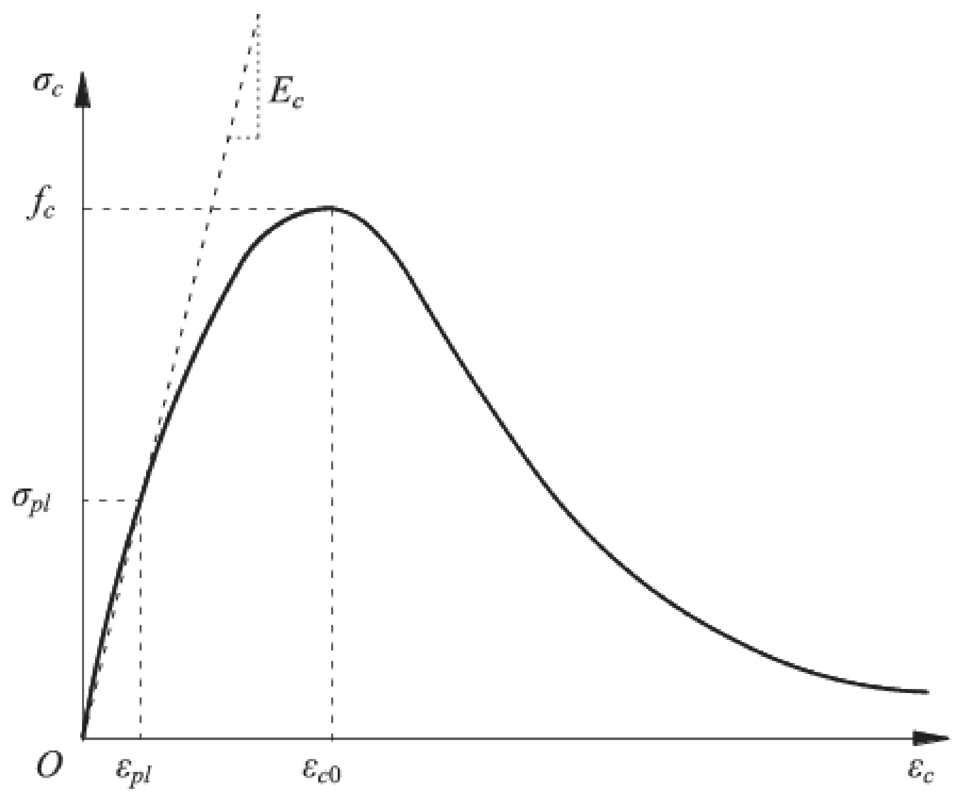

Figure 1.1 Stress-Strain Curve of Concrete (Lo et al., 2014)

CHAPTER 2: EFFECTS OF FIRE ON CONCRETE

2.1 Concept of Fire

Fire has been used since early ancient times for cooking food however occasionally it can be our enemy in various incidents. Different factors are responsible for setting fire, they may be of wild source or unintentional or illegitimate reasons like using dry bushes, oil or petrol as a fuel source (Onundi et. al., 2019). Approximately 8 in every 1,000,000 people are subjected to death each year due to fire in Europe and more are being hospitalized because of fire (Akhimien et.al., 2018).

Rapid oxidation of any flammable substance can set fire (“GUIDELINE 5", 2014). There are FOUR basic elements for any fire to put on and those are Heat, Oxygen, Fuel and Chemical Chain Reaction ("Guide & Fire", 2015). This makes a Fire Tetrahedron. Fire can be categorized in 5 classes depending upon the type of fuel being used i.e.:

i. Class A fires (ordinary combustible materials like wood, paper etc.)
ii. Class B fires (flammable liquids)
iii. Class C fires (energized electrical equipment)
iv. Class D fires (combustible metals)
v. Class K fires (combustible cooking appliances) (GUIDELINE 5, 2014).

2.2 Effects of Fire on Plain Concrete

Undesirable fires are one of the huge dangers for buildings (Jacob et al., 2013). Research regarding fire effects on concrete and concrete structures mainly related to buildings, have been conducted by various researchers. The central areas of studies were:

a) The consideration of intricate behavior of material
b) The overall safety perspective of building before, during & after fire event (Khoury, 2000).

Designing a building element with concrete requires a specified minimum cover for structural reinforcements. This cover cannot be sufficient sometimes to protect the structural elements of the building individually, that are being exposed to elevated temperatures for a long time. This severely reduces the bearing capacity and properties of materials being used in the buildings. Hence it is very essential to be aware of the performances of different construction materials at high temperatures as if controlled improperly can subsequently lead to the collapse of building (Onundi et. al., 2019). Although concrete show very good behavior in fire because of its two important properties i.e., it is non-combustible, and it act as a good insulating agent having low thermal conductivity.

Concrete act as a shielding insulating material towards steel reinforcement. Therefore reinforced cement concrete behaves very well under high temperatures unless and until spalling phenomenon occurs due to fire that may breakdown the concrete masses from the surface of concrete (Jacob et al., 2013). There are two disadvantages of concrete under fire. First is the weakening of mechanical properties during elevated temperature that may cause due to physicochemical changes in the material itself and second is explosive spalling that can result in corrosion of material, decrease in size of that element and may expose the reinforcing steel to high temperatures.

Mechanical properties of concrete can be worsening on heating due to three "material factors" i.e. (1) Physicochemical variations in the coarse aggregates (2) thermal unsuitability between the coarse aggregates and the concrete paste and (3) physicochemical changes in the concrete mix. However, there are some "environmental factors" as well i.e. heating rate; outside sealing includes moisture loss from the surface; applied loading; and temperature level (Onundi et. al., 2019).

2.3 Behavior of Concrete at Elevated Temperatures

The concrete properties are significantly impacted when it is heated at high temperature which occurs in case of fire. At low temperature, the properties do not vary too much but as the temperature is increased further, the mechanical properties are severely reduced.

Normal concrete does not rupture when heated at around 100°C and the properties are greatly reduced at higher temperatures. The researchers worked to investigate the reason behind this and performed various experiments. When concrete is heated, differential strains are generated because the coarse aggregates expand, and cement sand paste shrinks due to heat. This led to the answer of transient creep phenomenon which is closely related to the thermal strains induced by applied loads (LITS). When the concrete is constantly exposed to high temperatures of above 100°C then then mechanical properties are badly impacted and it becomes quote difficult to the model the behavior. (Khoury, 2000).

It can be said that mechanical characterization of heated concrete without considering the impact of LITS will not give accurate findings. (Fletcher et al., 2006) studied the concrete physical properties at a microstructure level and inferred that the microstructure changes significantly for the normal and high-performance concrete under high temperature. Moreover, the behavior of ultra-high-performance concrete was not as per the expectation which means that it is more impacted due to heating.

Another useful aspect of concrete at elevated temperature is the stacking which helps in compaction and eventually helps in restraining the chipping-off and expansion of concrete. Moreover, the behavior of sealed and unsealed concrete also varies a lot in the presence of fire. When an unsealed concrete specimen is heated at high temperature, the moisture will be totally lost, and pores will be created inside the concrete. Heat fumes when enter inside the pores will develop such a significant pore pressure that it will rupture the concrete and spalling phenomenon will follow. Whereas the principal method in moist sealed concrete is related to hydrothermal chemical reactions that might bring more vulnerable or much stronger gel relying on ratio of CaO/SiO_2 (C/S ratio) used.

Structural concrete failures occur in case of fire depending upon the type of fire, applied loadings and the building type being subjected to fire. Failure of concrete could also happen because of reduction in tensile strength, bending strength, bond breakage, decrease of shear strength, reduced compressive strength and chipping-off (also known as concrete spalling). Hence, the concrete elements (beams, columns etc.) should be designed in such a way as to meet the applicable loading requirements without any failure for the specified timeframe during a given fire event. It should be ensured that the structural element dimensions are sufficient to keep the heat passing through that specific structural part within acceptable limits. Moreover, an adequate cover to the steel reinforcement should be provided to protect the steel from thermal impacts. (Khoury, 2000).

When exposed to heat, concrete reacts not simply in momentary physical changes, for example enlargement, yet by going through different chemical changes. This reaction is particularly unpredictable due to the non-consistency of the material. Concrete comprises of both cement and aggregate components, and these may respond to high temperature in different ways. Several of these are reversible after cooling, yet others are nonreversible and may considerably deteriorate the solid structure after fire.

Most permeable concrete structures contain a specific quantity of water in them. This will clearly turn into vapors if the temperature considerably goes beyond the level range of 100-140° C or somewhere in the vicinity, generally building up the pressure inside concrete material. If the temperature comes to about 400° C, the calcium hydroxide content in cement will start to get dried out, creating more water vapors and furthermore causing a critical decrease in the physical quality of the material. Such chemical and physical variations in concrete will significantly reduce the compressive strength of material (Fletcher et al., 2006).

2.4 Spalling Impacts on Strength of Concrete

Spalling is the process in which pieces of concrete get chipped off and are removed from the surface of concrete frequently at genuinely high velocities. This is caused due to the fire flames with high heating rates ranging between 20–30^{o} C/min (Khoury, 2000). The process is commonly accepted to happen at high temperature. Spalling may altogether decrease or even dispose of the concrete layer off the reinforcement bars, hence subjecting the reinforcement material to relatively high temperatures. This decreases the strength and quality of steel reinforcement and therefore reduces the mechanical properties of that structure cumulatively. One more huge effect of spalling on the physical quality of structures happens through decrease of the concrete cross-section available to keep up the applied loading, while increases the pressure on rest of the concrete areas (Fletcher et al., 2006).

2.5 Cracking Impacts on strength of Concrete

Thermal expansion and desiccation of concrete because of heating can cause the development of cracks or fissures in concrete as compared to, or in addition with explosive spalling as well. These gaps may create passages for direct heat towards reinforcement bars, potentially generating more heating pressure and further breaking. Compressive loads which may emerge from thermal expansion can be extremely helpful in material compaction and smothering the development of fissures; this may result in very minor reduction of elastic modulus and compressive strength as compared to samples that bear less loading (Fletcher et al., 2006).

The typical routine afterward fire, is to eliminate and substitute the 'overheated' layer. However, if the concrete does not spall off in the period of fire, this layer will keep on protecting the reinforcing bars and inner concrete while serving as a heat barrier. However, the tendency of protection from dangerous reagents will be significantly reduced. (Khoury, 2000).

2.6 Improvements in Fire Resistance Property of Concrete

Different kinds of fibers can be mixed into concrete to alleviate the impacts of spalling. For instance, bringing polypropylene fibers into the concrete mixture that is at the point when the concrete is exposed to heat, the polypropylene fibers will melt down, making paths inside the concrete for the expulsion of water vapors and whatever other vaporous gases, which will subsequently decrease the development of pressure inside the concrete. There have been many discussions with respect to whether monofilament or multi-filament fibers are well capable to reduce spalling phenomenon.

Besides, the melted down polypropylene strands can create an obstruction for the movement of vapors deeper in concrete, avoiding the pressure development at greater penetrations instead of compelling the vapors to emit. On the other hand, polypropylene fibers can aid in the process of cracking at greater depths inside the concrete that can reduce spalling issue at the surface, but can have unfavorable structural outcomes (Fletcher et al., 2006). The concrete spalling phenomenon can be avoided by the introduction of polypropylene fibers in the concrete blend while mixing. Another suitable option is to cover the exposed concrete surface with a heat barrier by sealing it. (Khoury, 2000).

Researches have been conducted on the impacts of enclosing a concrete with an assortment of fabrics so as to evaluate any improvement in spalling prevention. A metal surface can function quite well in improving the spalling resistance in case of fire. Carbon fiber or glass fiber surfaces can also be used but the benefits are lesser in case of these materials. Steel fabric can be used to reduces spalling by providing horizontal controlled strain to the concrete element that is more than the inner pore-pressure causing spalling. The reason why carbon and glass fibers does not work quite well in this case is the poor bondage of these elements as compared to steel fabric. These bonds break substantially at elevated temperatures and thus causes comparative decrease in capacity of the fabric to provide restriction. Nevertheless, it does not give the idea that the method stimulates breaking more inside the structure (Bisby et al., 2005).

2.7 Effects of Fire on Reinforced Concrete (RC)

Typical fires effect reinforced concrete (RC) elements by rising the temperature of concrete mass. This increase in temperature weakens the mechanical properties of concrete and steel. Though, when it is exposed to persistent fire exposure or uncommonly elevated temperatures, concrete can endure substantial distress. Yet, high temperatures can decrease the compressive strength of concrete to a certain extent that the material holds no helpful structural strength (Khoury, 2000).

According to IS 456:2000 a structure or basic structural component needed to have resistance for fire must be planned to have a suitable level of protection from fire penetration, heat conduction and disaster (Jacob et al., 2013). Structural frameworks (like columns and beams), floors, rooftop frames and load bearing walls, should be capable of withholding stresses and strains applied to them because of huge fires. The beam-column frame structure should also carry their own self-weight without failure for the specific time interval as per the design. The International Building Code 2006 (IBC) comprises of prescriptive necessities for concrete structures in section 720 of the code. This section covers up various construction materials and assemblies that meet specified fire resistance evaluations (Bilow et al., 2008).

2.8 Fire Test and Evaluation methods

Resistance of fire can be characterized as the capacity of a component (not a material) of structure to satisfy its planned purpose for the design life in case of a fire (Khoury, 2000). Various fire test methods are used nowadays to evaluate the fire resistance properties of concrete building elements and sections. The test methods by ASTM (American Society of Testing Materials) are generally adopted for evaluation. The particular ASTM standard is ASTM E 119, Standard Methods of Fire Tests of Building Construction and Materials.

The fire tests are performed by following standard procedures of heating the specimen in the blast furnace. The concrete samples or cores are taken and subjected to controlled fire flames from underneath, top and sides. If beams are to be tested, then it’s important to keep their sides and bottom open. The walls are tested by heating from both sides and concrete columns are subjected to heat from all the sides. The temperature inside the furnace is increased in each timeframe as per the standard time vs temperature curve provided by ASTM E 119. The test is concluded when any of the recorded conditions are met.

(Bilow et al., 2008). Furthermore, there are 3 basic evaluation methods of fire resistance that is fire testing, prescriptive method and performance-based method (Khoury, 2000).

2.9 Factors Affecting Fire Resistance

Variables influencing resistance of fire for concrete components as per BS 8110 are:

1. Size
2. Shape of components
3. Properties and disposition of reinforcement or tendon
4. The applied loading.
5. The type of concrete, including cement, sand and aggregate.
6. Reinforcement cover.
7. Support conditions.
8. The thickness of section and its capability to retain heat. (floor/walls)
9. The establishment of surface insulation (Khoury, 2000).

CHAPTER 3: EXPERIMENTAL STUDIES

The primary purpose of this research work was to study the post-peak behavior of concrete at elevated temperatures under compression. Hence experimental data from various research was collected and then analyzed. Many researchers have studied the post-peak behavior of concrete by performing different experiments. The major focus here was to collect the experimental data obtained from compression testing of cylindrical concrete samples in a strain-controlled environment at various temperatures. Furthermore, calculations were carried out to study the changes in toughness of concrete with the increase in temperature.

For this purpose, experimental data from 8 different research papers was collected. It contains total 83 stress-strain curves obtained from compression testing of concrete samples at elevated temperatures. The experimental data was collected for various kinds of concrete including plain, poly-propylene fiber reinforced and steel fiber reinforced concrete. The experimental data used for this study is discussed below.

3.1 Experimental Study by Colombo (2010)

The research by (Colombo et al., 2010) was performed to study the mechanical characterization of steel-fiber reinforced concrete used for the production of precast roof elements. They carried out further investigation to study the toughness degradation in bending, uniaxial tension and compression of concrete once exposed to elevated temperatures. The tests performed were four point bending tests, uniaxial compression tests and fixed-end uniaxial tension tests.

The cylindrical compressive strength of samples at room temperature was around 75 MPa. The samples contained steel fibers content of 50 kg/m^3. The steel fibers were hooked-end and made of low-carbon steel. The length of added steel fibers was 30mm and length to diameter ratio was 45.

The samples were thermally treated in a furnace by applyinhg some thermal cycles up to several extreme temperatures; trying to decrease as much as possible the temperature gradients inside the samples. The samples were then heated up to the maximum temperatures of (200° C, 400° C and 600° C). A heating rate equal to 30° C/hour was used to reach the specified extreme temperature. Afterward, the samples were stabilized for 2 hours under a constant temperature to guarantee a uniform temperature inside the specimens. Then the cooling process was carried out with a rate of 12°C/hour down to the minimum temperature of 100°C. After this, the furnace was opened to bring the specimen temperature down to room temperature.

The experiments were performed in three different parts. The first phase is the mechanical characterization of the material which is carried out by performing four point bending tests on notched specimen. After the test, two cylindrical samples with 150 mm length and a diameter of 75 mm were cored from each specimen. One of those was tested in uniaxial compression, whereas the other was used in a fixed end uniaxial tension test.

The results of uniaxial tests performed on the cored concrete samples by (Colombo et al., 2010) are shown in the below figures 3.1 and 3.2. All the tests were displacement controlled and the displacement rate was equal to 0.1 mm/min in the loading as well as unloading phases.

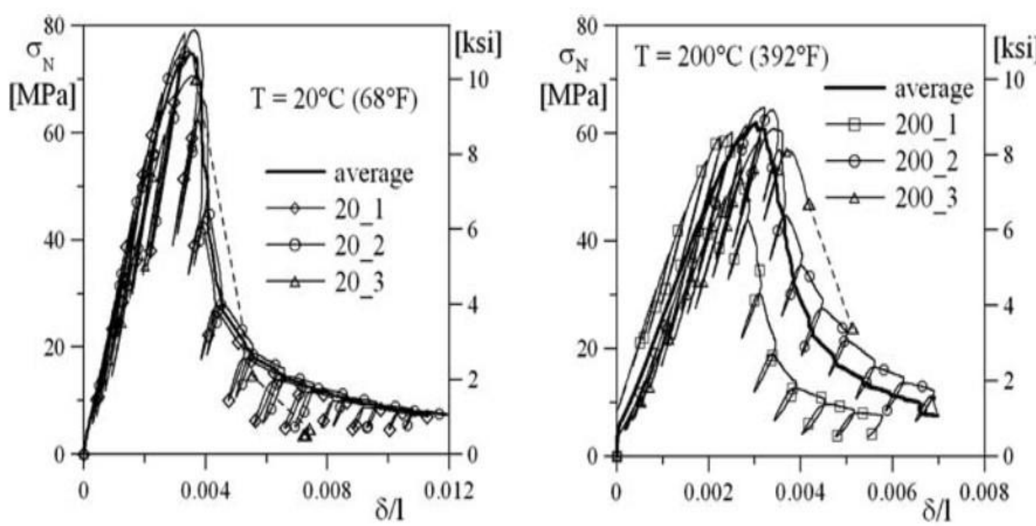

Figure 3.1 (Colombo et al., 2010)

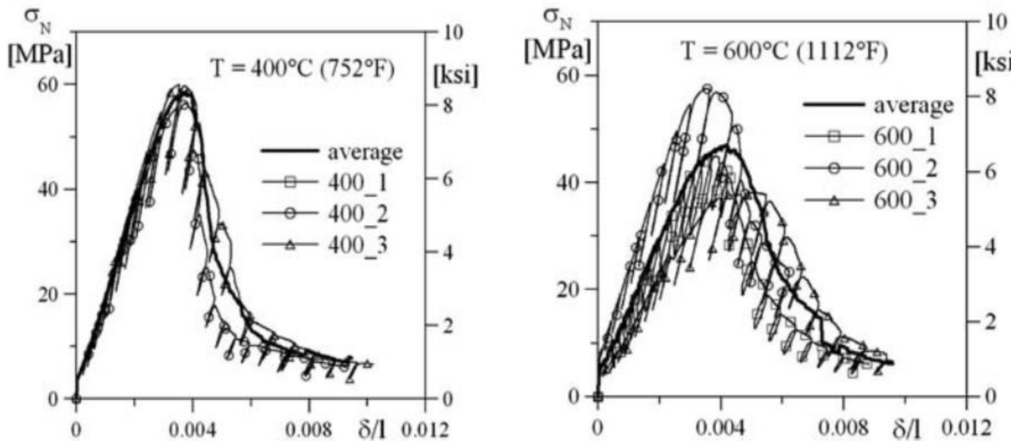

Figure 3.2 (Colombo et al., 2010)

3.2 Experimental Study by Anupama Krishna (2019)

The experimental research carried out by (Anupama Krishna et al., 2019) to study mechanical properties of concrete specimens at high temperatures was very helpful for the current research. The mechanical properties of primary focus in the research carried out by (Anupama Krishna et al., 2019) were compressive andtensile strength, young's modulus, and stress vs strain curves obtained from compression testing. So, specimens of standard sizes were casted and tested after heating at temperatures ranging between 100^{o}C to 1000^{o}C in an electrical furnace.

Ordinary Portland cement (OPC) was utilized in this experimentation and sieve analysis was performed for the coarse and fine grains. The testing of concrete mix was performed according to IS 81421976 and mix design for M20 concrete was performed as per IS 10262-2009. While the water to cement ratio was maintained at 0.45. Then the slump value of 60mm with a target mean strength of 28 MPa was used for the design purpose. Thus, the achieved compressive strength was 32.4 MPa.

Tests were performed on standard 150x150mm cubes and 150x300mm cylinders to study the compression strength and tensile strength. The relationships between stresses and strains were also obtained by compression testing of concrete specimens at elevated temperatures. The curing of concrete samples was carried out for twenty-eight days and then the samples were dried at room temperature in the laboratory for twenty-four hours. After that, the specimens were placed in oven at 105° C for twenty-four hours. Then the samples were heated at high temperature from 100° C to 1000° C. Finally, the samples were air cooled and tests were performed as per the standards.

In total, there were 30 concrete cylinders tested to study the stress-strain correlation of concrete at elevated temperatures. These stress vs strain curves are shown in the below figure 3.3 and have been used in this study to further research the toughness of concrete at high temperatures.

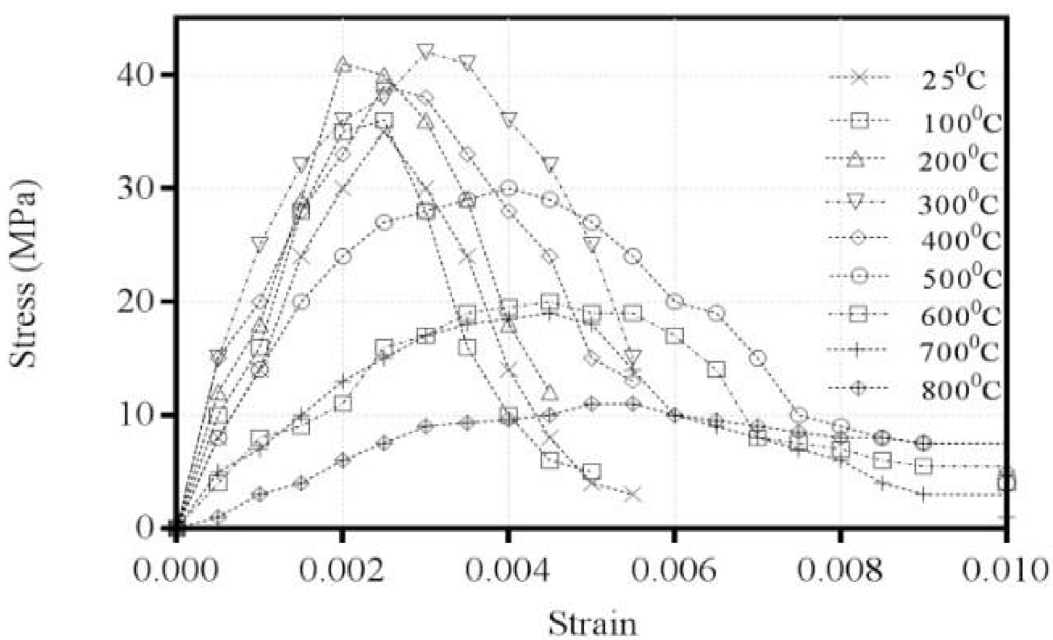

Figure 3.3 (Anupama Krishna et al., 2019)

3.3 Experimental Study by Chang (2006)

Some other experiments carried out by (Chang et al., 2006) were also referenced for this research analysis of post-peak behavior of concrete at high temperatures. Chang (2006) performed a study on the whole stress-strain correlation of concrete specimens once heated to a temperature of 100° C to 800° C. The concrete samples were casted in a standard mold of 150mm diameter and 300mm height. The samples were heated and then cooled at room temperature before final testing which was performed after 1 month. Regression analysis was carried out to formulate the relations of the mechanical properties with temperature. The testing results include the compression strength, strain at peak value of stress and the young's modulus. A total of 108 samples were tested by Chang (2006) to achieve the comprehensive stress-strain curves at elevated temperatures. The heating rate was chosen from 1° C to 4.5 °C per minute with an increase of 0.5 °C per minute respectively in consistent to the testing temperatures ranging from 100 to 800 °C with an increase of 100 °C.

The stress-strain curves gained from the experimental study of Chang (2006) are shown in the below figure 3.4:

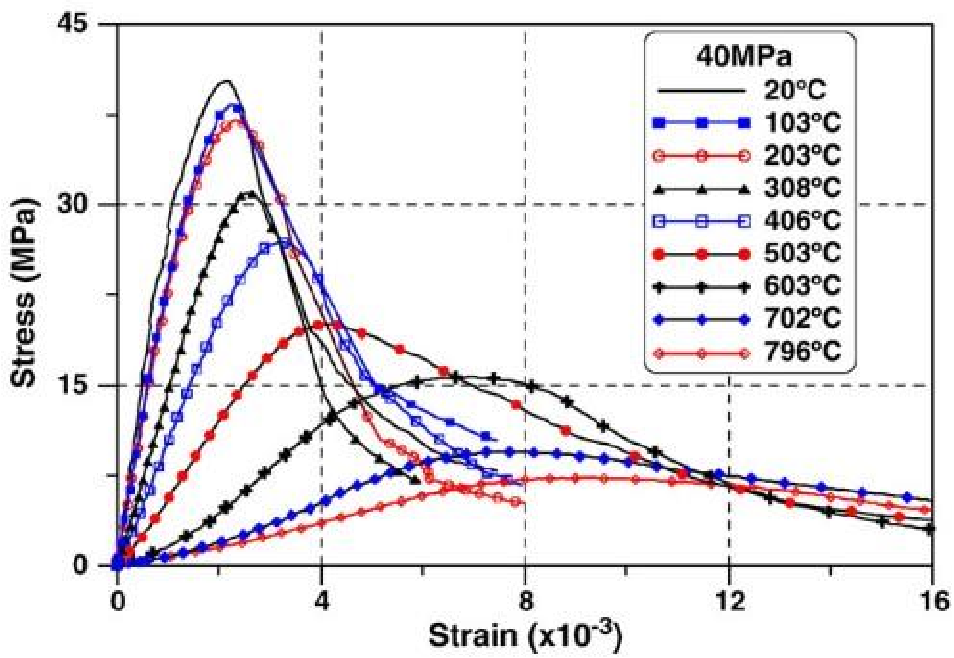

Figure 3.4 (Chang et al., 2006)

It is observed from the above curves that with the increase in temperature, the variance between initial tangent elastic modulus and the secant modulus at peak stress decreases. As the temperature is increased to more than 600° C, the initial tangent modulus becomes lesser than the secant modulus of concrete. It is obvious from the above graphs that the stress-strain curves for the unheated concrete samples vary a lot from the ones produced for heated concrete samples. These shapes strictly depend on the maximum attained temperature of the specimens. Moreover, it is also observed that as the temperature further increases, the post peak curves become flatter.

3.4 Experimental Study by Fu (2005)

Another research was carried out by (Fu et al., 2005) to study the stress-strain relationships of ordinary concrete and high-strength concrete at increased temperatures. In that research steel molds of 7.5 cm diameter and 15 cm in length, were utilized for molding the concrete specimen. The samples were de-molded twenty-four hours after casting and were poured in a water container for a duration of twenty-eight days. For each of the defined set of experiments 2 samples from the similar category were utilized to find out the mechanical characteristics at various temperatures levels (20^{o}C, 100^o C, 200^o C, 400^o C and 600^o C).

For each type of concrete, the specimens were tested at room temperature and then at higher temperatures of 100^o C, 200^o C, 400^o C and 600^o C. The specimens were heated in the furnace with a heating rate of 28^o C per minute. The heating of samples was carried out up to the target temperature and then the temperature was maintained in the furnace for 60 minutes to thermally stabilize the samples.

In the unstressed tests, the samples were heated up to the preferred temperatures and kept at that temperature for 60 min to obtain thermal stability. Finally, the specimens were tested under compression loading. To attain a comprehensive relation of load in contrast to deflection, the concrete samples were tested under a strain-controlled environment in order to calculate the post-peak portion of the stress-strain curves.

A distinctive pattern of strength deviation was noted in every single stage. The strength stayed comparatively unaffected up to 100^o C. Similarly, a difference in strengths was observed in the concrete with fly ash and metakaolin. The normal strength concrete displayed a small increase in compressive strength at a temperature of 100^o C. Up to 400^0 C, all the high strength concrete mixes had greater strength than the normal strength concretes except for the temperature of 100^o C to 200^o C. When temperature was increased more than 400^o C, the compression strength of high strength concrete and normal strength concrete decreased faster to around 60% of the compressive strength at room temperature.

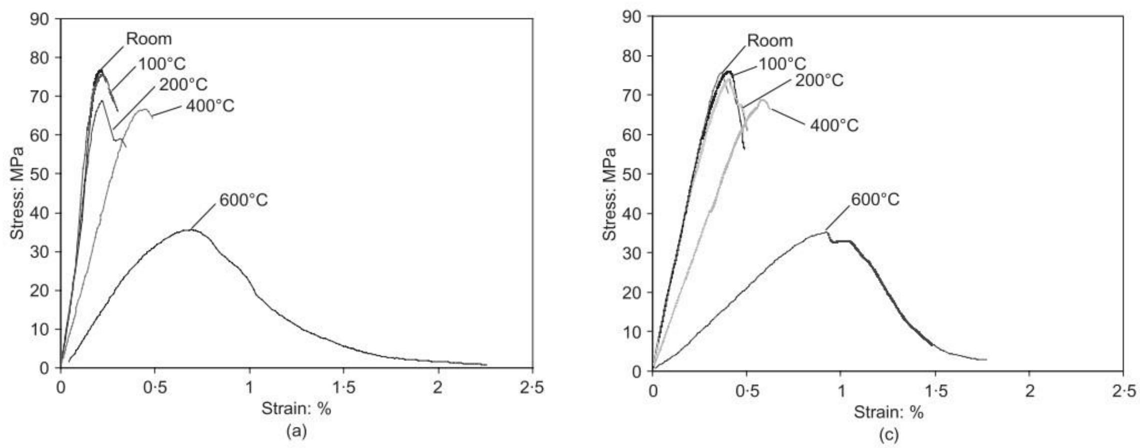

Figure 3.5 (Fu et al., 2005)

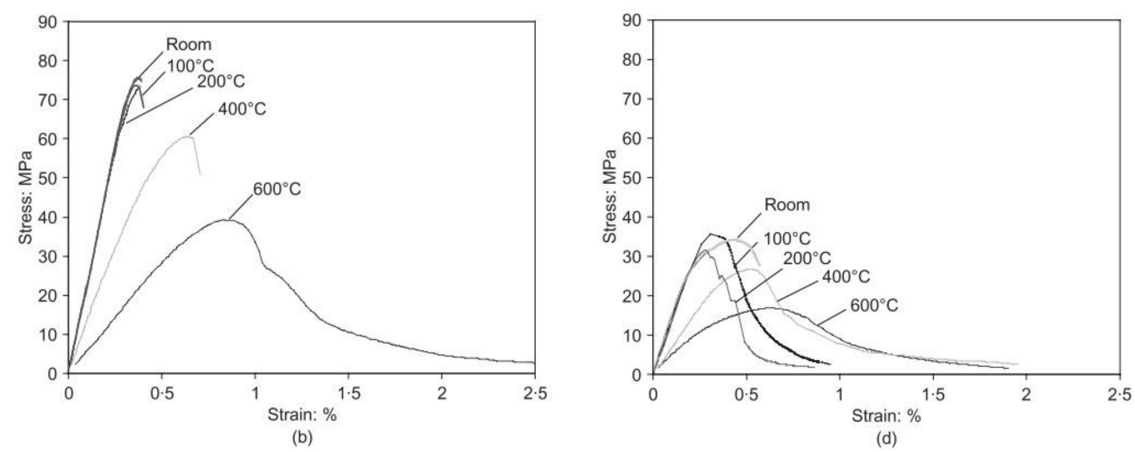

Figure 3.6 (Fu et al., 2005)

3.5 Experimental Study by (Nematzadeh & Mousavimehr, 2019)

In this study, the compressive stress strain curves of concrete comprising various waste materials was studied. These materials include PET and crumb rubber which were added in concrete specimens which were then tested at elevated temperatures. These materials were then added together in specific proportion as a natural sand substitute and the specimens were then tested once exposed to higher temperatures of 200°C, 400°C, 600°C, and 800°C. The physico-mechanical properties of concrete samples like compression strength, young's modulus, strain at peak value of stress, ultimate strain etc. were measured after exposing the specimens to high temperatures. At that point, they proposed several formulas to compute the mechanical properties. Moreover, a comparison was carried out between the results obtained from experiments and the ones produced by using international codes. (Nematzadeh & Mousavimehr, 2019) also did a comparison between their proposed relationships and the experimental results obtained by other researchers. Finally, they used the empirical equations for estimating the mechanical properties of concrete and proposed a stress vs strain model for concrete containing waste materials.

For the preparation of specimen, type II Portland cement was utilized in present research. Crushed dolomite rock was employed as a coarse aggregate. In addition, fine aggregate with fineness modulus of (2.6%), specific gravity of (2.63%), and water absorbency of (1.73%) was used as the fine aggregate.

Polyethylene terephthalate (PET) flakes were used in this research and added to the concrete mix. These were taken from a plastic waste obtained from a recycling factory, washed, and shredded in the form of PET flakes and then added to the concrete as fine aggregate.

Another recycled material additive used by (Nematzadeh & Mousavimehr, 2019) in their research was crumb tire rubber. This crumb rubber was provided by a tire recycling plant based in Iran. The material was washed and cleaned before finally adding it into the concrete.

Figure 3.7 (Nematzadeh & Mousavimehr, 2019)

Thermal gravimetric analysis experimentations were performed in accordance with ISO 11357 (ISO 1997) by means of an electric furnace starting from room temperature to a maximum temperature of around 600°C and the heating rate was 10°C per minute. The specimens were then heated in the presence of argon gas (inert) gas to limit the chemical activity.

In this study, a total of 96 cylindrical shaped samples with dimensions of 100mmx200mm were utilized. The main aim of their research was to measure the concrete mechanical properties with and without the addition of recycled concrete materials. The major properties of interest in this research were compressive strength and elastic modulus of concrete and they studied how these properties vary with the addition of recycled plastic fibers and waste rubber material when specimens are heated at high temperatures. Three similar samples were made for every experimental group and the results are stated as an average of three specimens.

The concrete specimens were labeled for easy identification of the constituents. R samples are the reference specimens without the addition of recycled materials. P15 denotes a sample comprising plastic flakes substituting 15% of the sand by volume. T15 denotes a sample comprising waste rubber substituting 15% of the sand by volume. Lastly, P7.5 T7.5

represents a sample comprising a mixture of plastic flakes and waste rubber substituting 7.5% of the volume of sand.

Five different sets were prepared for the testing of concrete samples at various temperatures which are 23°C, 200°C, 400°C, 600°C, and 800°C. The samples were first pre-heated at a temperature of 110°C for 24hrs to remove the moisture. After that, they were exposed to a temperature ranging between 200°C–800°C. During the testing, the room temperature was around 23°C and the testing was carried out at higher temperatures in order to compare the results with those obtained from room temperature testing of specimens. The specimens were heated in an electric furnace and the target temperature was maintained for at least 1 hour after its achieved inside the furnace. Finally, the samples were removed from the furnace and allowed to be cooled at room temperature. Various thermocouples installed inside the furnace enabled the correct measurement of temperature inside the furnace.

The results show that a significant reduction in the concrete properties was observed with the increase in temperature. Furthermore, the provided codes accurately evaluate the tentative results of compression strength at elevated temperatures and the young's modulus at all the high temperatures. On the other hand, it was observed that the values of strain at peak stress were over-estimated by the proposed relations.

The stress vs strain curves for different sets of concrete samples obtained by (Nematzadeh & Mousavimehr, 2019) are presented in the next figures:

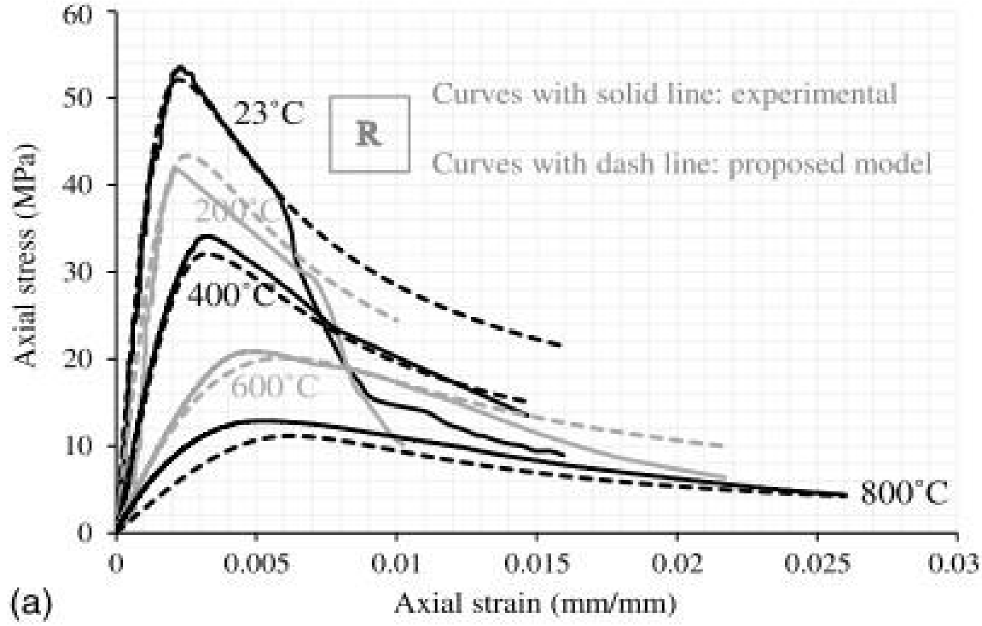

Figure 3.8 (Nematzadeh & Mousavimehr, 2019)

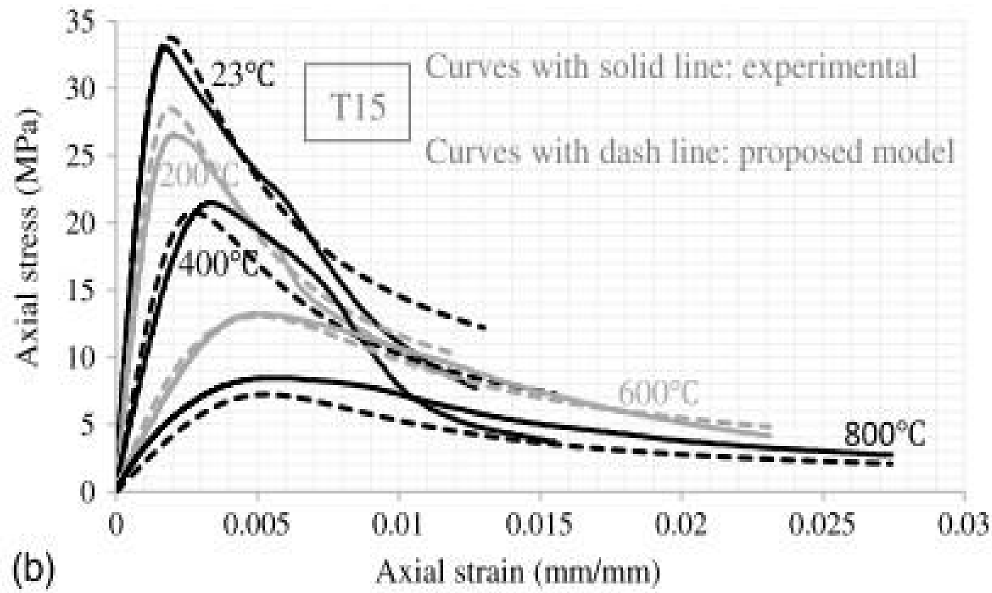

Figure 3.9 (Nematzadeh & Mousavimehr, 2019)

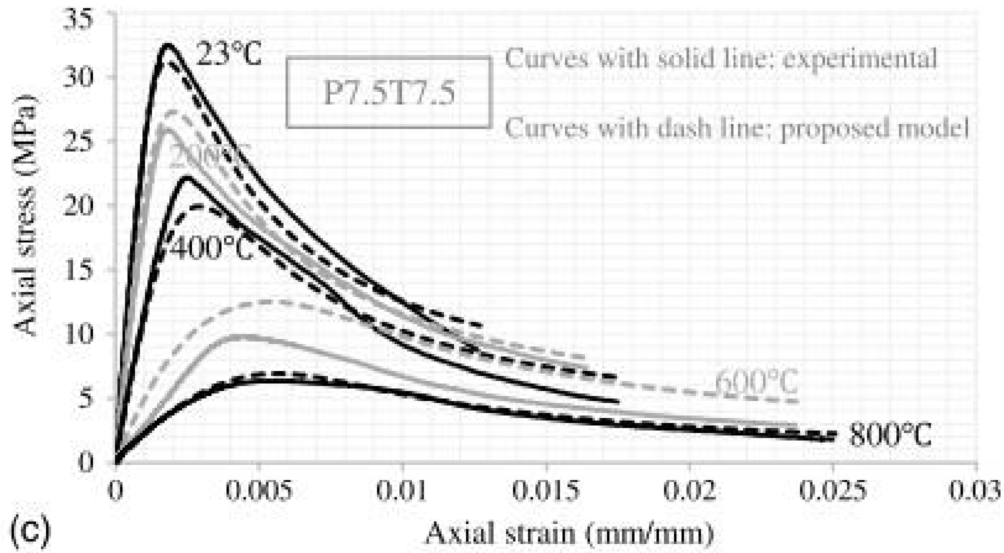

Figure 3.10 (Nematzadeh & Mousavimehr, 2019)

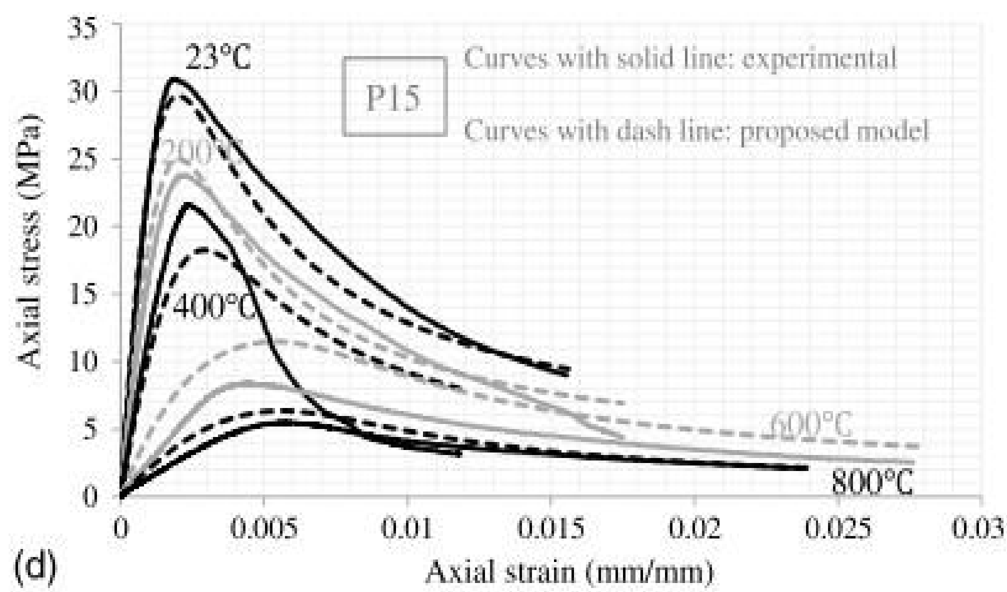

Figure 3.11 (Nematzadeh & Mousavimehr, 2019)

3.6 Experimental Study by (Shi et al., 2002)

A research carried out by (Shi et al., 2002) focused on the changes in mechanical properties of concrete based on various stress-temperature paths. They considered constant temperature and increased stress path vs constant stress and increased temperature path of concrete. The concrete strain for the first case could be obtained easily by experimentation while for the second case, it is quite difficult to compute the strains because the temperature inside the concrete specimen varies alot. So (Shi et al., 2002) proposed a new model for the temperature-flow mapping that allows one to obtain the mechanical properties and relate them with either of the cases mentioned earlier.

For studying the performance of concrete under the first case, (Shi et al., 2002) prepared 40 specimens of concrete. The mixed proportion was 1: 0.617: 2.083: 4.4 for cement, water, sand and aggregate, respectively. OPC with river sand as fine aggregate and limestone as coarse aggregate was used for the preparation of specimens. The average compressive strength achieved for the specimens was around 33 MPa. The dimensions of concrete samples were 100mm x300mm.

The stress-strain curves obtained at various temperature's by (Shi et al., 2002) are shown in the figure below:

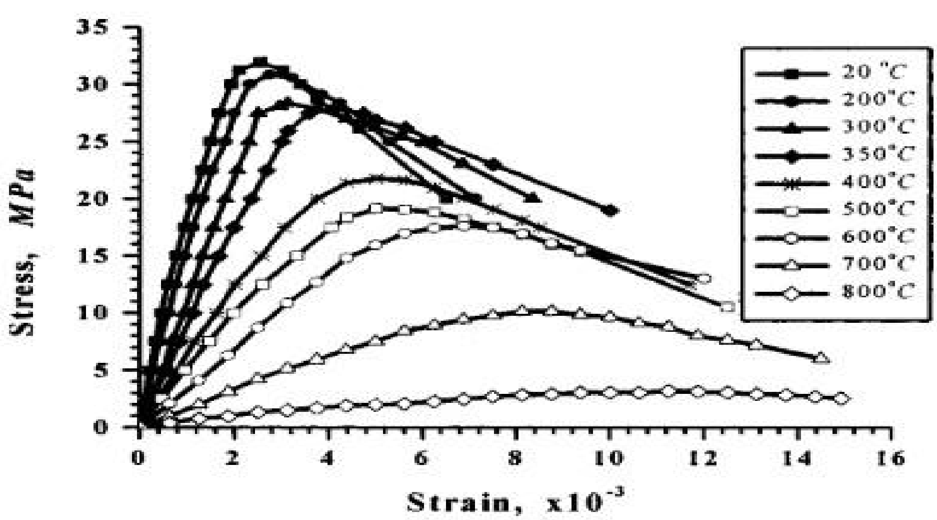

Figure 3.12 (Shi et al., 2002)

3.7 Experimental Study by (Lo Monte et al., 2015)

A research was performed by (Lo Monte et al., 2015) in which they studied the mechanical properties of heat-damaged concrete comprising of stretched polystyrene synthesized particles. Three different types of concrete mixes were used namely M0, M1 and M2. The mix type M0 was used as a reference, M1 mix was a typical was and the M2 mix contained high cement content.

For each type of concrete mix, 11 cylinders were casted out of which 10 were used in compression testing while the 11th one was used in indirect tension test. The compression tests were performed at temperatures of 20ºC, 150ºC, 300ºC, 500ºC and 700ºC. (Two samples were tested at each temperature for each mix type). The diameter and height of samples tested at room temperature were 150mm and 300mm, respectively. While the diameter and height of samples tested at elevated temperatures were 100mm and 200mm, respectively. All the compression tests were displacement controlled in this research.

In our research, we used the stress-strain curves for M0 concrete, and these are displayed in the figure below:

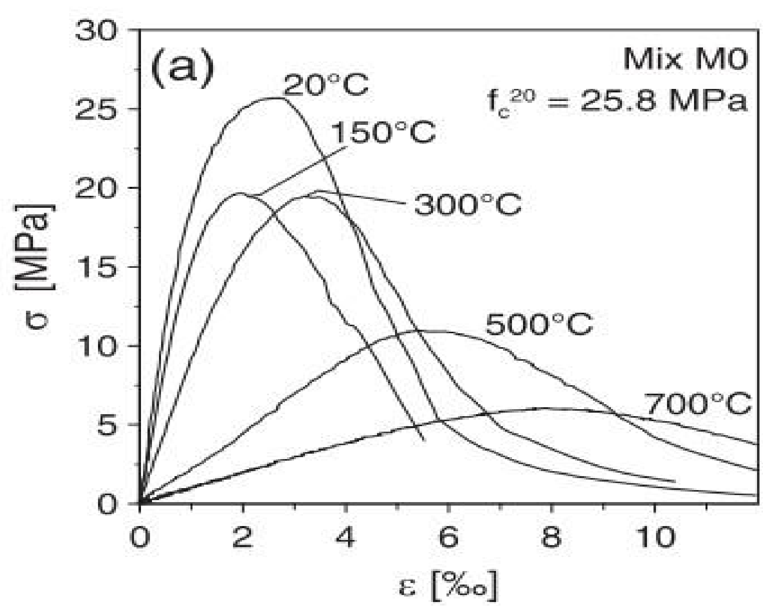

Figure 3.13 (Shi et al., 2002)

3.8 Experimental Study by (Poon et al., 2004)

A research was performed by (Poon et al., 2004) to characterize the compressive behavior of high performance fiber reinforced concrete when heated at very high temperatures. High performance concrete was used in this study with different cement constituents. Ordinary Portland cement concrete was used with some additions of metakaolin (MK), silica fumes (SF), steel fibers and polypropylene fibers in different proportions. The specimens with different proportions of aforementioned elements were heated at temperatures of 600^oC and 800^oC and the mechanical properties were studied.

Various concrete mixes was prepared in a small mixer and for each mix, a total of twelve samples, comprising three 10x10cm cubes and nine cylinders with 10cm diameter and 20 cm height were casted in steel molds. The samples were treated in water bath at 27^oC for 28 days after removing from the molds at day one. The specimens were then treated at a temperature of 20^oC and a humidity of 75% for another 28 days. Testing of the 3 cubes and 3 of the 9 cylindrical samples was carried out soon after the treatment under aforementioned conditions.

The remaining six cylinders were heated in an electric furnace at two different temperatures of 600^oC and 800^oC (three samples at each temperature). The specimens were heated at a constant rate of 2.5^oC per minute to reach the target temperatures. Afterwards, the heat was provided for an extra hour and then the specimens were cooled down naturally to reach the ambient temperature.

The results of the stress-strain relationships as studied by (Poon et al., 2004) are shown in the figures below:

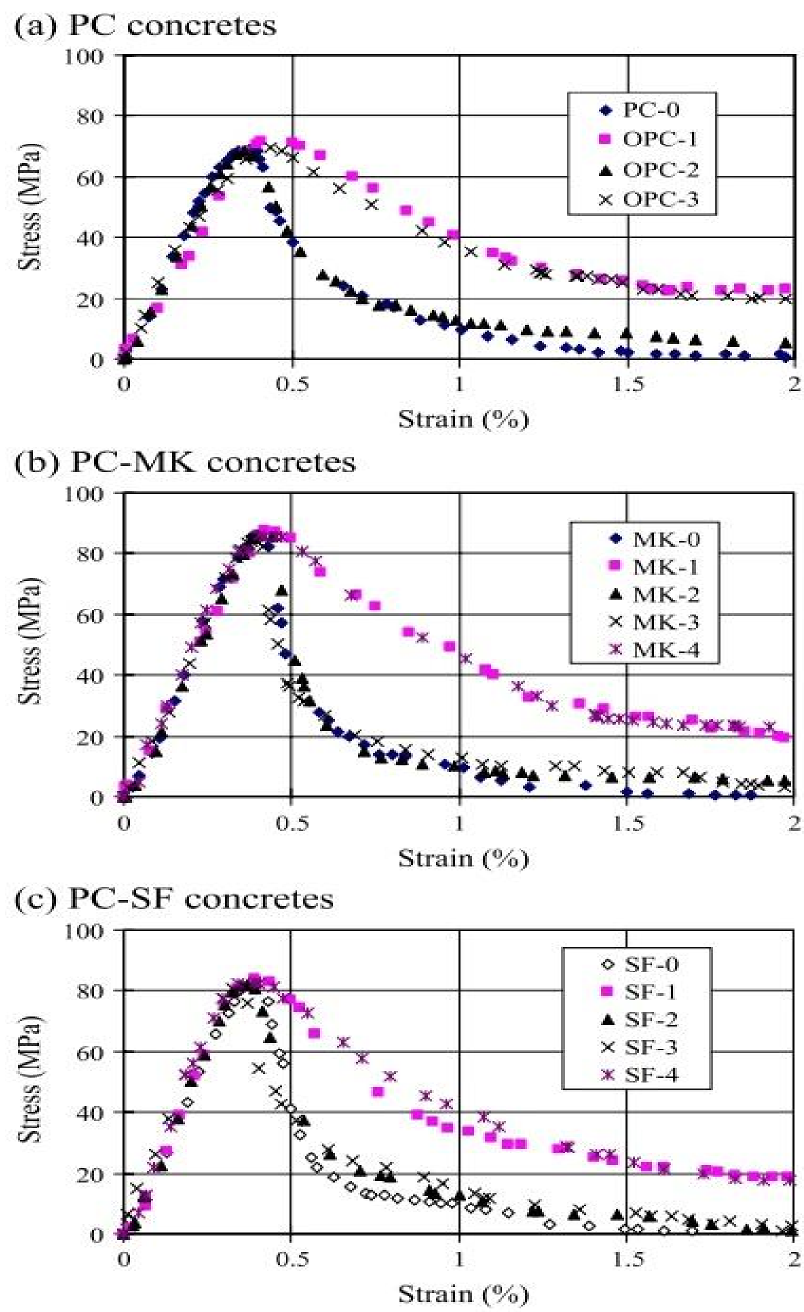

Fig. 1. Stress−strain curves of unheated concrete cylinders.

Figure 3. 14 (Poon et al., 2004)

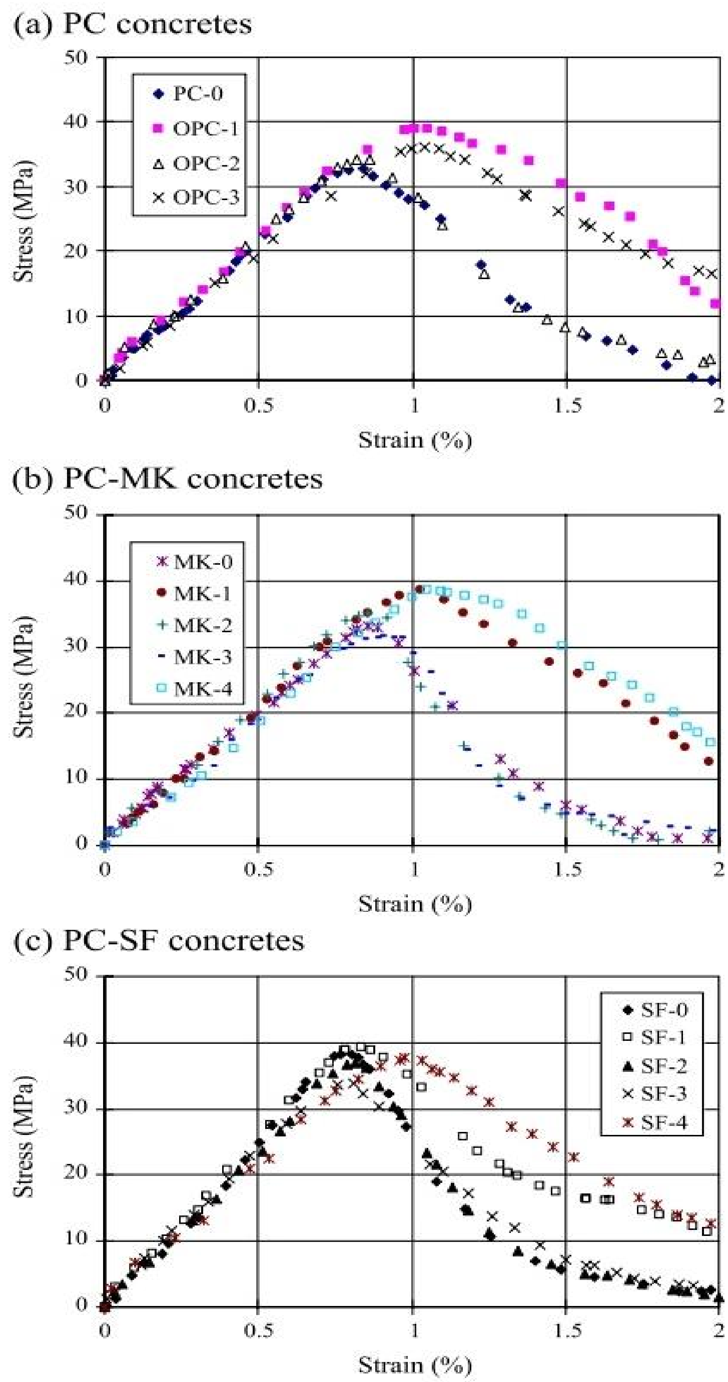

. Stress–strain curves of concrete cylinders after exposure to 600 °C.

Figure 3.15 (Poon et al., 2004)

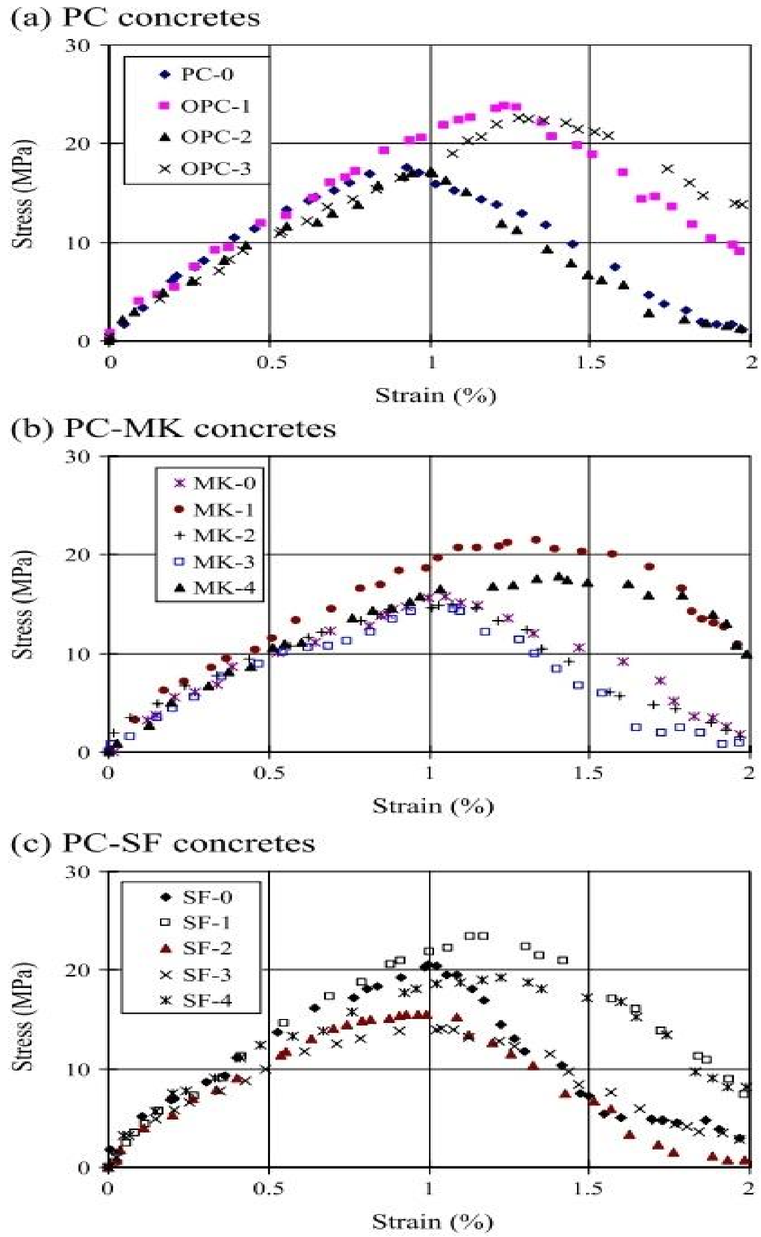

Fig. 4. Stress–strain curves of concrete cylinders after exposure to 800 °C.

Figure 3.16 (Poon et al., 2004)

In our research, we have used the stress-strain curves for the samples P-0, OPC-1, MK-0, MK-1, SF-0, and SF-1 at room temperature, 600°C and 800°C.

CHAPTER 4: ANALYSIS OF RESULTS & DISCUSSION

Several researchers have worked on the behavior of concrete and studied its mechanical characteristics at high temperatures. However, there are only limited researchers who have researched on the toughness of concrete by calculating post-peak stress-strain curves at high temperatures. (Nematzadeh et al., 2019) in their research proposed unique functions to predict the pre-peak as well as post-peak portion of concrete stress-strain curve under compression. The reason behind this is the change in post-peak behavior due to cracks propagation. This is also true when concrete specimens are heated at high temperature.

The experiments performed by different researchers that are described earlier in chapter 3 have been used as a base to analyze the post-peak behavior of concrete. The characterization of concrete toughness at elevated temperatures has been carried out in this research by following the procedures described by (Fantilli et al., 2008). The post-peak behavior of concrete based materials in compression is characterized by stress-inelastic displacement relations. Fantilli (2008) introduced a function to express such relations in their research. While in this present study that function has been validated with the experimental data presented in chapter 3 respectively and then a comparison is made between the experimental post-peak curves and those produced by that function. The pre-peak portion of the experimental curves are also validated by comparing them with the mathematical model proposed in UNI EN 1992-1-2_2005 (Euro Code 2) for concrete at elevated temperatures.

4.1 Fracture Toughness of Concrete

The presence of strain localization in the post-peak portion of stress-strain curve of concrete in tension is generally acceptable. However, strains that exceed the tensile strength are localized in the process zone and the unloading happens in the remaining part of the sample that is in tension. Here the stress-strain relationship is utilized for the ascending branch. The softening stage can be modeled by means of stress-crack opening displacement relationships as per the fictitious crack model proposed by (Hillerborg et al., 1976). The area under the stress-COD curve constitutes the fracture toughness A_F of the concrete.

The below equation can be used for the computation of inelastic displacements in concrete specimen as proposed by (Fantilli et al., 2008).

$$w = \left(\varepsilon_c - \varepsilon_{c1} + \frac{\Delta\sigma_c}{E_c}\right) * H \qquad \text{Equation. 1}$$

The value of the function F (w) can be computed simply by dividing the value of post-peak stress at a particular step with the compressive strength of concrete (f'_c).

A graph between the function F (w) and the inelastic displacements (w) can be plotted and the area under the curve gives us the fracture toughness A_F of the concrete. The graphs obtained for various experiments are attached in the Annex-II of this report.

4.2 Procedure

For various types of concrete specimens, we extracted the stress-strain curves from various research papers that have been discussed earlier in chapter 3. The geometrical and mechanical properties of concrete specimens that include height (H), compressive strength (f'_c), Youngs modulus (E_c) and strain at peak stress (ε_{c1}) were also calculated. The stress-strain graphs were imported in AutoCAD, scaled, and marked to get the values of stresses at uniform increments of strain. The points on the curve were then imported to MS Excel to get the complete stress-strain curve. Then the equation 1 was used to compute the inelastic displacements (w) of concrete specimens for the post-peak portion of the stress-strain curve. Furthermore, the value of function F (w) is also computed as for the various points that were marked in AutoCAD on the stress-strain curve. Finally, the area under the curve plotted between F (w) and w was computed up to a limiting value of w=1mm to get the fracture toughness A_F of the specimen. The same steps were repeated to compute the A_F of concrete samples at elevated temperatures. The results are shown in the table attached in Annex-I.

The impact of elevated temperature on the characteristics of concrete was calculated by plotting the following four relations based on the data provided in Annex-II.

1. Compressive strength (f'c) vs Temperature.

2. Elastic Modulus (E) vs Temperature.
3. Fracture Toughness (A_F) vs Temperature.
4. Strain at Peak (ε_{c1}) vs Temperature.

The results are shown in the following graphs:

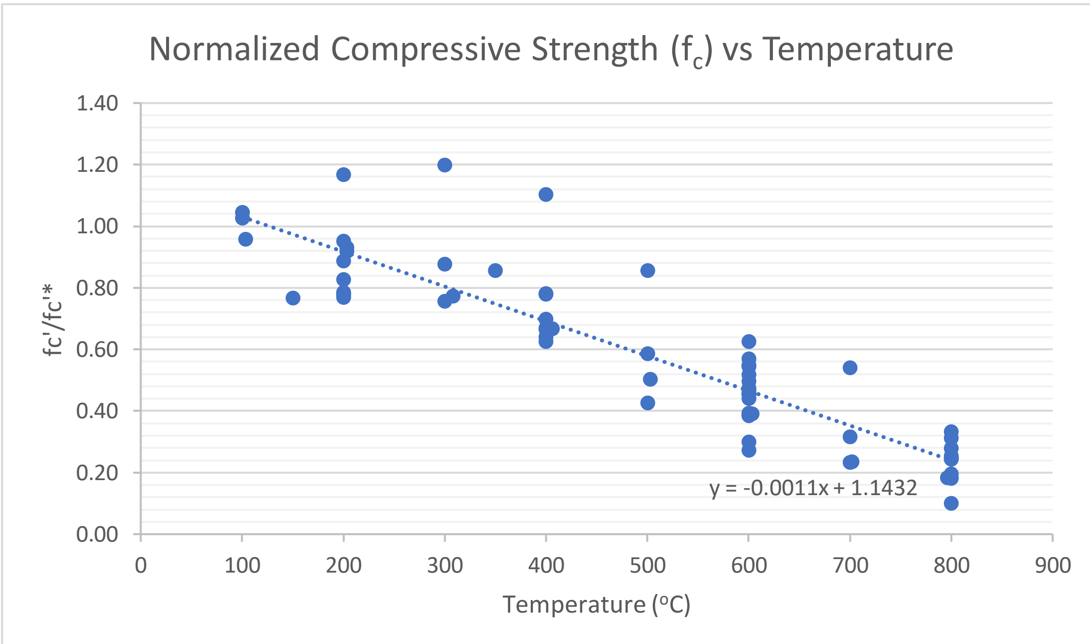

Figure 4.1

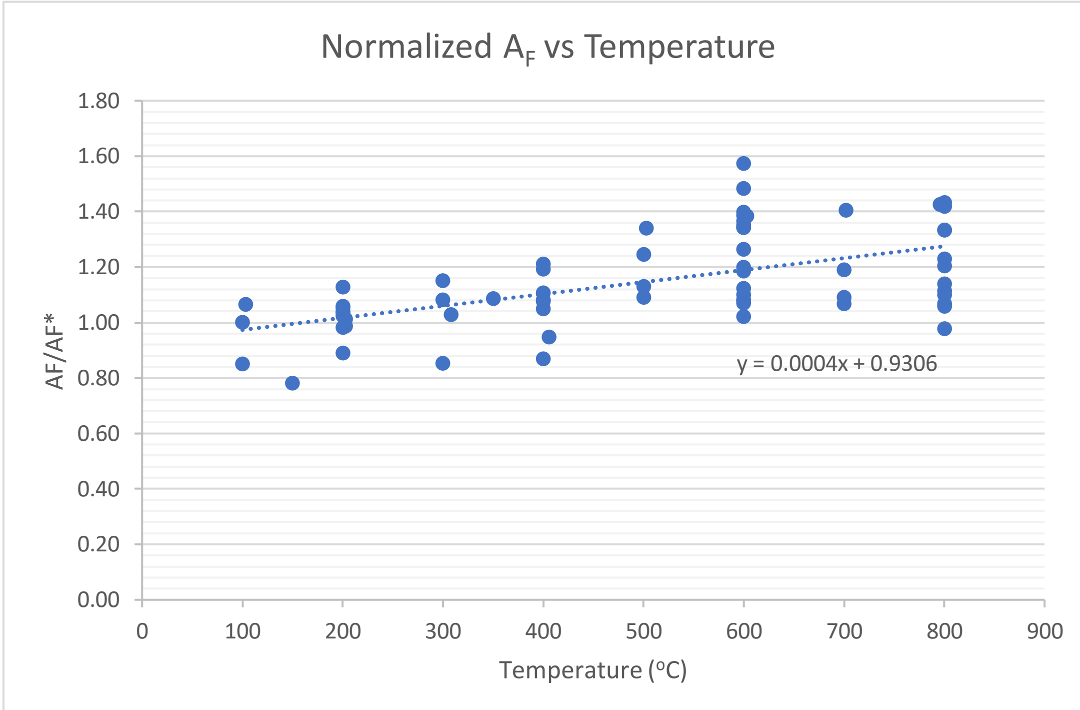

Figure 4.2

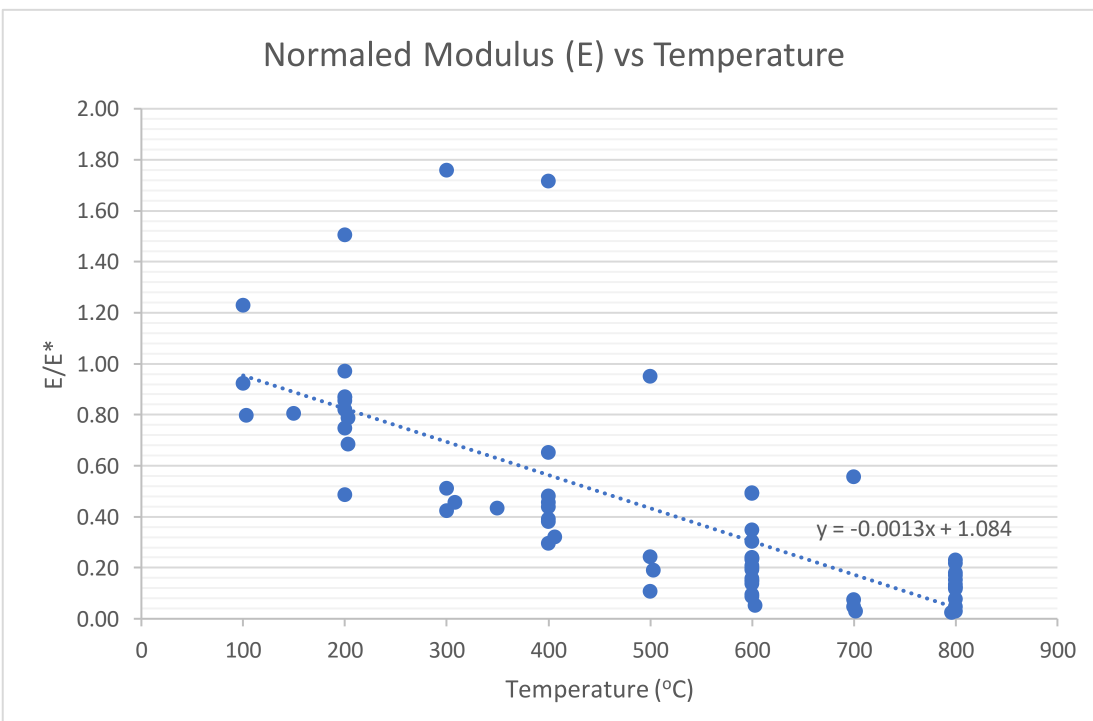

Figure 4.3

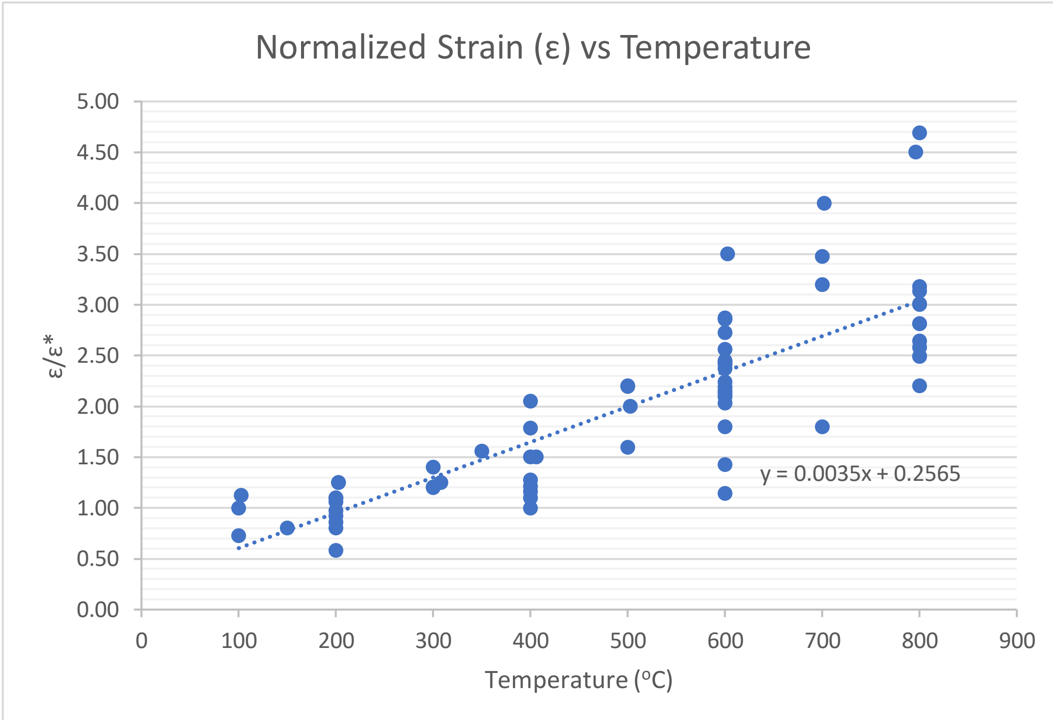

Figure 4.4

A complete database containing the data for all the stress-strain curve used in this research was prepared and the summary is attached in the Annex-I of this report. It includes the experimental mechanical properties at room temperature as well as at elevated temperatures. It also includes the mechanical properties obtained from the proposed function at room temperature and elevated temperature. Moreover, the graphs obtained for various stress-strain curves are provided in Annex-II of this report. These graphs show a comparison between the experimental post-peak curve and the post-peak curve obtained by the model for various types of concretes at elevated temperature.

CHAPTER 5: CONCLUSION

This research intended to compute the toughness of concrete when exposed to elevated temperatures while working on the post-peak portion of stress strain curves. Based on this research, we have reached the following conclusions:

1. There are no major deviations in compressive strength, elastic modulus, strain, and toughness parameter (A_f) when the specimens are heated up to 100°C. The variation in mechanical properties becomes more significant when concrete is heated at high temperatures (above 600°C).
2. The compressive strength of concrete specimen decreases with the increase in temperature. At very high temperature (around 800°C), the strength reduces to around 20% of the total strength at room temperature.
3. The elastic modulus also tends to decline with the rise in temperature of concrete. The elastic modulus reduces to half at a temperature ranging between (400°C to 500°C).
4. The strain-at-peak-stress increases as the temperature is increased. The stress-strain curves become flatter at high temperatures and the peak shifts forward in most of the cases. At high temperature of around 800°C, the strain-at-peak-stress becomes approximately three times of the strain-at-peak-stress at room temperature.
5. The tough parameter (A_F) remains almost constant up to 100°C and then increases with the increase in temperature. However, the results deviate a lot at higher temperatures ranging between 600°C to 800°C.
6. The projected model for the deviation of A_f with temperature works quite well with in a temperature range of 100°C to 600°C. A further temperature increase significantly impacts the properties of concrete and it becomes tough to calculate the toughness behavior of concrete at temperatures above 600°C. There is a huge standard deviation in the statistics at temperatures of 600°C and 800°C, so the model is deviating from the experimental results.

REFERENCES

1. 2006 International Building Code, International Code Council, Inc., Falls Church, VA, 2006, pp. 109-155.
2. Abid, M., Hou, X., Zheng, W., & Hussain, R. R. (2019). Effect of fibers on high-temperature mechanical behavior and microstructure of reactive powder concrete. Materials, 12(2). https://doi.org/10.3390/ma12020329
3. ACI 214.4-03. Guide for Obtaining Cores and Interpreting Compressive Strength Results, American Concrete Institute, Farmington Hills, MI (2013).
4. Agarwal A, Nanda B, and Maity D (2014). Experimental investigation on chemically treated bamboo reinforced concrete beams and columns. Construction and Building Materials, 71: 610-617.
5. Ahmed, A. and Sturges, J., Materials Science in Construction: An Introduction. Routledge, 2014
6. Ajagbe, W. O., Tijani, M. A., Arohunfegbe, I. S. and Akinleye, M. T. (2018). Assessment of fine aggregates from different sources in Ibadan and environs for concrete production. Nigerian Journal of Technological Development. Accepted for publication on 13/12/2017.
7. Ajagbe, W., & Tijani, M. A. (2018). Compressive Strength of Concrete Made from Aggregates of Different Sources Compressive Strength of Concrete Made from Aggregates of Different Sources. USEP Journal of Research Information in Civil Engineering, 15(1), 1963–1974.
8. Akhimien, N., & Adamolekun, M. O. (2018). Fire safety, (January 2017).
9. American Concrete Institute - ACI. ACI 363R-92. State of the art report on High-Strength Concrete. In: ACI Manual of Concrete Practice (MCP), Part 5. Farmington Hills: American Concrete Institute; 2002.
10. Anupama Krishna, D., Priyadarsini, R. S., & Narayanan, S. (2019). Effect of elevated temperatures on the mechanical properties of concrete. Procedia Structural Integrity, 14, 384–394. https://doi.org/10.1016/j.prostr.2019.05.047
11. ASTM C 42/C 42M-90. Standard Test Method for Obtaining and Testing Drilled Cores and Sawed Beams of Concrete, Annual Book of ASTM Standards (2008).

12. ASTM E 119-00a, "Standard Test Methods for Fire Tests of Building Construction and Materials," ASTM International, West Conshohocken, PA, 2000, 21 pp.
13. Behbahani H, Nematollahi B, and Farasatpour M (2011). Steel fiber reinforced concrete: A review. In the International Conference on Structural Engineering Construction and Management (ICSECM2011), Kandy, Sri-Lanka.
14. Bilow, D. N., & Kamara, M. E. (2008). Fire and concrete structures. Proceedings of the 2008 Structures Congress - Structures Congress 2008: Crossing the Borders, 314(1). https://doi.org/10.1061/41016(314)299
15. Bisby, L. A., Green, M. F., & Kodur, V. K. R. (2005). Modeling the behavior of fiber reinforced polymer-confined concrete columns exposed to fire. *Journal of Composites for Construction*, *9*(1), 15–24. https://doi.org/10.1061/(ASCE)1090-0268(2005)9:1(15)
16. BS EN 12504-1:2009. Testing Concrete in Structures. Cored Specimens. Taking, Examining and Testing in Compression, British Standards Institution (2009)
17. Chang, Y. F., Chen, Y. H., Sheu, M. S., & Yao, G. C. (2006). Residual stress-strain relationship for concrete after exposure to high temperatures. Cement and Concrete Research, 36(10), 1999–2005. https://doi.org/10.1016/j.cemconres.2006.05.029
18. Colombo, M., Di Prisco, M., & Felicetti, R. (2010). Mechanical properties of steel fibre reinforced concrete exposed at high temperatures. Materials and Structures/Materiaux et Constructions, 43(4), 475–491. https://doi.org/10.1617/s11527-009-9504-0
19. Committee, A. C. I. (2019). 318-19 Building Code Requirements for Structural Concrete and Commentary. 318-19 Building Code Requirements for Structural Concrete and Commentary. https://doi.org/10.14359/51716937
20. Fantilli, A. P., Mihashi, H., & Vallini, P. (2008). Post-Peak Behavior of Cement-Based Materials. 104.
21. Fletcher, I., Borg, A., Hitchen, N., & Welch, S. (2006). Performance of concrete in fire: A review of the state of the art, with a case study of the Windsor Tower fire. 4th

International Workshop in Structures in Fire, 779–790. Retrieved from http://www.era.lib.ed.ac.uk/handle/1842/1987

22. Fowler, D. N. and Quiroga N. (2003). The effect of aggregates characteristic on the performance of Portland cement concrete. International Centre for Aggregates Research. (ICAR 104-1F382 p.).
23. Fu, Y. F., Wong, Y. L., Poon, C. S., & Tang, C. A. (2005). Stress-strain behaviour of high-strength concrete at elevated temperatures. Magazine of Concrete Research, 57(9), 535–544. https://doi.org/10.1680/macr.2005.57.9.535
24. Gollu, V. K., Allam. D. and Erla S. (2016). Causes of concrete failure. International Journal of Advanced Technology in Engineering and Science. 4(4), 198-206
25. Guide, A. B., & Fire, T. O. (2015). FIRE AND FIRE.
26. GUIDELINE 5 . CLASSES OF FIRE , TYPES OF PORTABLE FIRE EXTINGUISHERS , INSPECTION & MAINTENANCE OF FIRE EXTINGUISHERS IN UNIVERSITY BUILDINGS. (2014), 1–5.
27. Gunes, O. (2015). Turkey's grand challenge: Disaster-proof building inventory within 20 years. Case Studies in Construction Materials, 2, 18–34. https://doi.org/10.1016/j.cscm.2014.12.003
28. Jacob, B., Balaji, A., & John, E. (2013). Open Access Behaviour of concrete structures under fire - a comparative study between IS 456 : 2000 and finite element software ANSYS American Journal of Engineering Research (AJER), 62–66.
29. Japan Society of Civil Engineers, Method of tests for compressive strength and compressive toughness of steel fiber reinforced concrete. Standard SF-5, JSCE Concrete Library, No. 3, 1984, pp. 63-66.
30. Jiang, X, The Effect of Creep in Tension on Cracking Resistance of Concrete, Dissertation, Submitted for degree of M.Sc., Dept of Civil Engineering, Leeds University, 1997
31. Khoury, G. A. (2000). Effect of fire on concrete and concrete structures.
32. Kristiawan, S. A. (2006). Strength, shrinkage and creep of concrete in tension and compression. Civil Engineering Dimension, 8(2), 73–80.

33. Lakhiar MT, Sohu S, Bhatti IA, Bhatti N, Abbasi SA, and Tarique M (2018). Flexural performance of concrete reinforced by plastic fibers. Engineering, Technology and Applied Science Research, 8(3): 3041-3043.

34. Lo Monte, F., Bamonte, P., & Gambarova, P. G. (2015). Physical and mechanical properties of heat-Damaged structural concrete containing expanded polystyrene syntherized particles. Fire and Materials, 39(1), 58–71. https://doi.org/10.1002/fam.2230

35. Lo, S. H., Li, L., & Su, R. K. L. (2014). Optimization of partial interaction in bolted side-plated reinforced concrete beams. Computers and Structures, 131(January), 70–80. https://doi.org/10.1016/j.compstruc.2013.10.007

36. Malagavelli, V., & Paturu, N. R. (2011). Polyester fibers in the concrete an experimental investigation. Advanced Materials Research, 261–263, 125–129. https://doi.org/10.4028/www.scientific.net/AMR.261-263.125

37. Marar, K., Eren, Ö., & Yitmena, I. (2011). Compression specific toughness of normal strength steel fiber reinforced concrete (NSSFRC) and high strength steel fiber reinforced concrete (HSSFRC). Materials Research, 14(2), 239–247. https://doi.org/10.1590/S1516-14392011005000042

38. Mindess S and Banthia N. Fiber Reinforced Cementitious Composites: Current Practice and Future Prospects. In: *Proceedings of V. M. Malhotra Symposium Concrete Technology*: Past, Present, and Future; 1994; Berkeley. Detroit: American Concrete Institute; 1994. p. 417-446.

39. Mohammed, H., Mechanical Properties Of Ultra High Strength Fiber Reinforced Concrete (Doctoral dissertation, The University of Akron), 2015.

40. Mosaberpanah, M. A., & Eren, O. (2016). Relationship between 28-days Compressive Strength and Compression Toughness Factor of Ultra High Performance Concrete Using Design of Experiments. Procedia Engineering, 145, 1565–1571. https://doi.org/10.1016/j.proeng.2016.04.197

41. N. Kabashi, C. Krasniqi, and A. Dautaj, “Evaluation the compressive strength in concrete structures using the in-situ test methods,” J. Civ. Eng. Environ. Sci., 2, No. 1, 001–004 (2016).

42. Nematzadeh, M., & Mousavimehr, M. (2019). Residual Compressive Stress–Strain Relationship for Hybrid Recycled PET–Crumb Rubber Aggregate Concrete after Exposure to Elevated Temperatures. Journal of Materials in Civil Engineering, 31(8), 04019136. https://doi.org/10.1061/(asce)mt.1943-5533.0002749
43. Neves, R. D., & Fernandes de Almeida, J. C. O. (2005). Compressive behaviour of steel fibre reinforced concrete. Structural Concrete, 6(1), 1–8. https://doi.org/10.1680/stco.2005.6.1.1
44. Neville, A. M. (2011). Properties of concrete. 5th edition, Pearson Education Limited, Essex, England.
45. Noorzaei, J., Hakim, S. J. S., Jaafar, M. S. and Thanoon, W. A. M. (2007). Development of artificial neural networks for predicting concrete compressive strength. International Journal of Engineering and Technology. 4(2), 141-153.
46. O. Arioz, M. Tuncan, K. Ramyar, and A. Tuncan, "Assessing concrete strength by means of small diameter cores," Constr. Build. Mater., 22, 981–988 (2008).
47. Oad, R. (2018). Effect of steel fibres on the compressive and flexural strength of concrete. International Journal of ADVANCED AND APPLIED SCIENCES, 5(10), 16–21. https://doi.org/10.21833/ijaas.2018.10.003
48. Of, E., & Mansur, O. B. M. A. (1999). in C Ompression. Test, 11(February), 21–29.
49. Onundi, L. O., Oumarou, M. Ben, & Alkali, A. M. (2019). Effects of Fire on the Strength of Reinforced Concrete Structural Members, 7(1), 1–12. https://doi.org/10.12691/ajcea-7-1-1.
50. Otter DE and Naaman AE. Properties of Steel Fiber Reinforced Concrete Under Cyclic Loading. *ACI Materials Journal*. 1988; 85(4):254-261.
51. Park, S.H., Kim, D.J., Ryu, G.S. and Koh, K.T., Tensile behavior of ultra high performance hybrid fiber reinforced concrete. Cement and Concrete Composites, 34(2), 2012, pp.172-184.
52. Perceka, W., Liao, W. C., & Wang, Y. De. (2016). High strength concrete columns under axial compression load: Hybrid confinement efficiency of high strength transverse reinforcement and steel fibers. Materials, 9(4), 6–13. https://doi.org/10.3390/ma9040264

53. Poon, C. S., Shui, Z. H., & Lam, L. (2004). Compressive behavior of fiber reinforced high-performance concrete subjected to elevated temperatures. Cement and Concrete Research, 34(12), 2215–2222. https://doi.org/10.1016/j.cemconres.2004.02.011

54. Ragavendra, S., Reddy, I. P., & Dongre, A. (2017). Fibre Reinforced Concrete- A Case Study. 33rd National Convention of Architectural Engineers and National Seminar on “Architectural Engineering Aspect for Sustainable Building Envelopes” ArchEn-BuildEn-2017, Hyderabad, India, (December), 1–16.

55. Rajasekhar, K. (2017). Stress Strain Behaviour of Confined Normal Grade Concrete, 5(3), 84–89.

56. Rana A (2013). Some studies on steel fiber reinforced concrete. International Journal of Emerging Technology and Advanced Engineering, 3(1): 120-127.

57. Resplendino, J. and Toulemonde, F., Designing and Building with UHPFRC. John Wiley & Sons, 2013

58. S. Biondi, and E. Candigliota, “In situ tests for seismic assessment of R.C. structures,” in: Proc. of the 14th World Conf. on Earthquake Engineering (Oct. 12–17, 2008, Beijing) (2008).

59. Shetty, M. S. (2005). Concrete technology theory and practice. 6th ed. Chand and Company Limited, New Delhi.

60. Shi, X., Tan, T.-H., Tan, K.-H., & Guo, Z. (2002). Concrete Constitutive Relationships Under Different Stress-Temperature Paths. Journal of Structural Engineering, 128(12), 1511–1518. https://doi.org/10.1061/(asce)0733-9445(2002)128:12(1511)

61. Shirinabadi, R., & Moosavi, E. (2020). Evaluation of Compression Strength of Concrete Specimens via Experimental Results and Numerical Simulation. Strength of Materials, 52(1), 138–148. https://doi.org/10.1007/s11223-020-00159-w

62. Sohu S, Halid A, Nagapan S, Fattah A, Latif I, and Ullah K (2017). Causative factors of cost overrun in highway projects of Sindh province of Pakistan. In the IOP Conference Series: Materials Science and Engineering, IOP Publishing, Bandung, Indonesia, 271(1): 012036.

63. Sorelli LG, Meda A, and Plizzari GA (2006). Steel fiber concrete slabs on ground: A structural matter. ACI Structural Journal, 103(4): 551-558.
64. Vasudevan, R., S.K. Nigam, R. Velkennedy, A. R. Chandra Sekar and B. Sundarakannan, Proceedings of the International Conference on Sustainable Solid Waste Management (2007), Chennai, India, pp.105-111.
65. Wenjun Qu, Xiaoliang Zhang and Haiqun Huang, Journal of Composites for Construction, ASCE (2009), Vol. 13(5), pp. 350 –359, Oct. 2009.

Appendices

Annex I

Sr #	Type of concrete	Room Temperature Parameters					Additive Details		Parameters at Elevated Temperature									Parameters Obtained From Model								References
		w/c	f_c'* (Mpa)	A_F^*	E* (Mpa)	ε_{c1}*	Type of Additive	Additive Quantity	Max. temperature attained (^oC)	f_c' (Mpa)	A_F	E (Mpa)	ε_{c1}	f_c/f_c*	A_F/A_F*	E/E*	$\varepsilon_{c1}/\varepsilon_{c1*}$	f_{ct}/f_c	fcT	$\varepsilon_{c1}/\varepsilon_{c1*}$	$\varepsilon_{c1}T$	E/E*	ET	A_F/A_F*	A_FT	
1	Steel Fiber Reinforced	0.43	75	0.43	25015	0.004	Hooked End Steel Fibers	50 kg/m^3	200	62	0.44	20520	0.003	0.83	1.02	0.82	0.86	0.92	69.22	0.96	0.0033	0.82	20612	1.01	0.44	Colombo, M., Di Prisco, M., & Felicetti, R. (2010). Mechanical properties of steel fibre reinforced concrete exposed at high temperatures. Materials and Structures/Materiaux et Constructions, 43(4), 475–491. https://doi.org/10.1617/s11527-009-9504-0
2	Steel Fiber Reinforced	0.43	75	0.43	25015	0.004	Hooked End Steel Fibers	50 kg/m^3	400	59	0.52	16275	0.0035	0.78	1.19	0.65	1.00	0.70	52.73	1.66	0.0058	0.56	14108	1.09	0.47	Colombo, M., Di Prisco, M., & Felicetti, R. (2010). Mechanical properties of steel fibre reinforced concrete exposed at high temperatures. Materials and Structures/Materiaux et Constructions, 43(4), 475–491. https://doi.org/10.1617/s11527-009-9504-0
3	Steel Fiber Reinforced	0.43	75	0.43	25015	0.004	Hooked End Steel Fibers	50 kg/m^3	600	47	0.59	12332	0.004	0.63	1.37	0.49	1.14	0.48	36.23	2.36	0.0082	0.30	7605	1.17	0.51	Colombo, M., Di Prisco, M., & Felicetti, R. (2010). Mechanical properties of steel fibre reinforced concrete exposed at high temperatures. Materials and Structures/Materiaux et Constructions, 43(4), 475–491. https://doi.org/10.1617/s11527-009-9504-0
4	Plain Concrete	0.45	35	0.65	17300	0.003	-	-	100	36	0.56	21260	0.0025	1.03	0.85	1.23	1.00	1.03	35.99	0.61	0.0015	0.95	16504	0.97	0.64	Anupama Krishna, D., Priyadarsini, R. S., & Narayanan, S. (2019). Effect of elevated temperatures on the mechanical properties of concrete. Procedia Structural Integrity, 14, 384–394. https://doi.org/10.1016/j.prostr.2019.05.047
5	Plain Concrete	0.45	35	0.65	17300	0.003	-	-	200	41	0.74	26040	0.002	1.17	1.13	1.51	0.80	0.92	32.16	0.96	0.0024	0.82	14255	1.01	0.66	Anupama Krishna, D., Priyadarsini, R. S., & Narayanan, S. (2019). Effect of elevated temperatures on the mechanical properties of concrete. Procedia Structural Integrity, 14, 384–394. https://doi.org/10.1016/j.prostr.2019.05.047
6	Plain Concrete	0.45	35	0.65	17300	0.003	-	-	300	42	0.75	30440	0.003	1.20	1.15	1.76	1.20	0.81	28.32	1.31	0.0033	0.69	12006	1.05	0.69	Anupama Krishna, D., Priyadarsini, R. S., & Narayanan, S. (2019). Effect of elevated temperatures on the mechanical properties of concrete. Procedia Structural Integrity, 14, 384–394. https://doi.org/10.1016/j.prostr.2019.05.047
7	Plain Concrete	0.45	35	0.65	17300	0.003	-	-	400	38	0.71	29700	0.00275	1.10	1.08	1.72	1.10	0.70	24.49	1.66	0.0041	0.56	9757	1.09	0.71	Anupama Krishna, D., Priyadarsini, R. S., & Narayanan, S. (2019). Effect of elevated temperatures on the mechanical properties of concrete. Procedia Structural Integrity, 14, 384–394. https://doi.org/10.1016/j.prostr.2019.05.047
8	Plain Concrete	0.45	35	0.65	17300	0.003	-	-	500	30	0.82	16440	0.004	0.86	1.25	0.95	1.60	0.59	20.66	2.01	0.0050	0.43	7508	1.13	0.74	Anupama Krishna, D., Priyadarsini, R. S., & Narayanan, S. (2019). Effect of elevated temperatures on the mechanical properties of concrete. Procedia Structural Integrity, 14, 384–394. https://doi.org/10.1016/j.prostr.2019.05.047
9	Plain Concrete	0.45	35	0.65	17300	0.003	-	-	600	20	0.83	8490	0.0045	0.57	1.26	0.49	1.80	0.48	16.83	2.36	0.0059	0.30	5259	1.17	0.77	Anupama Krishna, D., Priyadarsini, R. S., & Narayanan, S. (2019). Effect of elevated temperatures on the mechanical properties of concrete. Procedia Structural Integrity, 14, 384–394. https://doi.org/10.1016/j.prostr.2019.05.047
10	Plain Concrete	0.45	35	0.65	17300	0.003	-	-	700	19	0.71	9640	0.0045	0.54	1.09	0.56	1.80	0.37	13.00	2.71	0.0068	0.17	3010	1.21	0.79	Anupama Krishna, D., Priyadarsini, R. S., & Narayanan, S. (2019). Effect of elevated temperatures on the mechanical properties of concrete. Procedia Structural Integrity, 14, 384–394. https://doi.org/10.1016/j.prostr.2019.05.047
11	Plain Concrete	0.45	35	0.65	17300	0.003	-	-	800	11	0.87	2160	0.0055	0.31	1.33	0.12	2.20	0.26	9.17	3.06	0.0076	0.04	761	1.25	0.82	Anupama Krishna, D., Priyadarsini, R. S., & Narayanan, S. (2019). Effect of elevated temperatures on the mechanical properties of concrete. Procedia Structural Integrity, 14, 384–394. https://doi.org/10.1016/j.prostr.2019.05.047
12	Plain Concrete	-	40	0.67	33040	0.002	-	-	203	37	0.68	22600	0.0025	0.93	1.01	0.68	1.25	0.92	36.41	0.97	0.0019	0.82	27096	1.01	0.68	Bastami, M., Aslani, F., & Omran, M. E. (2010). High-temperature mechanical properties of concrete. International Journal of Civil Engineering, 8(4), 337–351.
13	Plain Concrete	-	40	0.68	31500	0.002	-	-	103	38	0.72	25120	0.00225	0.96	1.07	0.80	1.13	1.03	41.18	0.62	0.0012	0.95	29928	0.97	0.66	Chang, Y. F., Chen, Y. H., Sheu, M. S., & Yao, G. C. (2006). Residual stress-strain relationship for concrete after exposure to high temperatures. *Cement and Concrete Research* , *36* (10), 1999–2005. https://doi.org/10.1016/j.cemconres.2006.05.029
14	Plain Concrete	-	40	0.68	31500	0.002	-	-	203	37	0.67	24800	0.0025	0.92	0.99	0.79	1.25	0.92	36.78	0.97	0.0019	0.82	25833	1.01	0.69	Chang, Y. F., Chen, Y. H., Sheu, M. S., & Yao, G. C. (2006). Residual stress-strain relationship for concrete after exposure to high temperatures. *Cement and Concrete Research* , *36* (10), 1999–2005. https://doi.org/10.1016/j.cemconres.2006.05.029
15	Plain Concrete	-	40	0.68	31500	0.002	-	-	308	31	0.70	14360	0.0025	0.77	1.03	0.46	1.25	0.80	32.16	1.33	0.0027	0.68	21533	1.05	0.72	Chang, Y. F., Chen, Y. H., Sheu, M. S., & Yao, G. C. (2006). Residual stress-strain relationship for concrete after exposure to high temperatures. *Cement and Concrete Research* , *36* (10), 1999–2005. https://doi.org/10.1016/j.cemconres.2006.05.029
16	Plain Concrete	-	40	0.68	31500	0.002	-	-	406	27	0.64	10100	0.003	0.67	0.95	0.32	1.50	0.70	27.85	1.68	0.0034	0.56	17520	1.09	0.74	Chang, Y. F., Chen, Y. H., Sheu, M. S., & Yao, G. C. (2006). Residual stress-strain relationship for concrete after exposure to high temperatures. *Cement and Concrete Research* , *36* (10), 1999–2005. https://doi.org/10.1016/j.cemconres.2006.05.029

Sr #	Type of concrete	Room Temperature Parameters					Additive Details		Parameters at Elevated Temperature									Parameters Obtained From Model								References
		w/c	f_c'* (Mpa)	A_F^*	E* (Mpa)	ε_{c1}*	Type of Additive	Additive Quantity	Max. temperature attained (°C)	f_c' (Mpa)	A_F	E (Mpa)	ε_{c1}	f_c/f_c*	A_F/A_F*	E/E*	$\varepsilon_{c1}/\varepsilon_{c1*}$	f_{ct}/f_c	fcT	$\varepsilon_{c1}/\varepsilon_{c1*}$	ε_{c1}T	E/E*	ET	A_F/A_F*	A_FT	
17	Plain Concrete	-	40	0.68	31500	0.002	-	-	503	20	0.91	5960	0.004	0.50	1.34	0.19	2.00	0.59	23.58	2.02	0.0040	0.43	13548	1.13	0.77	Chang, Y. F., Chen, Y. H., Sheu, M. S., & Yao, G. C. (2006). Residual stress-strain relationship for concrete after exposure to high temperatures. *Cement and Concrete Research* , *36* (10), 1999–2005. https://doi.org/10.1016/j.cemconres.2006.05.029
18	Plain Concrete	-	40	0.68	31500	0.002	-	-	603	16	0.94	1640	0.007	0.39	1.38	0.05	3.50	0.48	19.19	2.37	0.0047	0.30	9453	1.17	0.80	Chang, Y. F., Chen, Y. H., Sheu, M. S., & Yao, G. C. (2006). Residual stress-strain relationship for concrete after exposure to high temperatures. *Cement and Concrete Research* , *36* (10), 1999–2005. https://doi.org/10.1016/j.cemconres.2006.05.029
19	Plain Concrete	-	40	0.68	31500	0.002	-	-	702	9	0.95	900	0.008	0.24	1.40	0.03	4.00	0.37	14.83	2.71	0.0054	0.17	5399	1.21	0.82	Chang, Y. F., Chen, Y. H., Sheu, M. S., & Yao, G. C. (2006). Residual stress-strain relationship for concrete after exposure to high temperatures. *Cement and Concrete Research* , *36* (10), 1999–2005. https://doi.org/10.1016/j.cemconres.2006.05.029
20	Plain Concrete	-	40	0.68	31500	0.002	-	-	796	7	0.97	740	0.009	0.18	1.42	0.02	4.50	0.27	10.70	3.04	0.0061	0.05	1550	1.25	0.85	Chang, Y. F., Chen, Y. H., Sheu, M. S., & Yao, G. C. (2006). Residual stress-strain relationship for concrete after exposure to high temperatures. *Cement and Concrete Research* , *36* (10), 1999–2005. https://doi.org/10.1016/j.cemconres.2006.05.029
21	High Strength Concrete	0.3	75	0.55	41024	0.002	-	-	600	34	0.81	6120	0.00625	0.46	1.48	0.15	2.86	0.48	36.35	2.36	0.0052	0.30	12471	1.17	0.64	Fu, Y. F., Wong, Y. L., Poon, C. S., & Tang, C. A. (2005). Stress-strain behaviour of high-strength concrete at elevated temperatures. Magazine of Concrete Research, 57(9), 535–544. https://doi.org/10.1680/macr.2005.57.9.535
22	MK Concrete	0.3	75	0.55	26240	0.004	-	-	600	35	0.86	3600	0.00875	0.46	1.57	0.14	2.41	0.48	36.38	2.36	0.0085	0.30	7977	1.17	0.64	Fu, Y. F., Wong, Y. L., Poon, C. S., & Tang, C. A. (2005). Stress-strain behaviour of high-strength concrete at elevated temperatures. Magazine of Concrete Research, 57(9), 535–544. https://doi.org/10.1680/macr.2005.57.9.535
23	PFA Concrete	0.3	76	0.55	24072	0.004	-	-	600	40	0.76	5744	0.00875	0.52	1.40	0.24	2.37	0.48	36.82	2.36	0.0087	0.30	7318	1.17	0.64	Fu, Y. F., Wong, Y. L., Poon, C. S., & Tang, C. A. (2005). Stress-strain behaviour of high-strength concrete at elevated temperatures. Magazine of Concrete Research, 57(9), 535–544. https://doi.org/10.1680/macr.2005.57.9.535
24	Normal Strength Concrete	0.3	35	0.55	14992	0.004	-	-	100	36	0.55	13824	0.00313	1.05	1.00	0.92	0.73	1.03	35.75	0.61	0.0026	0.95	14302	0.97	0.53	Fu, Y. F., Wong, Y. L., Poon, C. S., & Tang, C. A. (2005). Stress-strain behaviour of high-strength concrete at elevated temperatures. Magazine of Concrete Research, 57(9), 535–544. https://doi.org/10.1680/macr.2005.57.9.535
25	Normal Strength Concrete	0.3	35	0.55	14992	0.004	-	-	200	31	0.49	14560	0.0025	0.89	0.89	0.97	0.58	0.92	31.94	0.96	0.0041	0.82	12353	1.01	0.55	Fu, Y. F., Wong, Y. L., Poon, C. S., & Tang, C. A. (2005). Stress-strain behaviour of high-strength concrete at elevated temperatures. Magazine of Concrete Research, 57(9), 535–544. https://doi.org/10.1680/macr.2005.57.9.535
26	Normal Strength Concrete	0.3	35	0.55	14992	0.004	-	-	400	27	0.66	6832	0.005	0.78	1.21	0.46	1.16	0.70	24.33	1.66	0.0071	0.56	8455	1.09	0.59	Fu, Y. F., Wong, Y. L., Poon, C. S., & Tang, C. A. (2005). Stress-strain behaviour of high-strength concrete at elevated temperatures. Magazine of Concrete Research, 57(9), 535–544. https://doi.org/10.1680/macr.2005.57.9.535
27	Normal Strength Concrete	0.3	35	0.55	14992	0.004	-	-	600	17	0.73	5200	0.00625	0.50	1.34	0.35	1.43	0.48	16.72	2.36	0.0103	0.30	4558	1.17	0.64	Fu, Y. F., Wong, Y. L., Poon, C. S., & Tang, C. A. (2005). Stress-strain behaviour of high-strength concrete at elevated temperatures. Magazine of Concrete Research, 57(9), 535–544. https://doi.org/10.1680/macr.2005.57.9.535
28	Normal Strength Concrete-R	0.51	53	0.82	40800	0.002	-	-	200	42	0.87	19808	0.00203	0.79	1.06	0.49	0.92	0.92	49.30	0.96	0.0021	0.82	33619	1.01	0.83	Nematzadeh, M., & Mousavimehr, M. (2019). Residual Compressive Stress–Strain Relationship for Hybrid Recycled PET–Crumb Rubber Aggregate Concrete after Exposure to Elevated Temperatures. Journal of Materials in Civil Engineering, 31(8), 04019136. https://doi.org/10.1061/(asce)mt.1943-5533.0002749
29	Normal Strength Concrete-R	0.51	53	0.82	40800	0.002	-	-	400	34	0.86	17840	0.0033	0.64	1.05	0.44	1.50	0.70	37.55	1.66	0.0036	0.56	23011	1.09	0.89	Nematzadeh, M., & Mousavimehr, M. (2019). Residual Compressive Stress–Strain Relationship for Hybrid Recycled PET–Crumb Rubber Aggregate Concrete after Exposure to Elevated Temperatures. Journal of Materials in Civil Engineering, 31(8), 04019136. https://doi.org/10.1061/(asce)mt.1943-5533.0002749
30	Normal Strength Concrete-R	0.51	53	0.82	40800	0.002	-	-	600	21	0.92	8112	0.00536	0.39	1.12	0.20	2.44	0.48	25.80	2.36	0.0052	0.30	12403	1.17	0.96	Nematzadeh, M., & Mousavimehr, M. (2019). Residual Compressive Stress–Strain Relationship for Hybrid Recycled PET–Crumb Rubber Aggregate Concrete after Exposure to Elevated Temperatures. Journal of Materials in Civil Engineering, 31(8), 04019136. https://doi.org/10.1061/(asce)mt.1943-5533.0002749
31	Normal Strength Concrete-R	0.51	53	0.82	40800	0.002	-	-	800	13	0.93	7344	0.00548	0.25	1.14	0.18	2.49	0.26	14.05	3.06	0.0067	0.04	1795	1.25	1.03	Nematzadeh, M., & Mousavimehr, M. (2019). Residual Compressive Stress–Strain Relationship for Hybrid Recycled PET–Crumb Rubber Aggregate Concrete after Exposure to Elevated Temperatures. Journal of Materials in Civil Engineering, 31(8), 04019136. https://doi.org/10.1061/(asce)mt.1943-5533.0002749

Sr #	Type of concrete	Room Temperature Parameters					Additive Details		Parameters at Elevated Temperature									Parameters Obtained From Model								References
		w/c	f_c'* (Mpa)	A_F^*	E* (Mpa)	ε_{c1}*	Type of Additive	Additive Quantity	Max. temperature attained (°C)	f_c' (Mpa)	A_F	E (Mpa)	ε_{c1}	f_c/f_c*	A_F/A_F*	E/E*	$\varepsilon_{c1}/\varepsilon_{c1*}$	f_{ct}/f_c	fcT	$\varepsilon_{c1}/\varepsilon_{c1*}$	ε_{c1}T	E/E*	ET	A_F/A_F*	A_FT	
32	Normal Strength Concrete-P15	0.51	35	0.76	32400	0.002	PET Flakes	55.4 Kg/m^3	200	27	0.80	28192	0.00199	0.77	1.05	0.87	1.06	0.92	31.94	0.96	0.0018	0.82	26698	1.01	0.77	Nematzadeh, M., & Mousavimehr, M. (2019). Residual Compressive Stress–Strain Relationship for Hybrid Recycled PET–Crumb Rubber Aggregate Concrete after Exposure to Elevated Temperatures. Journal of Materials in Civil Engineering, 31(8), 04019136. https://doi.org/10.1061/(asce)mt.1943-5533.0002749
33	Normal Strength Concrete-P15	0.51	35	0.76	32400	0.002	PET Flakes	55.4 Kg/m^3	400	22	0.85	12624	0.00334	0.63	1.11	0.39	1.79	0.70	24.33	1.66	0.0031	0.56	18274	1.09	0.83	Nematzadeh, M., & Mousavimehr, M. (2019). Residual Compressive Stress–Strain Relationship for Hybrid Recycled PET–Crumb Rubber Aggregate Concrete after Exposure to Elevated Temperatures. Journal of Materials in Civil Engineering, 31(8), 04019136. https://doi.org/10.1061/(asce)mt.1943-5533.0002749
34	Normal Strength Concrete-P15	0.51	35	0.76	32400	0.002	PET Flakes	55.4 Kg/m^3	600	13	0.92	4736	0.00537	0.38	1.20	0.15	2.87	0.48	16.72	2.36	0.0044	0.30	9850	1.17	0.89	Nematzadeh, M., & Mousavimehr, M. (2019). Residual Compressive Stress–Strain Relationship for Hybrid Recycled PET–Crumb Rubber Aggregate Concrete after Exposure to Elevated Temperatures. Journal of Materials in Civil Engineering, 31(8), 04019136. https://doi.org/10.1061/(asce)mt.1943-5533.0002749
35	Normal Strength Concrete-P15	0.51	35	0.76	32400	0.002	PET Flakes	55.4 Kg/m^3	800	9	0.92	3792	0.00586	0.25	1.20	0.12	3.13	0.26	9.11	3.06	0.0057	0.04	1426	1.25	0.96	Nematzadeh, M., & Mousavimehr, M. (2019). Residual Compressive Stress–Strain Relationship for Hybrid Recycled PET–Crumb Rubber Aggregate Concrete after Exposure to Elevated Temperatures. Journal of Materials in Civil Engineering, 31(8), 04019136. https://doi.org/10.1061/(asce)mt.1943-5533.0002749
36	Normal Strength Concrete-T15	0.51	33	0.75	33000	0.002	Crumb Rubber	39.4 Kg/m^3	200	26	0.78	28240	0.00195	0.78	1.04	0.86	0.98	0.92	30.65	0.96	0.0019	0.82	27192	1.01	0.76	Nematzadeh, M., & Mousavimehr, M. (2019). Residual Compressive Stress–Strain Relationship for Hybrid Recycled PET–Crumb Rubber Aggregate Concrete after Exposure to Elevated Temperatures. Journal of Materials in Civil Engineering, 31(8), 04019136. https://doi.org/10.1061/(asce)mt.1943-5533.0002749
37	Normal Strength Concrete-T15	0.51	33	0.75	33000	0.002	Crumb Rubber	39.4 Kg/m^3	400	22	0.81	15856	0.00255	0.67	1.08	0.48	1.28	0.70	23.35	1.66	0.0033	0.56	18612	1.09	0.82	Nematzadeh, M., & Mousavimehr, M. (2019). Residual Compressive Stress–Strain Relationship for Hybrid Recycled PET–Crumb Rubber Aggregate Concrete after Exposure to Elevated Temperatures. Journal of Materials in Civil Engineering, 31(8), 04019136. https://doi.org/10.1061/(asce)mt.1943-5533.0002749
38	Normal Strength Concrete-T15	0.51	33	0.75	33000	0.002	Crumb Rubber	39.4 Kg/m^3	600	10	0.89	3156.8	0.00438	0.30	1.18	0.10	2.19	0.48	16.04	2.36	0.0047	0.30	10032	1.17	0.88	Nematzadeh, M., & Mousavimehr, M. (2019). Residual Compressive Stress–Strain Relationship for Hybrid Recycled PET–Crumb Rubber Aggregate Concrete after Exposure to Elevated Temperatures. Journal of Materials in Civil Engineering, 31(8), 04019136. https://doi.org/10.1061/(asce)mt.1943-5533.0002749
39	Normal Strength Concrete-T15	0.51	33	0.75	33000	0.002	Crumb Rubber	39.4 Kg/m^3	800	7	0.93	2560	0.00563	0.20	1.23	0.08	2.82	0.26	8.74	3.06	0.0061	0.04	1452	1.25	0.94	Nematzadeh, M., & Mousavimehr, M. (2019). Residual Compressive Stress–Strain Relationship for Hybrid Recycled PET–Crumb Rubber Aggregate Concrete after Exposure to Elevated Temperatures. Journal of Materials in Civil Engineering, 31(8), 04019136. https://doi.org/10.1061/(asce)mt.1943-5533.0002749
40	Normal Strength Concrete-P7.5T7.5	0.51	31	0.82	31630	0.002	PET Flakes, Crumb Rubber	27.67 Kg/m^3 19.70 Kg/m^3	200	24	0.81	23648	0.0022	0.77	0.98	0.75	1.10	0.92	28.55	0.96	0.0019	0.82	26063	1.01	0.83	Nematzadeh, M., & Mousavimehr, M. (2019). Residual Compressive Stress–Strain Relationship for Hybrid Recycled PET–Crumb Rubber Aggregate Concrete after Exposure to Elevated Temperatures. Journal of Materials in Civil Engineering, 31(8), 04019136. https://doi.org/10.1061/(asce)mt.1943-5533.0002749
41	Normal Strength Concrete-P7.5T7.5	0.51	31	0.82	31630	0.002	PET Flakes, Crumb Rubber	27.67 Kg/m^3 19.70 Kg/m^3	400	22	0.72	12064	0.00242	0.70	0.87	0.38	1.21	0.70	21.75	1.66	0.0033	0.56	17839	1.09	0.90	Nematzadeh, M., & Mousavimehr, M. (2019). Residual Compressive Stress–Strain Relationship for Hybrid Recycled PET–Crumb Rubber Aggregate Concrete after Exposure to Elevated Temperatures. Journal of Materials in Civil Engineering, 31(8), 04019136. https://doi.org/10.1061/(asce)mt.1943-5533.0002749
42	Normal Strength Concrete-P7.5T7.5	0.51	31	0.82	31630	0.002	PET Flakes, Crumb Rubber	27.67 Kg/m^3 19.70 Kg/m^3	600	8	0.91	2736	0.004063	0.27	1.10	0.09	2.03	0.48	14.95	2.36	0.0047	0.30	9616	1.17	0.96	Nematzadeh, M., & Mousavimehr, M. (2019). Residual Compressive Stress–Strain Relationship for Hybrid Recycled PET–Crumb Rubber Aggregate Concrete after Exposure to Elevated Temperatures. Journal of Materials in Civil Engineering, 31(8), 04019136. https://doi.org/10.1061/(asce)mt.1943-5533.0002749

Sr #	Type of concrete	Room Temperature Parameters					Additive Details		Parameters at Elevated Temperature									Parameters Obtained From Model								References
		w/c	f_c'* (Mpa)	A_F*	E* (Mpa)	ε_{c1}*	Type of Additive	Additive Quantity	Max. temperature attained (°C)	f_c' (Mpa)	A_F	E (Mpa)	ε_{c1}	f_c/f_c*	A_F/A_F*	E/E*	$\varepsilon_{c1}/\varepsilon_{c1*}$	f_{ct}/f_c	fcT	$\varepsilon_{c1}/\varepsilon_{c1*}$	ε_{c1}T	E/E*	ET	A_F/A_F*	A_FT	
43	Normal Strength Concrete-P7.5T7.5	0.51	31	0.82	31630	0.002	PET Flakes, Crumb Rubber	27.67 Kg/m^3 19.70 Kg/m^3	800	6	0.87	1446.4	0.005625	0.18	1.06	0.05	2.81	0.26	8.14	3.06	0.0061	0.04	1392	1.25	1.03	Nematzadeh, M., & Mousavimehr, M. (2019). Residual Compressive Stress–Strain Relationship for Hybrid Recycled PET–Crumb Rubber Aggregate Concrete after Exposure to Elevated Temperatures. Journal of Materials in Civil Engineering, 31(8), 04019136. https://doi.org/10.1061/(asce)mt.1943-5533.0002749
44	Normal Strength Concrete	0.617	33	0.87	22440	0.002	-	-	200	31	0.90	19440	0.00269	0.95	1.04	0.87	1.10	0.92	30.10	0.96	0.0023	0.82	18491	1.01	0.88	Shi, X., Tan, T.-H., Tan, K.-H., & Guo, Z. (2002). Concrete Constitutive Relationships Under Different Stress-Temperature Paths. Journal of Structural Engineering, 128(12), 1511–1518. https://doi.org/10.1061/(asce)0733-9445(2002)128:12(1511)
45	Normal Strength Concrete	0.617	33	0.87	22440	0.002	-	-	300	29	0.94	11440	0.00295	0.88	1.08	0.51	1.20	0.81	26.51	1.31	0.0032	0.69	15573	1.05	0.92	Shi, X., Tan, T.-H., Tan, K.-H., & Guo, Z. (2002). Concrete Constitutive Relationships Under Different Stress-Temperature Paths. Journal of Structural Engineering, 128(12), 1511–1518. https://doi.org/10.1061/(asce)0733-9445(2002)128:12(1511)
46	Normal Strength Concrete	0.617	33	0.87	22440	0.002	-	-	350	28	0.95	9700	0.00382	0.86	1.08	0.43	1.56	0.76	24.72	1.48	0.0036	0.63	14115	1.07	0.93	Shi, X., Tan, T.-H., Tan, K.-H., & Guo, Z. (2002). Concrete Constitutive Relationships Under Different Stress-Temperature Paths. Journal of Structural Engineering, 128(12), 1511–1518. https://doi.org/10.1061/(asce)0733-9445(2002)128:12(1511)
47	Normal Strength Concrete	0.617	33	0.87	22440	0.002	-	-	400	22	0.94	6600	0.00503	0.66	1.08	0.29	2.05	0.70	22.92	1.66	0.0041	0.56	12656	1.09	0.95	Shi, X., Tan, T.-H., Tan, K.-H., & Guo, Z. (2002). Concrete Constitutive Relationships Under Different Stress-Temperature Paths. Journal of Structural Engineering, 128(12), 1511–1518. https://doi.org/10.1061/(asce)0733-9445(2002)128:12(1511)
48	Normal Strength Concrete	0.617	33	0.87	22440	0.002	-	-	500	19	0.95	5452	0.00538	0.59	1.09	0.24	2.20	0.59	19.34	2.01	0.0049	0.43	9739	1.13	0.99	Shi, X., Tan, T.-H., Tan, K.-H., & Guo, Z. (2002). Concrete Constitutive Relationships Under Different Stress-Temperature Paths. Journal of Structural Engineering, 128(12), 1511–1518. https://doi.org/10.1061/(asce)0733-9445(2002)128:12(1511)
49	Normal Strength Concrete	0.617	33	0.87	22440	0.002	-	-	600	18	0.94	3526	0.00667	0.55	1.08	0.16	2.72	0.48	15.75	2.36	0.0058	0.30	6822	1.17	1.02	Shi, X., Tan, T.-H., Tan, K.-H., & Guo, Z. (2002). Concrete Constitutive Relationships Under Different Stress-Temperature Paths. Journal of Structural Engineering, 128(12), 1511–1518. https://doi.org/10.1061/(asce)0733-9445(2002)128:12(1511)
50	Normal Strength Concrete	0.617	33	0.87	22440	0.002	-	-	700	10	0.93	1692	0.00851	0.32	1.07	0.08	3.47	0.37	12.17	2.71	0.0066	0.17	3905	1.21	1.06	Shi, X., Tan, T.-H., Tan, K.-H., & Guo, Z. (2002). Concrete Constitutive Relationships Under Different Stress-Temperature Paths. Journal of Structural Engineering, 128(12), 1511–1518. https://doi.org/10.1061/(asce)0733-9445(2002)128:12(1511)
51	Normal Strength Concrete	0.617	33	0.87	22440	0.002	-	-	800	3	0.93	650	0.0115	0.10	1.07	0.03	4.69	0.26	8.58	3.06	0.0075	0.04	987	1.25	1.09	Shi, X., Tan, T.-H., Tan, K.-H., & Guo, Z. (2002). Concrete Constitutive Relationships Under Different Stress-Temperature Paths. Journal of Structural Engineering, 128(12), 1511–1518. https://doi.org/10.1061/(asce)0733-9445(2002)128:12(1511)
52	Normal Strength Concrete-M0	0.7	26	0.74	22680	0.003	-	-	150	20	0.58	18240	0.002	0.77	0.78	0.80	0.80	0.98	25.15	0.78	0.0020	0.89	20163	0.99	0.73	Lo Monte, F., Bamonte, P., & Gambarova, P. G. (2015). Physical and mechanical properties of heat-Damaged structural concrete containing expanded polystyrene syntherized particles. Fire and Materials, 39(1), 58–71. https://doi.org/10.1002/fam.2230
53	Normal Strength Concrete-M0	0.7	26	0.74	22680	0.003	-	-	300	19	0.63	9600	0.0035	0.76	0.85	0.42	1.40	0.81	20.91	1.31	0.0033	0.69	15740	1.05	0.78	Lo Monte, F., Bamonte, P., & Gambarova, P. G. (2015). Physical and mechanical properties of heat-Damaged structural concrete containing expanded polystyrene syntherized particles. Fire and Materials, 39(1), 58–71. https://doi.org/10.1002/fam.2230
54	Normal Strength Concrete-M0	0.7	26	0.74	22680	0.003	-	-	500	11	0.84	2404.4	0.0055	0.43	1.13	0.11	2.20	0.59	15.25	2.01	0.0050	0.43	9843	1.13	0.84	Lo Monte, F., Bamonte, P., & Gambarova, P. G. (2015). Physical and mechanical properties of heat-Damaged structural concrete containing expanded polystyrene syntherized particles. Fire and Materials, 39(1), 58–71. https://doi.org/10.1002/fam.2230
55	Normal Strength Concrete-M0	0.7	26	0.74	22680	0.003	-	-	700	6	0.88	1072	0.008	0.23	1.19	0.05	3.20	0.37	9.59	2.71	0.0068	0.17	3946	1.21	0.90	Lo Monte, F., Bamonte, P., & Gambarova, P. G. (2015). Physical and mechanical properties of heat-Damaged structural concrete containing expanded polystyrene syntherized particles. Fire and Materials, 39(1), 58–71. https://doi.org/10.1002/fam.2230
56	Ordinary Portland Concrete, PC-0	0.29	69	0.61	23456	0.004	-	-	600	33	0.84	4864	0.00838	0.47	1.39	0.21	2.24	0.48	33.39	2.36	0.0088	0.30	7131	1.17	0.71	Poon, C. S., Shui, Z. H., & Lam, L. (2004). Compressive behavior of fiber reinforced high-performance concrete subjected to elevated temperatures. Cement and Concrete Research, 34(12), 2215–2222. https://doi.org/10.1016/j.cemconres.2004.02.011
57	Ordinary Portland Concrete, PC-0	0.29	69	0.61	23456	0.004	-	-	800	18	0.86	3184	0.00931	0.26	1.42	0.14	2.49	0.26	18.19	3.06	0.0114	0.04	1032	1.25	0.76	Poon, C. S., Shui, Z. H., & Lam, L. (2004). Compressive behavior of fiber reinforced high-performance concrete subjected to elevated temperatures. Cement and Concrete Research, 34(12), 2215–2222. https://doi.org/10.1016/j.cemconres.2004.02.011
58	Ordinary Portland Concrete w/ metakaolin,MK-0	0.36	86	0.61	22160	0.004	-	-	600	33	0.82	5184	0.00832	0.39	1.35	0.23	2.10	0.48	41.60	2.36	0.0094	0.30	6737	1.17	0.71	Poon, C. S., Shui, Z. H., & Lam, L. (2004). Compressive behavior of fiber reinforced high-performance concrete subjected to elevated temperatures. Cement and Concrete Research, 34(12), 2215–2222. https://doi.org/10.1016/j.cemconres.2004.02.011

Sr #	Type of concrete	Room Temperature Parameters					Additive Details		Parameters at Elevated Temperature									Parameters Obtained From Model								References
		w/c	f_c'* (Mpa)	A_F^*	E* (Mpa)	ε_{c1}*	Type of Additive	Additive Quantity	Max. temperature attained (^oC)	f_c' (Mpa)	A_F	E (Mpa)	ε_{c1}	f_c/f_c*	A_F/A_F*	E/E*	$\varepsilon_{c1}/\varepsilon_{c1^*}$	f_{ct}/f_c	fcT	$\varepsilon_{c1}/\varepsilon_{c1^*}$	ε_{c1}T	E/E*	ET	A_F/A_F*	A_FT	
59	Ordinary Portland Concrete w/ metakaolin,MK-0	0.36	86	0.61	22160	0.004	-	-	800	16	0.87	2688	0.01049	0.18	1.43	0.12	2.64	0.26	22.66	3.06	0.0121	0.04	975	1.25	0.76	Poon, C. S., Shui, Z. H., & Lam, L. (2004). Compressive behavior of fiber reinforced high-performance concrete subjected to elevated temperatures. Cement and Concrete Research, 34(12), 2215–2222. https://doi.org/10.1016/j.cemconres.2004.02.011
60	Ordinary Portland Concrete w/ silicafume, SF-0	0.32	83	0.60	21664	0.004	-	-	600	38	0.81	5048	0.00825	0.46	1.34	0.23	2.13	0.48	40.01	2.36	0.0091	0.30	6586	1.17	0.70	Poon, C. S., Shui, Z. H., & Lam, L. (2004). Compressive behavior of fiber reinforced high-performance concrete subjected to elevated temperatures. Cement and Concrete Research, 34(12), 2215–2222. https://doi.org/10.1016/j.cemconres.2004.02.011
61	Ordinary Portland Concrete w/ silicafume, SF-0	0.32	83	0.60	21664	0.004	-	-	800	21	0.80	4960	0.01	0.25	1.33	0.23	2.58	0.26	21.79	3.06	0.0119	0.04	953	1.25	0.75	Poon, C. S., Shui, Z. H., & Lam, L. (2004). Compressive behavior of fiber reinforced high-performance concrete subjected to elevated temperatures. Cement and Concrete Research, 34(12), 2215–2222. https://doi.org/10.1016/j.cemconres.2004.02.011
62	Ordinary Portland Concrete w/ steel fibers, OPC-1	0.29	71	0.89	19542.4	0.004	Steel Fibers	1%	600	39	0.90	5920	0.01049	0.55	1.02	0.30	2.56	0.48	34.50	2.36	0.0097	0.30	5941	1.17	1.04	Poon, C. S., Shui, Z. H., & Lam, L. (2004). Compressive behavior of fiber reinforced high-performance concrete subjected to elevated temperatures. Cement and Concrete Research, 34(12), 2215–2222. https://doi.org/10.1016/j.cemconres.2004.02.011
63	Ordinary Portland Concrete w/ steel fibers, OPC-1	0.29	71	0.89	19542.4	0.004	Steel Fibers	1%	800	24	0.86	4240	0.01234	0.33	0.98	0.22	3.01	0.26	18.79	3.06	0.0125	0.04	860	1.25	1.11	Poon, C. S., Shui, Z. H., & Lam, L. (2004). Compressive behavior of fiber reinforced high-performance concrete subjected to elevated temperatures. Cement and Concrete Research, 34(12), 2215–2222. https://doi.org/10.1016/j.cemconres.2004.02.011
64	Ordinary Portland Concrete w/ metakaolin & steel fibers,MK-1	0.36	88	0.84	23280	0.004	Steel Fibers	1%	600	39	0.90	4456	0.01027	0.44	1.07	0.19	2.45	0.48	42.28	2.36	0.0099	0.30	7077	1.17	0.98	Poon, C. S., Shui, Z. H., & Lam, L. (2004). Compressive behavior of fiber reinforced high-performance concrete subjected to elevated temperatures. Cement and Concrete Research, 34(12), 2215–2222. https://doi.org/10.1016/j.cemconres.2004.02.011
65	Ordinary Portland Concrete w/ metakaolin & steel fibers,MK-1	0.36	88	0.84	23280	0.004	Steel Fibers	1%	800	21	0.92	3520	0.01334	0.24	1.10	0.15	3.18	0.26	23.03	3.06	0.0128	0.04	1024	1.25	1.05	Poon, C. S., Shui, Z. H., & Lam, L. (2004). Compressive behavior of fiber reinforced high-performance concrete subjected to elevated temperatures. Cement and Concrete Research, 34(12), 2215–2222. https://doi.org/10.1016/j.cemconres.2004.02.011
66	Ordinary Portland Concrete w/ silicafume & steel fibers,SF-1	0.32	84	0.81	23152	0.004	Steel Fibers	1%	600	39	0.87	5558.4	0.00838	0.47	1.08	0.24	2.15	0.48	40.44	2.36	0.0092	0.30	7038	1.17	0.94	Poon, C. S., Shui, Z. H., & Lam, L. (2004). Compressive behavior of fiber reinforced high-performance concrete subjected to elevated temperatures. Cement and Concrete Research, 34(12), 2215–2222. https://doi.org/10.1016/j.cemconres.2004.02.011
67	Ordinary Portland Concrete w/ silicafume & steel fibers,SF-1	0.32	84	0.81	23152	0.004	Steel Fibers	1%	800	23	0.90	3955.2	0.0117	0.28	1.11	0.17	3.00	0.26	22.03	3.06	0.0119	0.04	1019	1.25	1.01	Poon, C. S., Shui, Z. H., & Lam, L. (2004). Compressive behavior of fiber reinforced high-performance concrete subjected to elevated temperatures. Cement and Concrete Research, 34(12), 2215–2222. https://doi.org/10.1016/j.cemconres.2004.02.011

Annex II

Post-peak analysis of experimental data by (Colombo et al., 2010)

Room Temperature

Properties		
E_c	25015.33	Mpa
f_c'	74.98	Mpa
ε_{c1}	0.0035	
H	150	mm

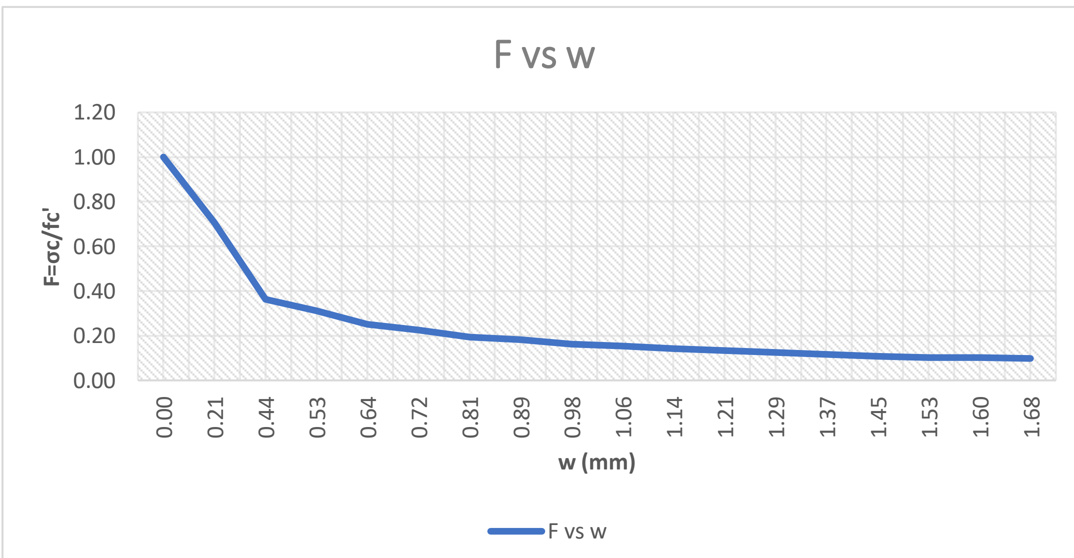

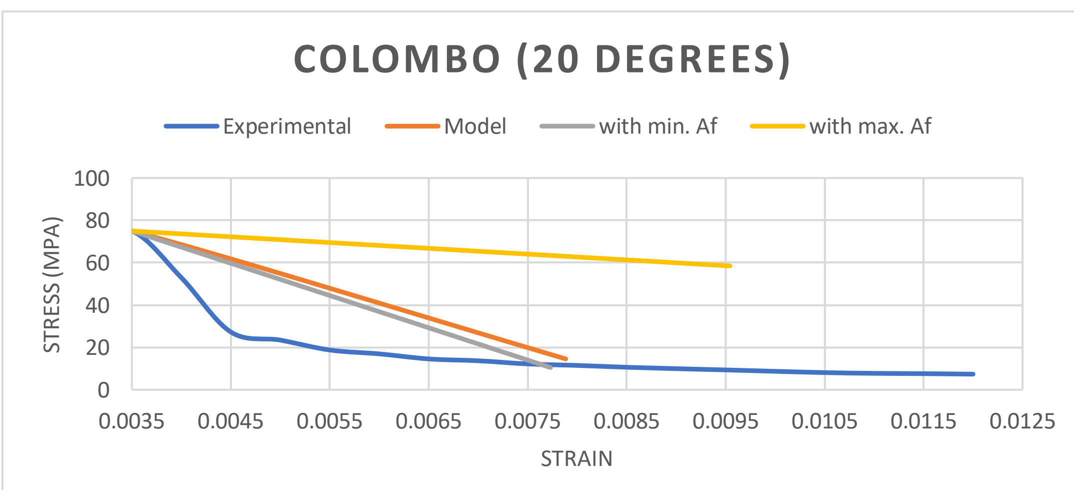

200°C

Properties		
E_c	20520	Mpa
f_c'	61.99	Mpa
ε_{c1}	0.003	
H	150	mm

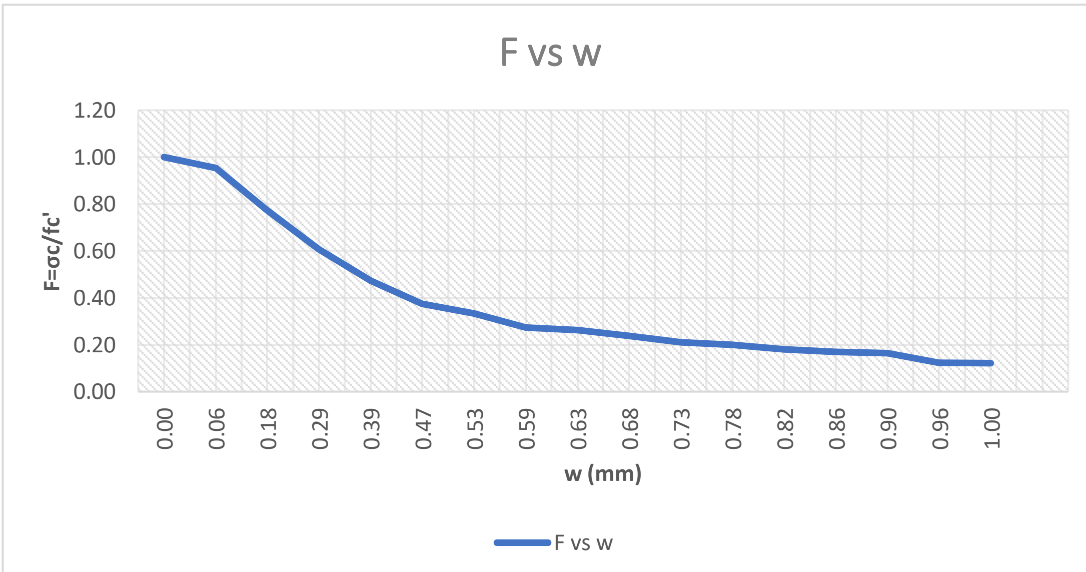

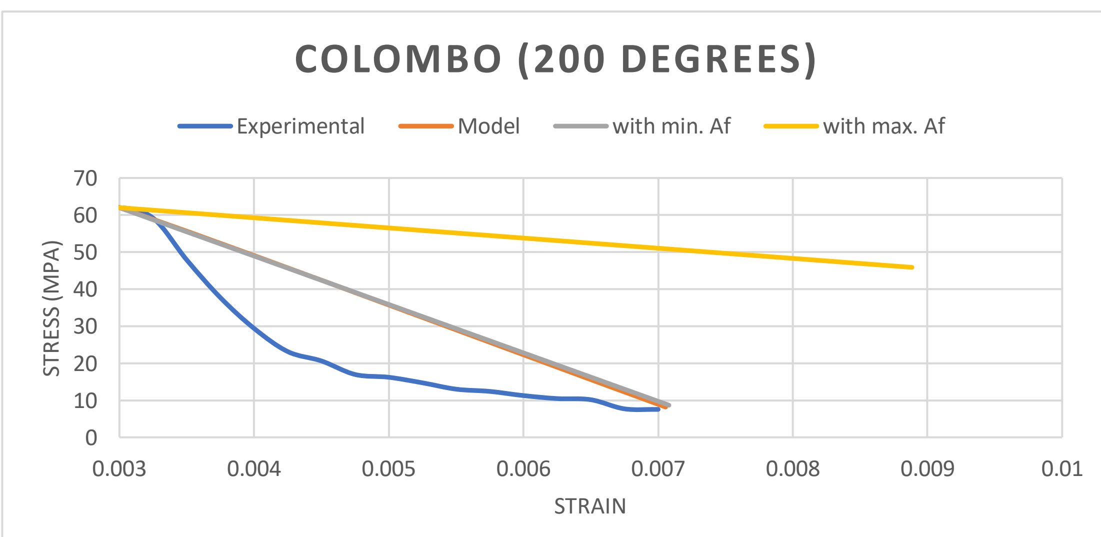

400°C

Properties		
E_c	16275	Mpa
f_c'	58.67	Mpa
ε_{c1}	0.0035	
H	150	mm

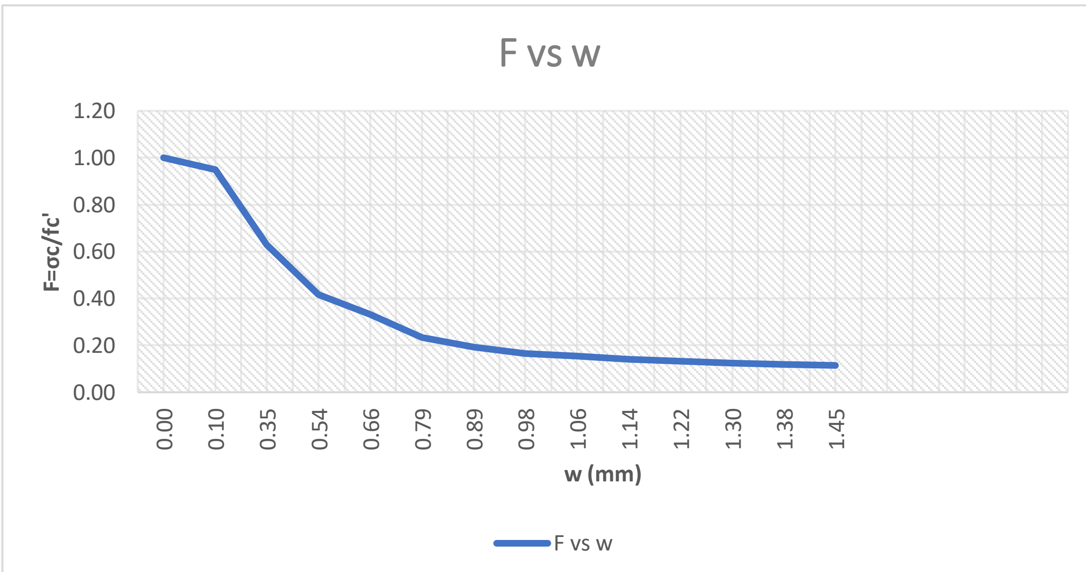

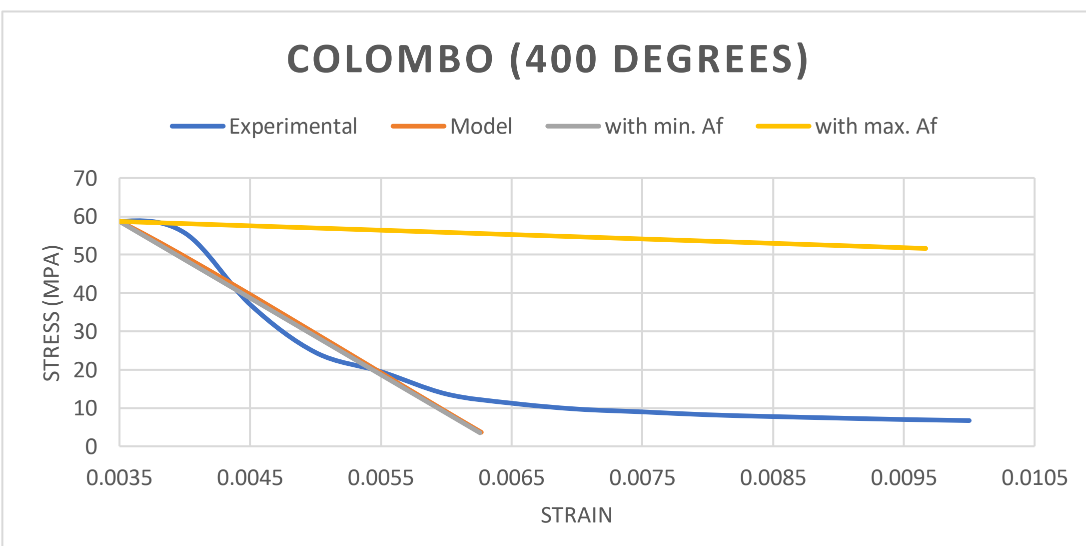

600ºC

Properties		
E_c	12331.8	Mpa
f_c'	46.92	Mpa
ε_{c1}	0.004	
H	150	mm

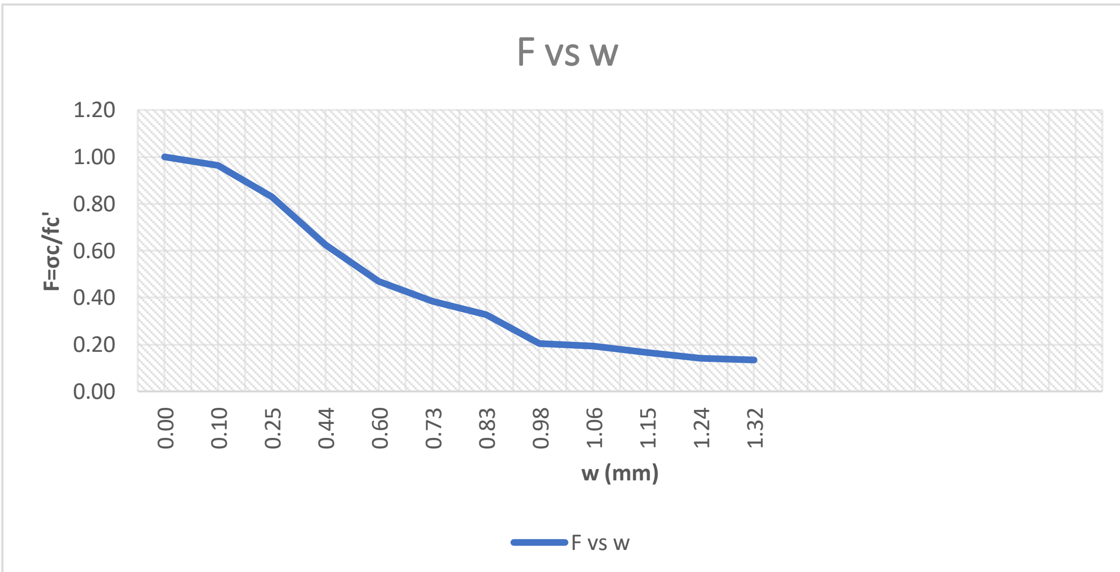

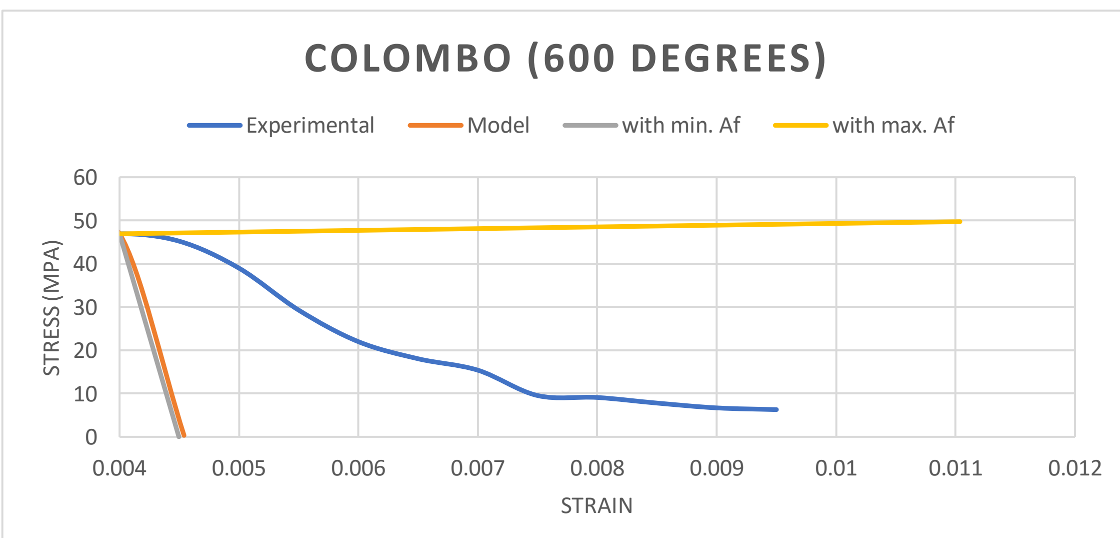

Post-peak analysis of experimental data by (Anumapa et al., 2019)

Room Temperature

Properties		
E_c	17300	Mpa
f_c'	34.83	Mpa
ε_{c1}	0.0025	
H	300	mm

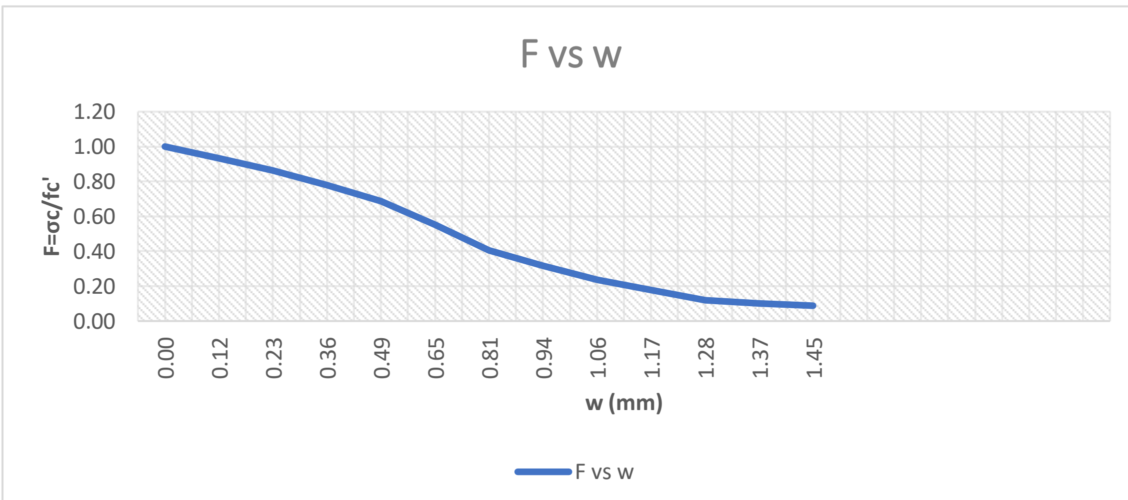

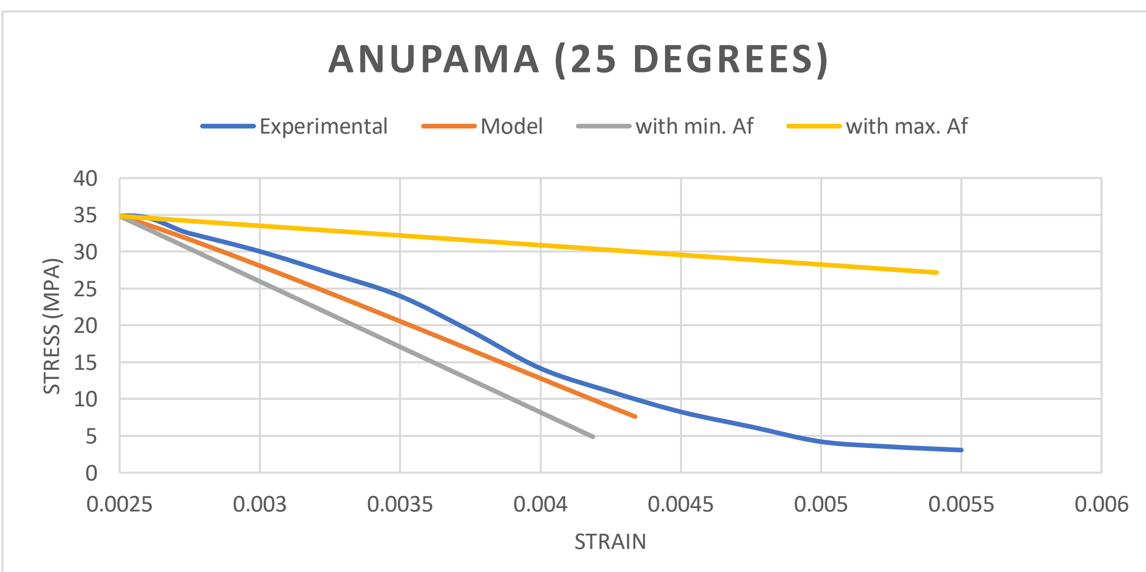

100°C

Properties		
E_c	21260	Mpa
f_c'	35.78	Mpa
ε_{c1}	0.0025	
H	300	mm

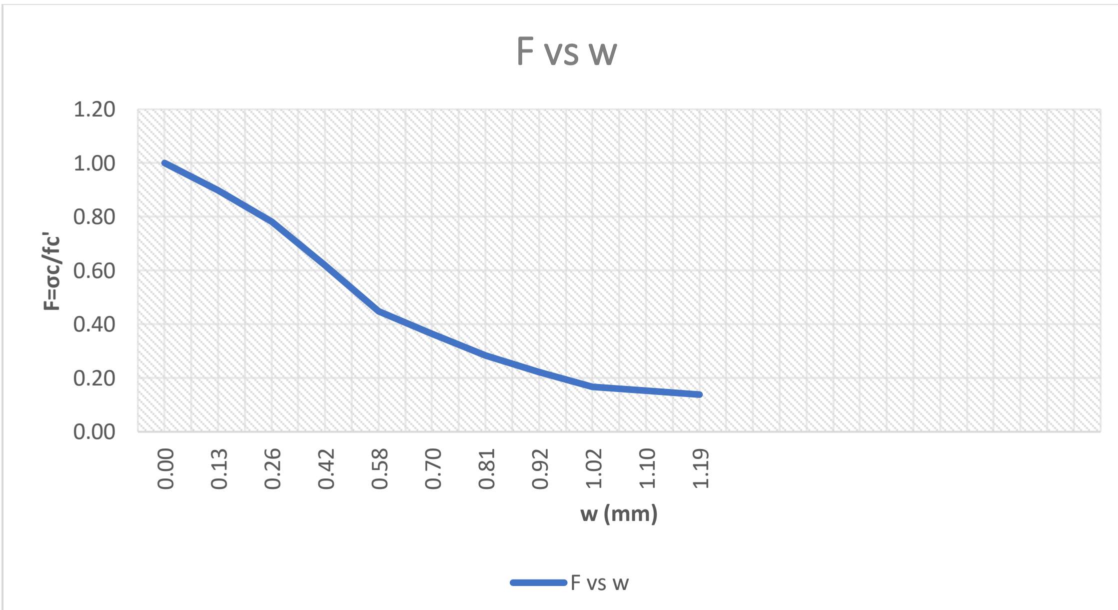

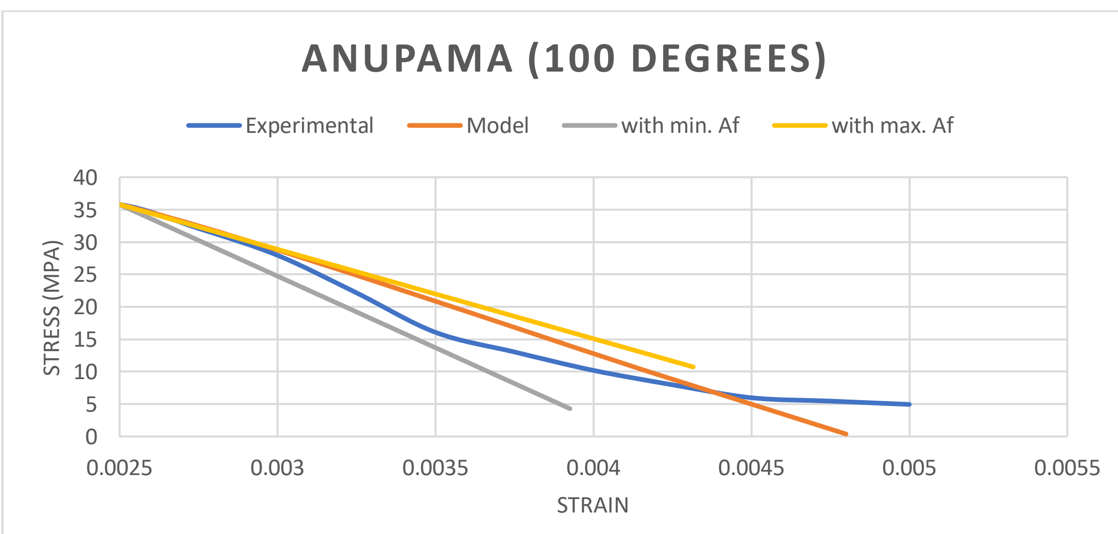

200ºC

Properties		
E_c	26040	Mpa
f_c'	40.72	Mpa
ε_{c1}	0.002	
H	300	mm

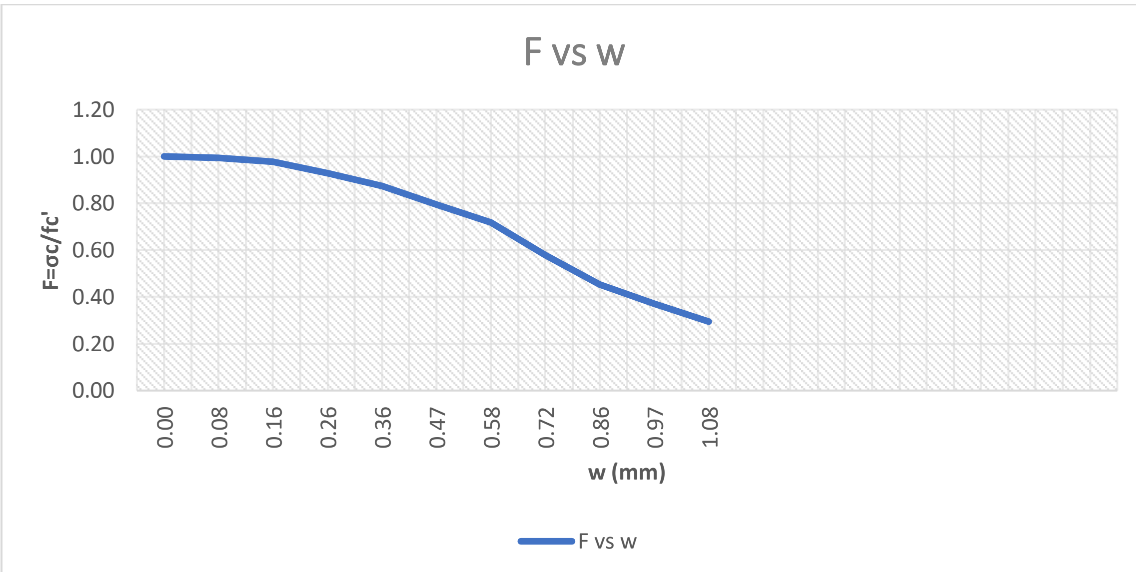

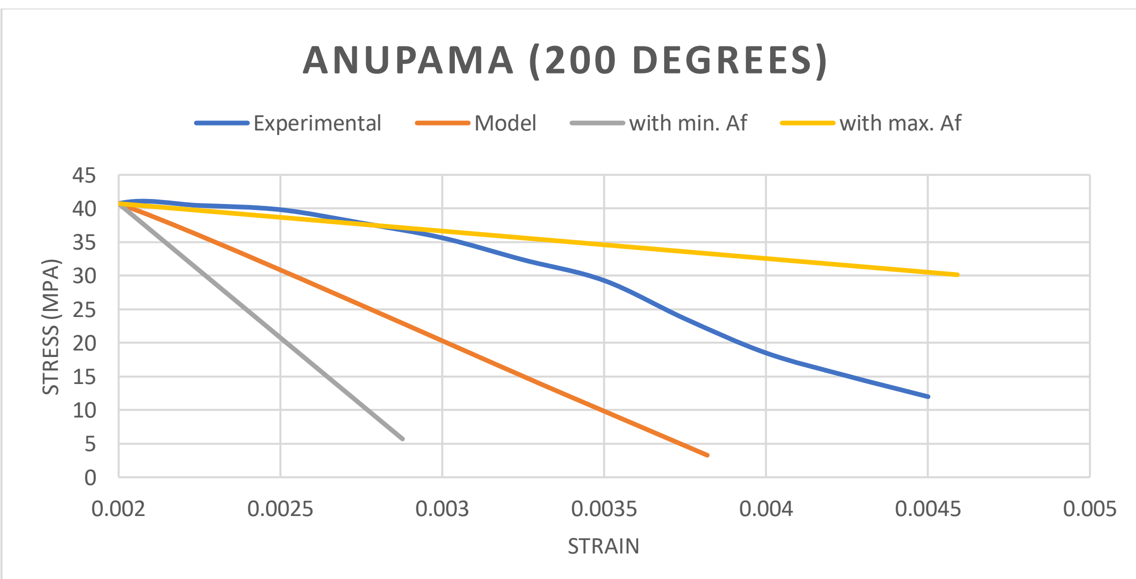

300°C

Properties		
Slope/E_c	30440	Mpa
f_c'	41.78	Mpa
ε_{c1}	0.003	
H	300	mm

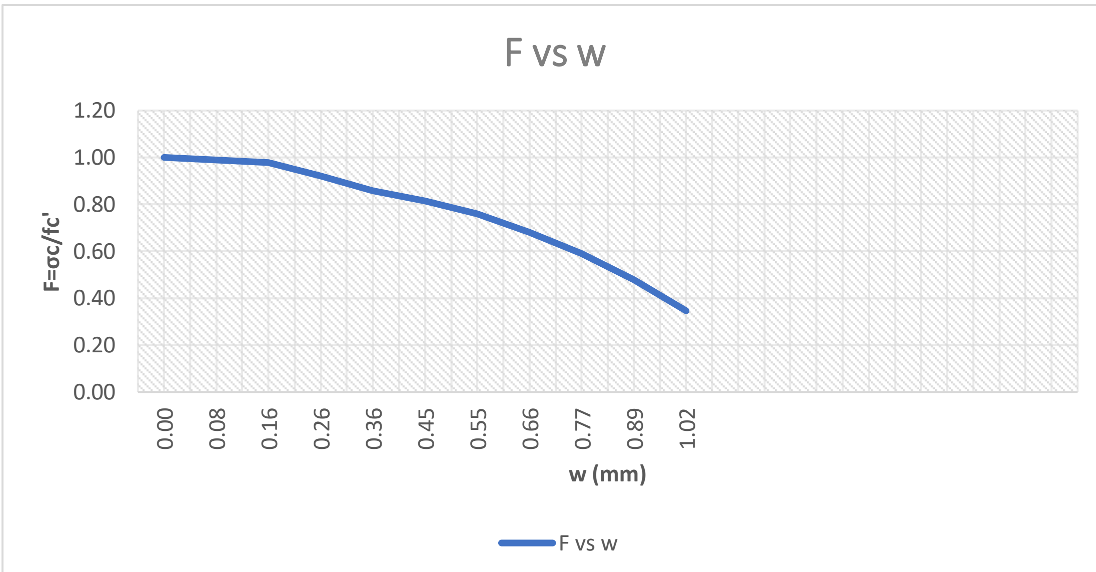

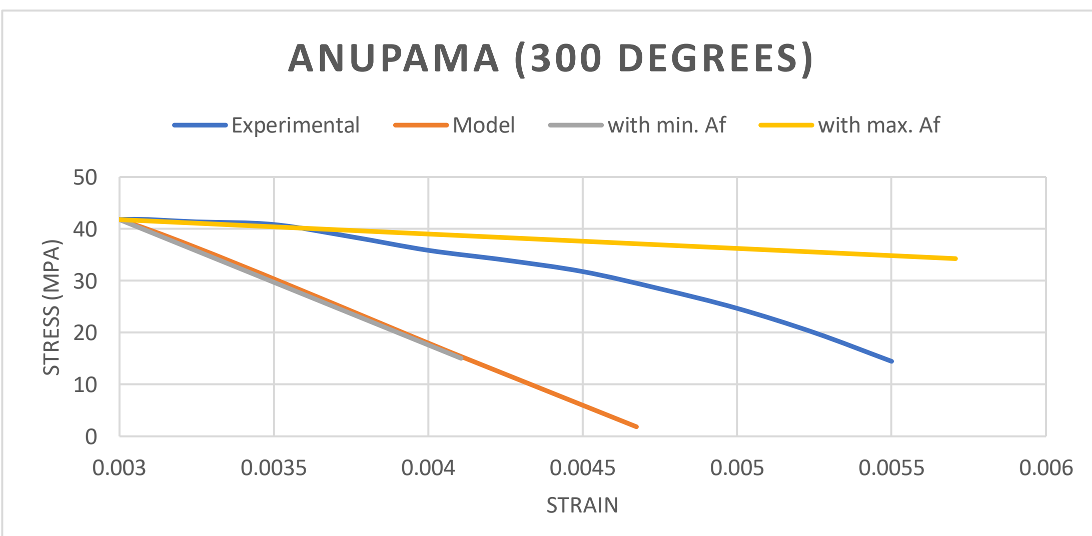

400°C

Properties		
E_c	29700	Mpa
f_c'	38.43	Mpa
ε_{c1}	0.00275	
H	300	mm

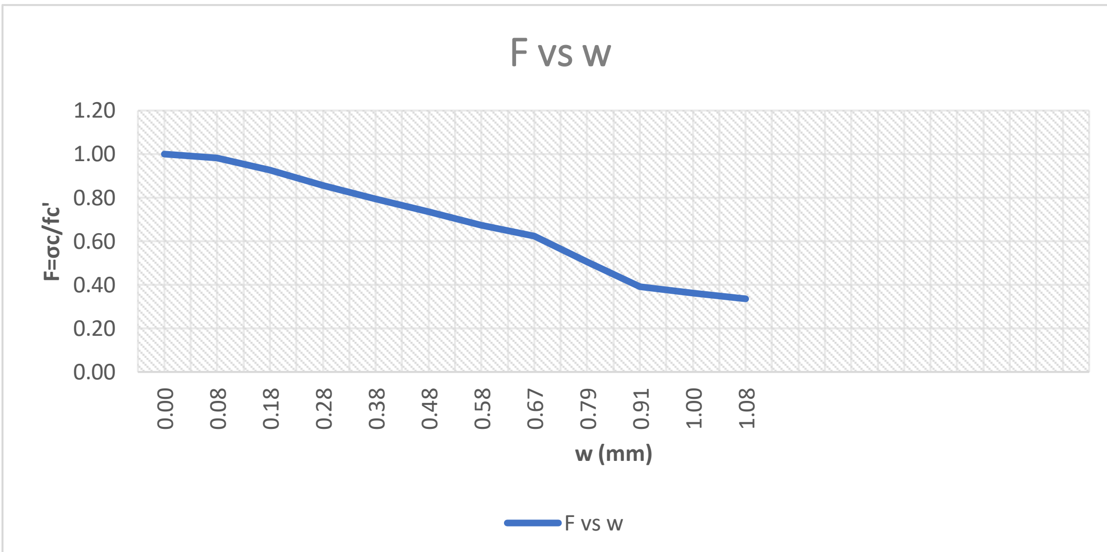

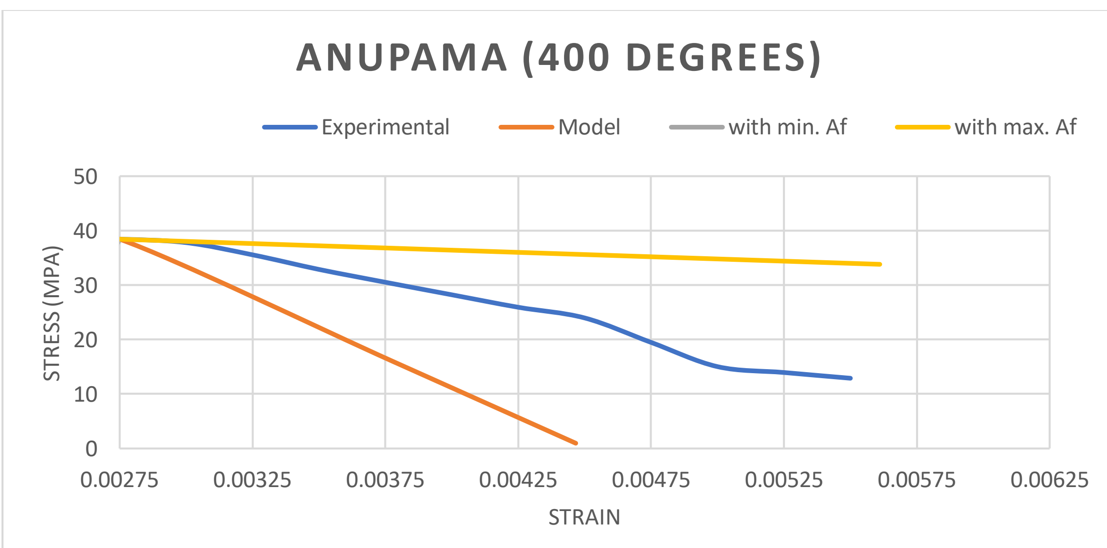

500^{o}C

Properties		
E_c	16440	Mpa
f_c'	29.84	Mpa
ε_{c1}	0.004	
H	300	mm

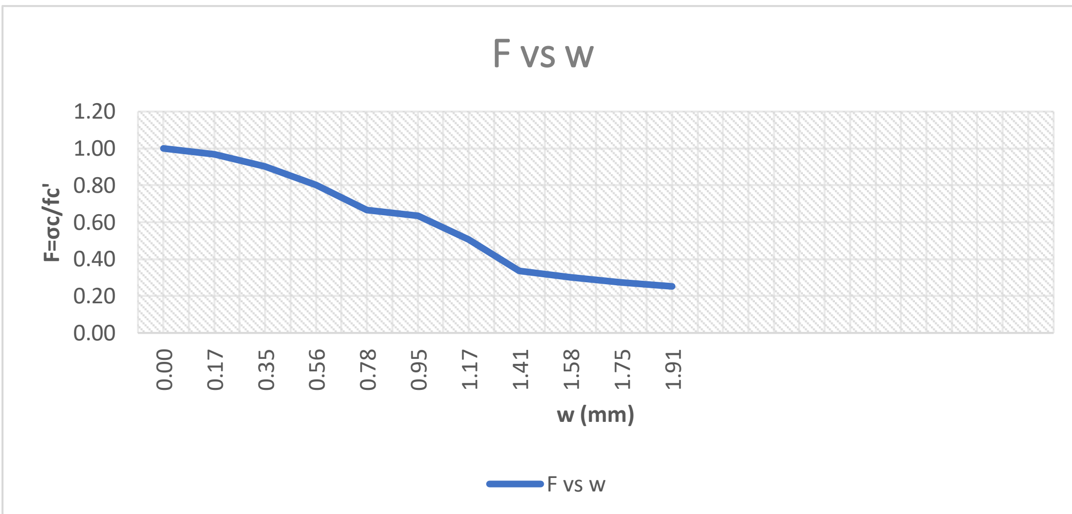

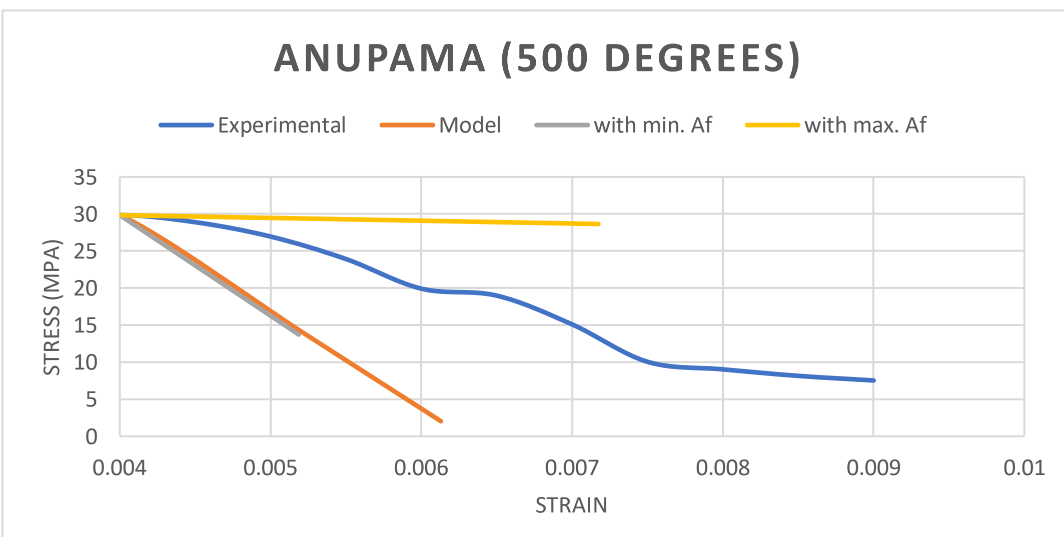

600°C

Properties		
E_c	8490	Mpa
f_c'	19.87	Mpa
ε_{c1}	0.0045	
H	300	mm

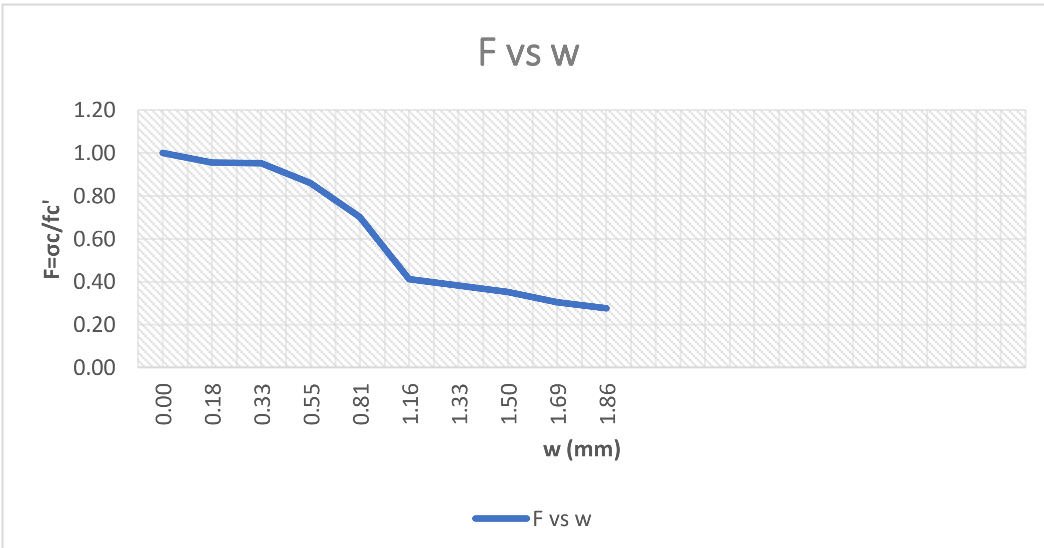

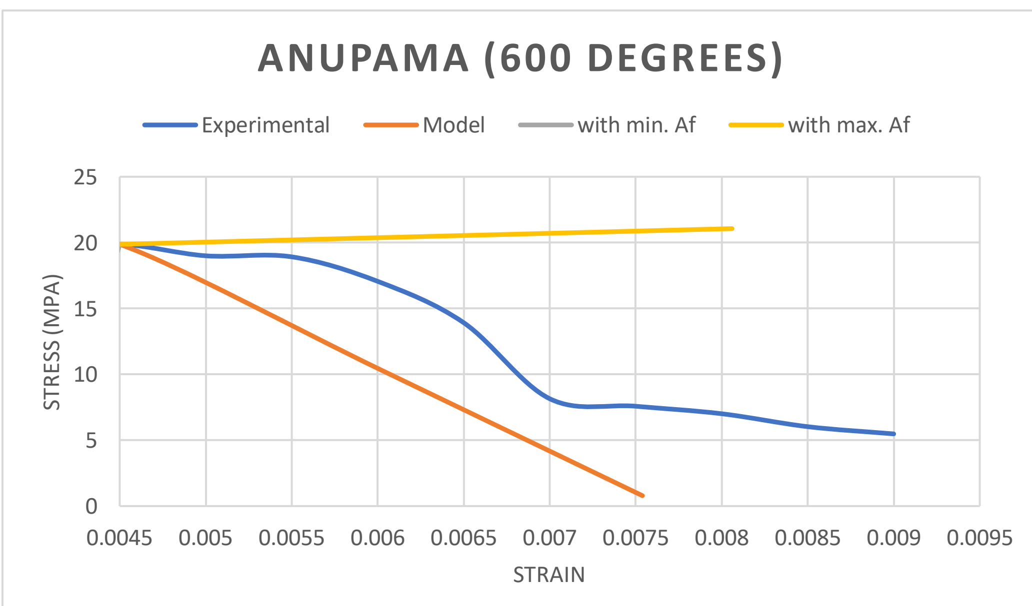

700°C

Properties		
E_c	9640	Mpa
f_c'	18.86	Mpa
ε_{c1}	0.0045	
H	300	mm

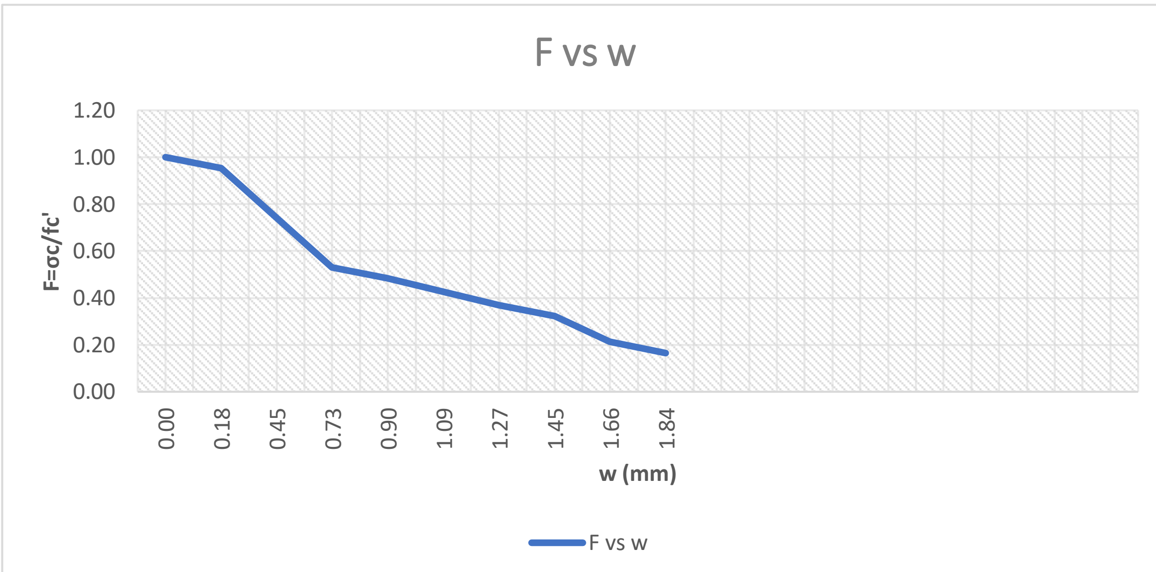

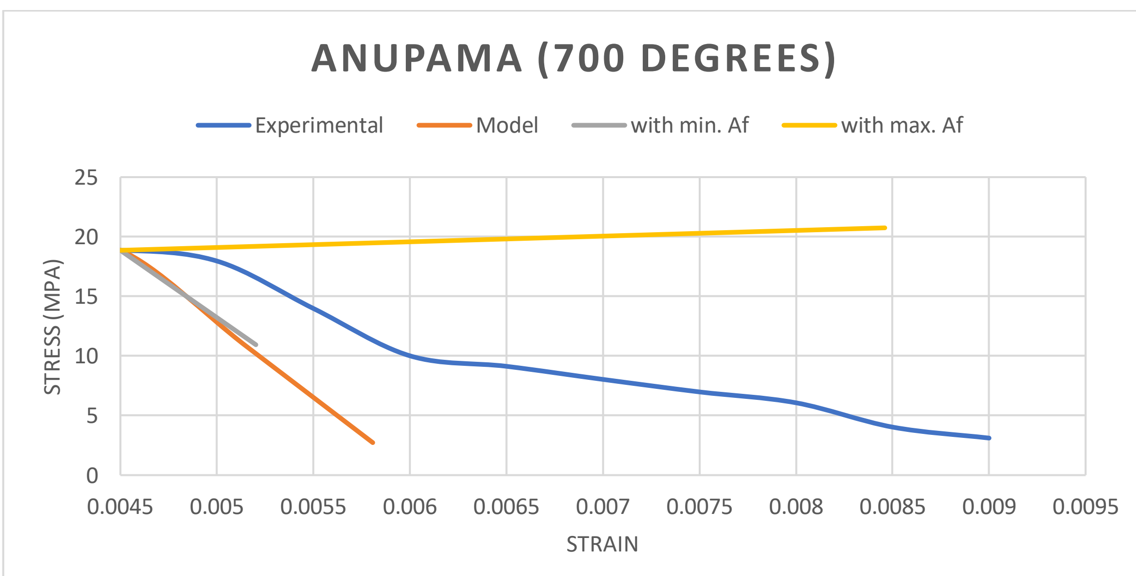

800^{o}C

Properties		
E_c	2160	Mpa
f_c'	10.92	Mpa
ε_{c1}	0.0055	
H	300	mm

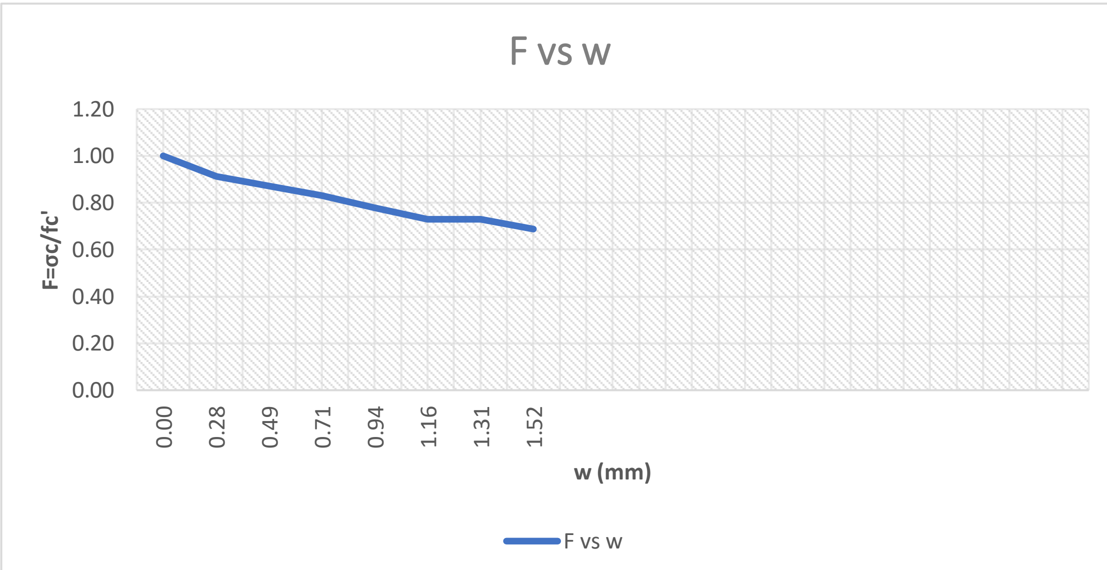

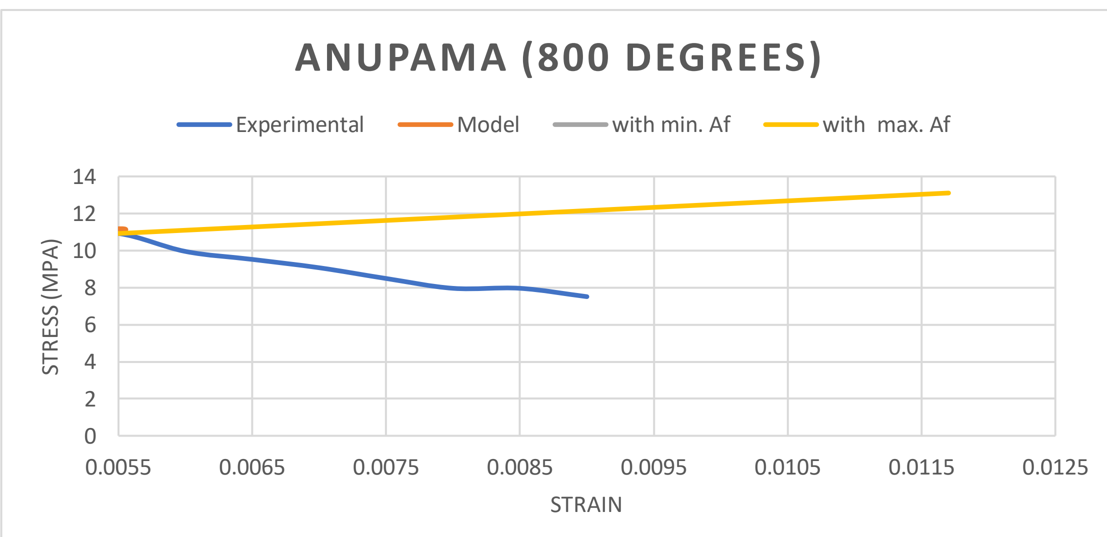

Post-peak analysis of experimental data by (Chang et al., 2006)

20°C

Properties		
E_c	31500	Mpa
f_c'	39.98	Mpa
ε_{c1}	0.00200	
H	300	mm

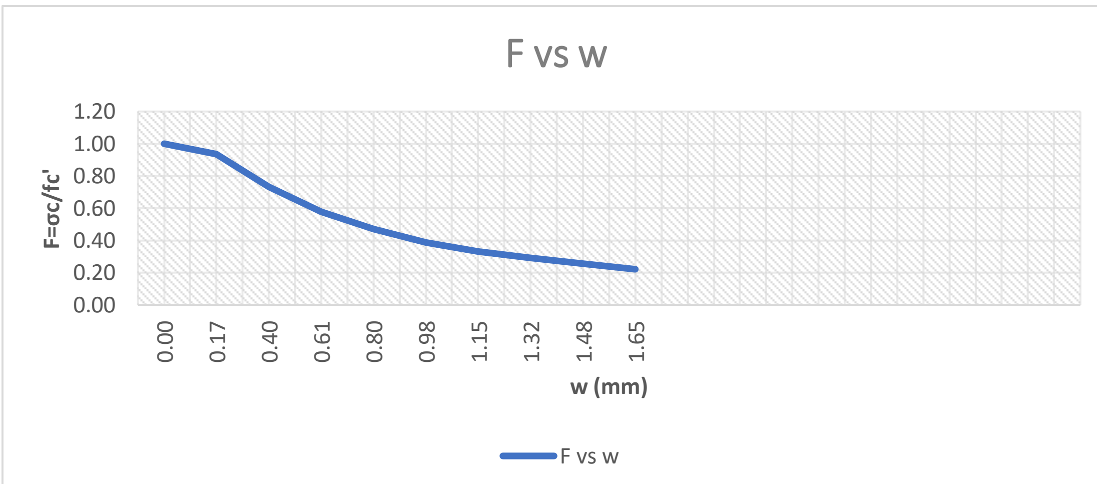

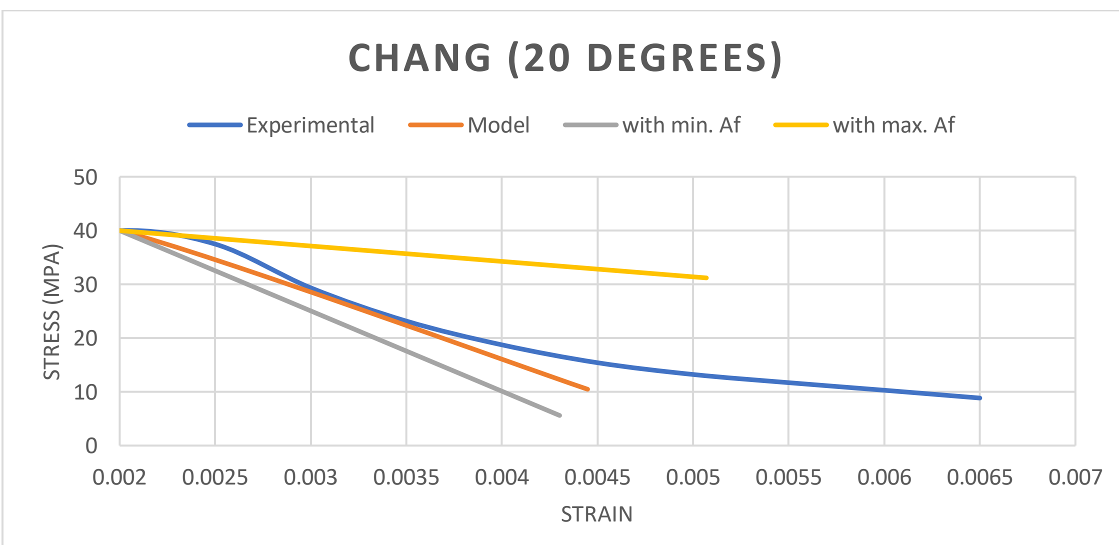

<u>103ºC</u>

Properties		
E_c	25120	Mpa
f_c'	38.35	Mpa
ε_{c1}	0.00225	
H	300	mm

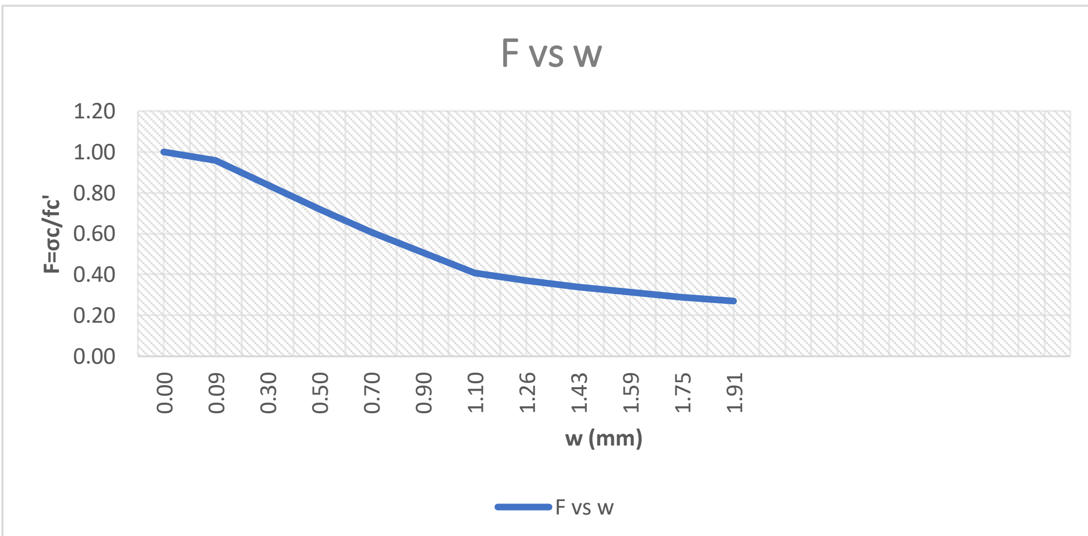

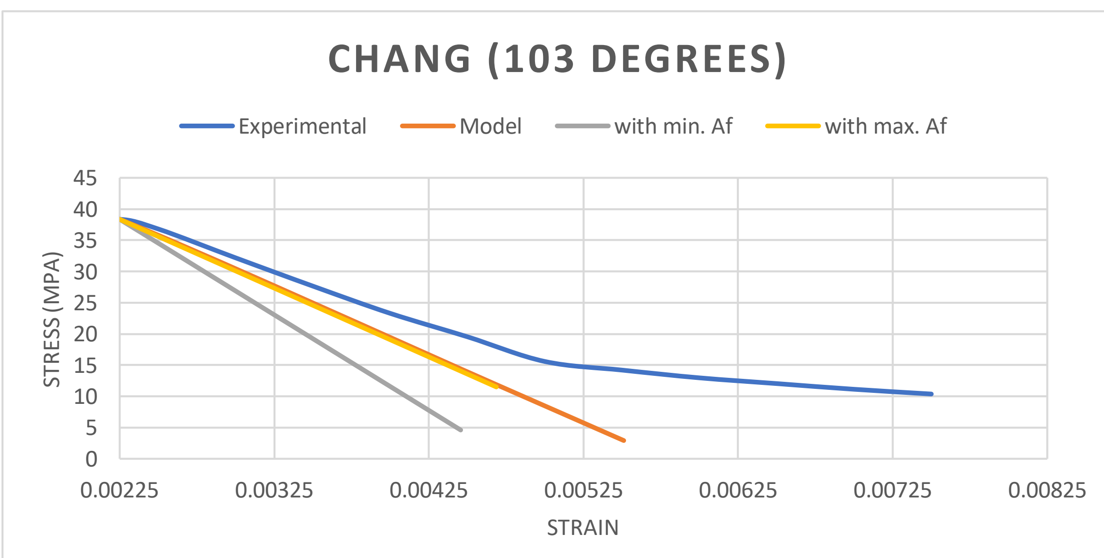

203°C

Properties		
E_c	24800	Mpa
f_c'	36.76	Mpa
ε_{c1}	0.00250	
H	300	mm

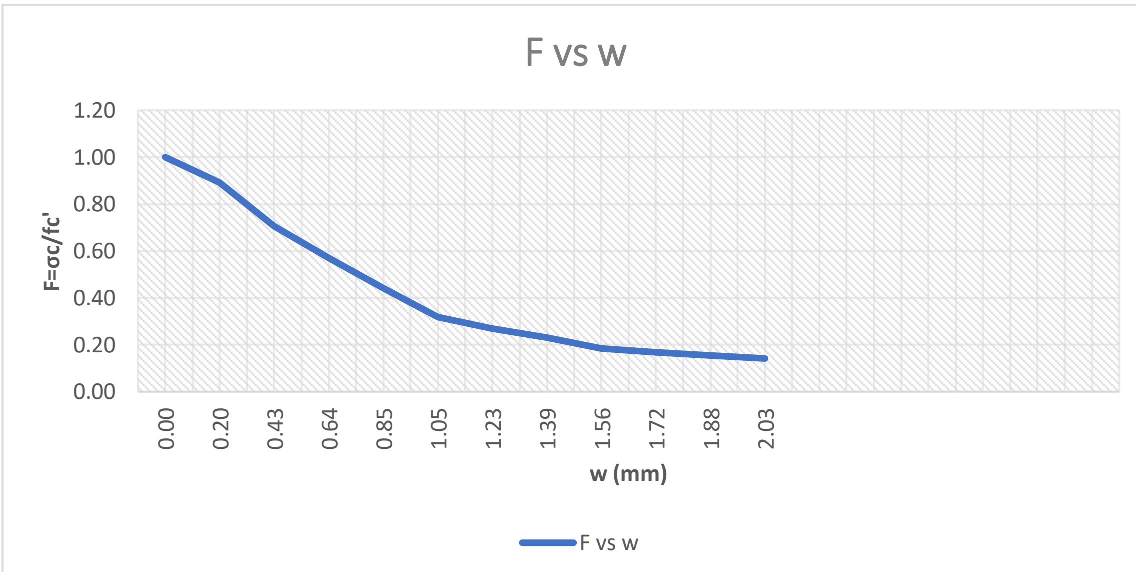

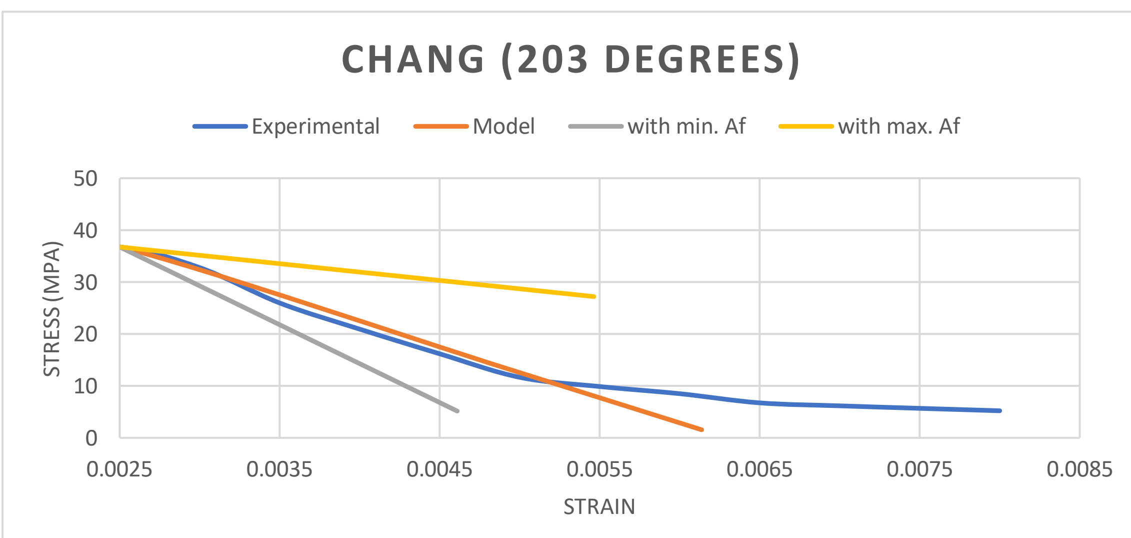

308°C

Properties		
E_c	14360	Mpa
f_c'	30.97	Mpa
ε_{c1}	0.00250	
H	300	mm

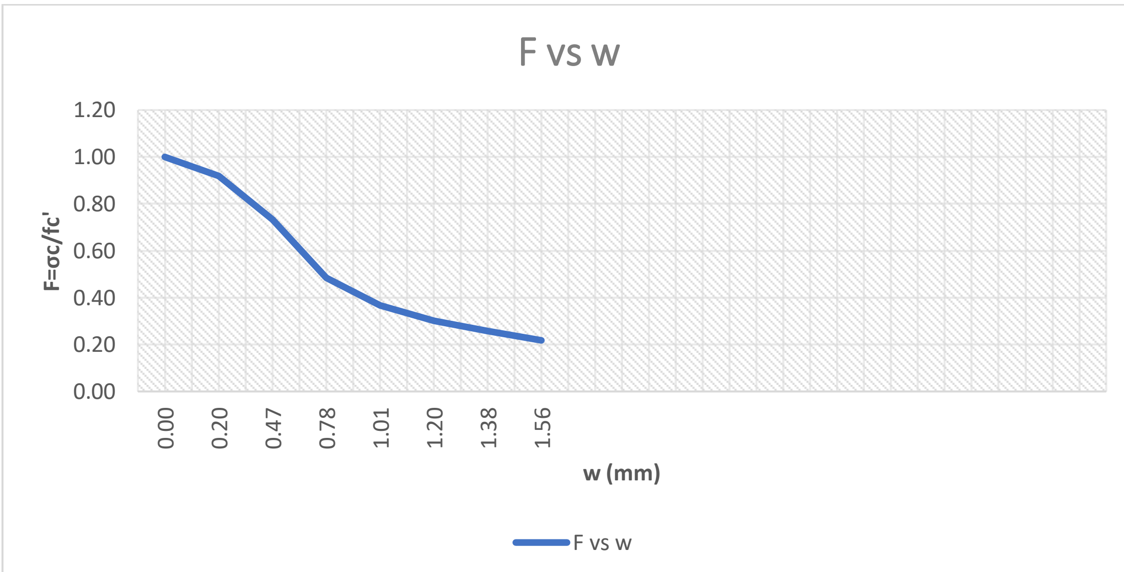

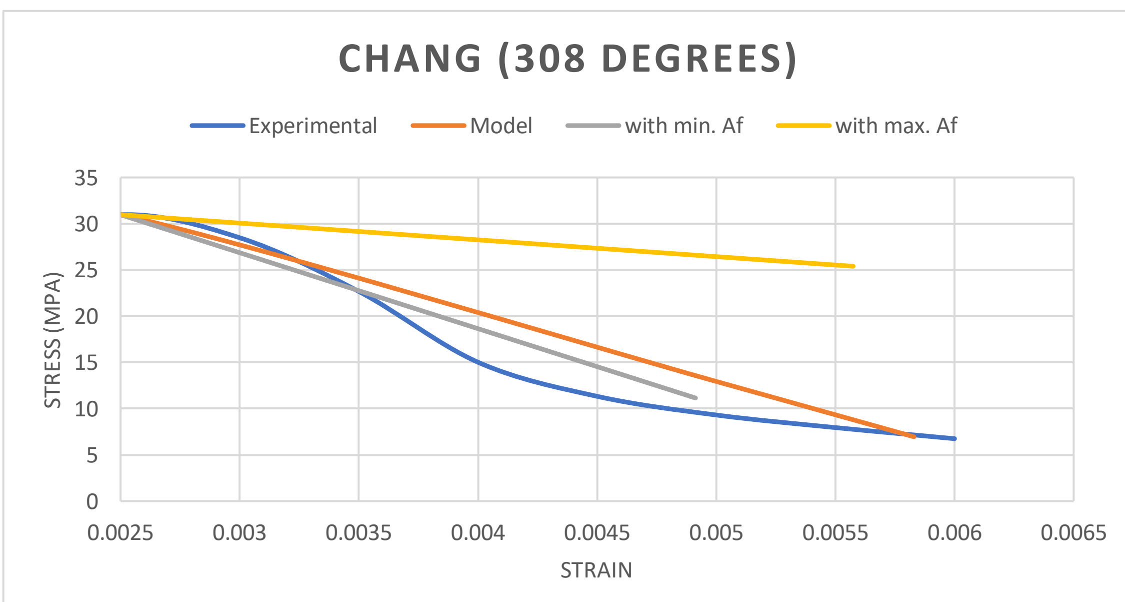

406°C

Properties		
E_c	10100	Mpa
f_c'	26.66	Mpa
ε_{c1}	0.00300	
H	300	mm

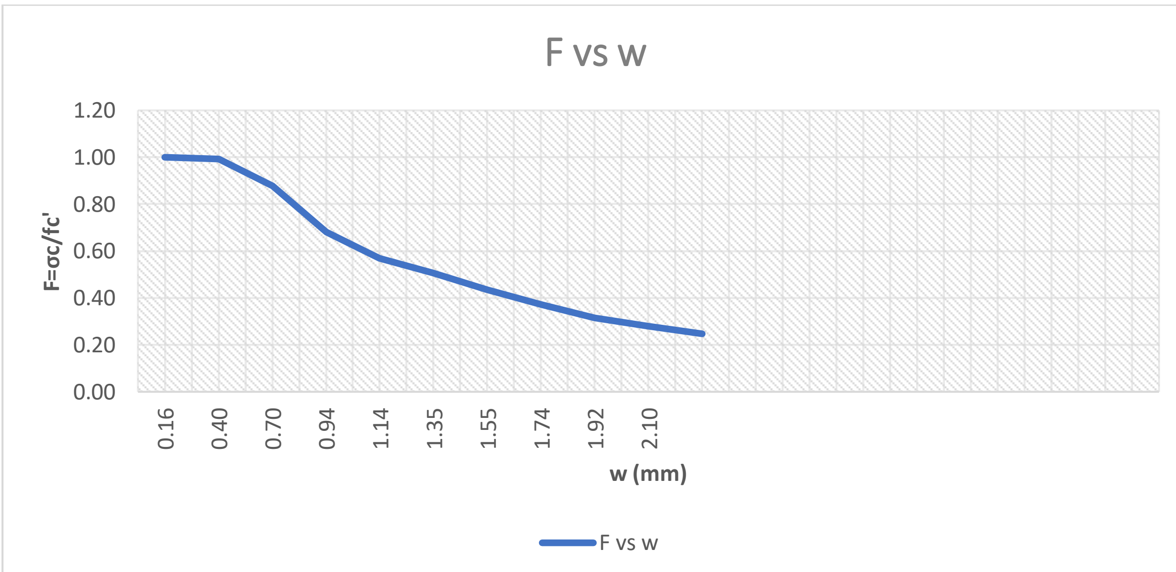

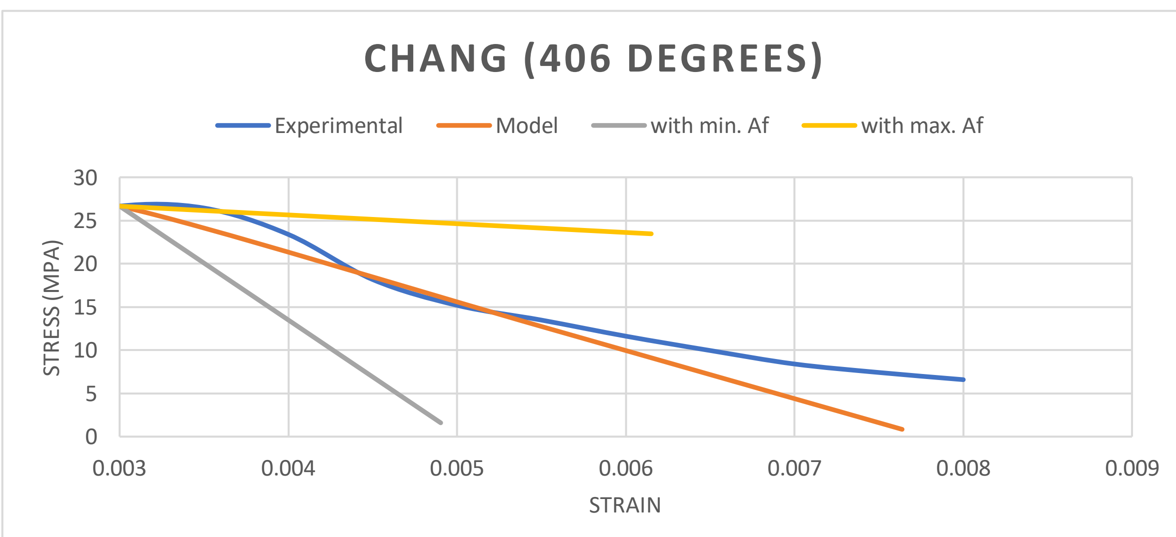

503ºC

Properties		
E_c	5960	Mpa
f_c'	20.15	Mpa
ε_{c1}	0.00400	
H	300	mm

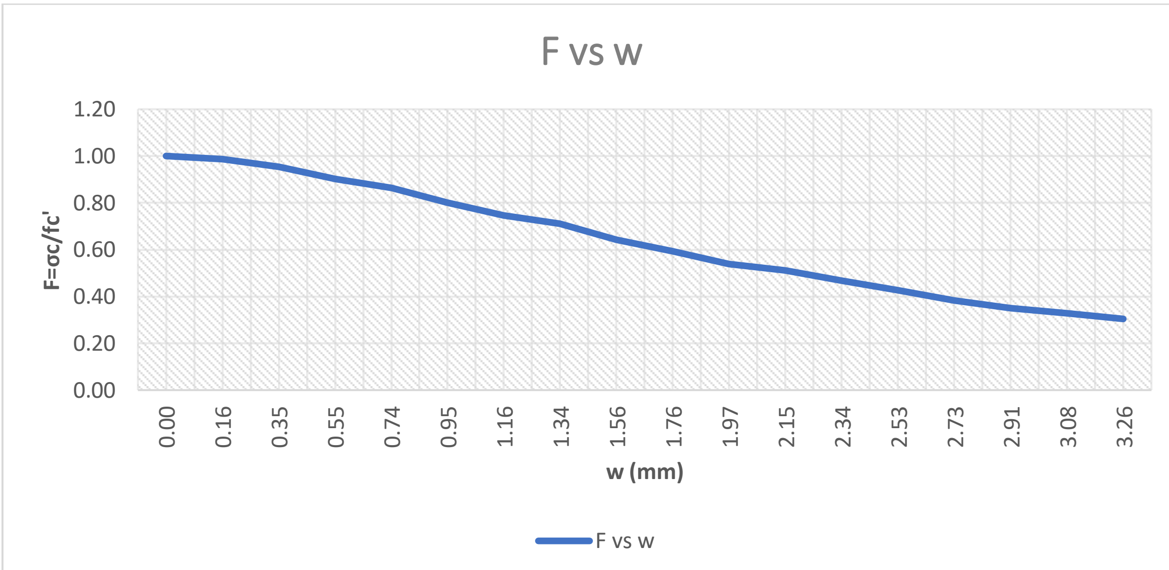

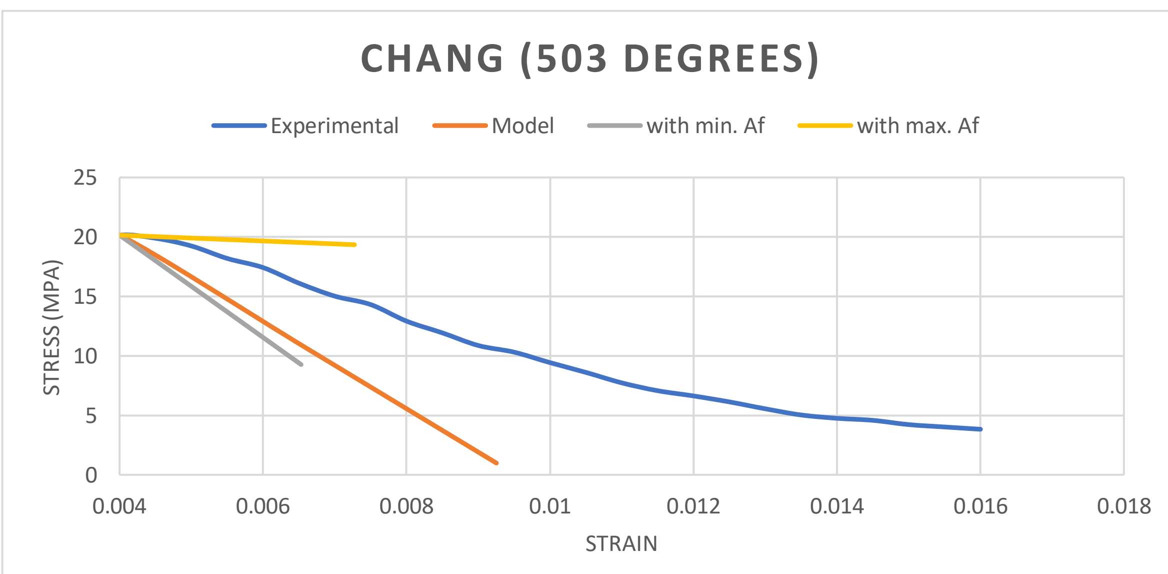

603ºC

Properties		
E_c	1640	Mpa
f_c'	15.69	Mpa
ε_{c1}	0.00700	
H	300	mm

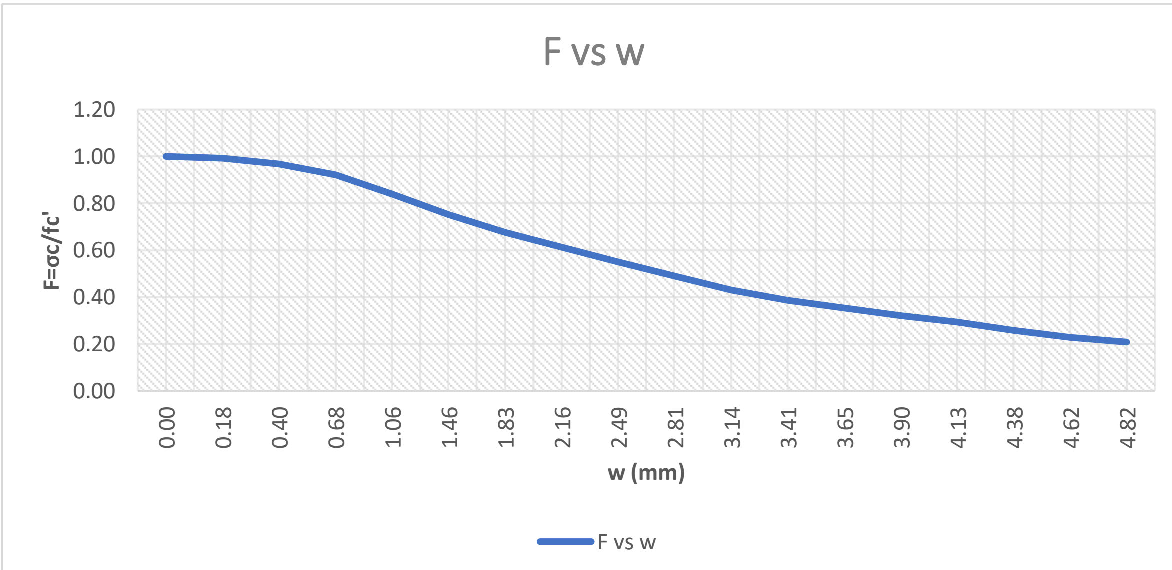

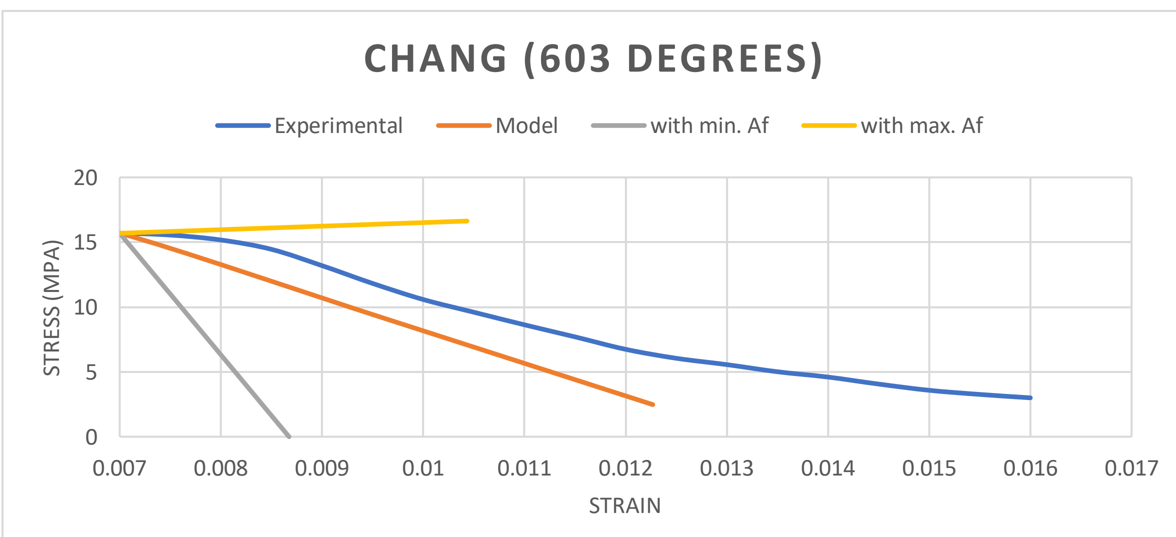

702°C

Properties		
E_c	900	Mpa
f_c'	9.45	Mpa
ε_{c1}	0.00800	
H	300	mm

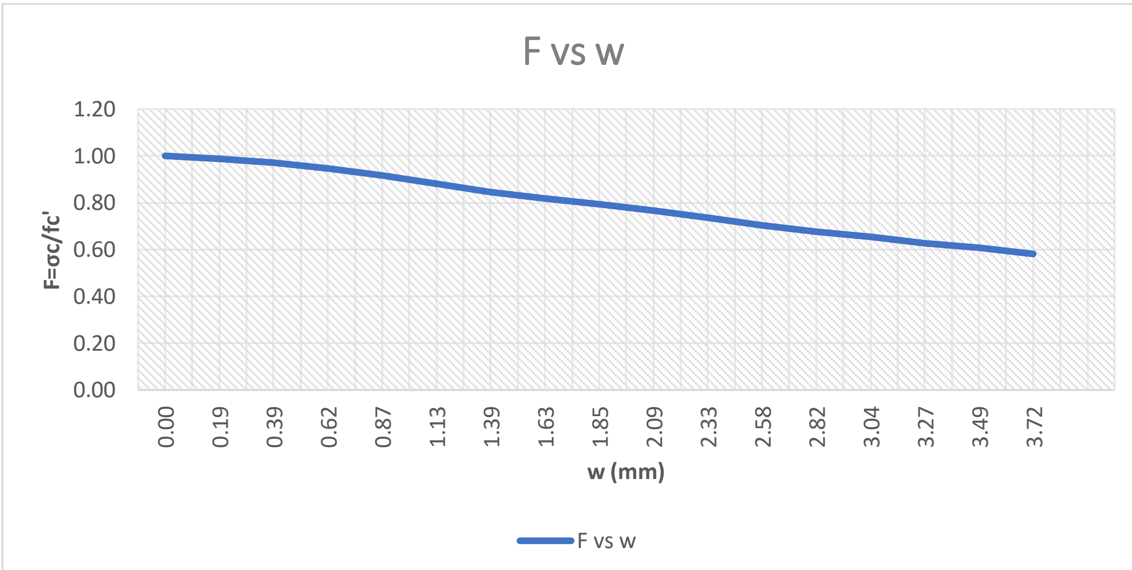

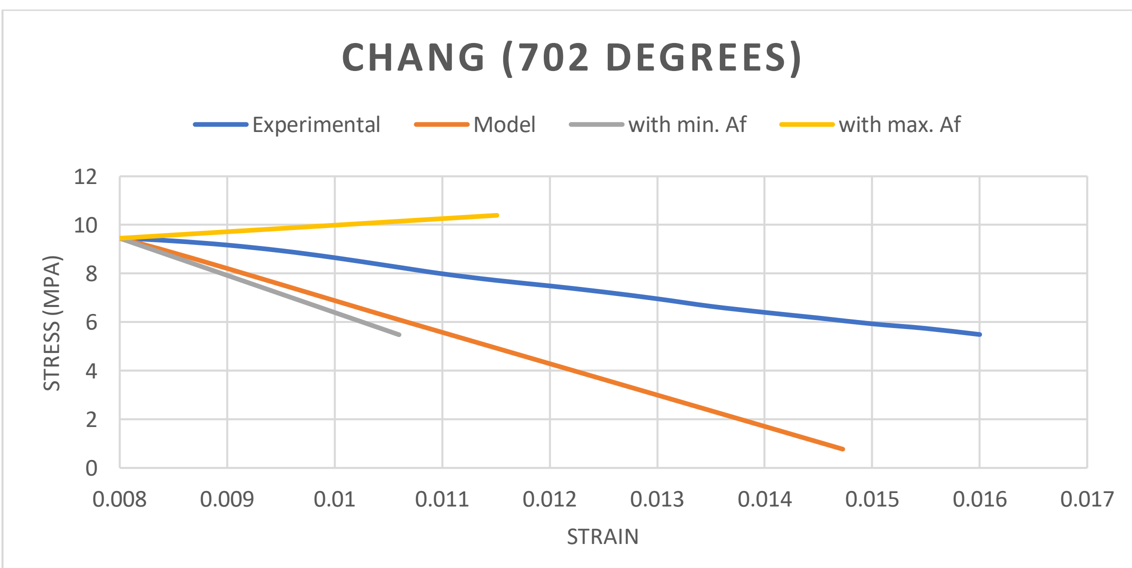

796°C

Properties		
Slope/E_c	740	Mpa
f_c'	7.35	Mpa
ε_{c1}	0.00900	
H	300	mm

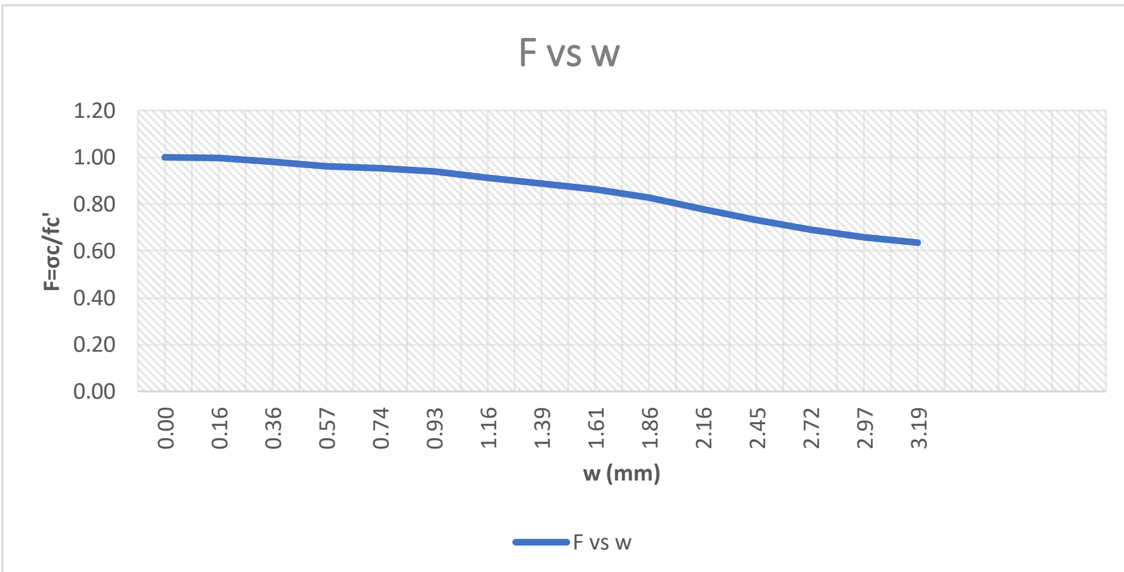

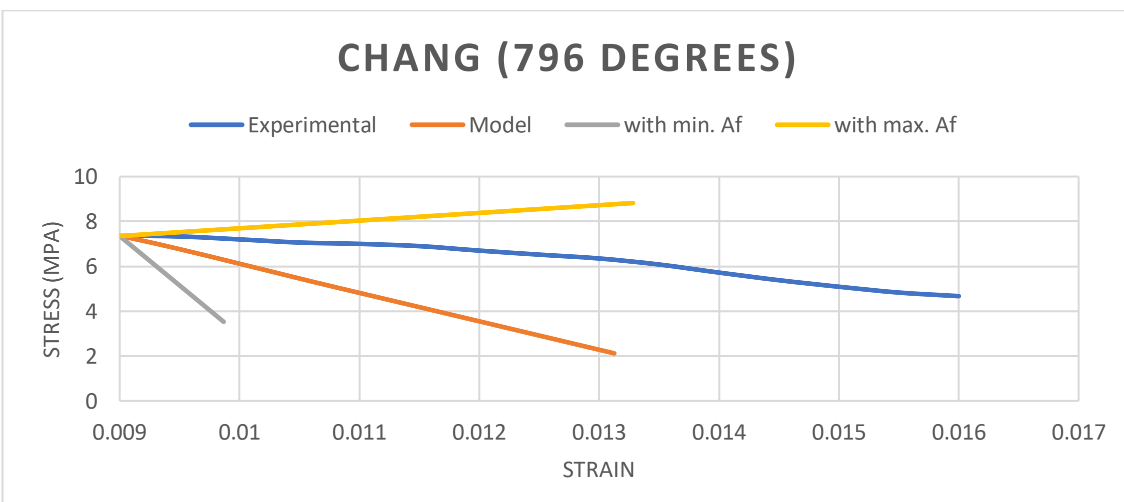

Post-peak analysis of experimental data by (Fu et al., 2005)

600°C (High Strength Concrete)

Properties		
E_c	6120	Mpa
f_c'	34.31	Mpa
ε_{c1}	0.00625	
H	150	mm

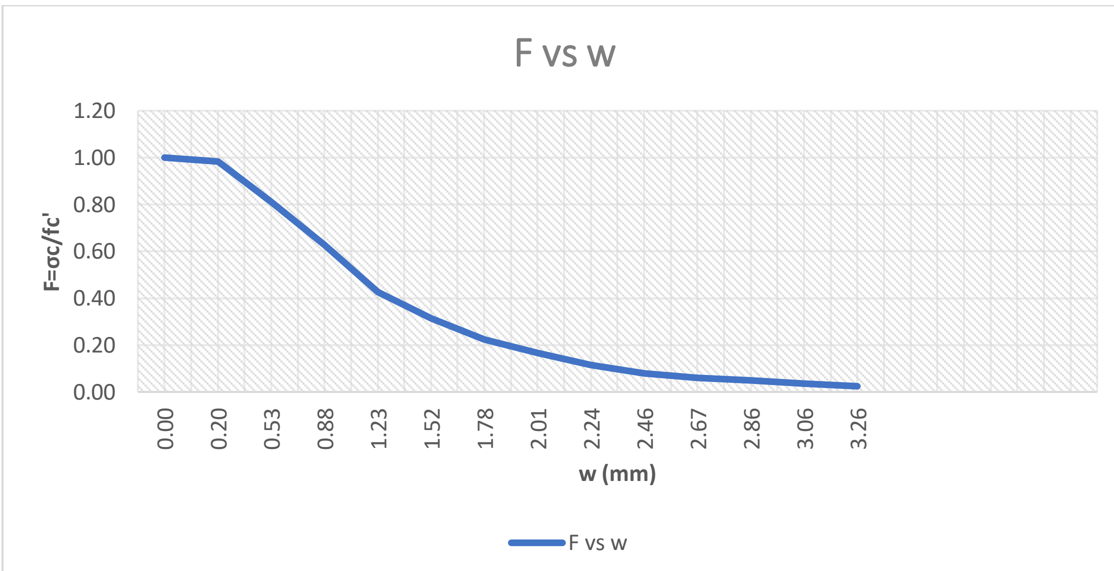

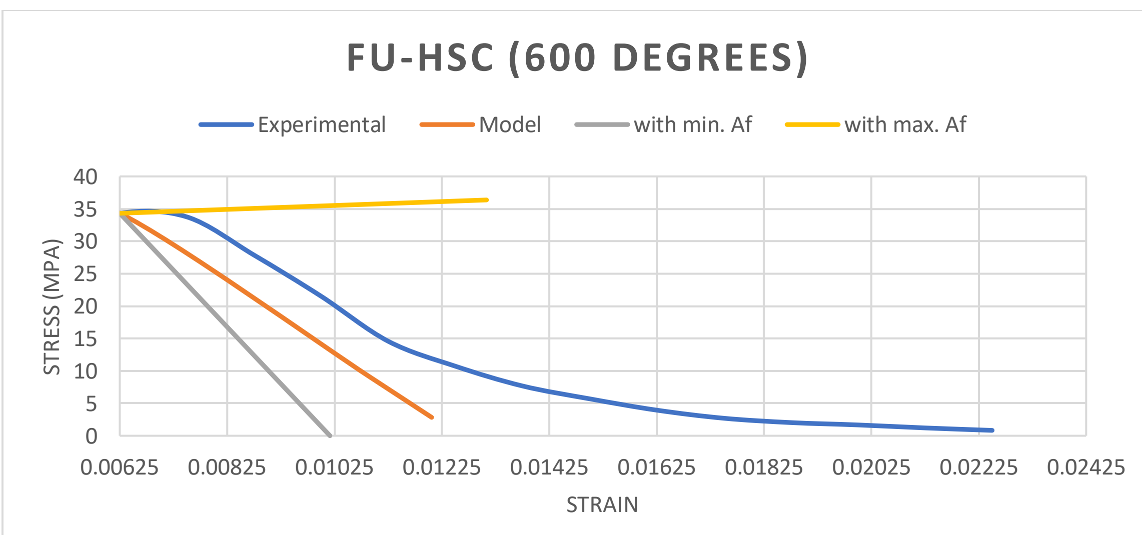

600°C (MK Concrete)

Properties		
E_c	3600	Mpa
f_c'	34.56	Mpa
ε_{c1}	0.00875	
H	150	mm

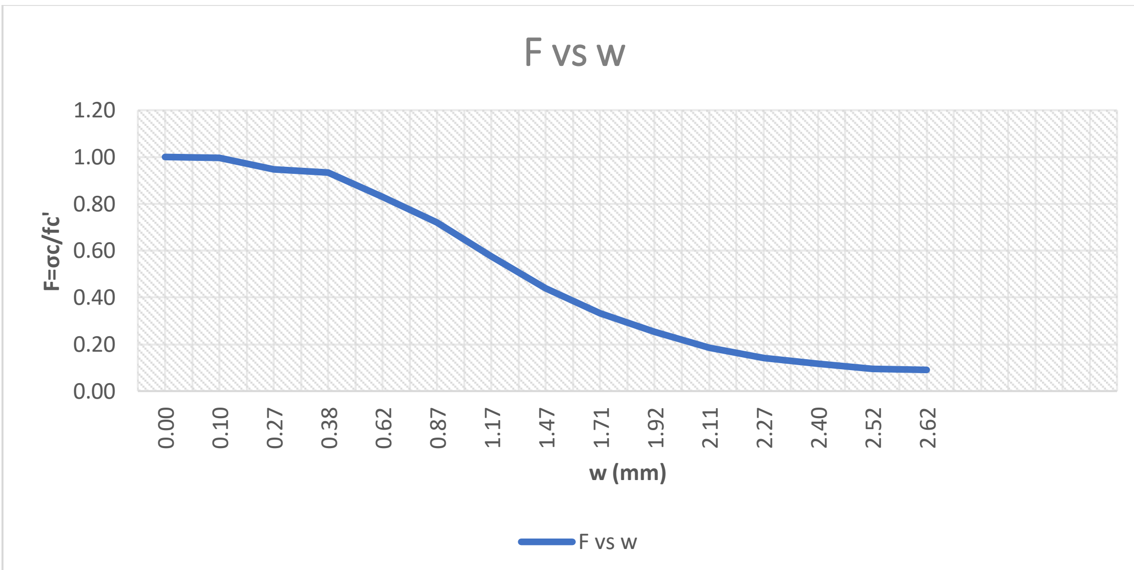

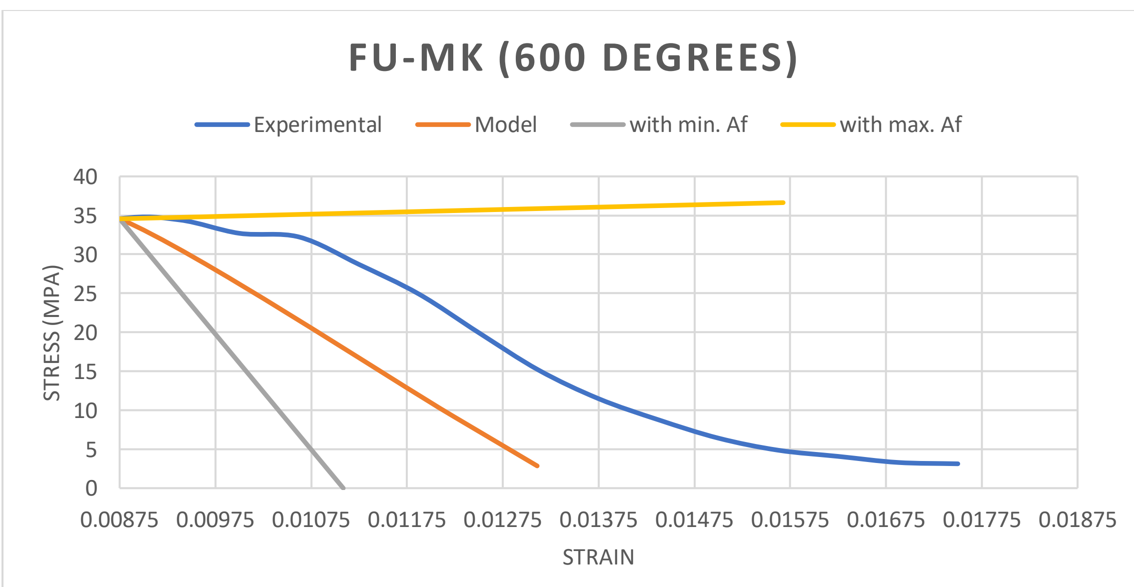

600°C (PFA Concrete)

Properties		
E_c	5744	Mpa
f_c'	39.54	Mpa
ε_{c1}	0.00875	
H	150	mm

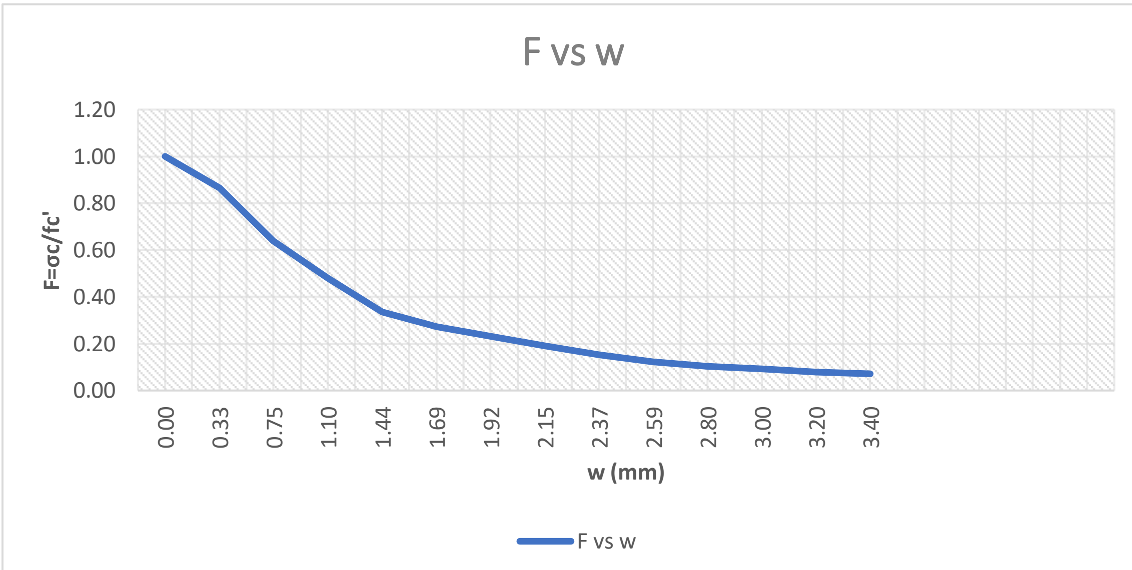

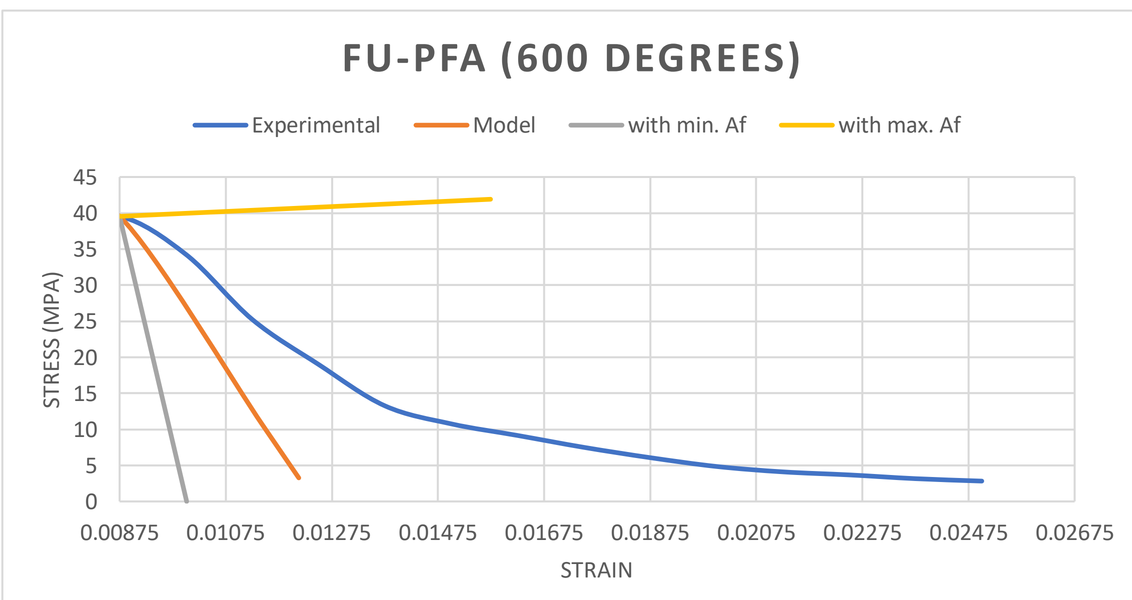

100°C (Normal Strength Concrete)

Properties		
E_c	13824	Mpa
f_c'	36.17	Mpa
ε_{c1}	0.00313	
H	150	mm

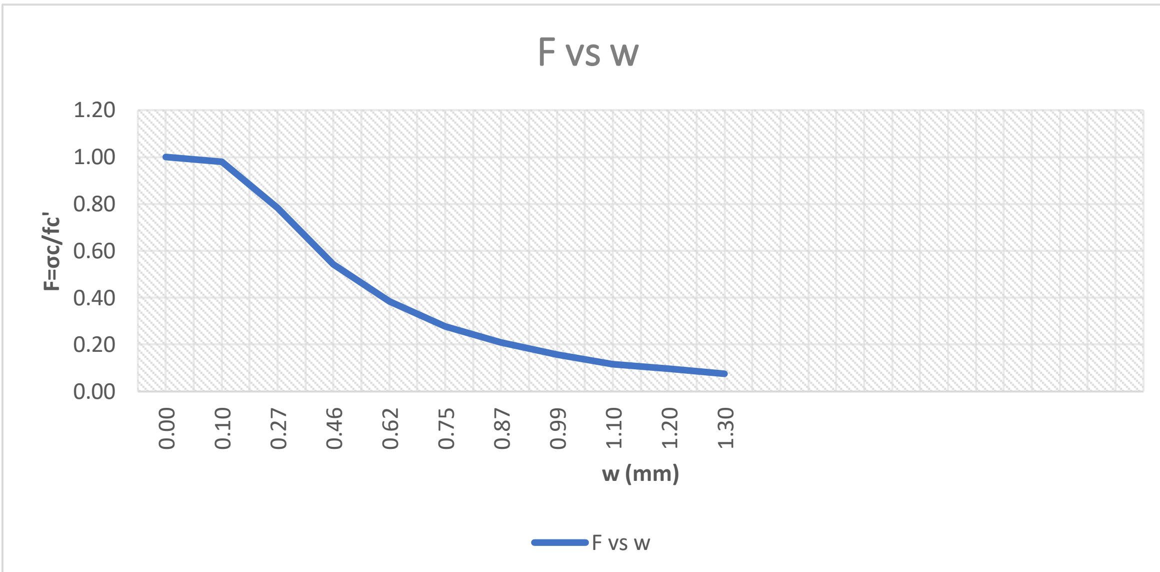

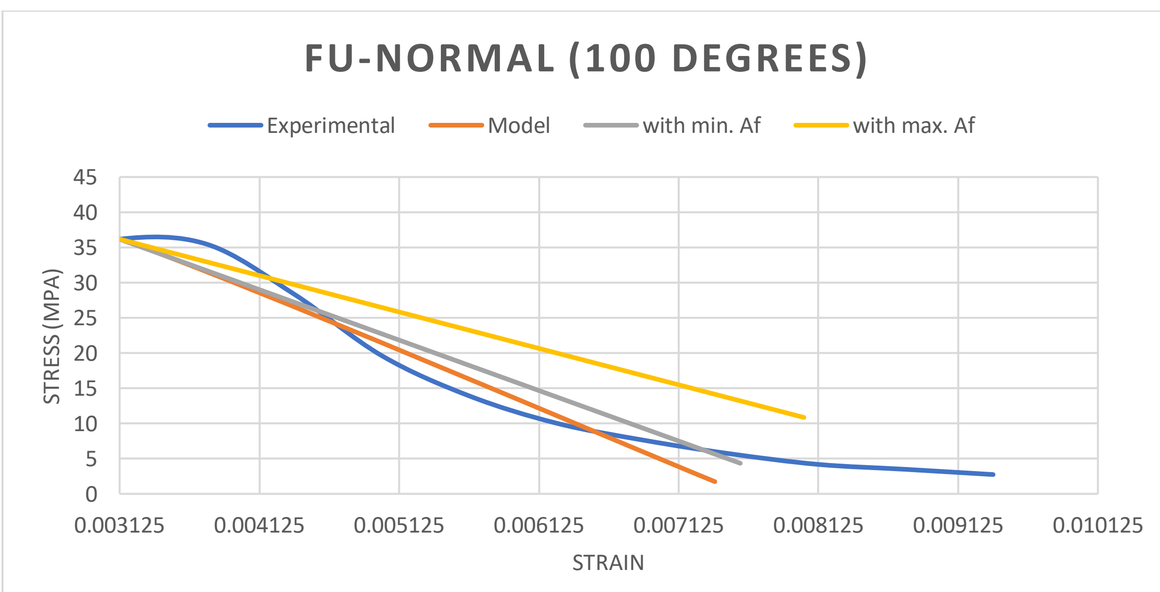

200°C (Normal Strength Concrete)

Properties		
E_c	14560	Mpa
f_c'	30.72	Mpa
ε_{c1}	0.00250	
H	150	mm

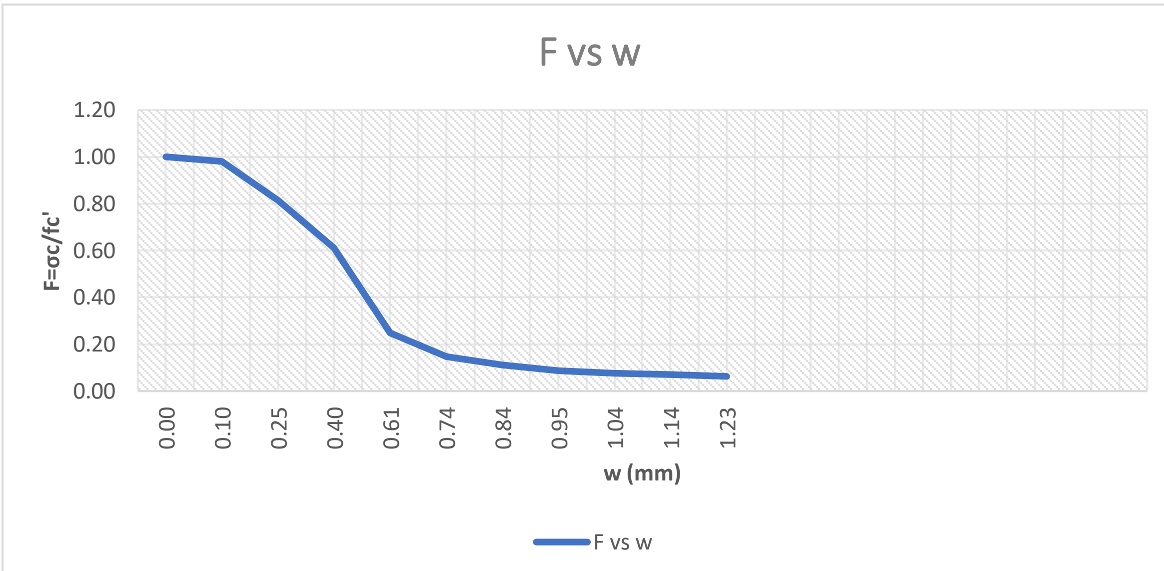

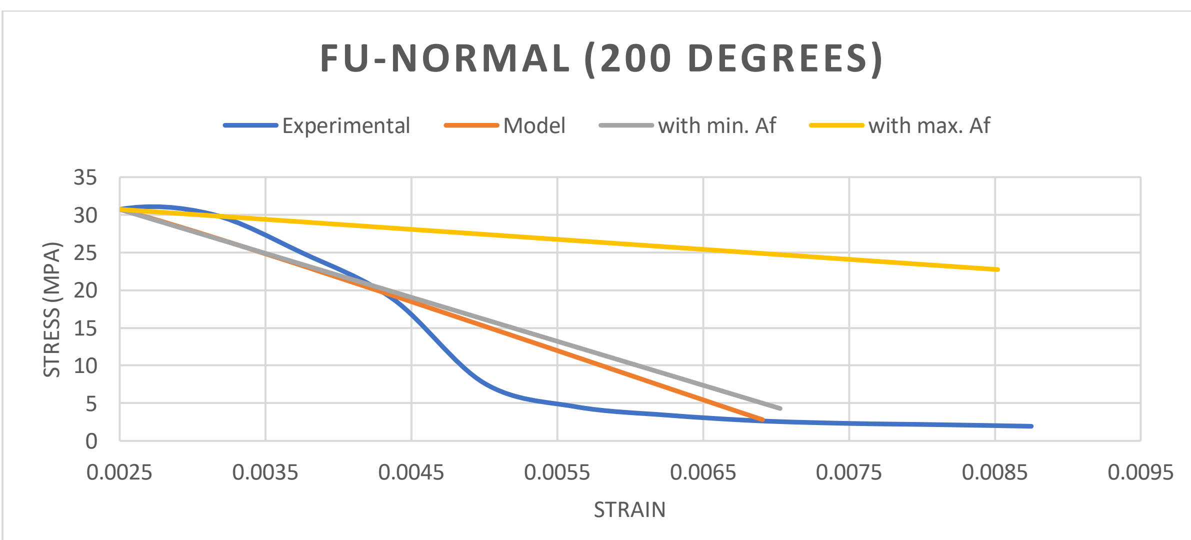

400°C (Normal Strength Concrete)

Properties7		
E_c	6832	Mpa
f_c'	26.97	Mpa
ε_{c1}	0.00500	
H	150	mm

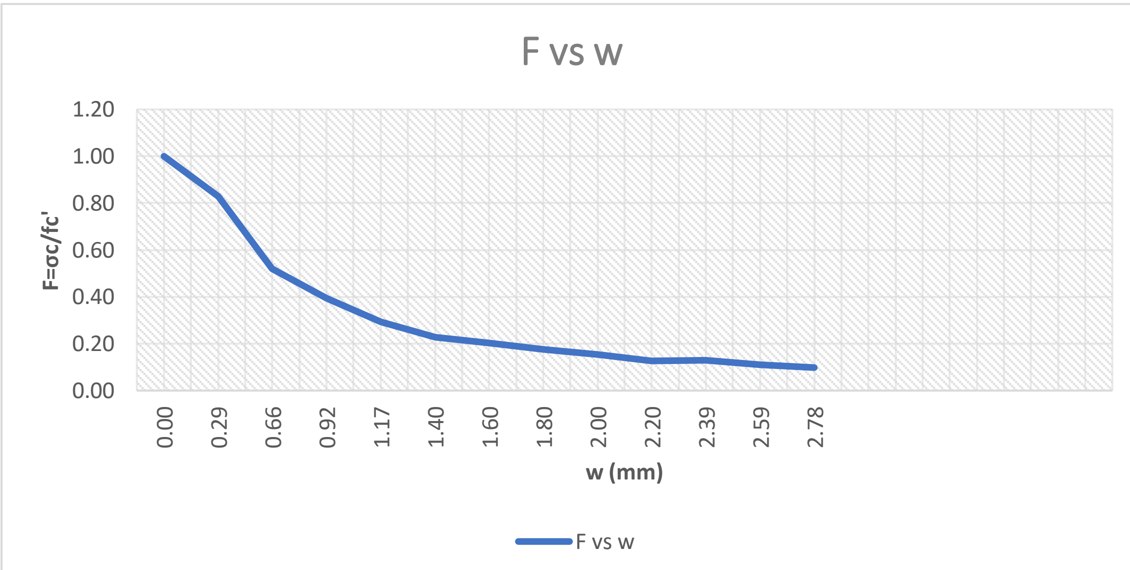

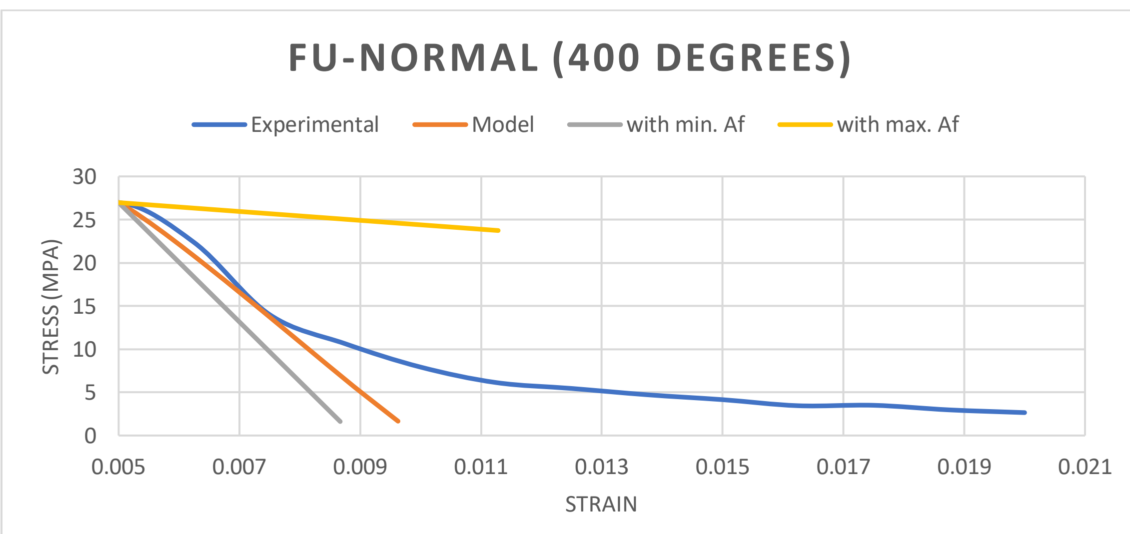

600°C (Normal Strength Concrete)

Properties		
E_c	5200	Mpa
f_c'	17.21	Mpa
ε_{c1}	0.00625	
H	150	mm

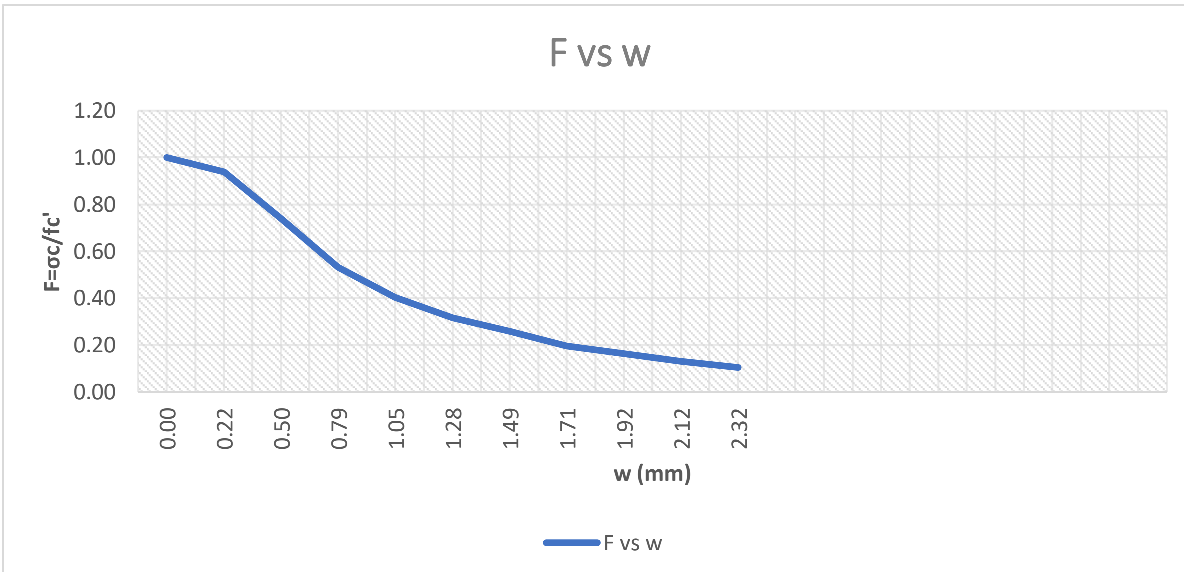

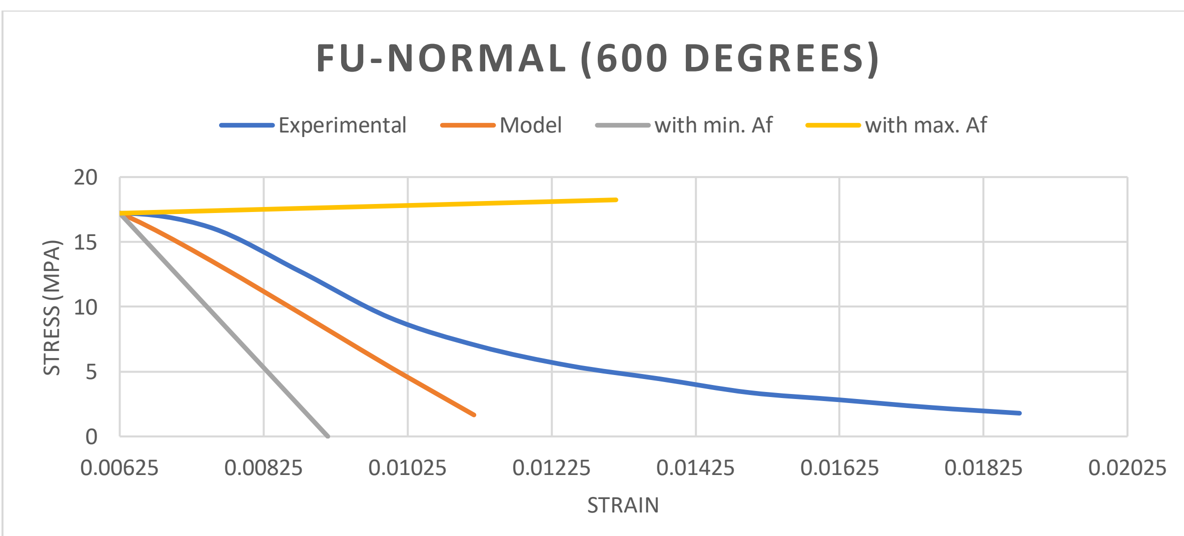

Post-peak analysis of experimental data by (Nematzadeh et al., 2019)

23°C (Normal Strength Concrete-R)

Properties		
E_c	40800	Mpa
f_c'	53.4	Mpa
ε_{c1}	0.00220	
H	200	mm

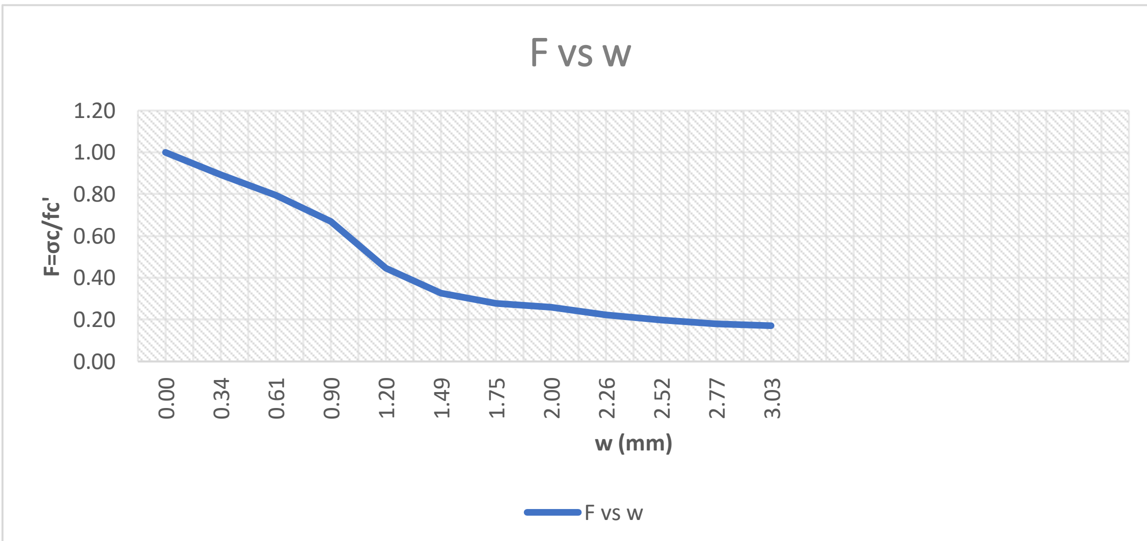

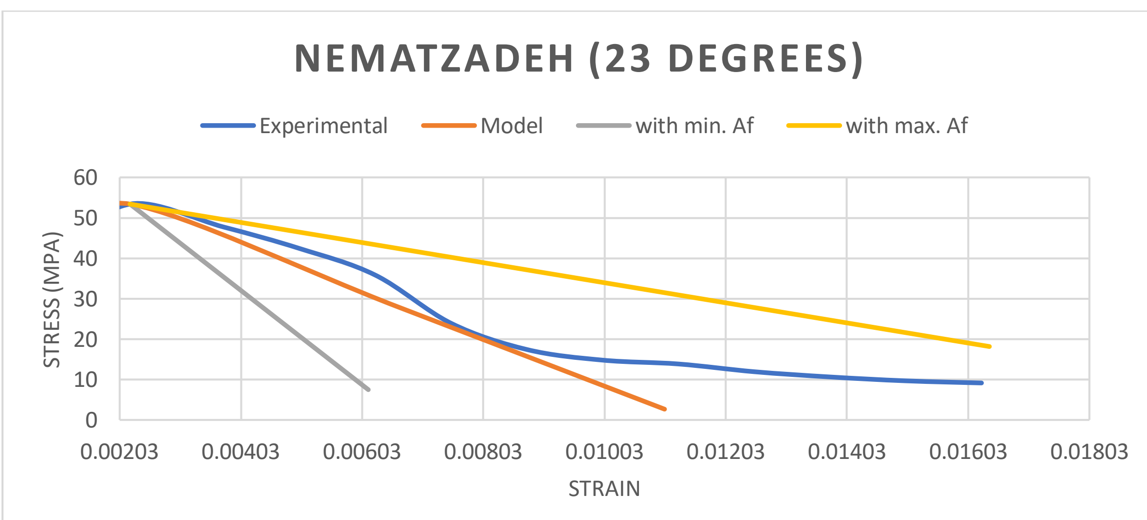

200°C (Normal Strength Concrete-R)

Properties		
E_c	19808	Mpa
f_c'	42	Mpa
ε_{c1}	0.00203	
H	200	mm

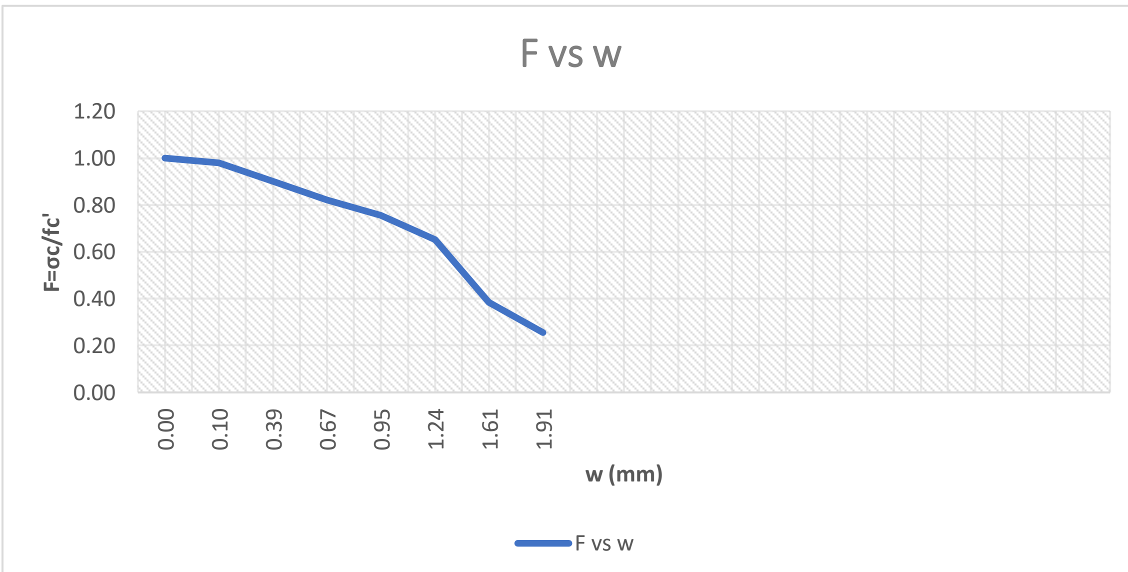

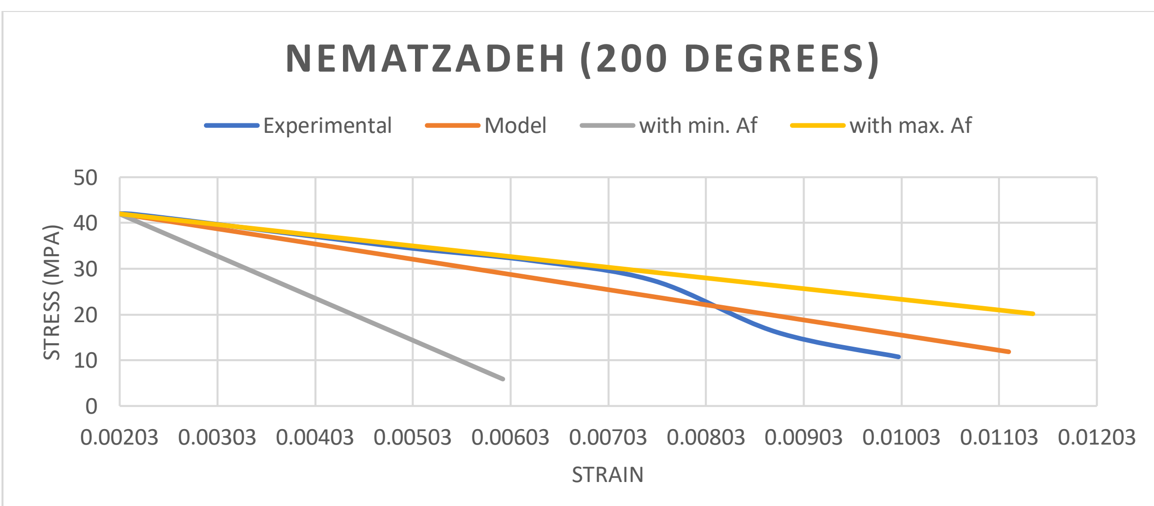

400°C (Normal Strength Concrete-R)

Properties		
E_c	17840	Mpa
f_c'	34.26	Mpa
ε_{c1}	0.00330	
H	200	mm

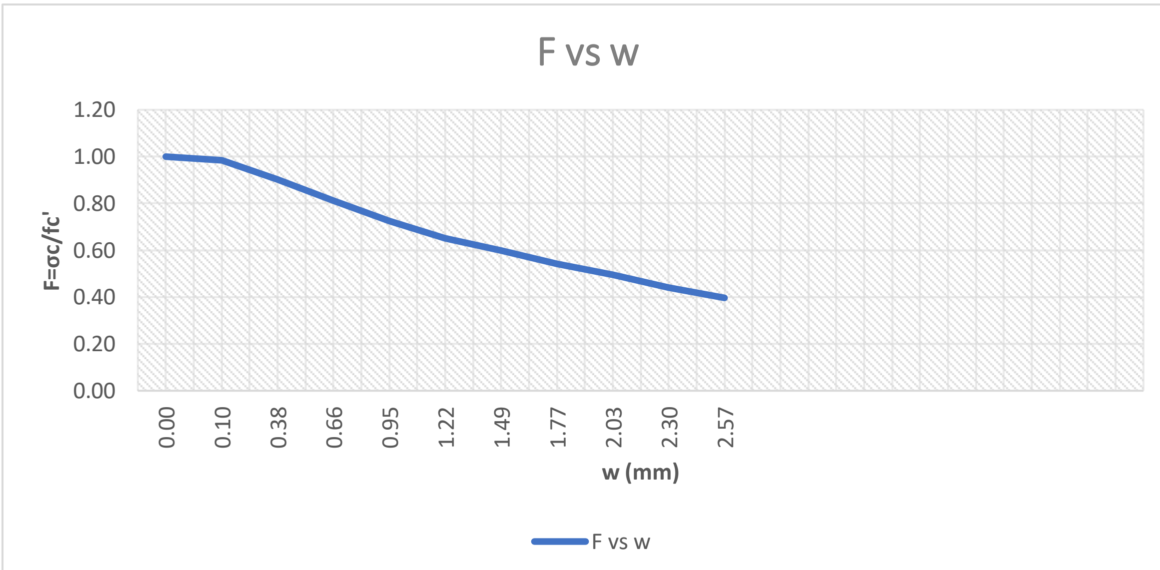

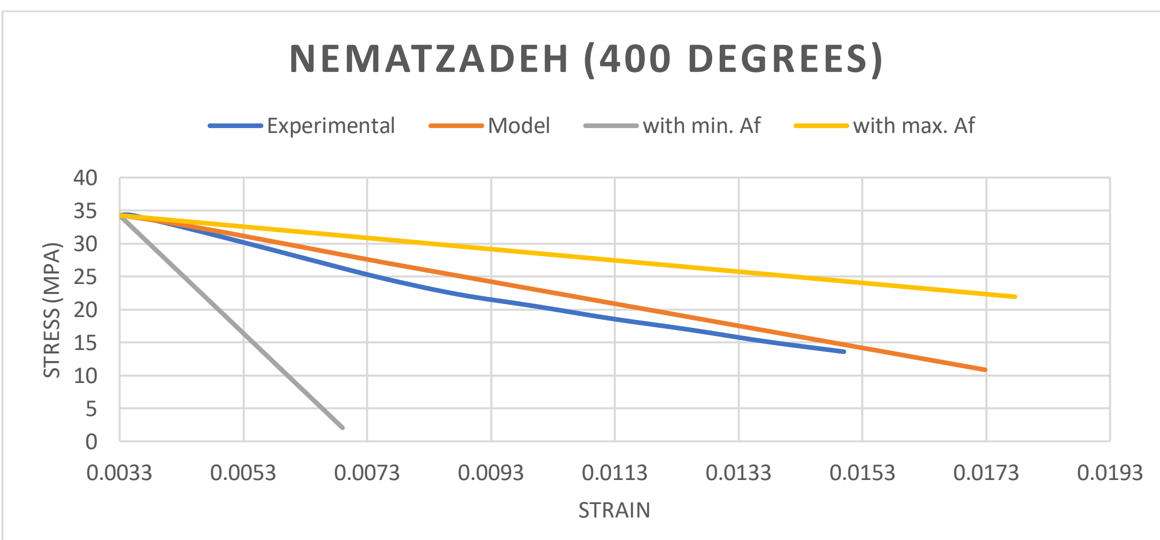

600^{o}C (Normal Strength Concrete-R)

Properties		
E_c	8112	Mpa
f_c'	21	Mpa
ε_{c1}	0.00536	
H	200	mm

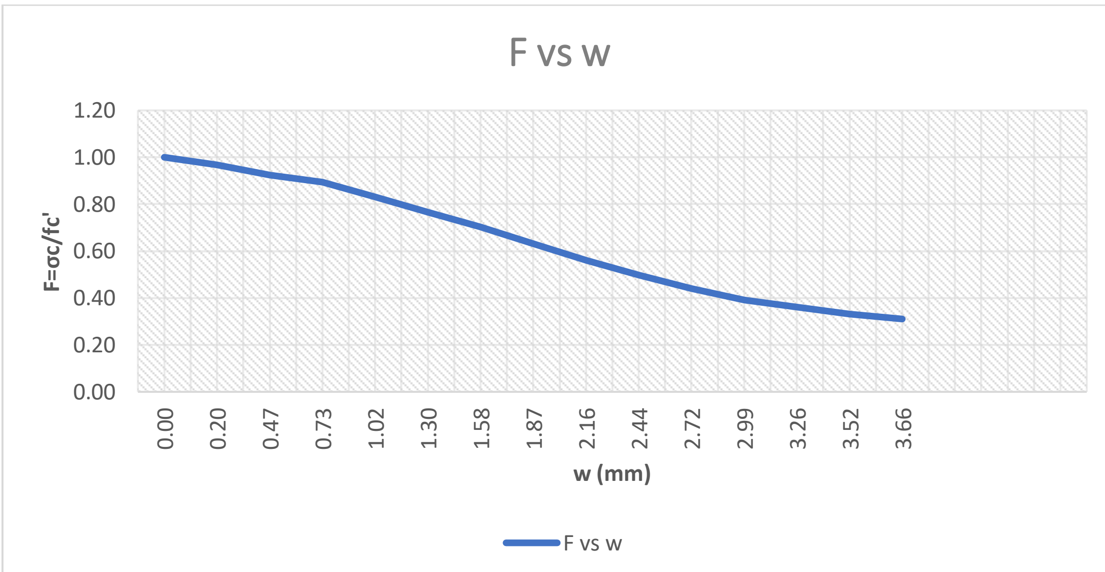

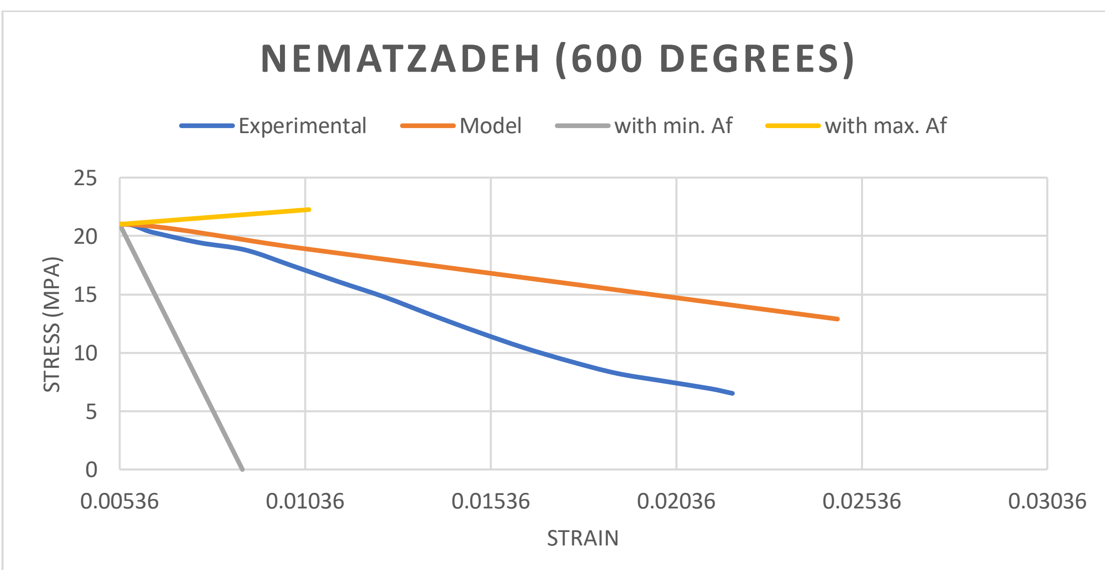

800°C (Normal Strength Concrete-R)

Properties		
E_c	7344	Mpa
f_c'	13.11	Mpa
ε_{c1}	0.00548	
H	200	mm

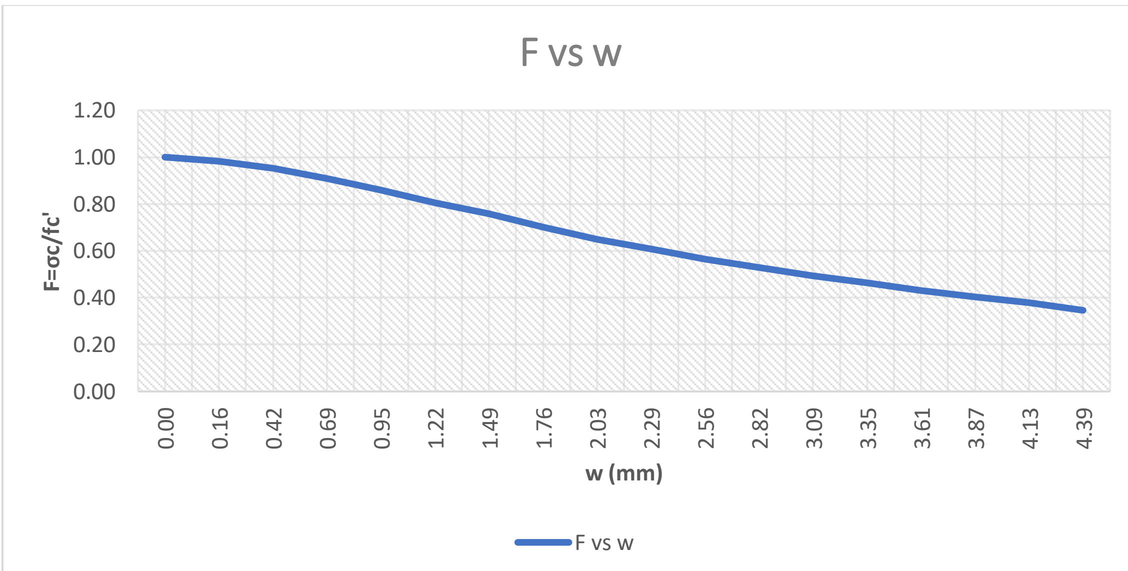

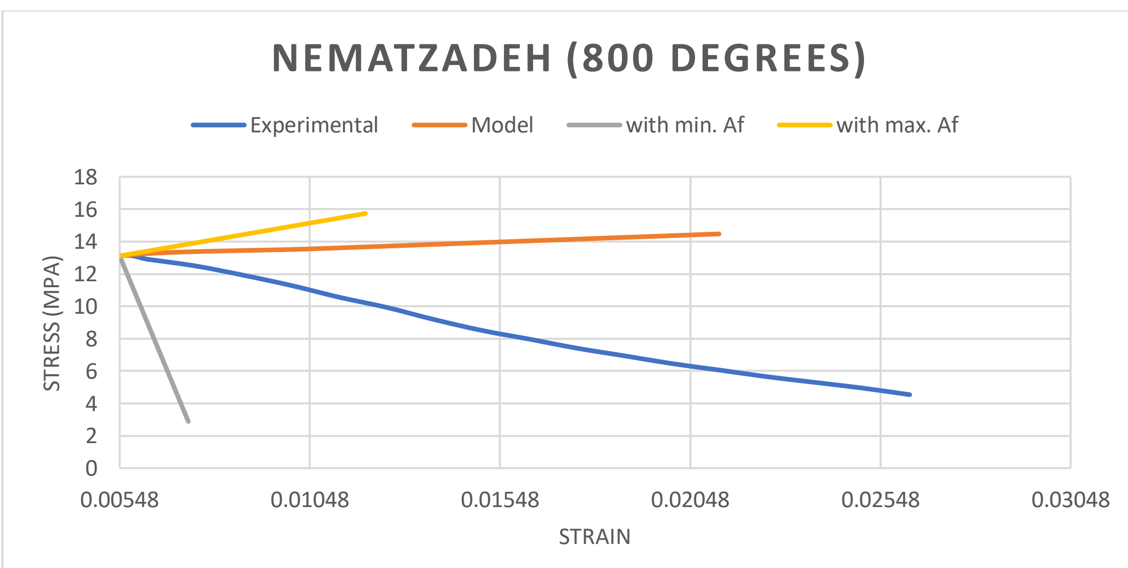

23°C (Normal Strength Concrete-P15)

Properties		
E_c	32400	Mpa
f_c'	34.6	Mpa
ε_{c1}	0.00187	
H	200	mm

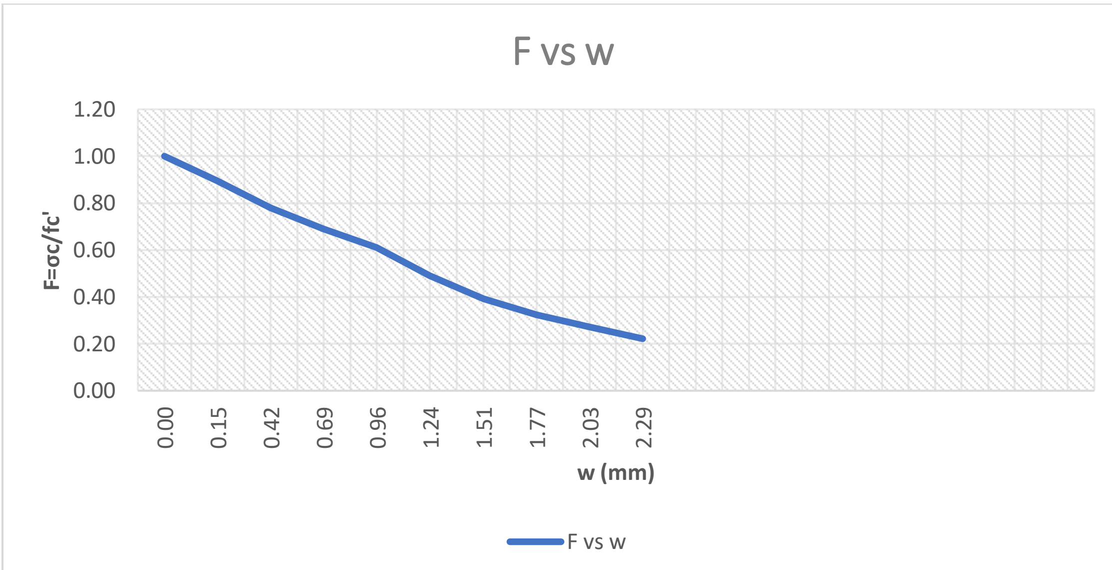

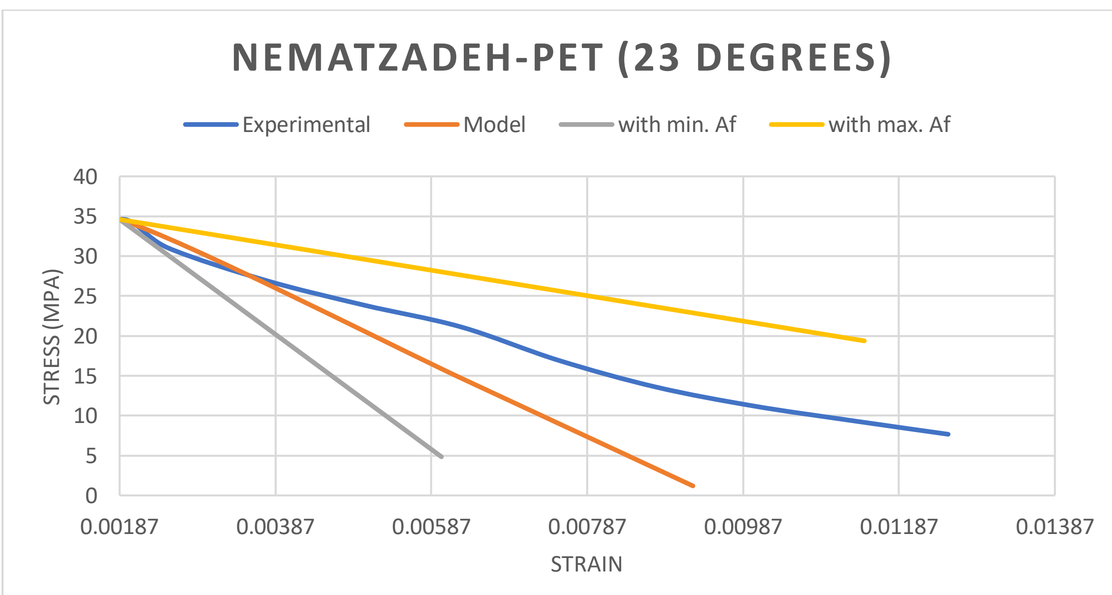

200^{o}C (Normal Strength Concrete-P15)

Properties		
E_c	28192	Mpa
f_c'	26.63	Mpa
ε_{c1}	0.00199	
H	200	mm

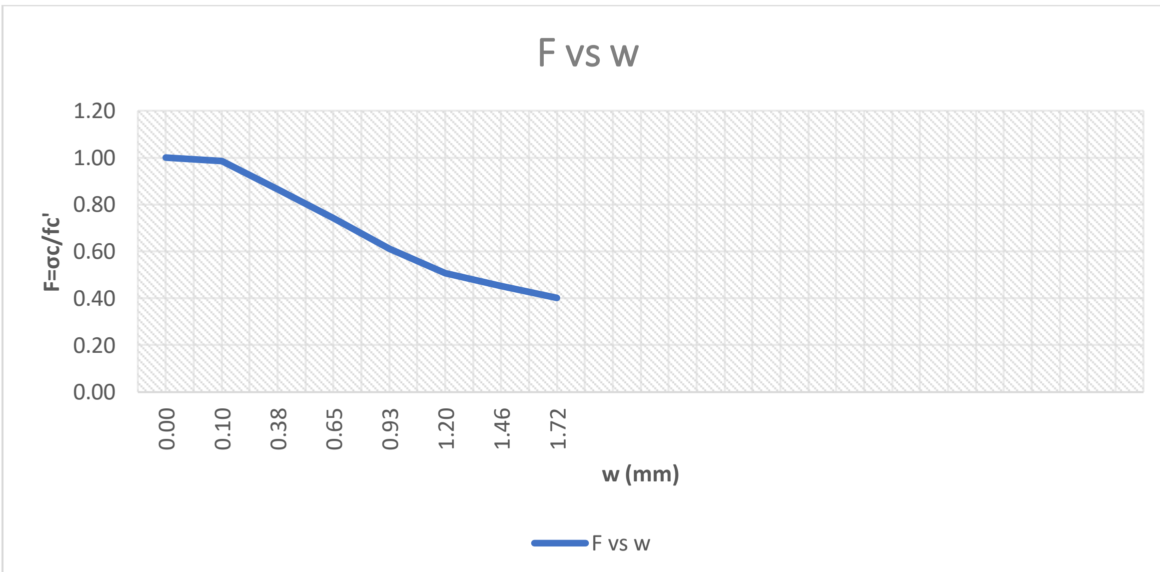

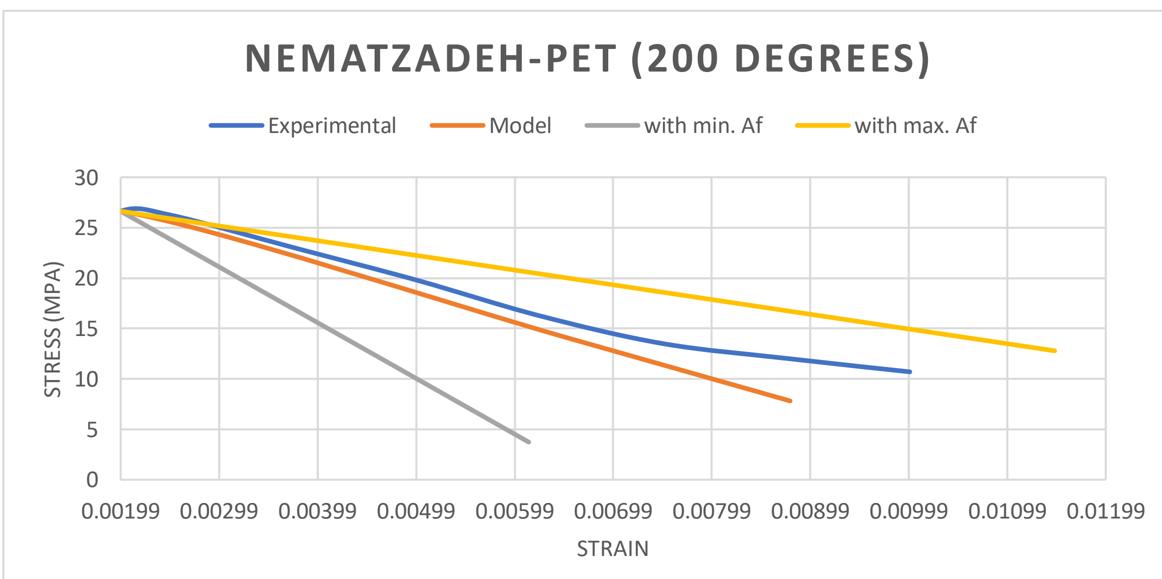

400^{o}C (Normal Strength Concrete-P15)

Properties		
E_c	12624	Mpa
f_c'	21.69	Mpa
ε_{c1}	0.00334	
H	200	mm

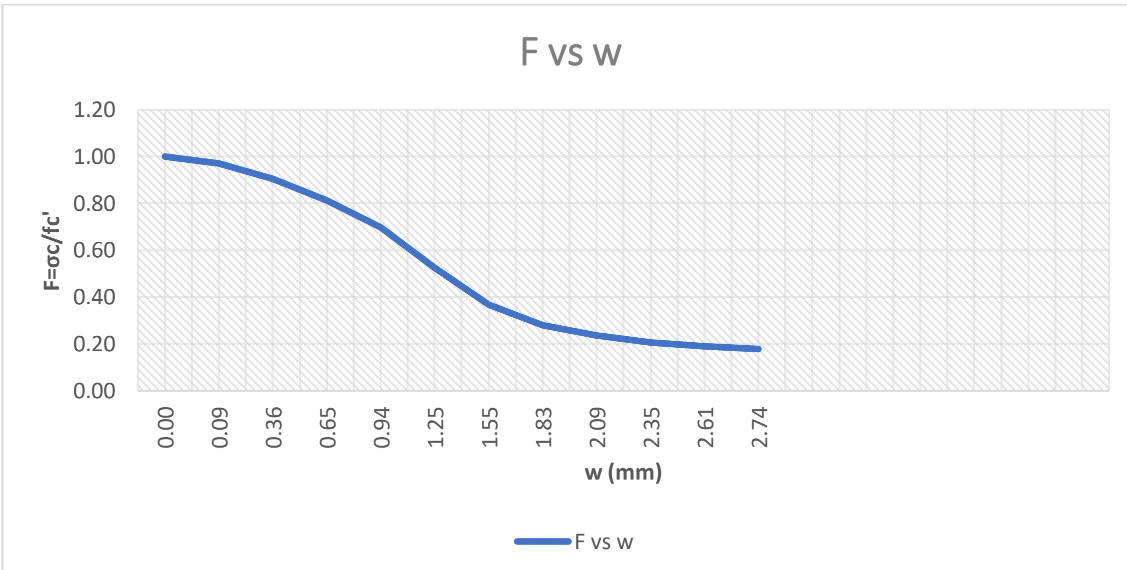

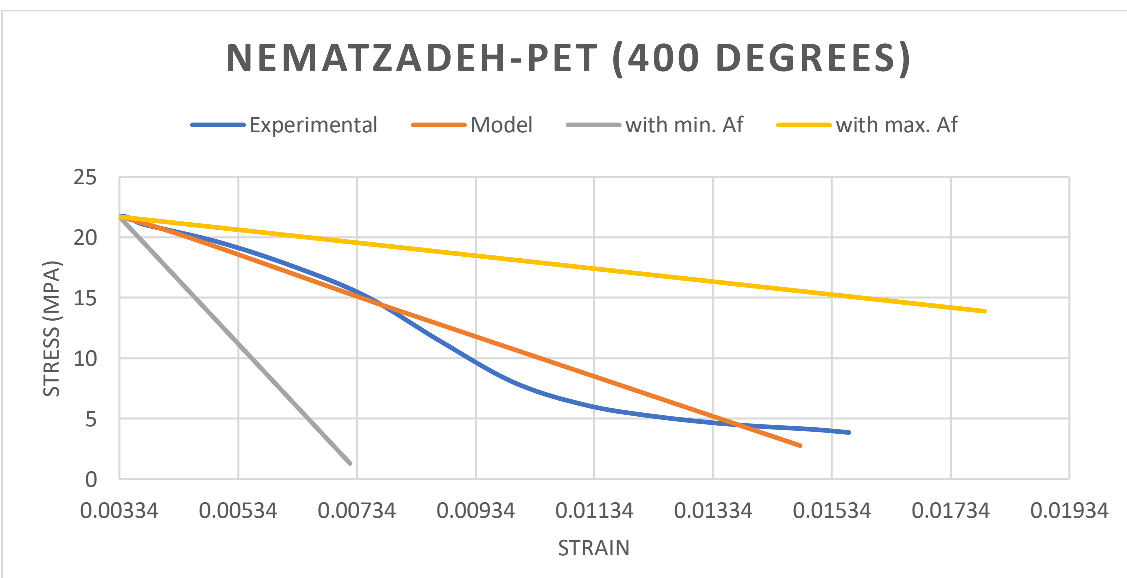

600°C (Normal Strength Concrete-P15)

Properties		
E_c	4736	Mpa
f_c'	13.32	Mpa
ε_{c1}	0.00537	
H	200	mm

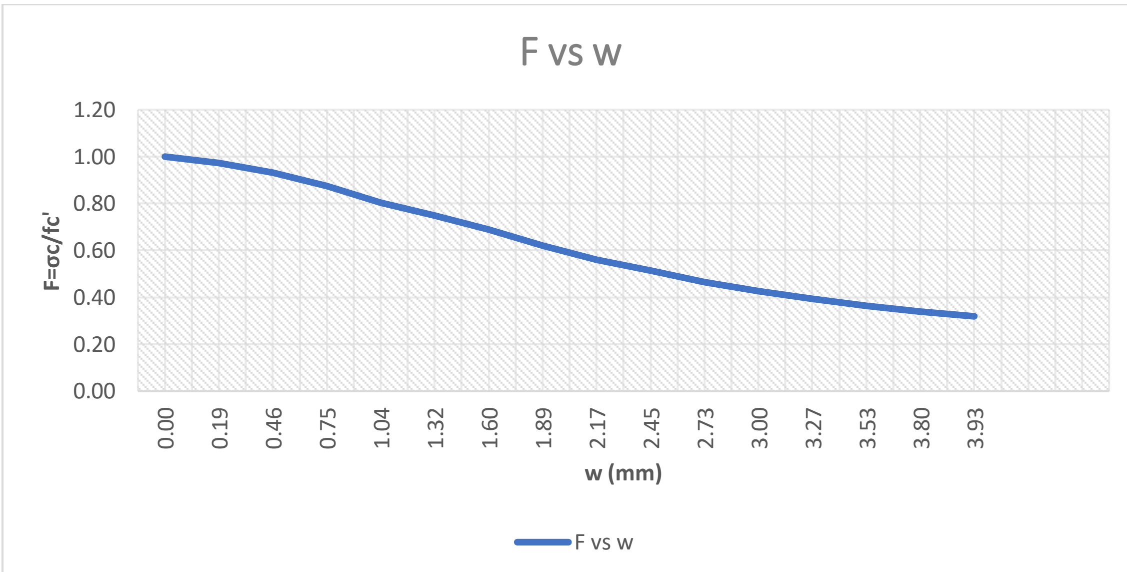

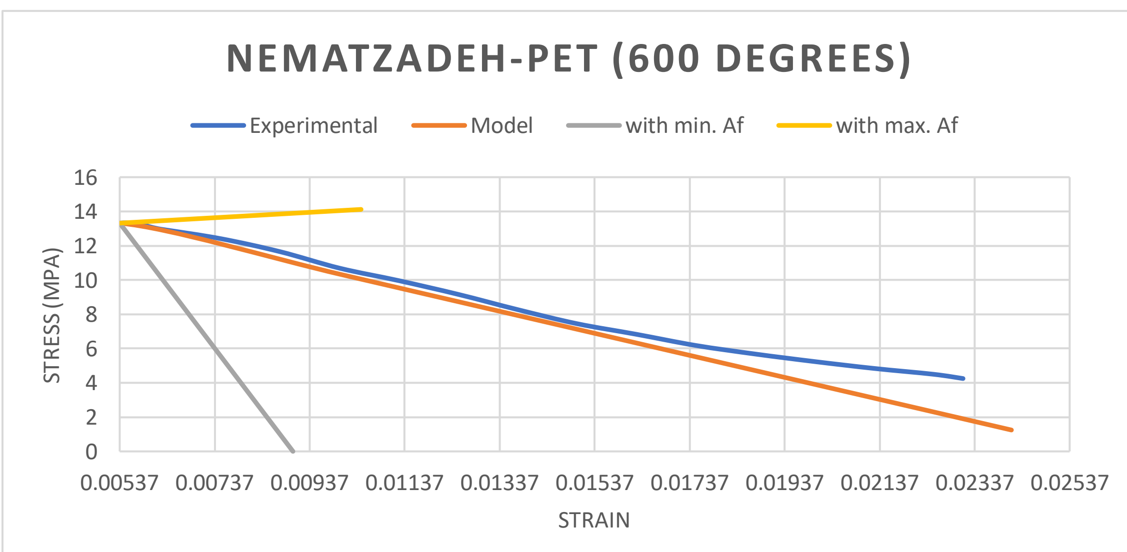

800^{o}C (Normal Strength Concrete-P15)

Properties		
E_c	3792	Mpa
f_c'	8.63	Mpa
ε_{c1}	0.00586	
H	200	mm

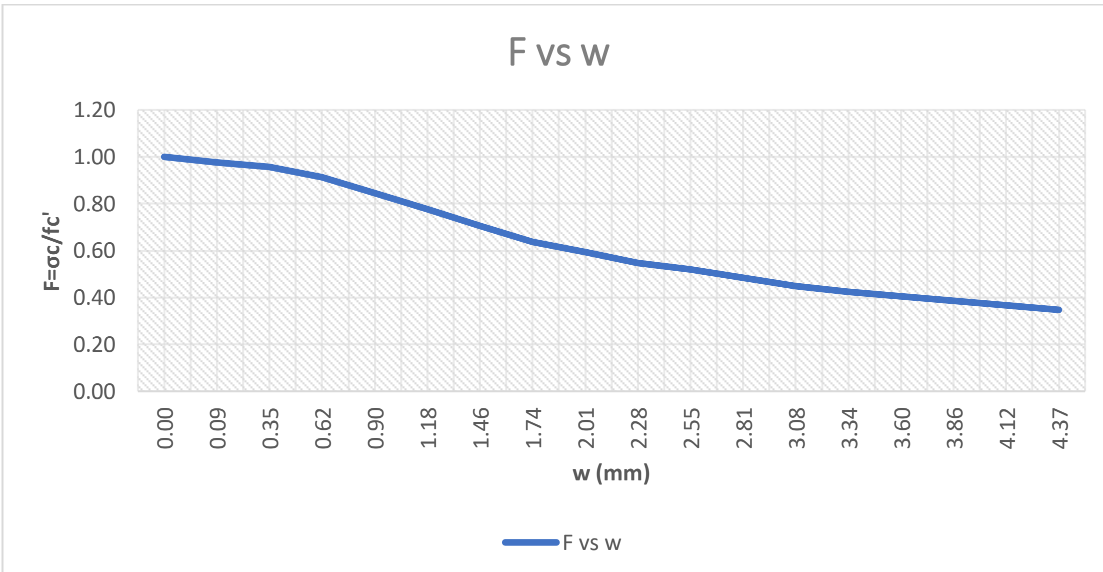

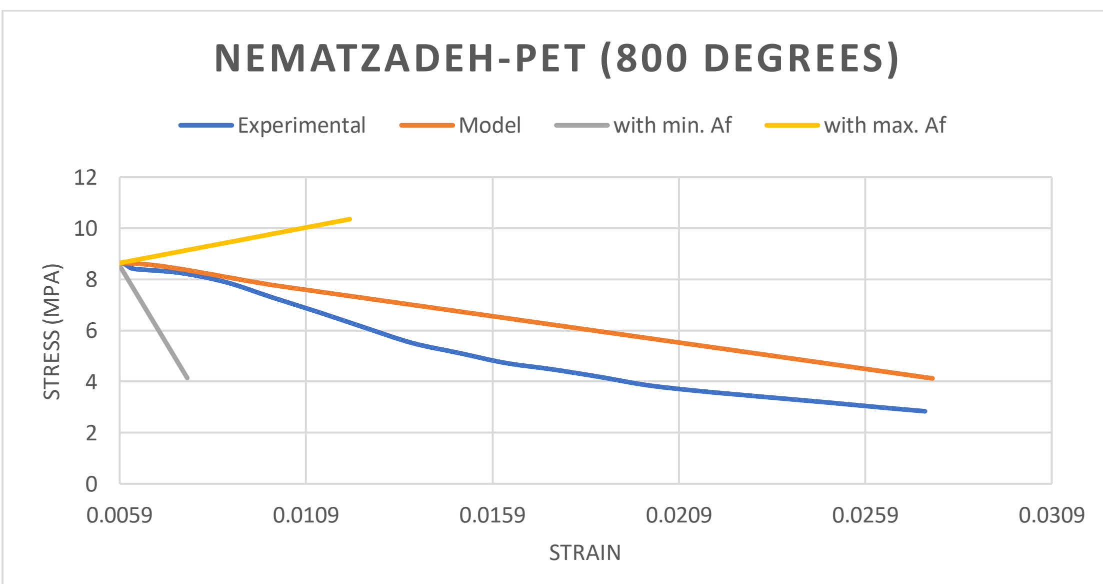

23°C (Normal Strength Concrete-T15)

Properties		
Slope/E_c	33000	Mpa
f_c'	33.2	Mpa
ε_{c1}	0.00200	
H	200	mm

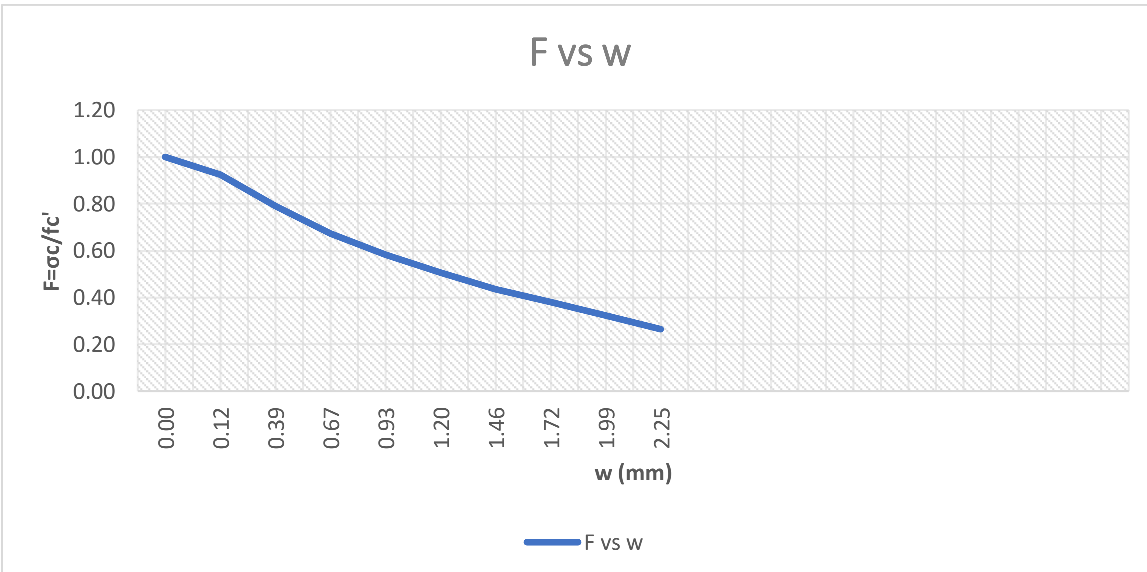

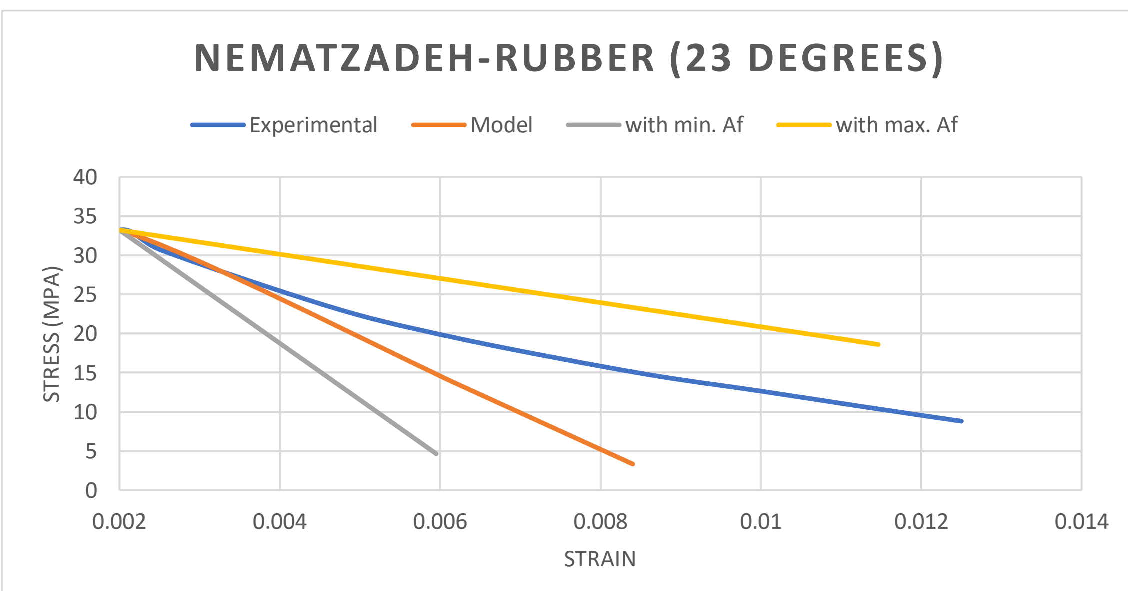

200°C (Normal Strength Concrete-T15)

Properties		
Slope/E_c	28240	Mpa
f_c'	25.98	Mpa
ε_{c1}	0.00195	
H	200	mm

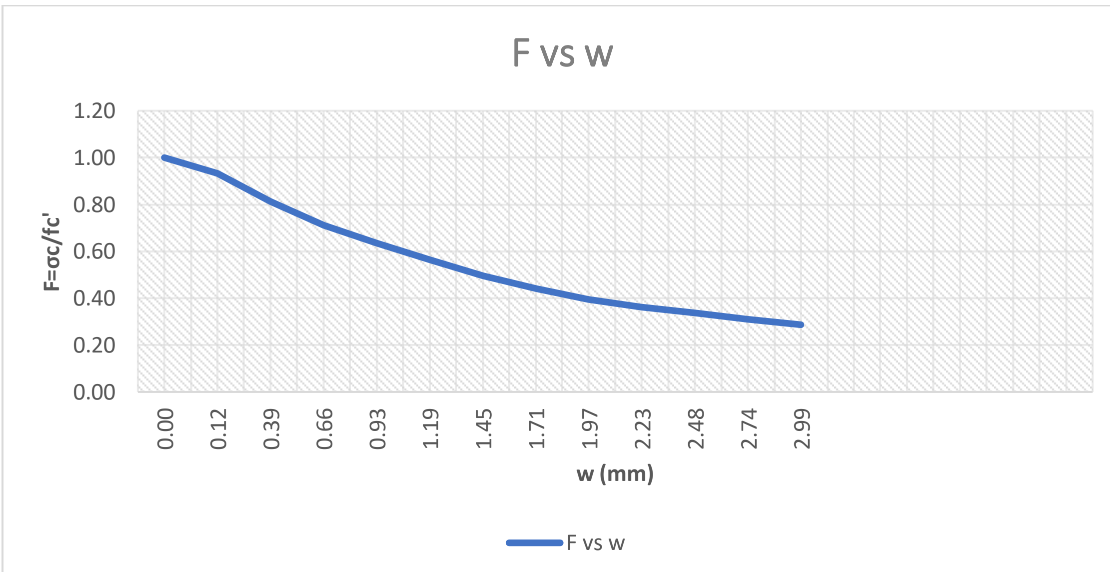

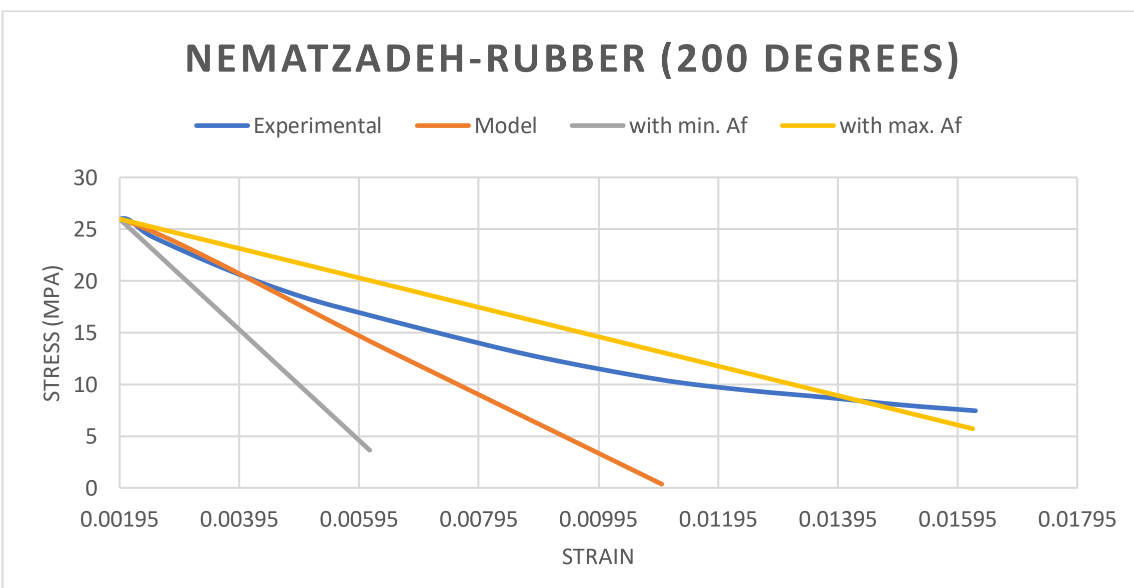

400°C (Normal Strength Concrete-T15)

Properties		
E_c	15856	Mpa
f_c'	22.27	Mpa
ε_{c1}	0.00255	
H	200	mm

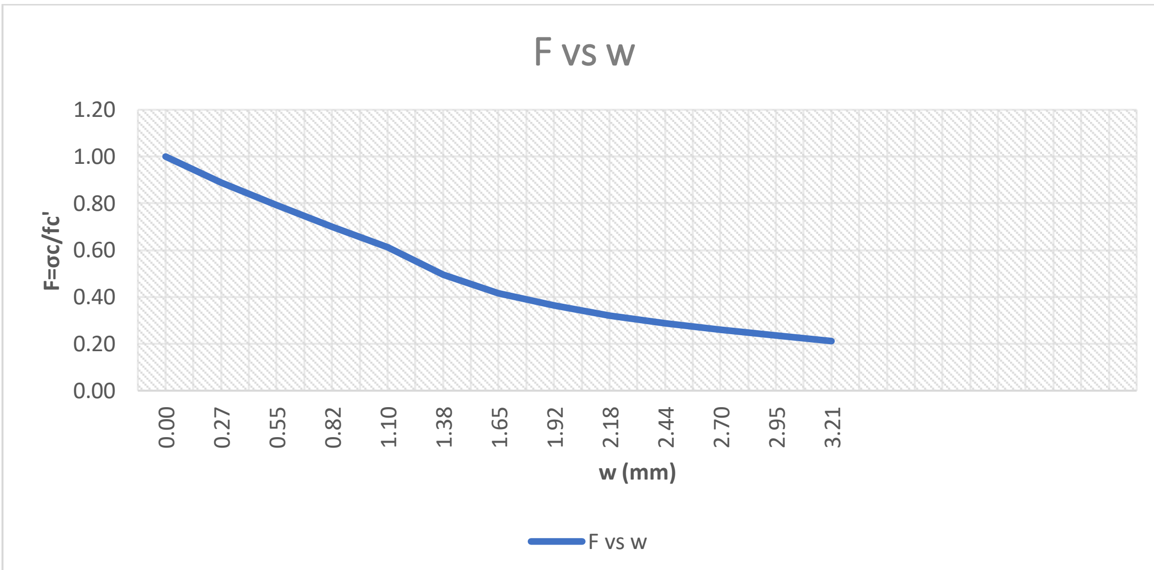

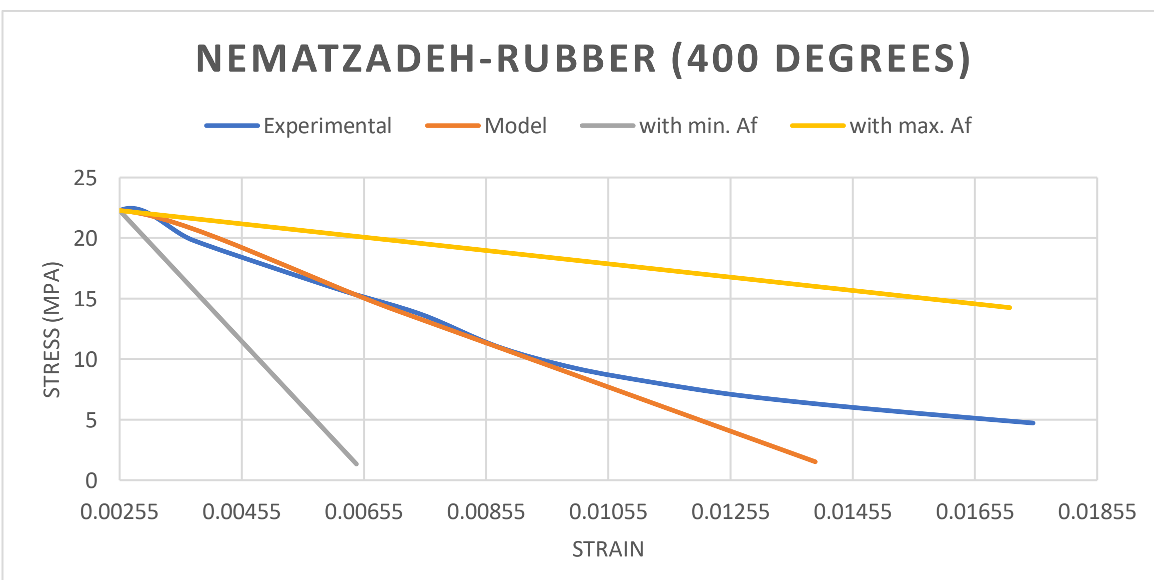

600ºC (Normal Strength Concrete-T15)

Properties		
E_c	3156.8	Mpa
f_c'	9.98	Mpa
ε_{c1}	0.00438	
H	200	mm

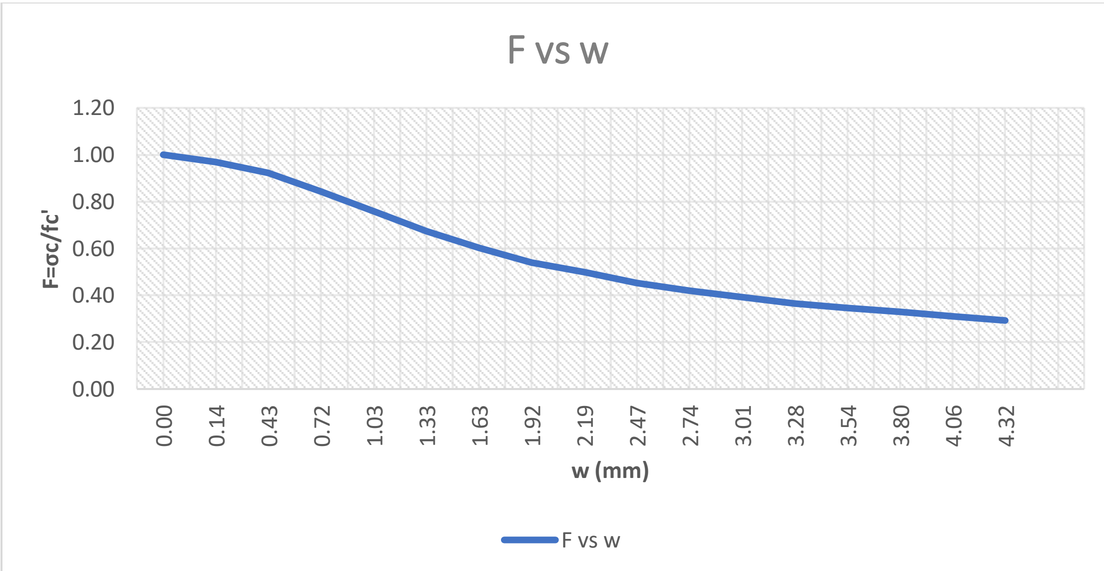

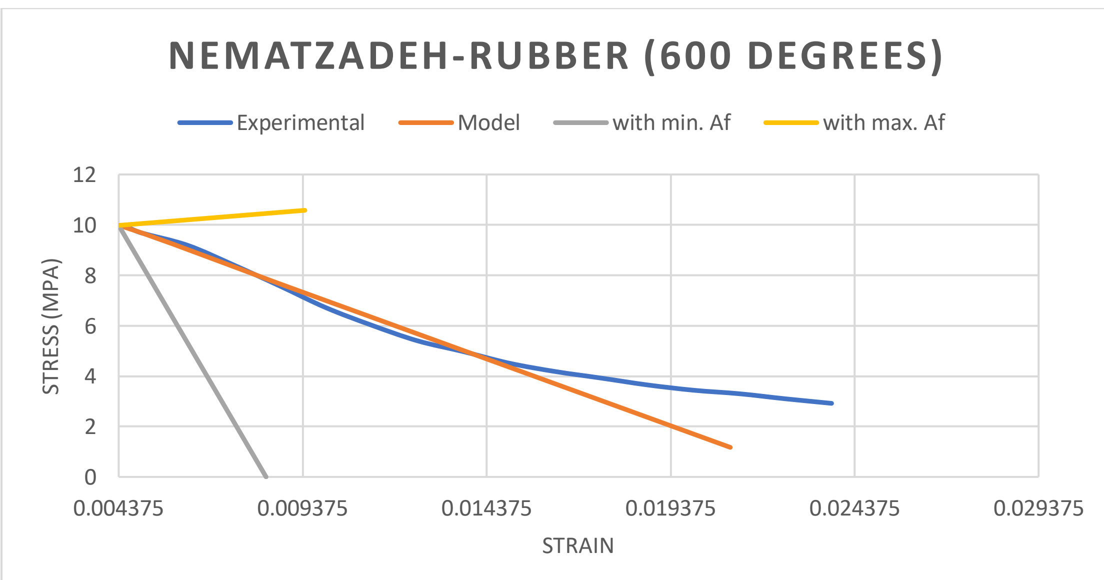

800°C (Normal Strength Concrete-T15)

Properties		
E_c	2560	Mpa
f_c'	6.51	Mpa
ε_{c1}	0.00563	
H	200	mm

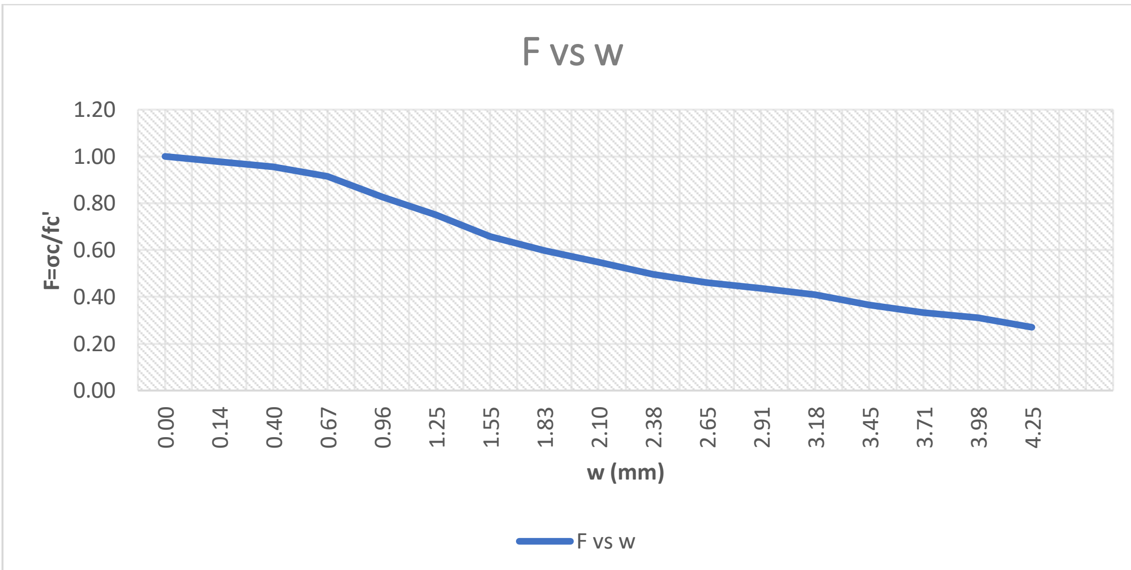

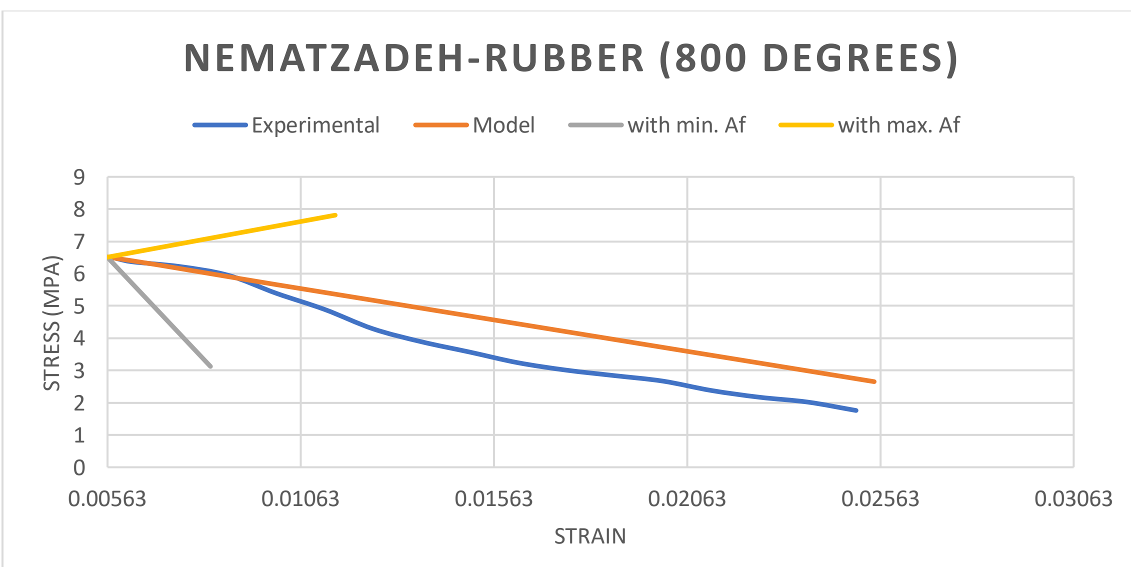

23°C (Normal Strength Concrete-P7.5T7.5)

Properties		
E_c	31630	Mpa
f_c'	30.93	Mpa
ε_{c1}	0.00200	
H	200	mm

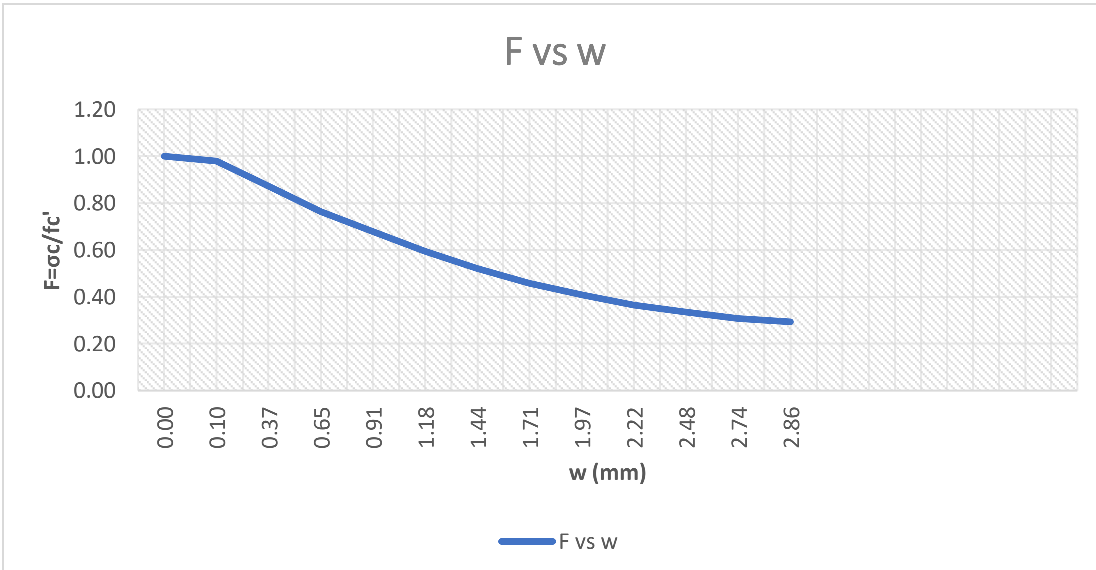

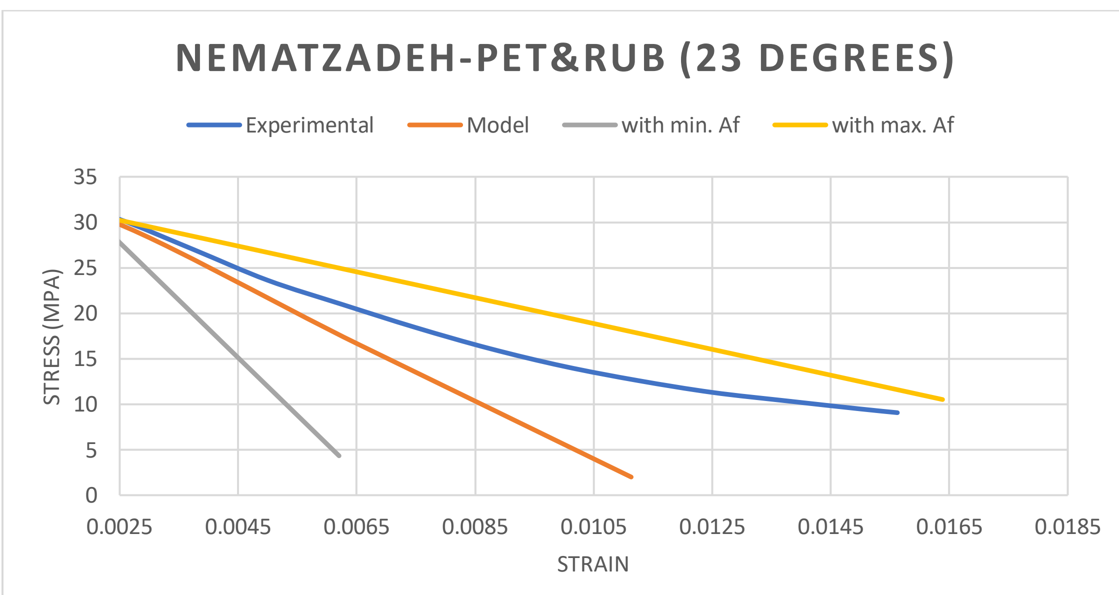

200^{o}C (Normal Strength Concrete-P7.5T7.5)

Properties		
E_c	23648	Mpa
f_c'	23.97	Mpa
ε_{c1}	0.00220	
H	200	mm

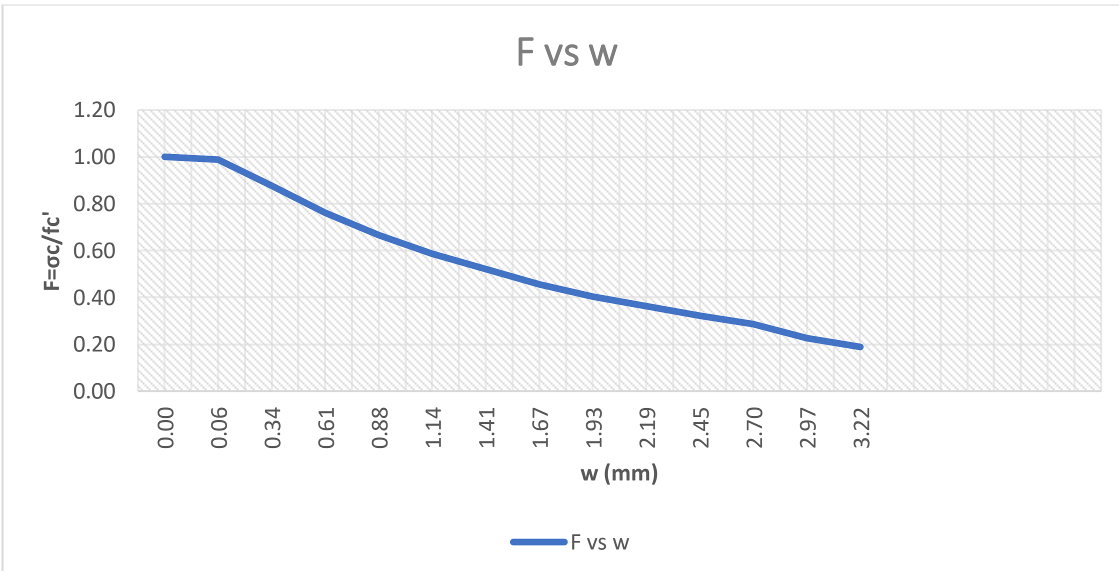

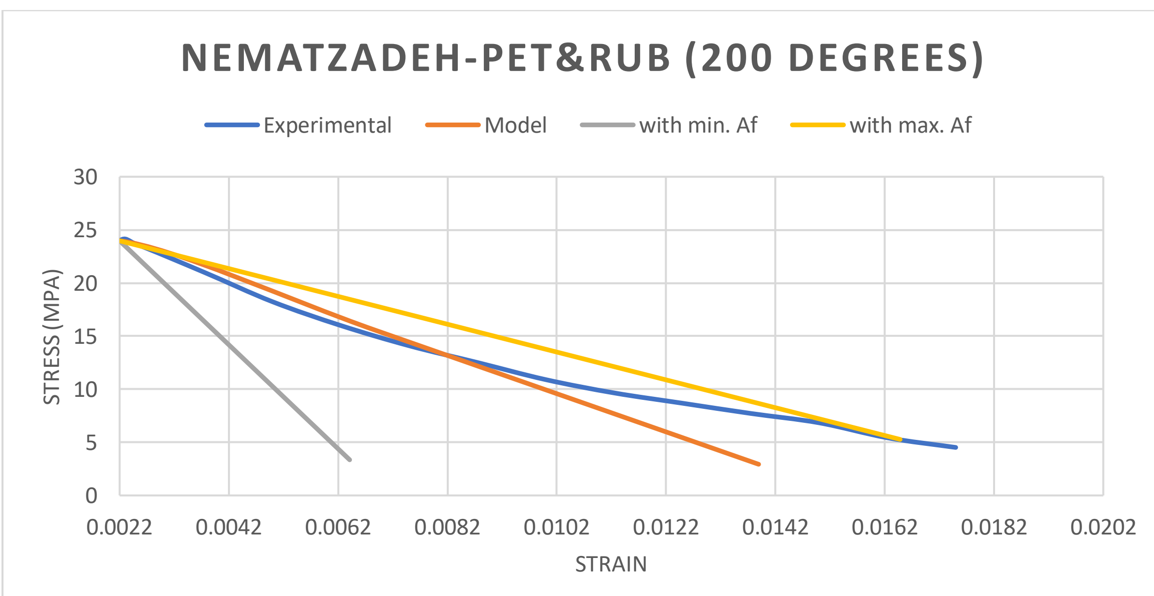

400°C (Normal Strength Concrete-P7.5T7.5)

Properties		
E_c	12064	Mpa
f_c'	21.6	Mpa
ε_{c1}	0.00242	
H	200	mm

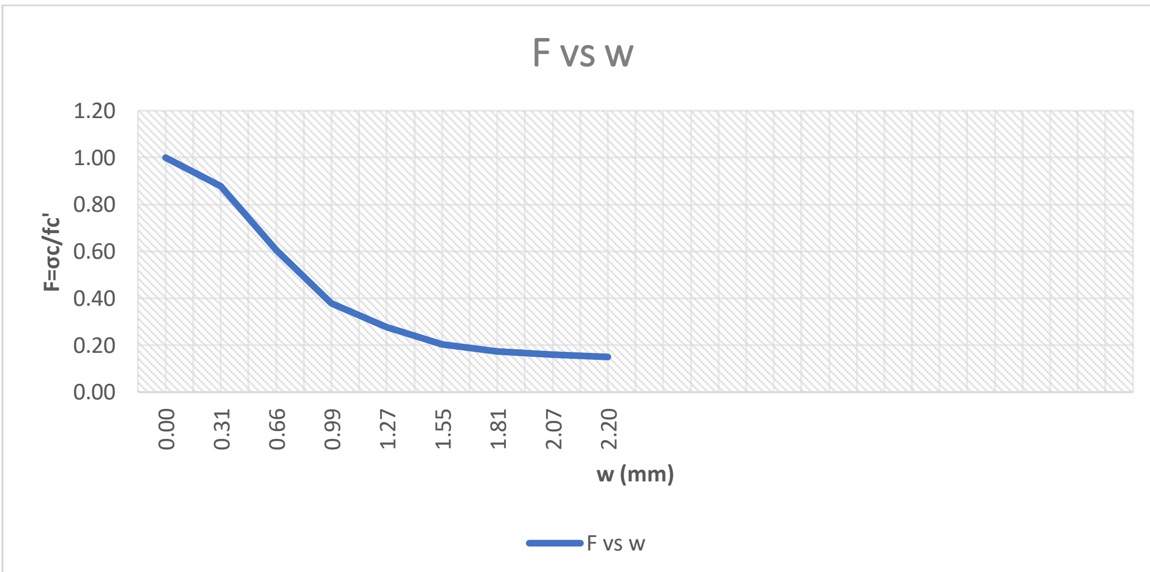

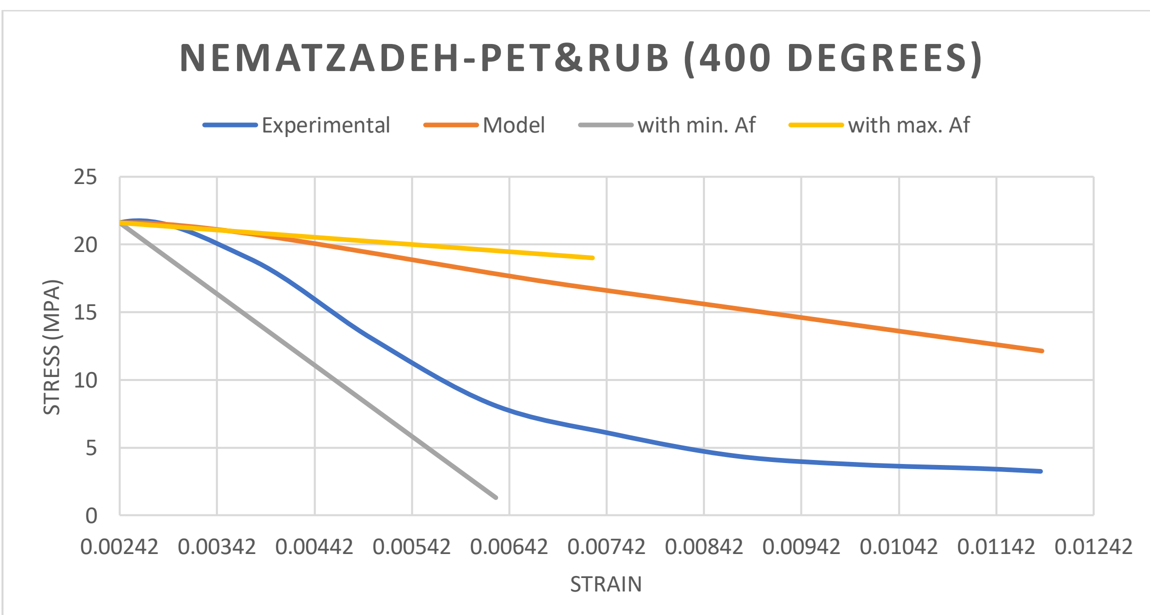

600°C (Normal Strength Concrete-P7.5T7.5)

Properties		
E_c	2736	Mpa
f_c'	8.48	Mpa
ε_{c1}	0.004063	
H	200	mm

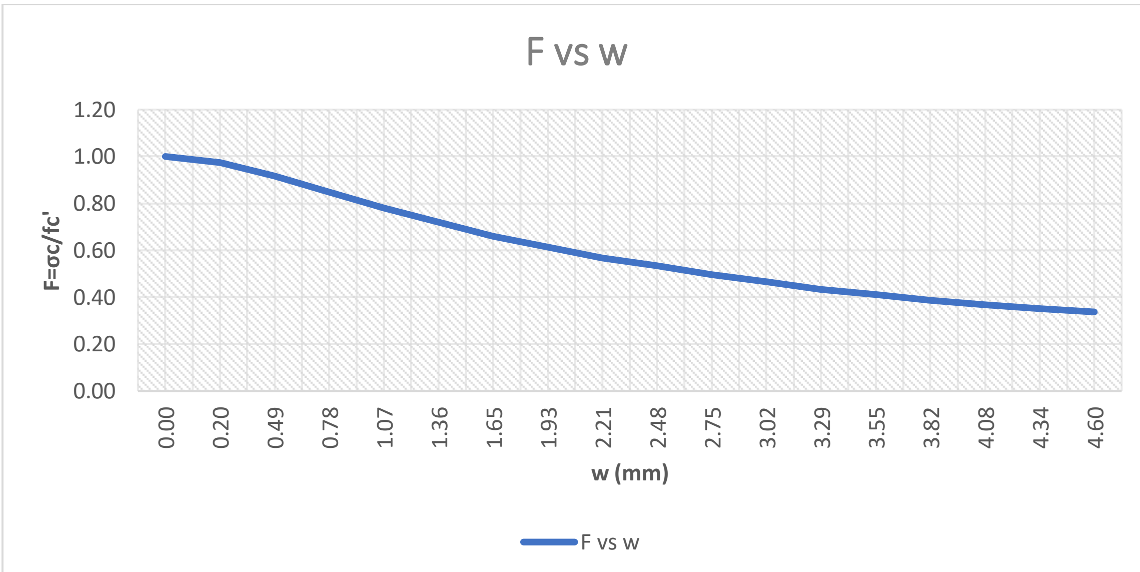

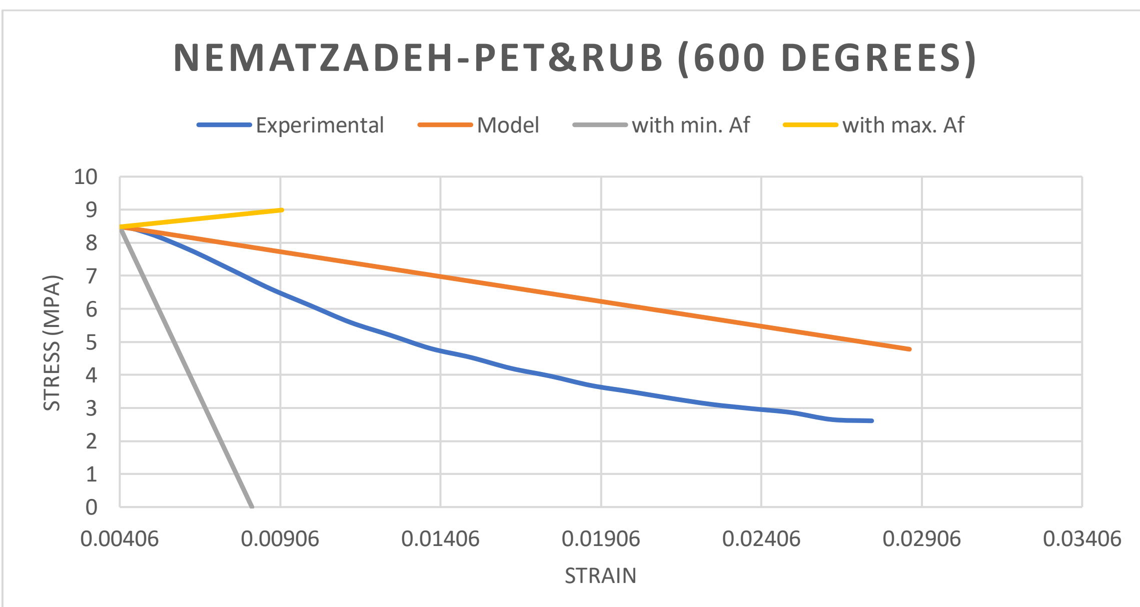

800°C (Normal Strength Concrete-P7.5T7.5)

Properties		
E_c	1446.4	Mpa
f_c'	5.63	Mpa
ε_{c1}	0.005625	
H	200	mm

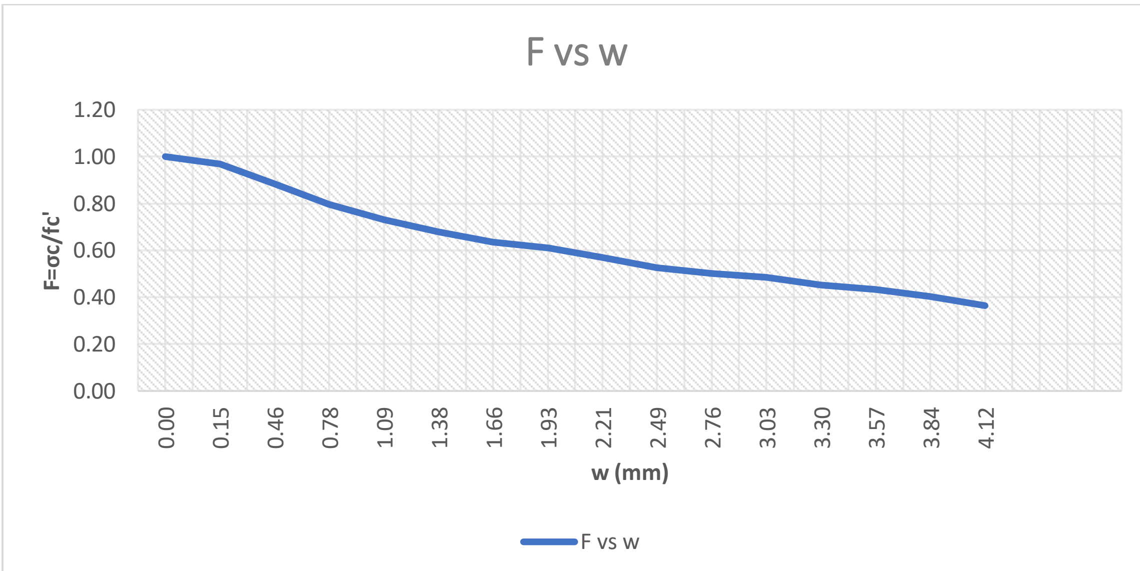

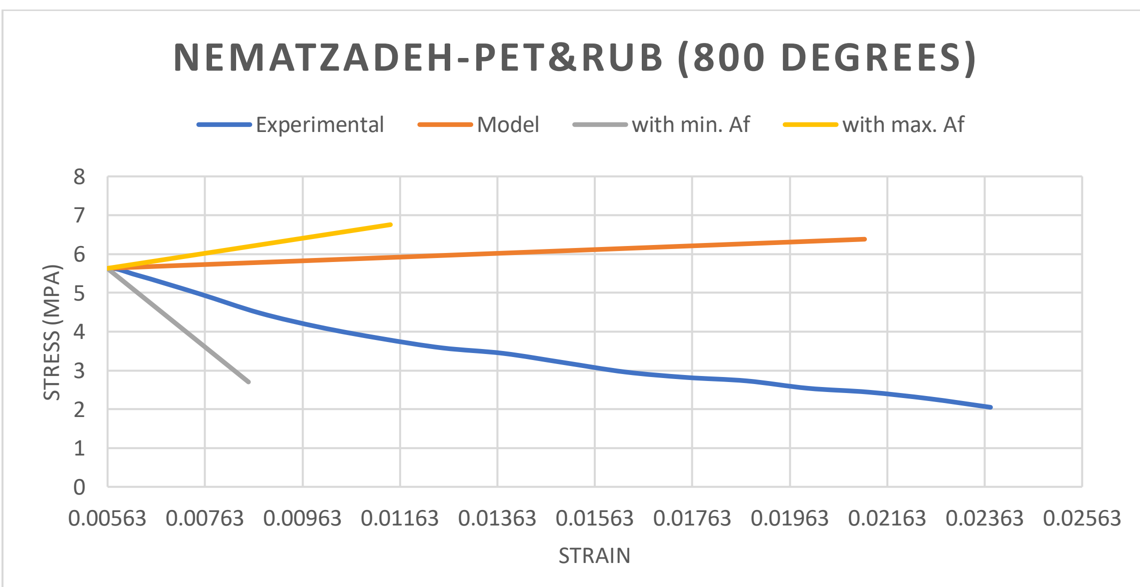

Post-peak analysis of experimental data by (Shi et al., 2002)

20°C (Normal Strength Concrete)

Properties		
E_c	22440	Mpa
f_c'	32.6	Mpa
ε_{c1}	0.002450	
H	300	mm

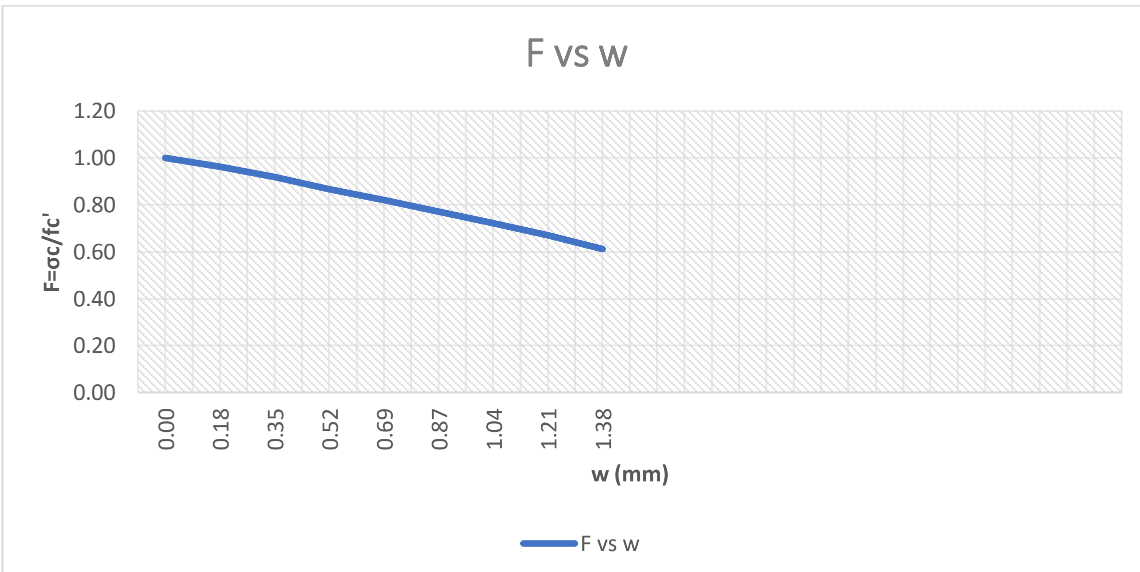

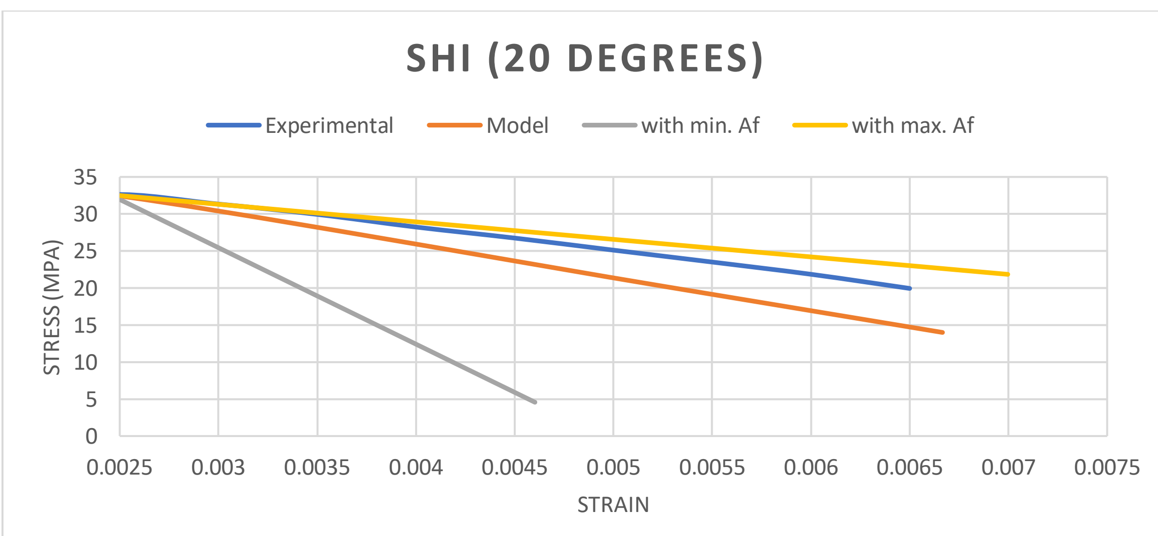

200°C (Normal Strength Concrete)

Properties		
E_c	19440	Mpa
f_c'	31.07	Mpa
ε_{c1}	0.002690	
H	300	mm

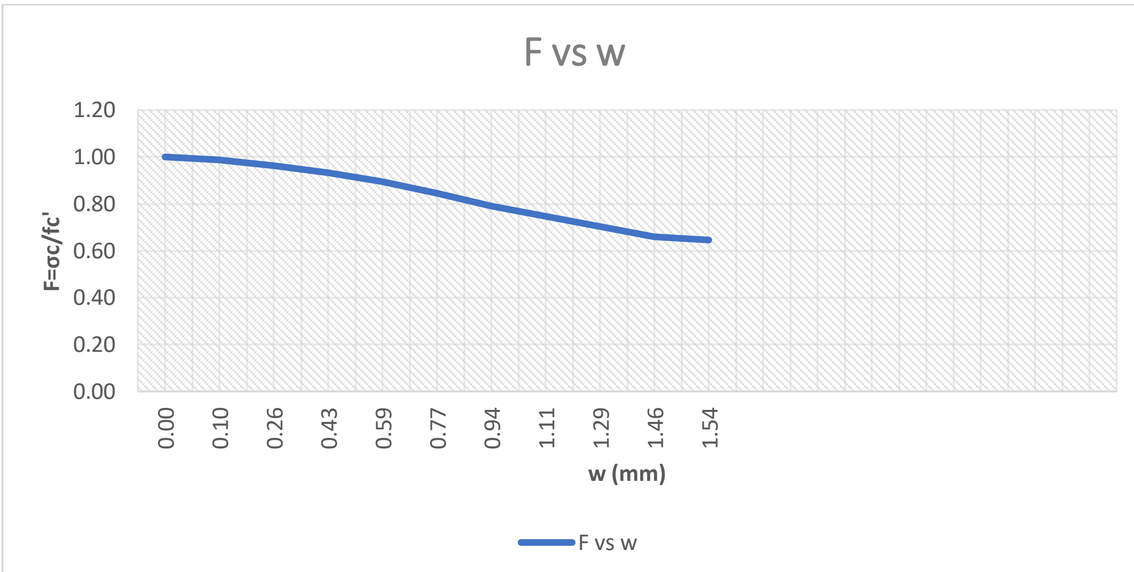

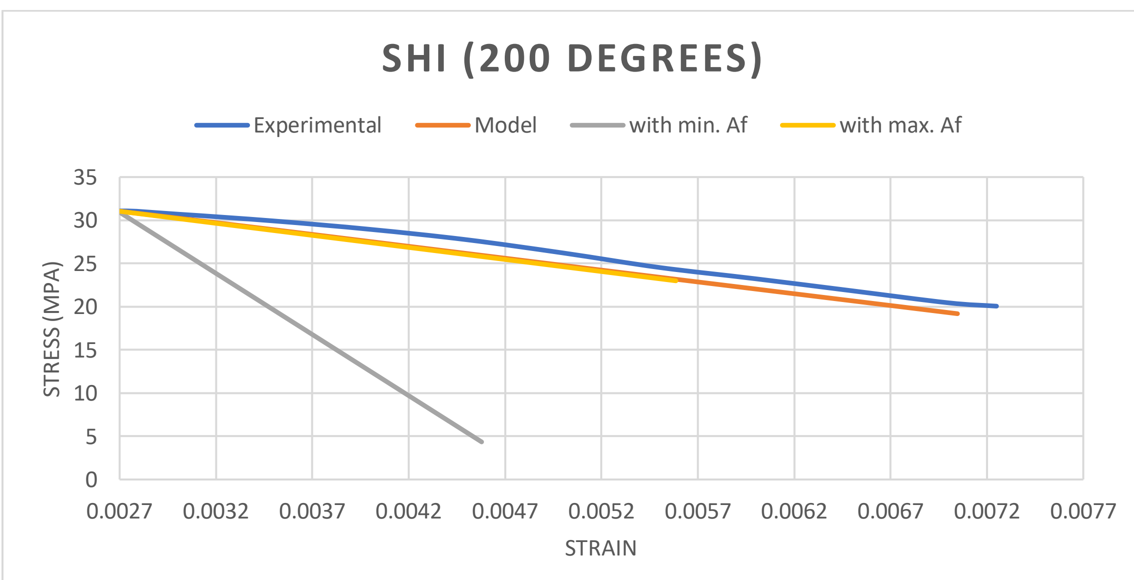

300°C (Normal Strength Concrete)

Properties		
E_c	11440	Mpa
f_c'	28.58	Mpa
ε_{c1}	0.002950	
H	300	mm

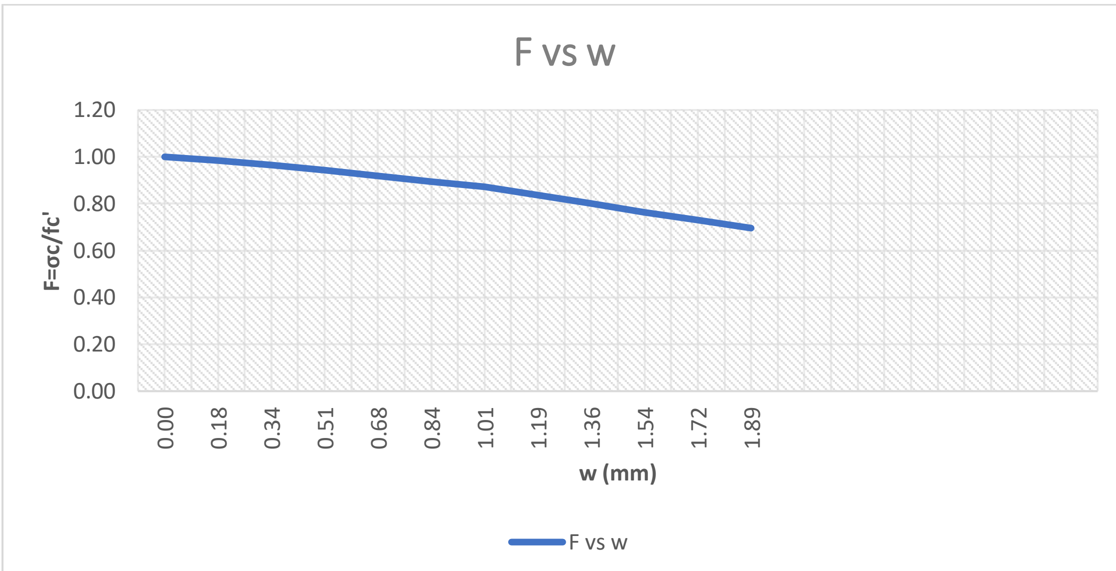

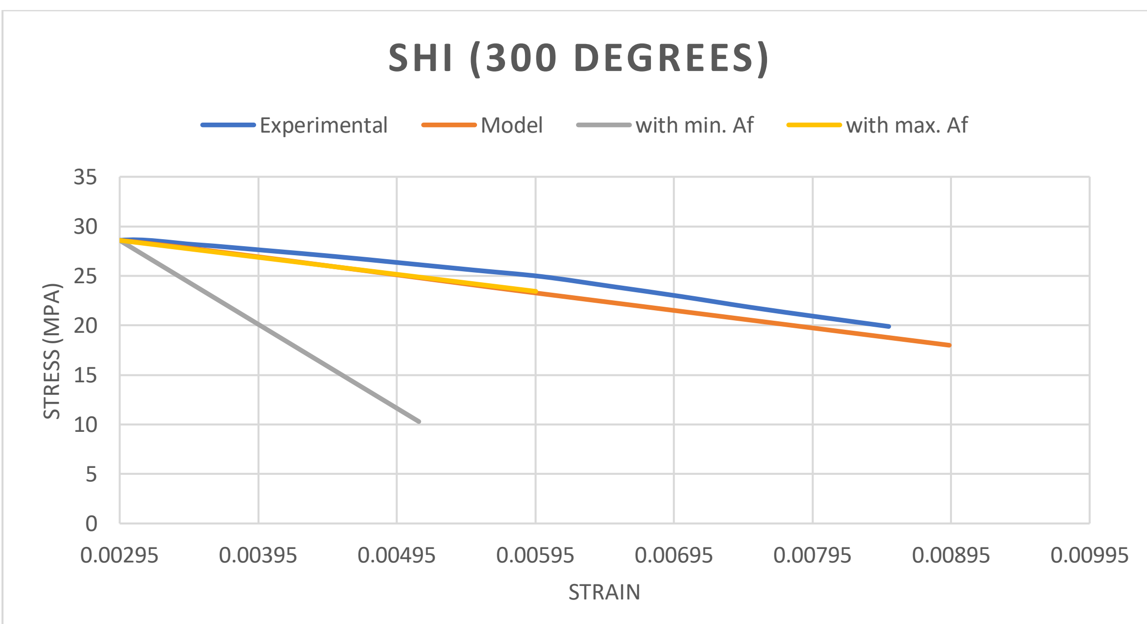

350°C (Normal Strength Concrete)

Properties		
E_c	9700	Mpa
f_c'	27.92	Mpa
ε_{c1}	0.003820	
H	300	mm

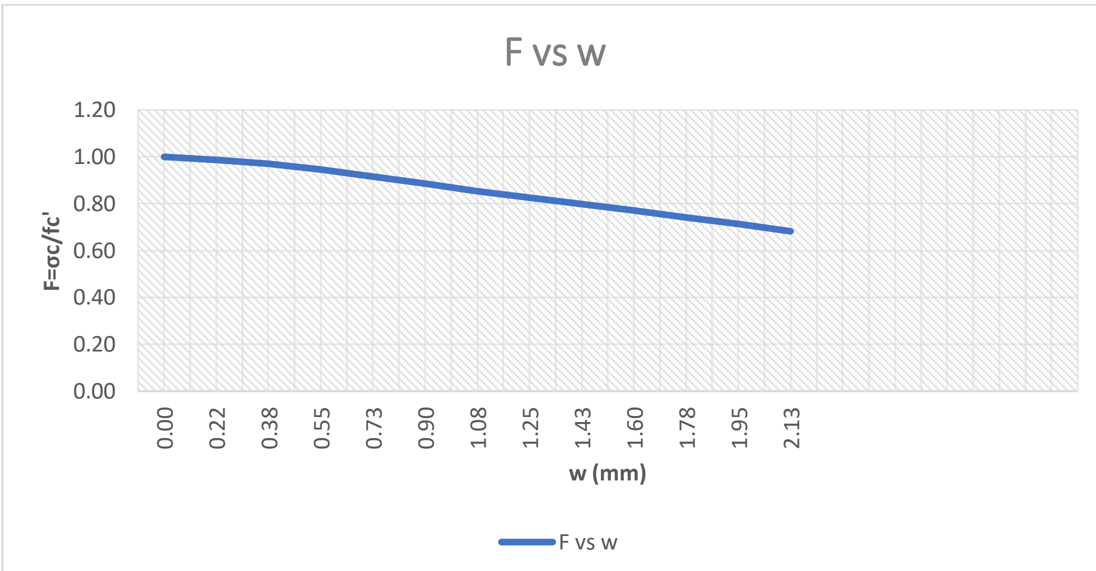

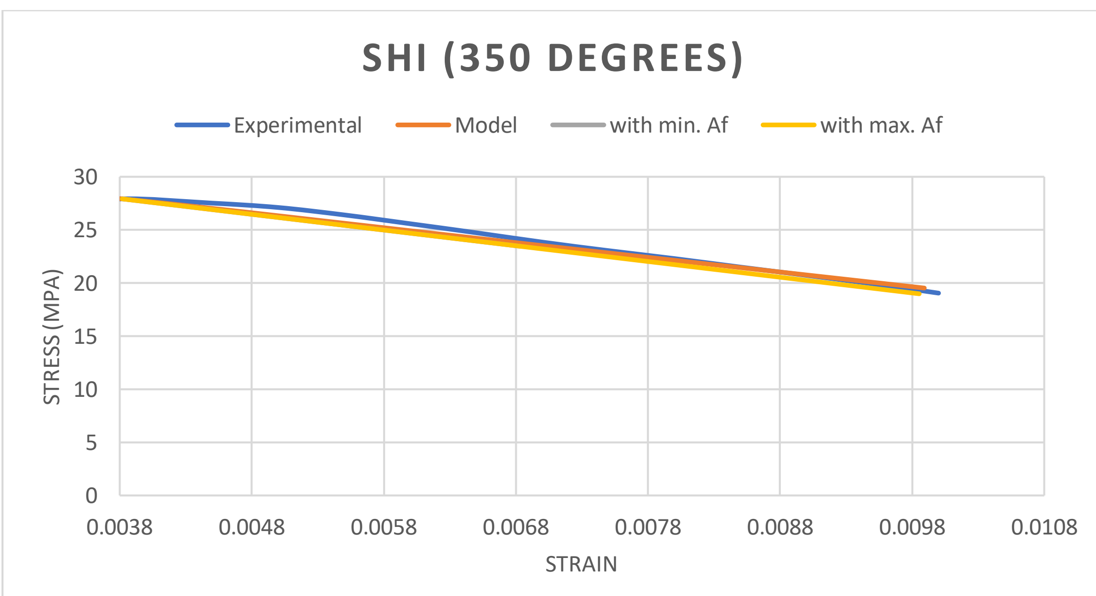

400°C (Normal Strength Concrete)

Properties		
E_c	6600	Mpa
f_c'	21.67	Mpa
ε_{c1}	0.005030	
H	300	mm

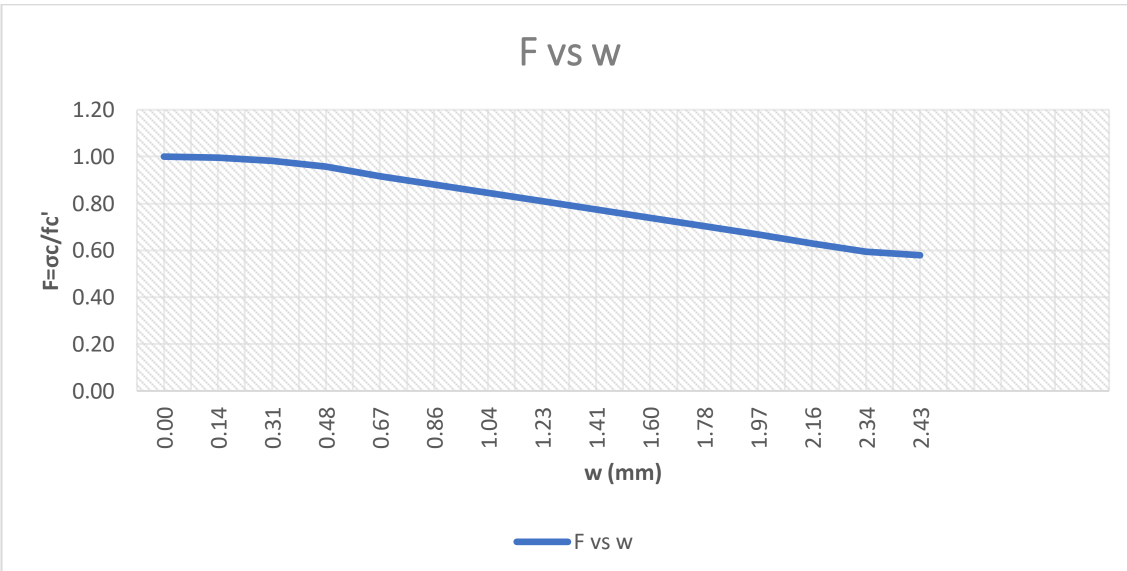

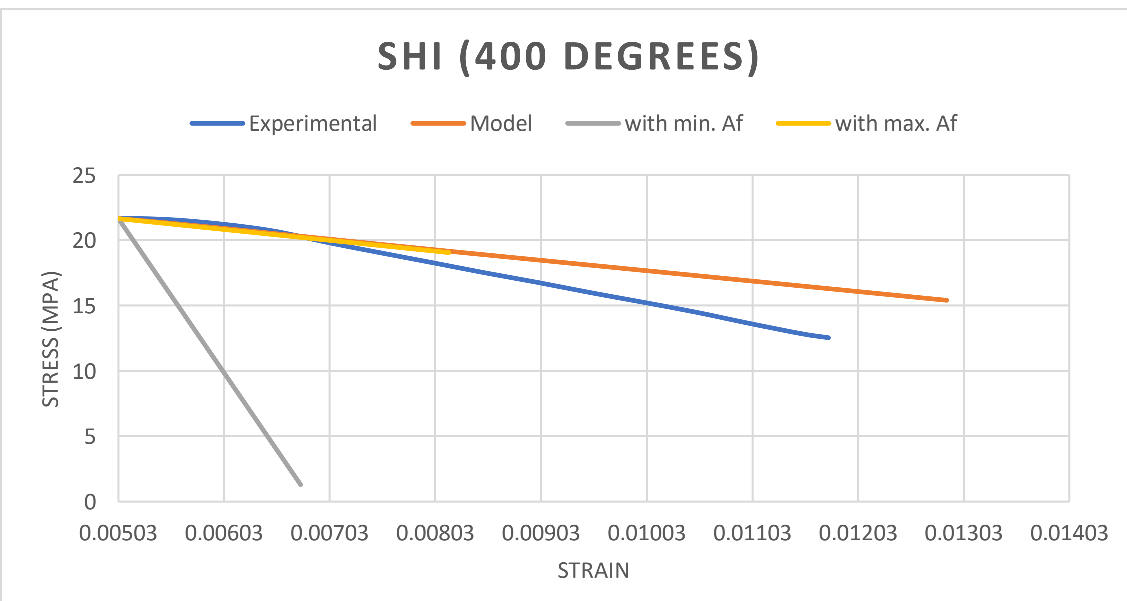

500°C (Normal Strength Concrete)

Properties		
E_c	5452	Mpa
f_c'	19.13	Mpa
ε_{c1}	0.005380	
H	300	mm

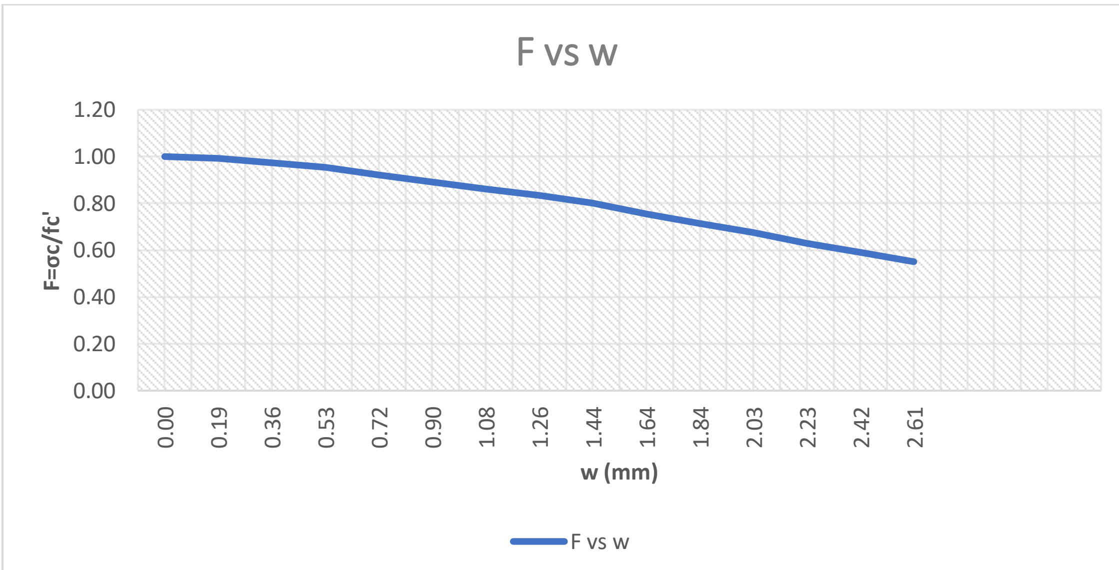

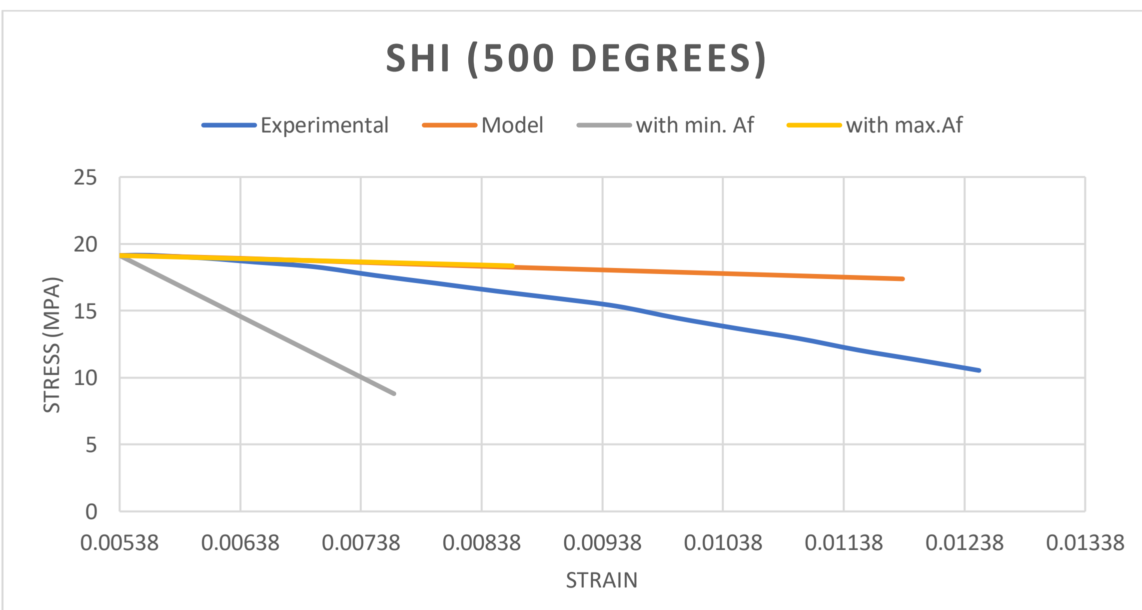

600°C (Normal Strength Concrete)

Properties		
E_c	3526	Mpa
f_c'	17.92	Mpa
ε_{c1}	0.006670	
H	300	mm

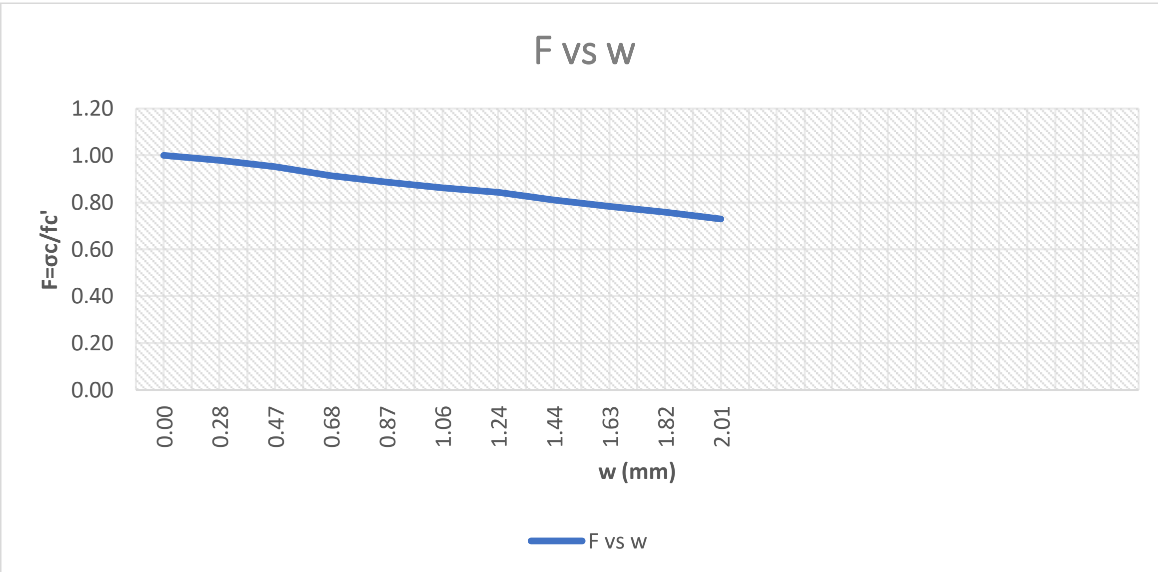

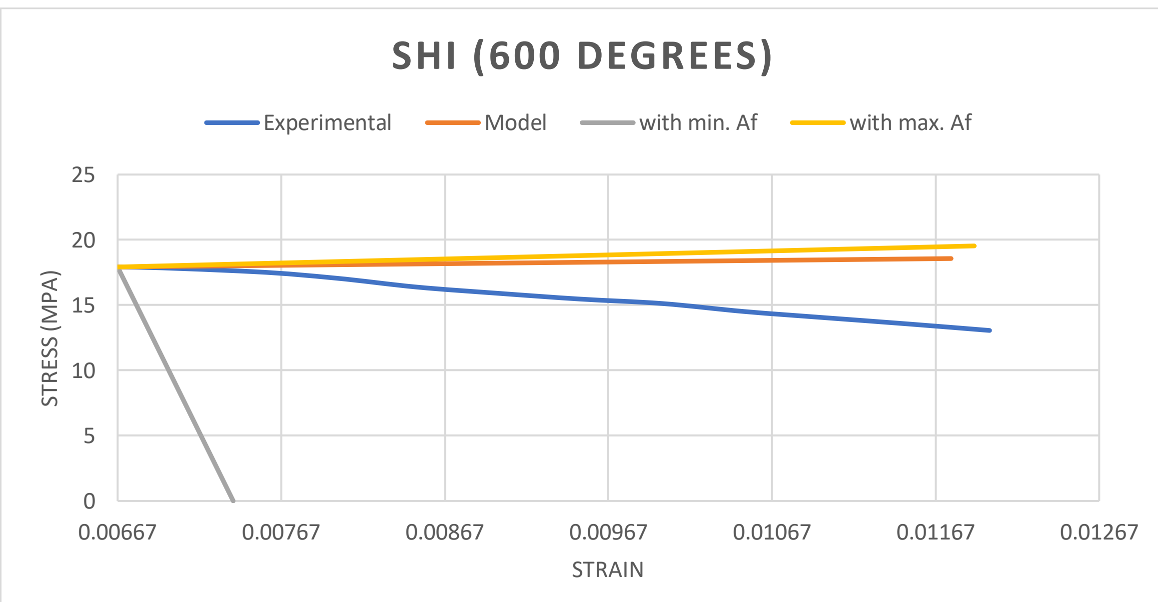

700°C (Normal Strength Concrete)

Properties		
E_c	1692	Mpa
f_c'	10.36	Mpa
ε_{c1}	0.008510	
H	300	mm

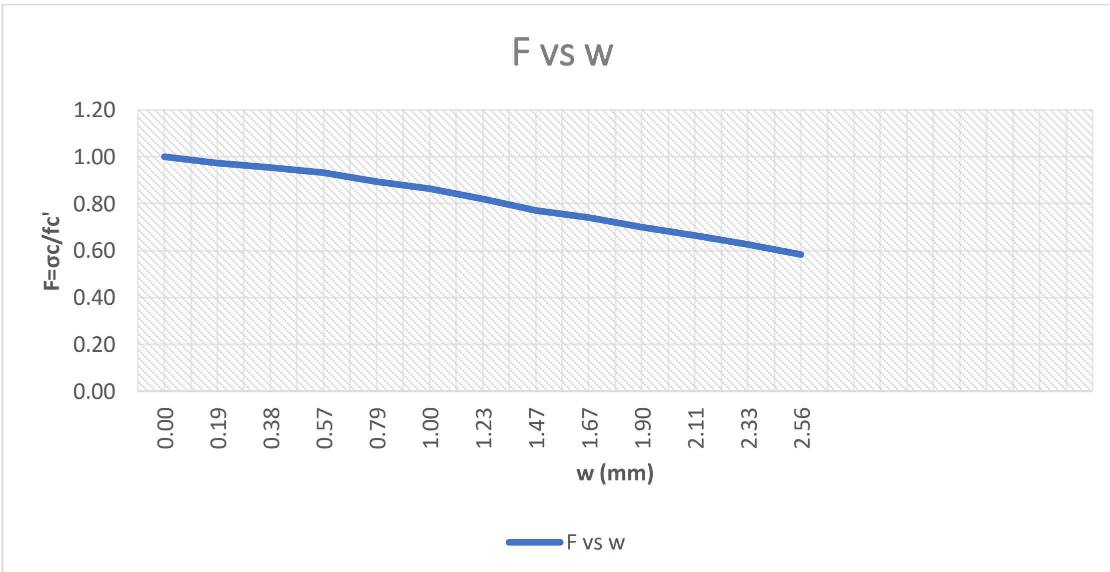

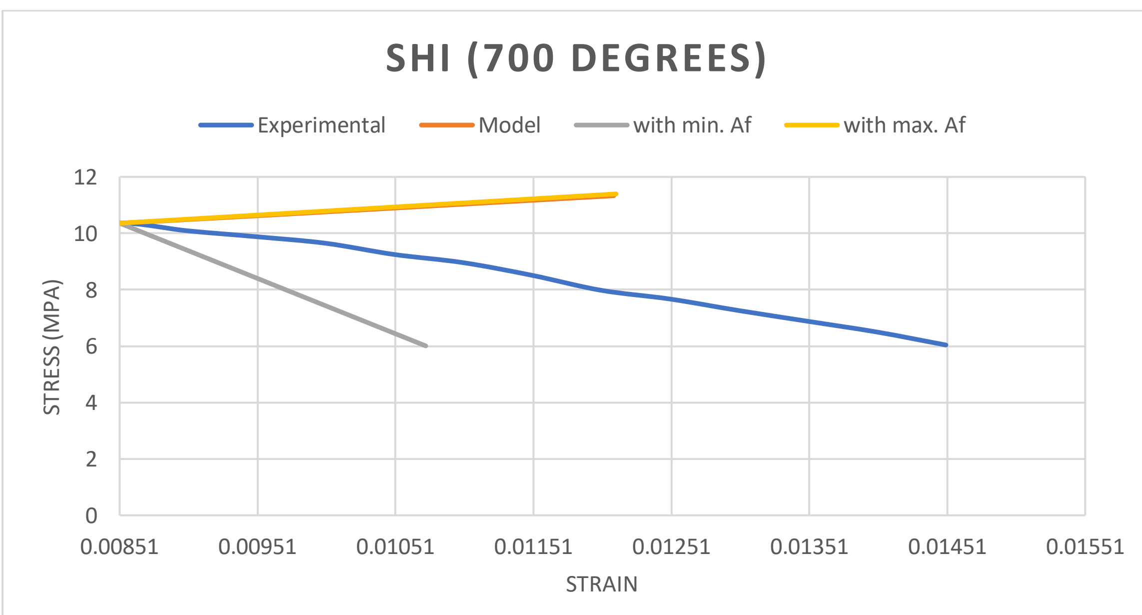

800°C (Normal Strength Concrete)

Properties		
E_c	650	Mpa
f_c'	3.26	Mpa
ε_{c1}	0.011500	
H	300	mm

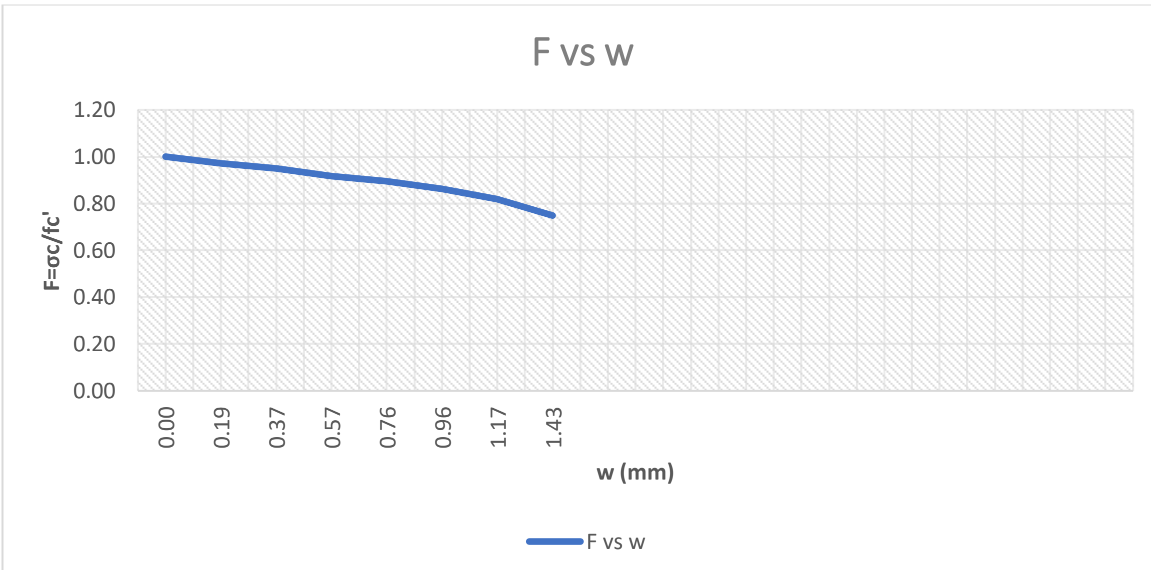

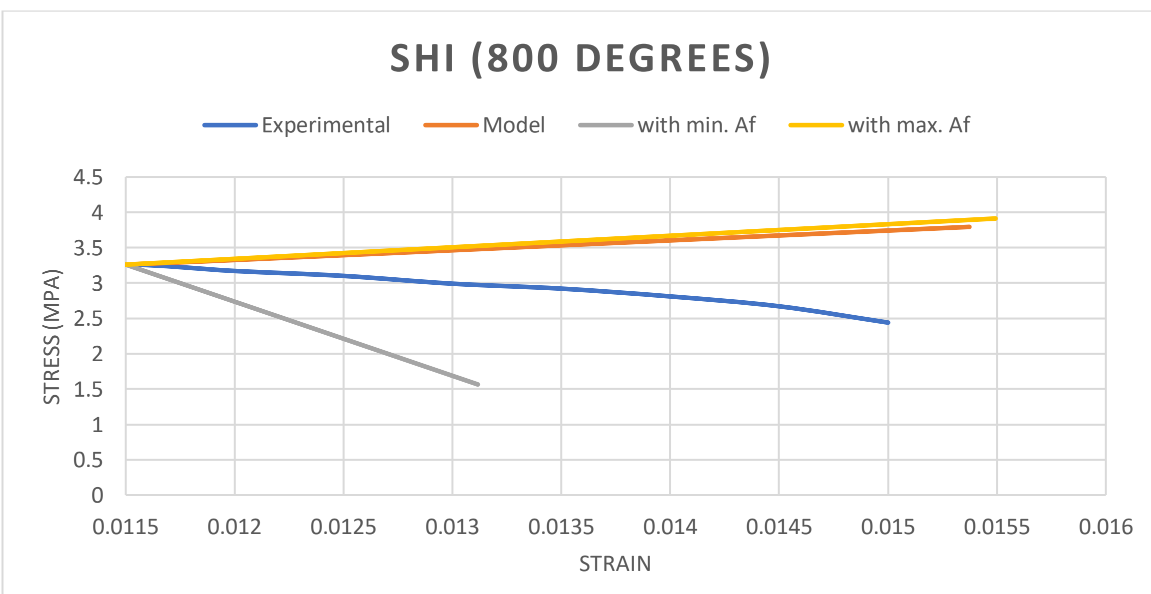

Post-peak analysis of experimental data by (Lo Monte et al., 2015)

20°C (M0 Concrete)

Properties		
E_c	22680	Mpa
f_c'	25.71	Mpa
ε_{c1}	0.002500	
H	300	mm

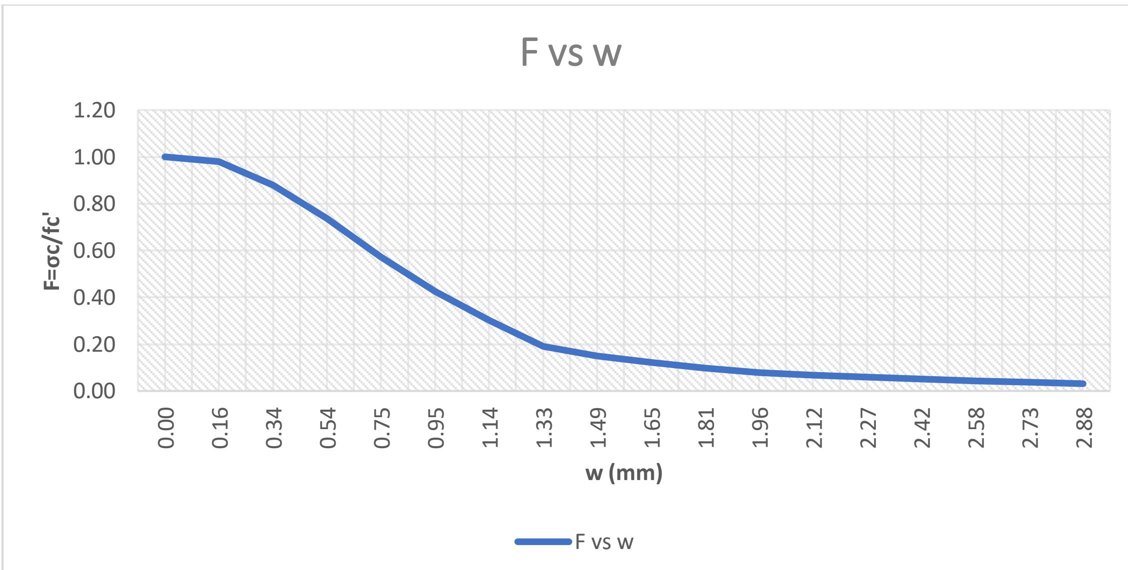

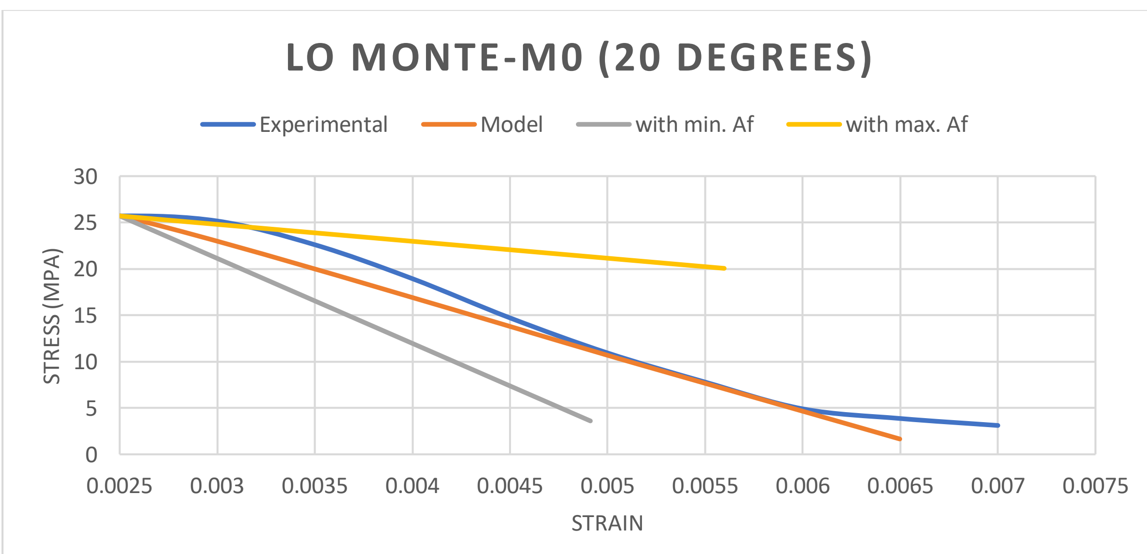

150^{o}C (M0 Concrete)

Properties		
E_c	18240	Mpa
f_c'	19.71	Mpa
ε_{c1}	0.002000	
H	200	mm

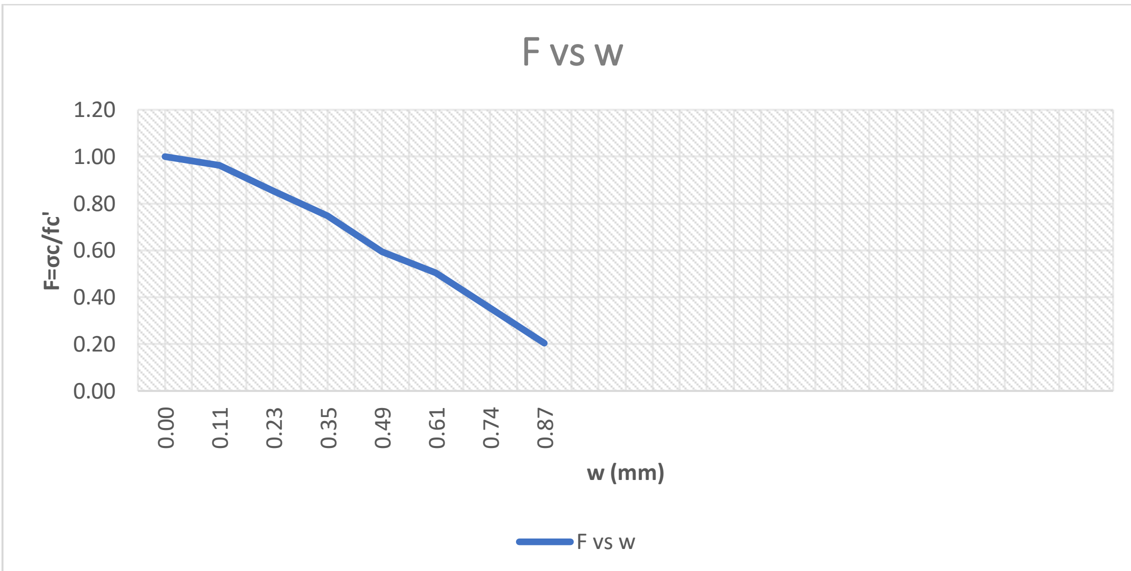

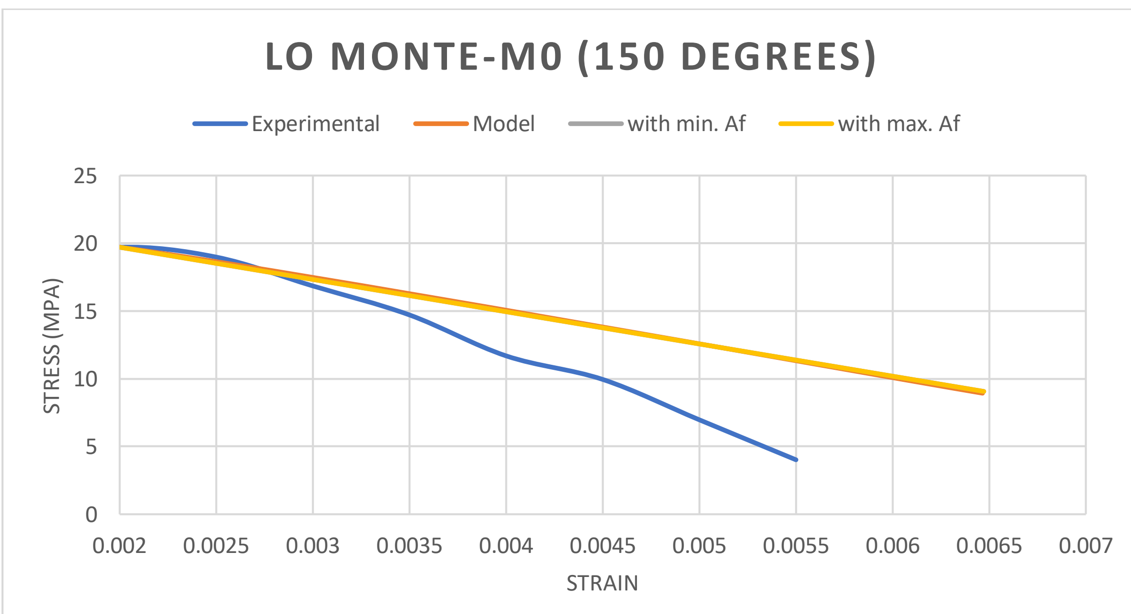

300°C (M0 Concrete)

Properties		
Slope/E_c	9600	Mpa
f_c'	19.46	Mpa
ε_{c1}	0.003500	
H	200	mm

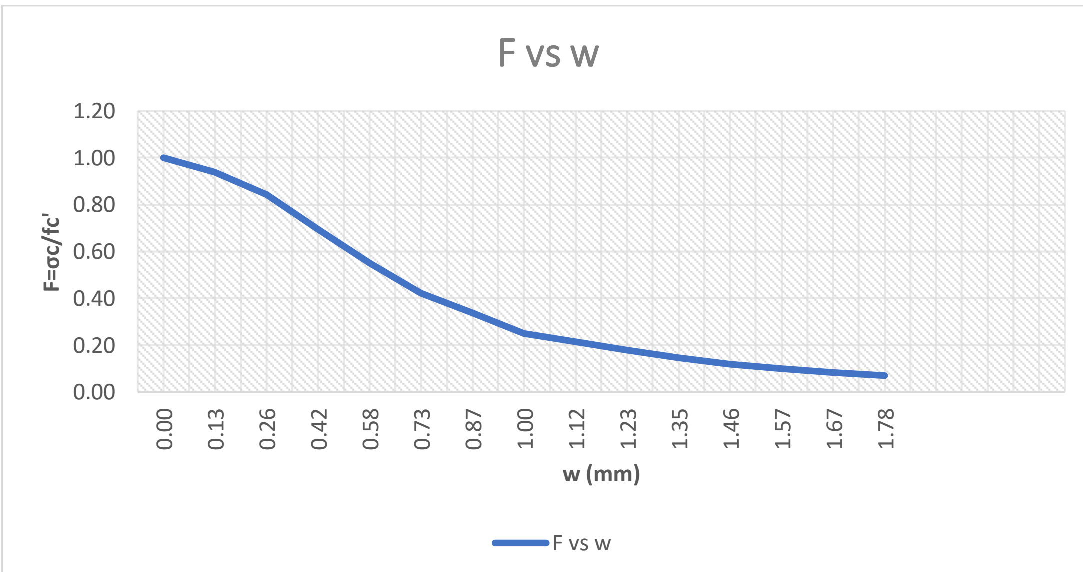

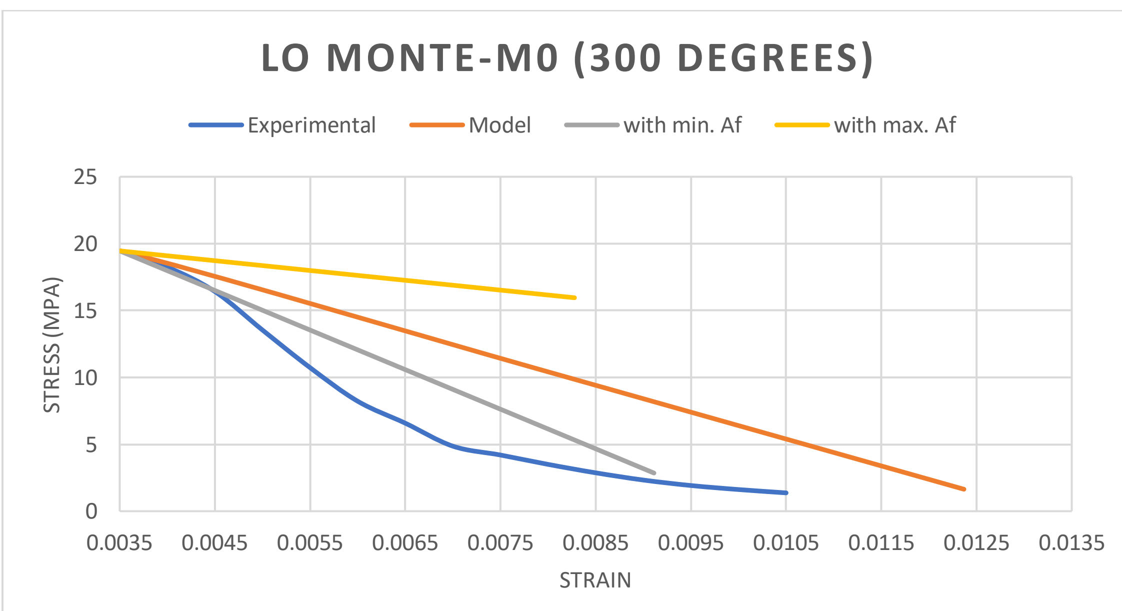

500°C (M0 Concrete)

Properties		
Slope/E_c	2404.4	Mpa
f_c'	11	Mpa
ε_{c1}	0.005500	
H	200	mm

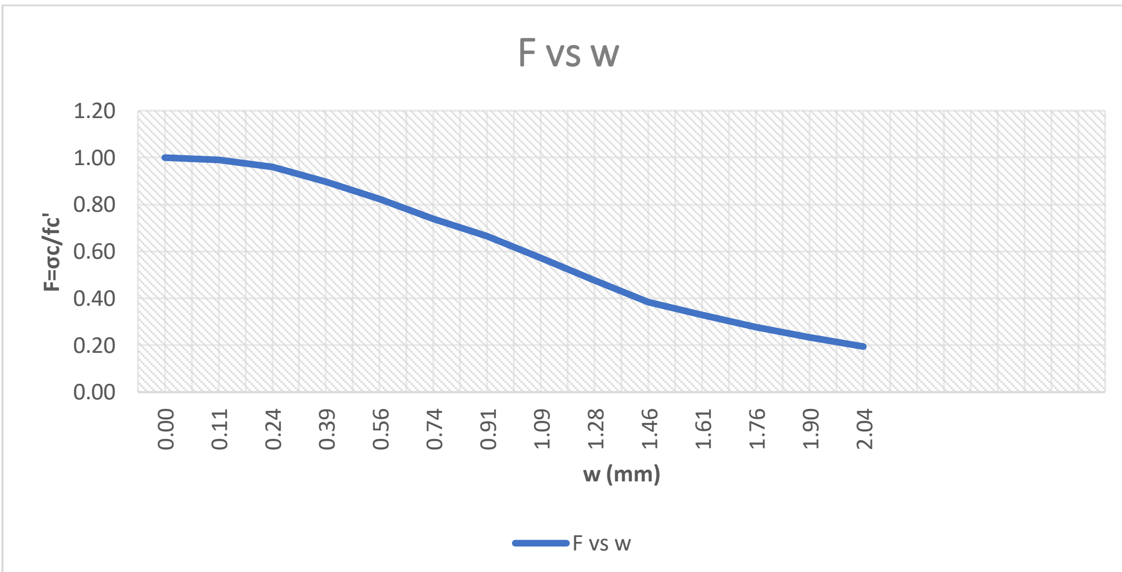

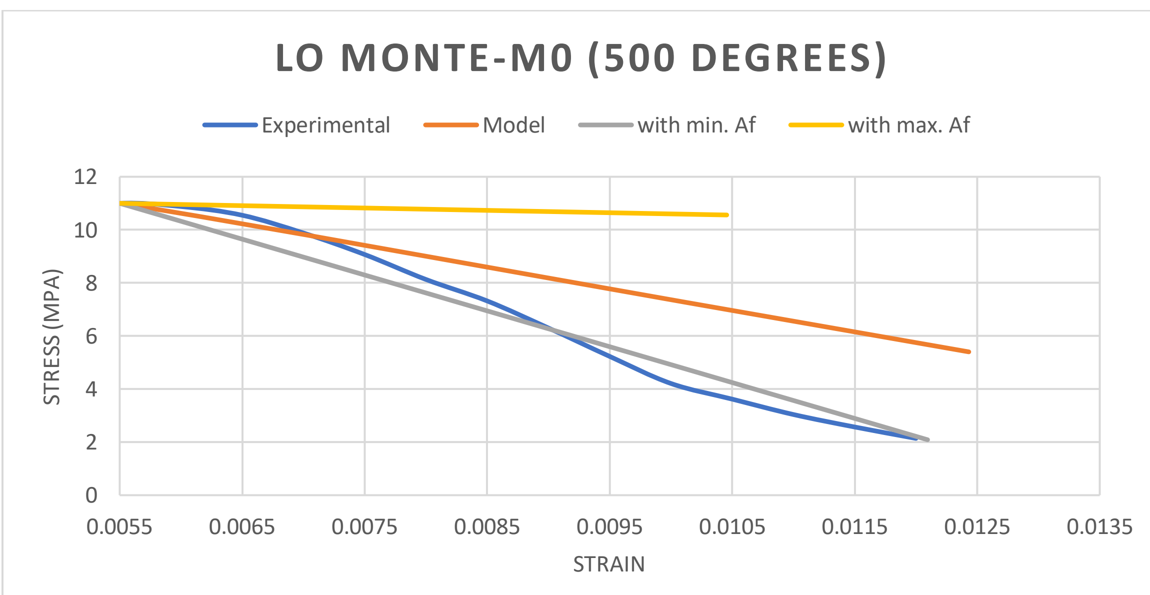

700°C (M0 Concrete)

Properties		
E_c	1072	Mpa
f_c'	6.03	Mpa
ε_{c1}	0.008000	
H	200	mm

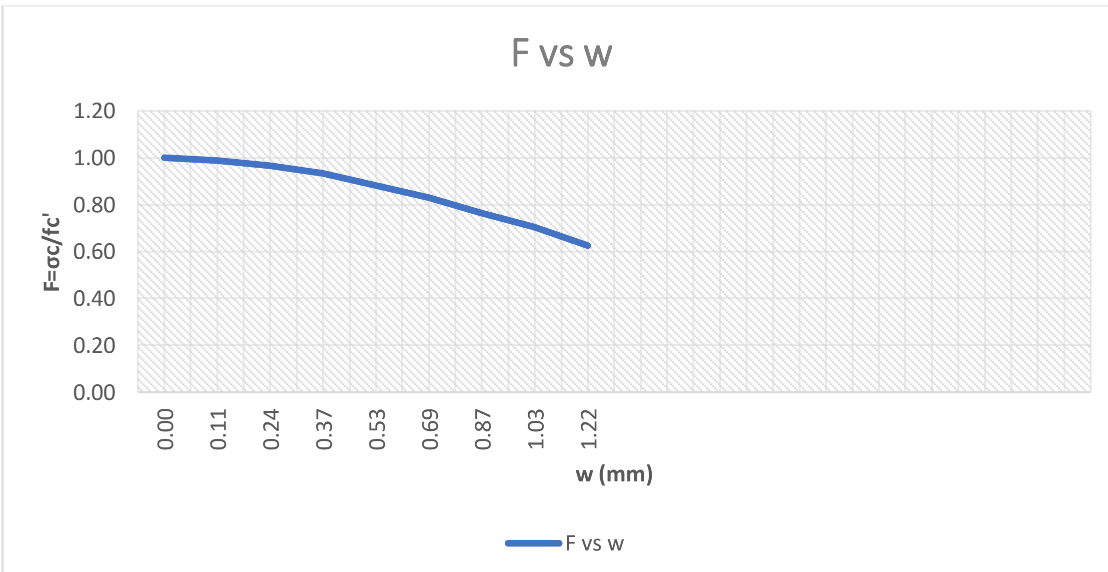

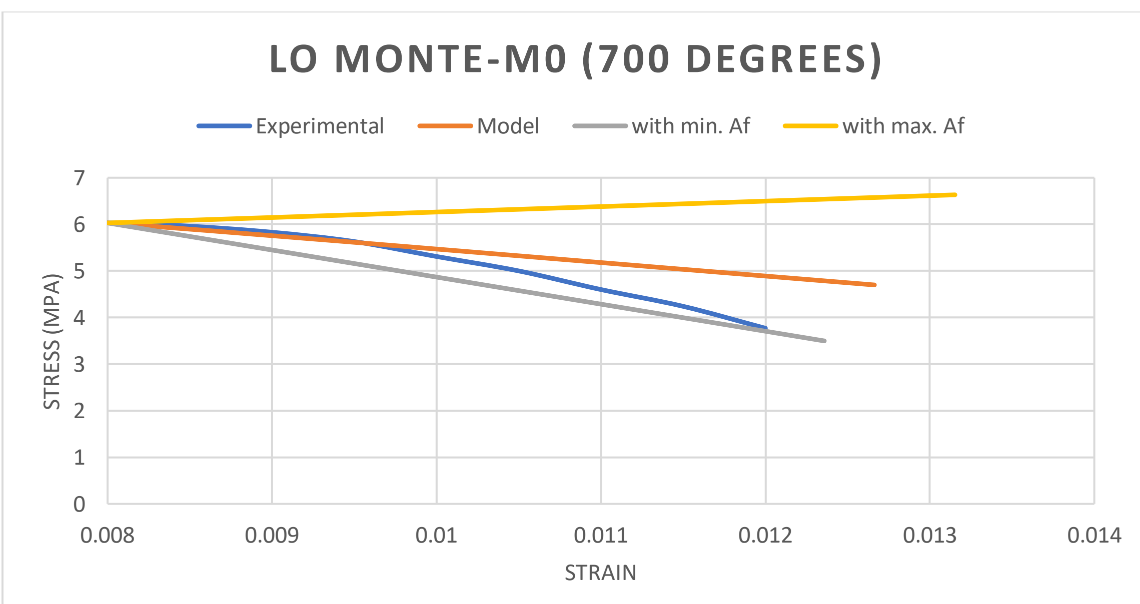

Post-peak analysis of experimental data by (Poon et al., 2004)

20°C (PC0 Concrete)

Properties		
E_c	23456	Mpa
f_c'	69.1	Mpa
ε_{c1}	0.003740	
H	200	mm

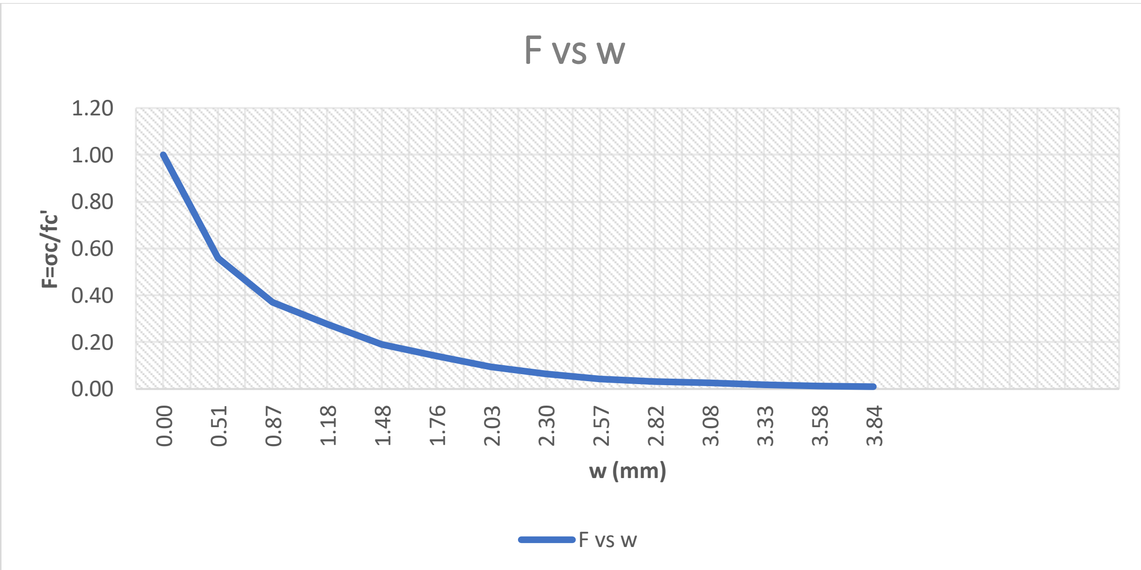

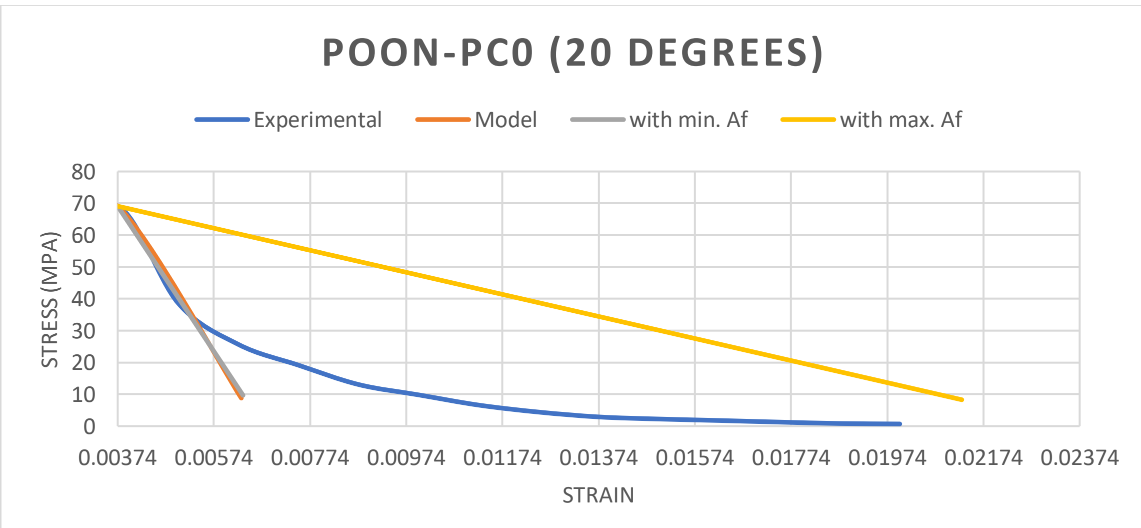

600^{o}C (PC0 Concrete)

Properties		
E_c	4864	Mpa
f_c'	32.79	Mpa
ε_{c1}	0.008380	
H	200	mm

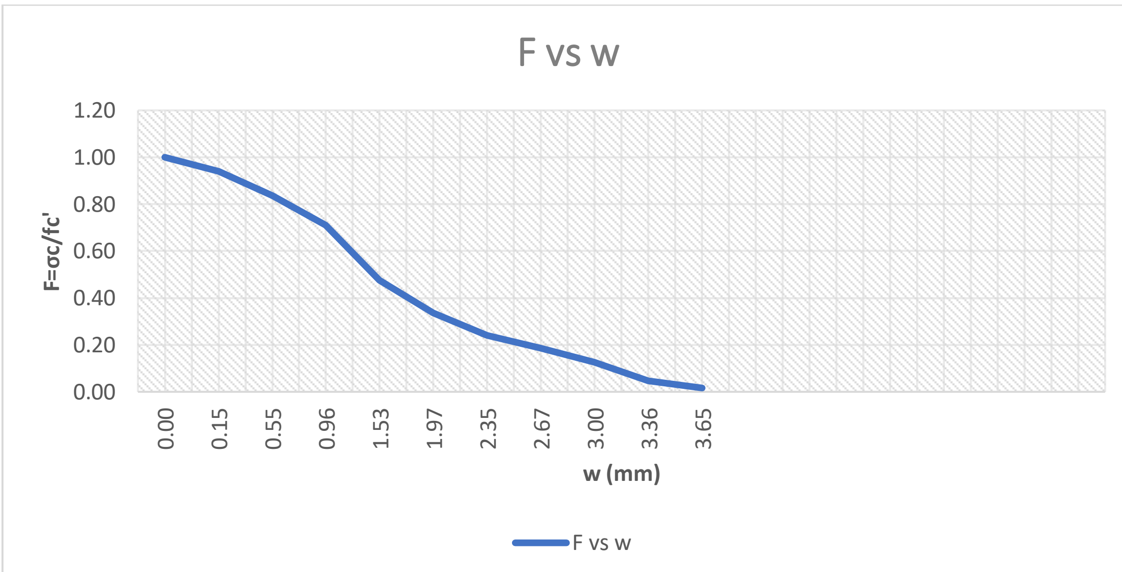

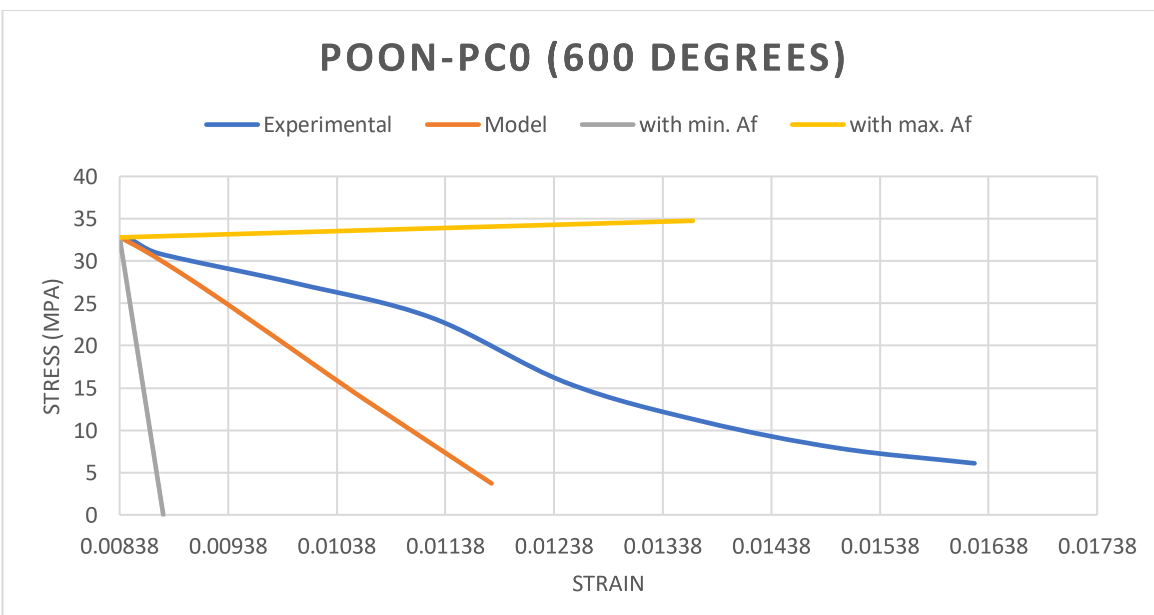

800^{o}C (PC0 Concrete)

Properties		
E_c	3184	Mpa
f_c'	17.64	Mpa
ε_{c1}	0.009310	
H	200	mm

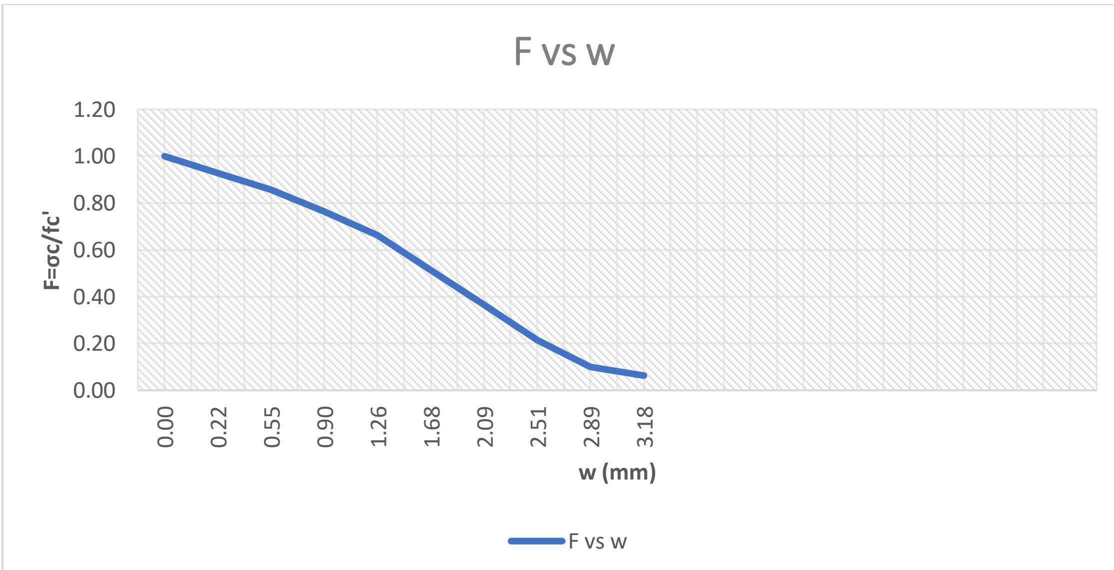

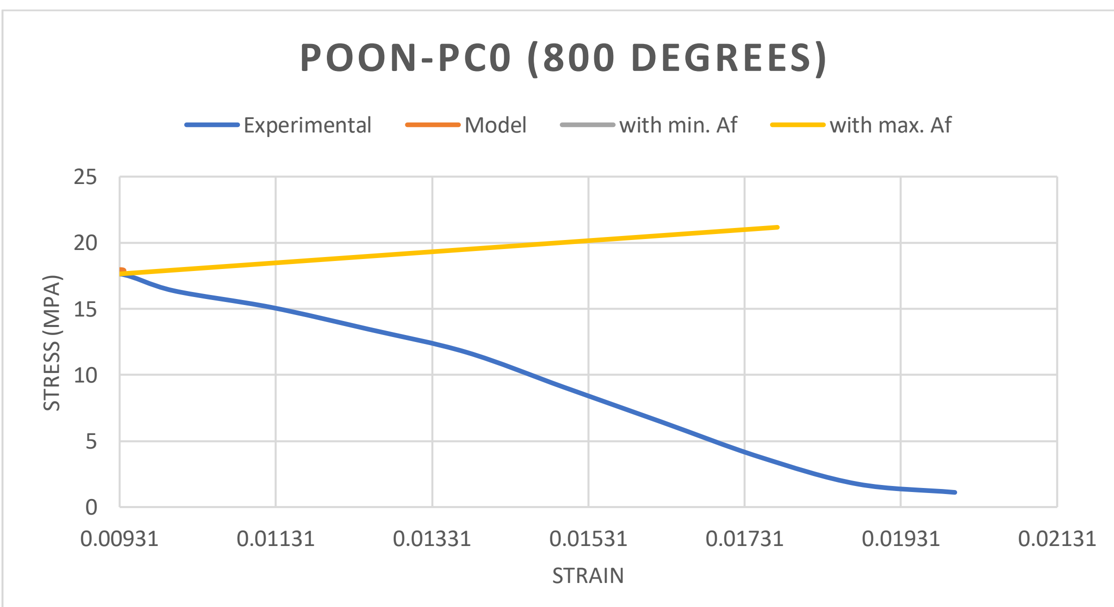

20°C (MK0 Concrete)

Properties		
E_c	22160	Mpa
f_c'	86.1	Mpa
ε_{c1}	0.003970	
H	200	mm

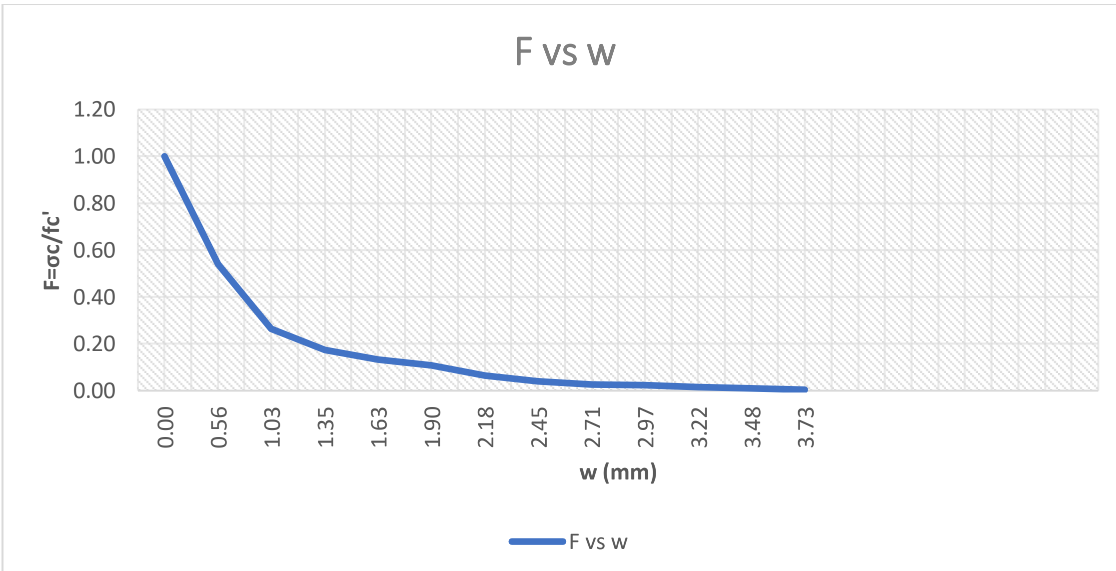

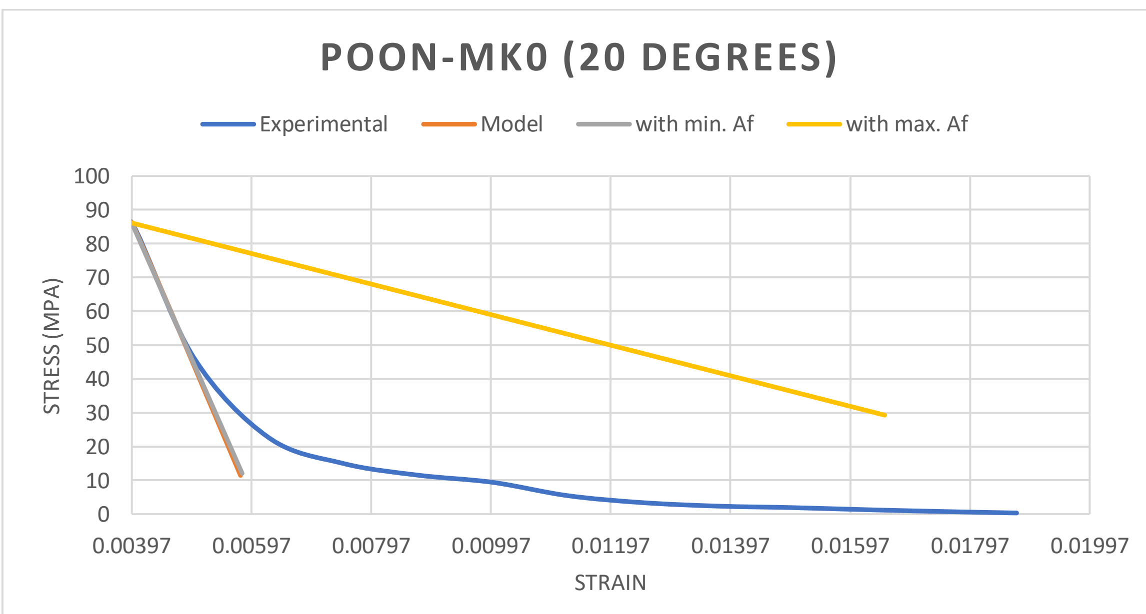

600°C (MK0 Concrete)

Properties		
E_c	5184	Mpa
f_c'	33.28	Mpa
ε_{c1}	0.008320	
H	200	mm

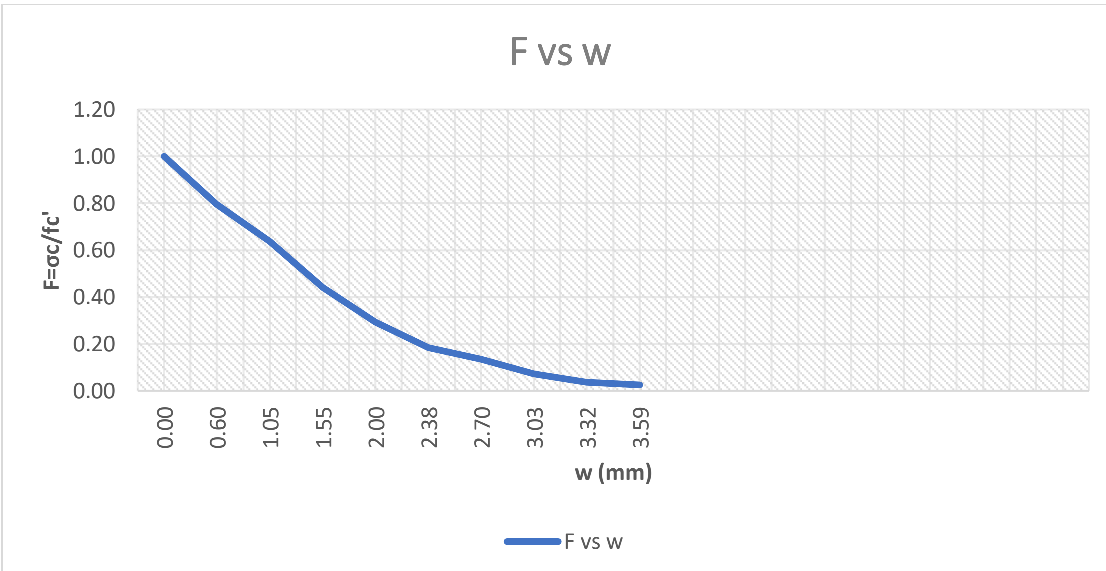

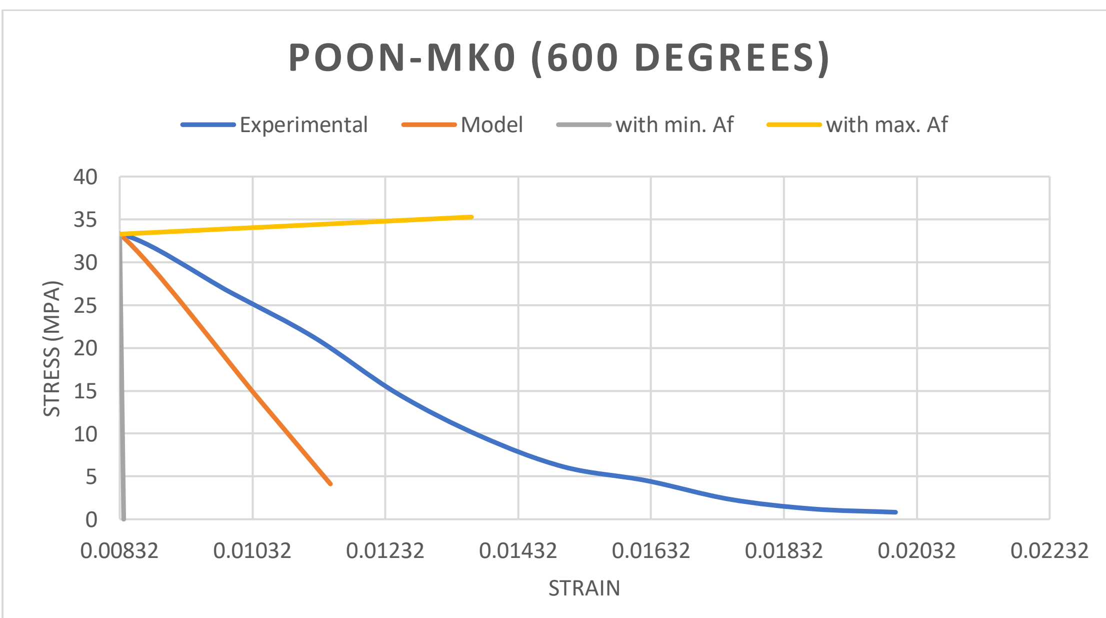

800°C (MK0 Concrete)

Properties		
E_c	2688	Mpa
f_c'	15.76	Mpa
ε_{c1}	0.010490	
H	200	mm

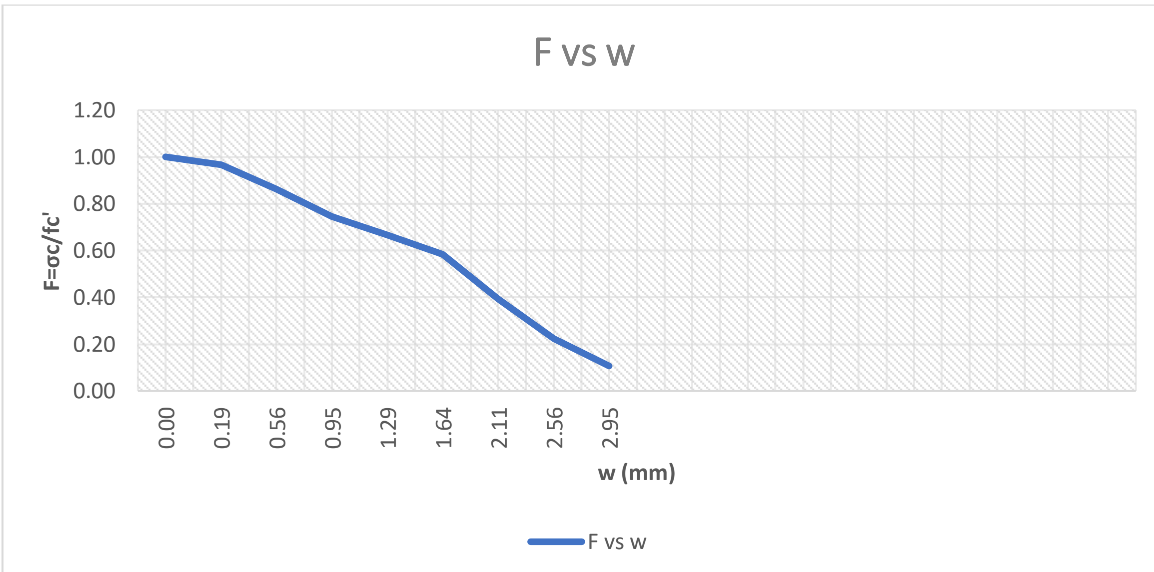

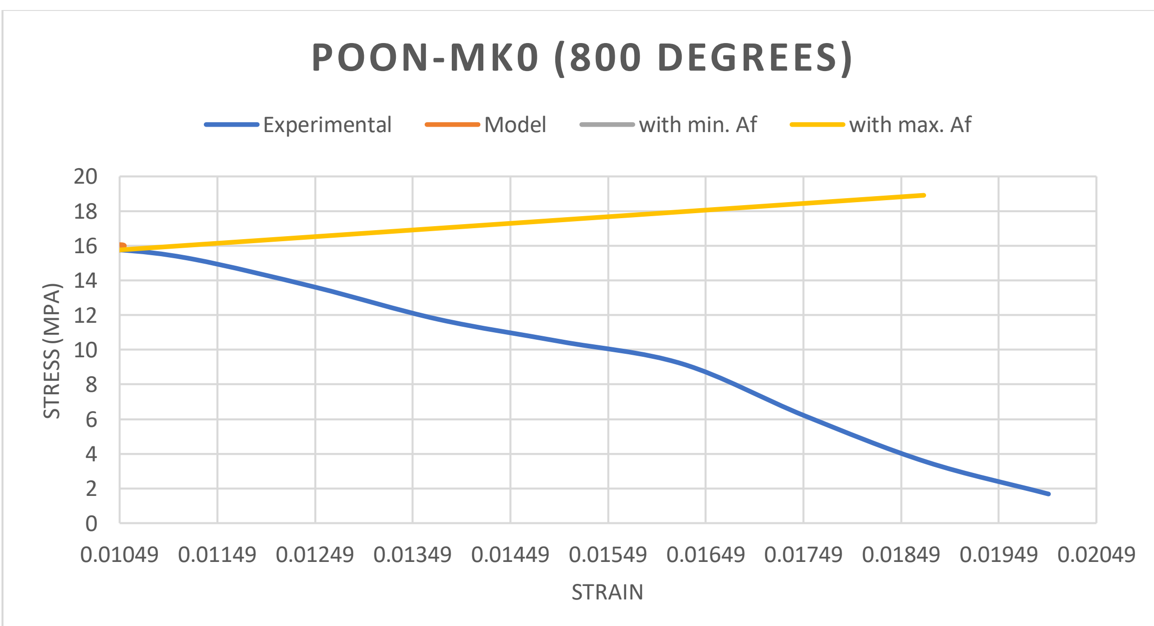

20°C (SF0 Concrete)

Properties		
E_c	21664	Mpa
f_c'	82.8	Mpa
ε_{c1}	0.003880	
H	200	mm

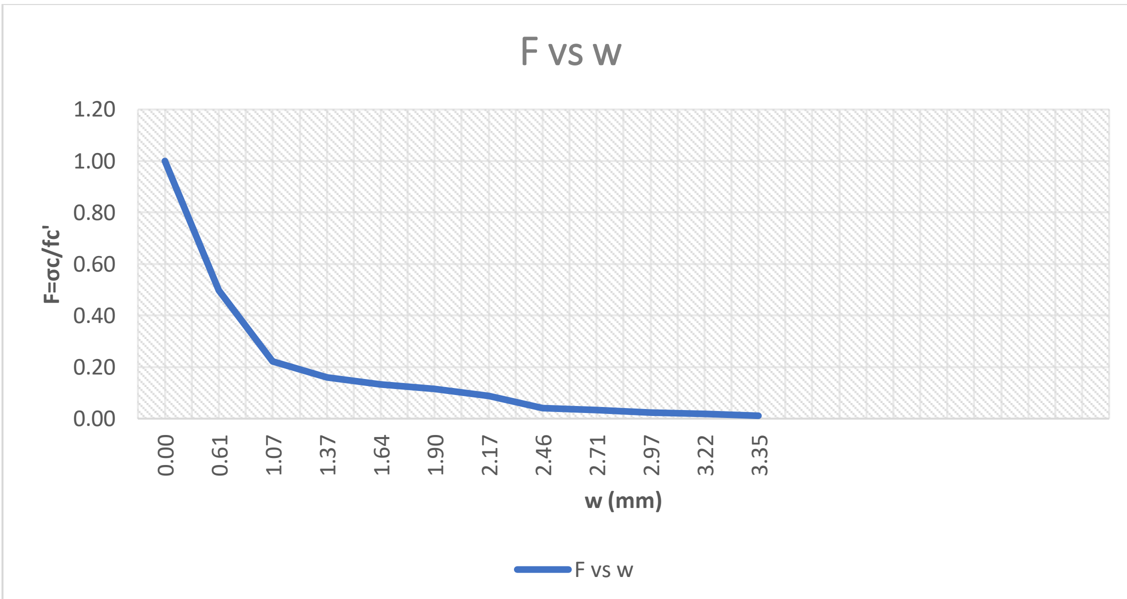

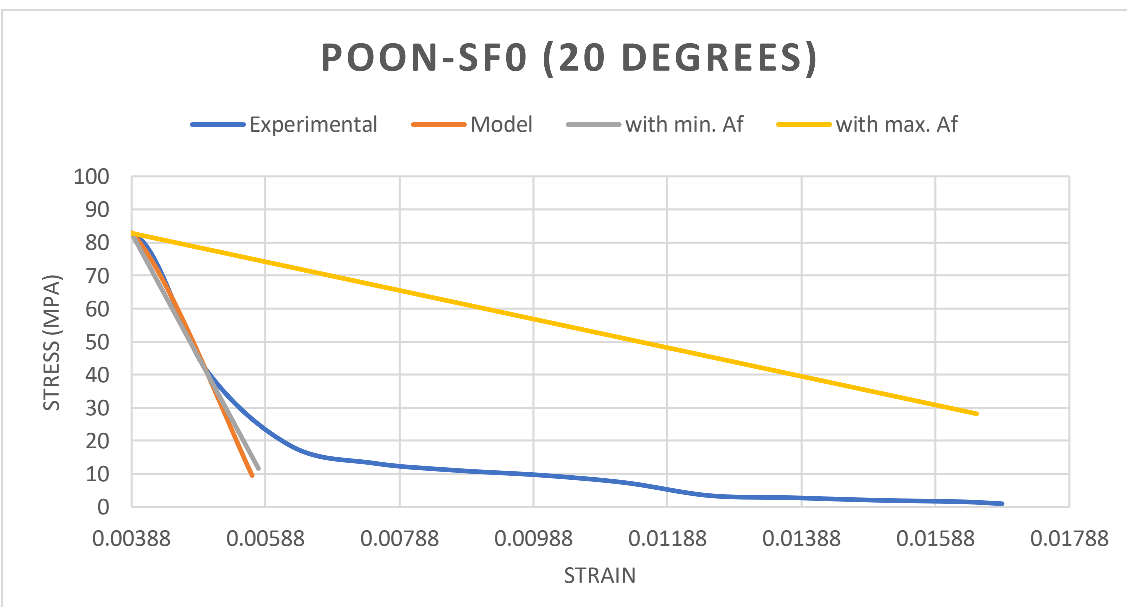

600°C (SF0 Concrete)

Properties		
Slope/E_c	5048	Mpa
f_c'	37.84	Mpa
ε_{c1}	0.008250	
H	200	mm

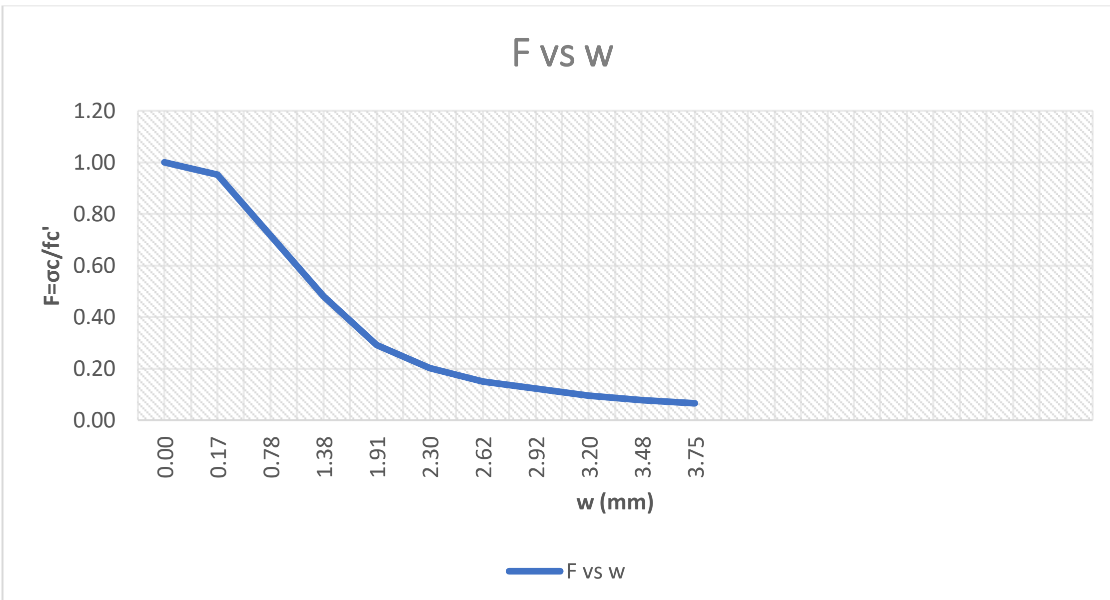

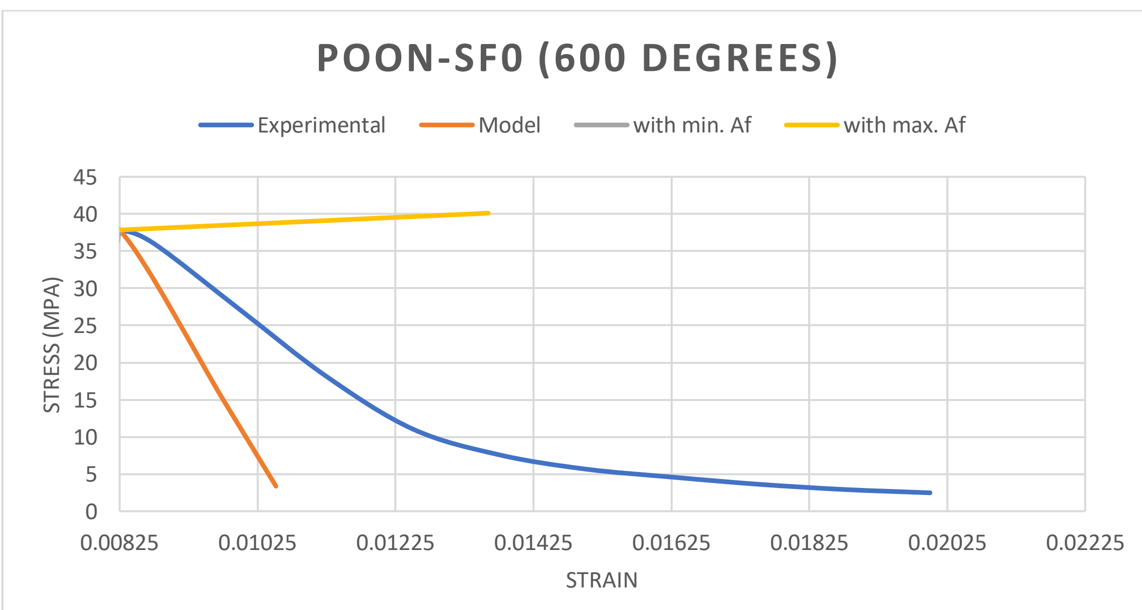

800°C (SF0 Concrete)

Properties		
E_c	4960	Mpa
f_c'	20.55	Mpa
ε_{c1}	0.010000	
H	200	mm

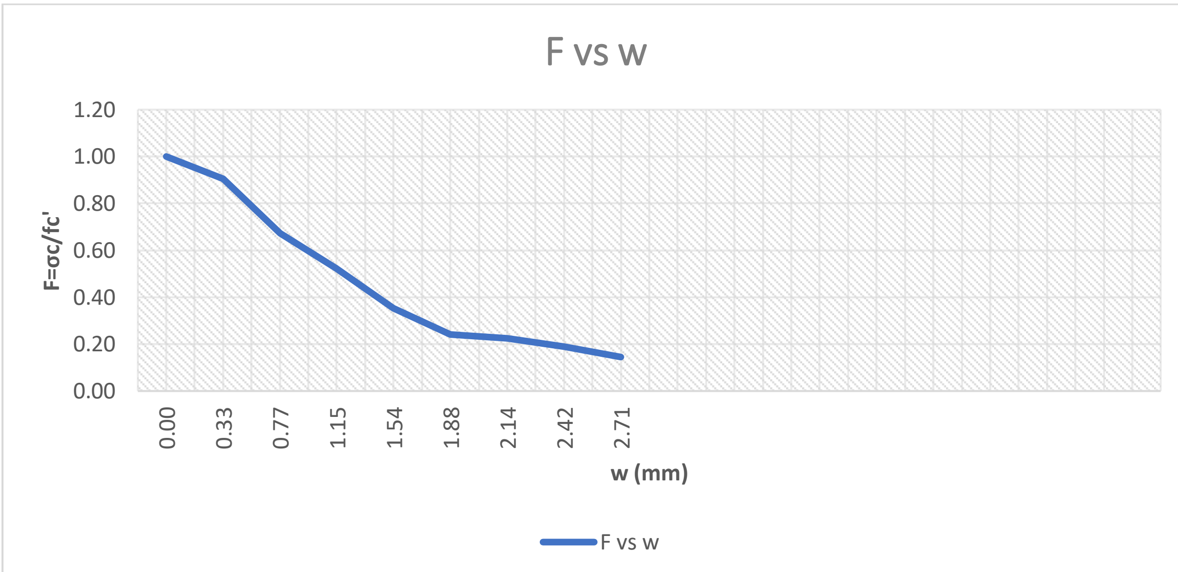

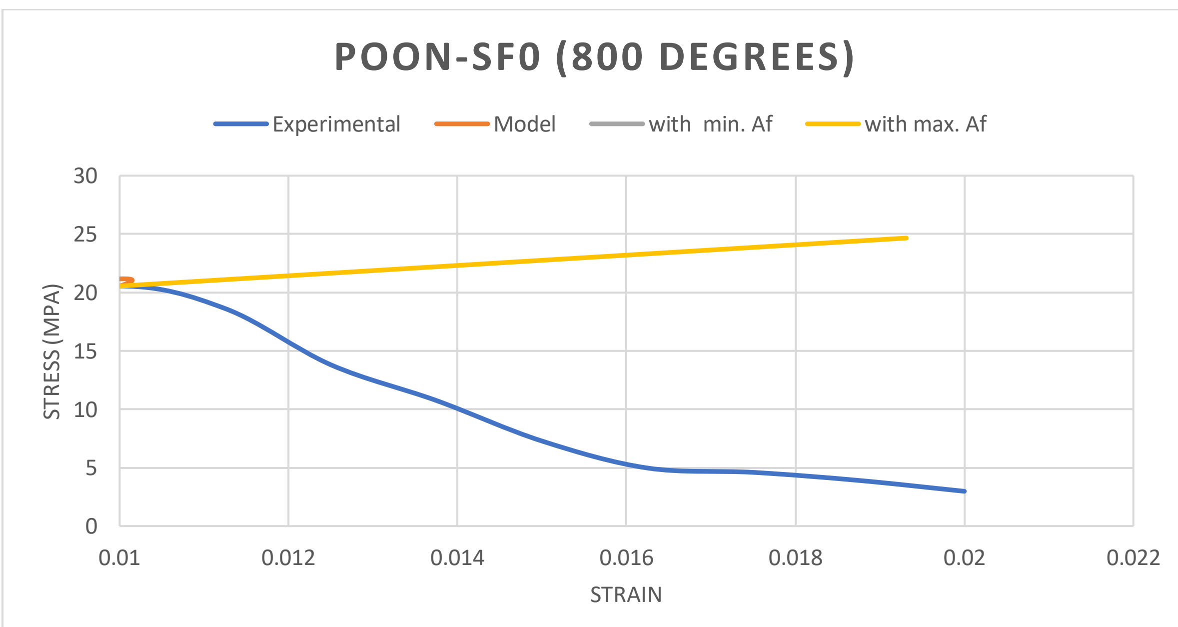

20°C (OPC1 Concrete)

Properties		
E_c	19542.4	Mpa
f_c'	71.4	Mpa
ε_{c1}	0.004100	
H	200	mm

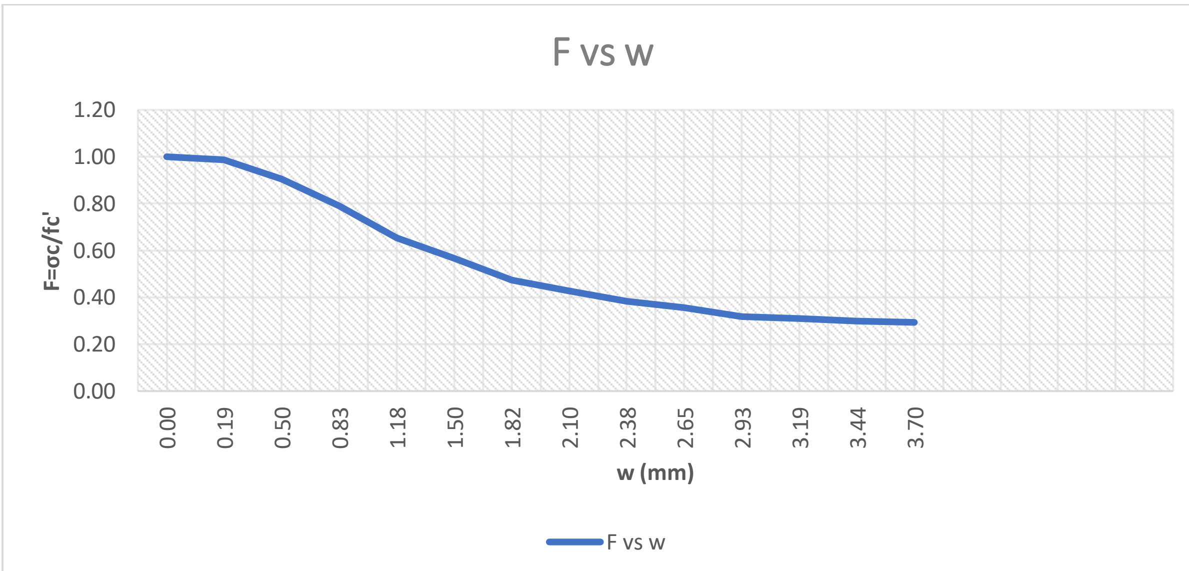

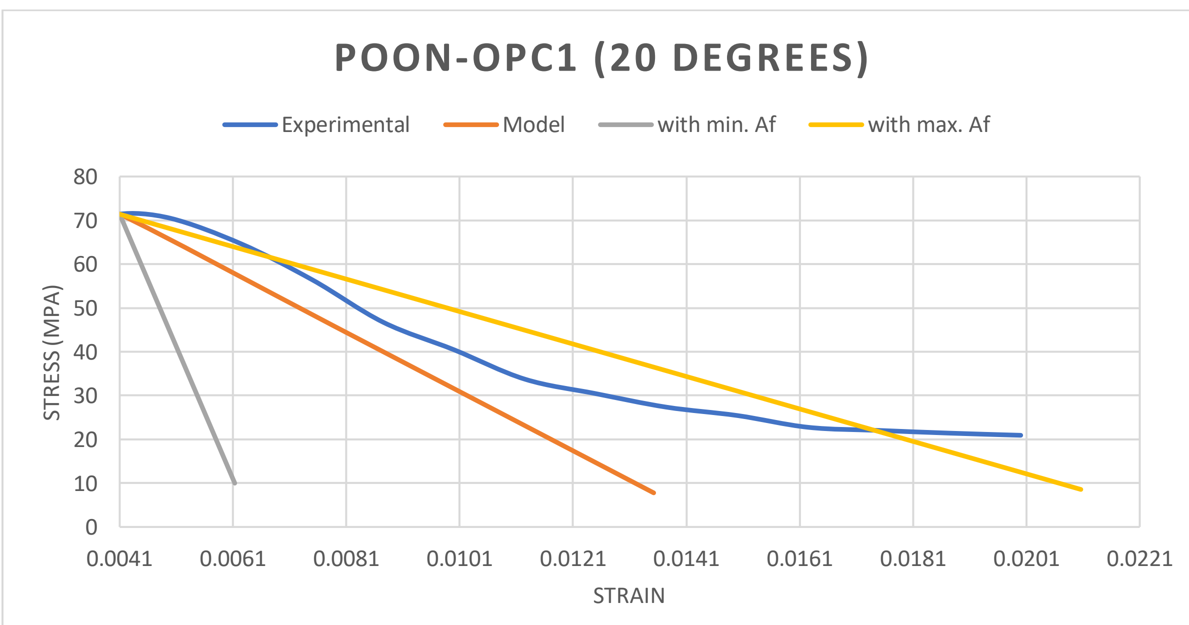

600°C (OPC1 Concrete)

Properties		
E_c	5920	Mpa
f_c'	38.95	Mpa
ε_{c1}	0.010490	
H	200	mm

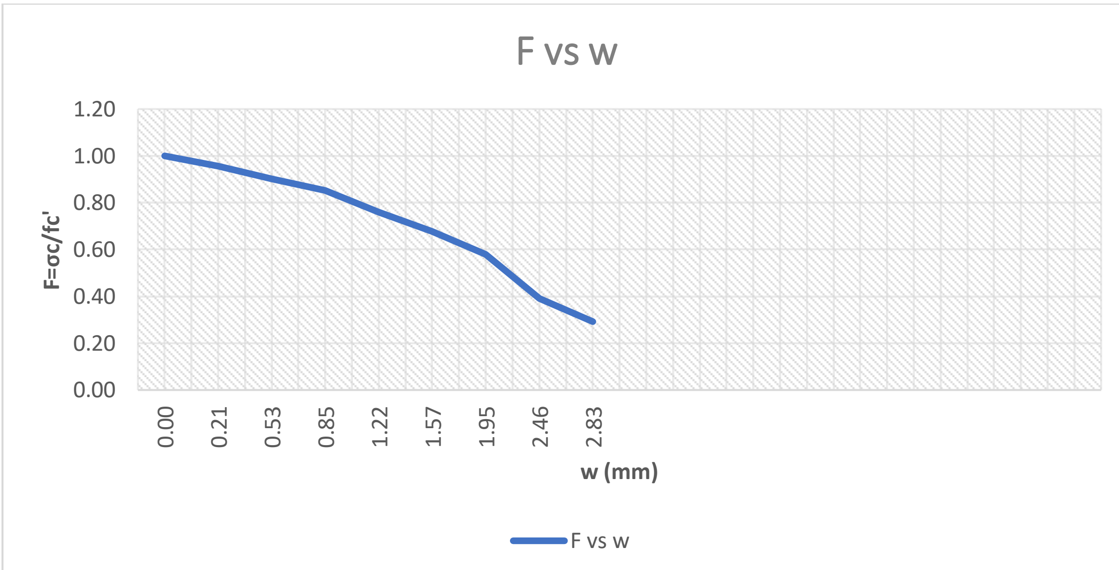

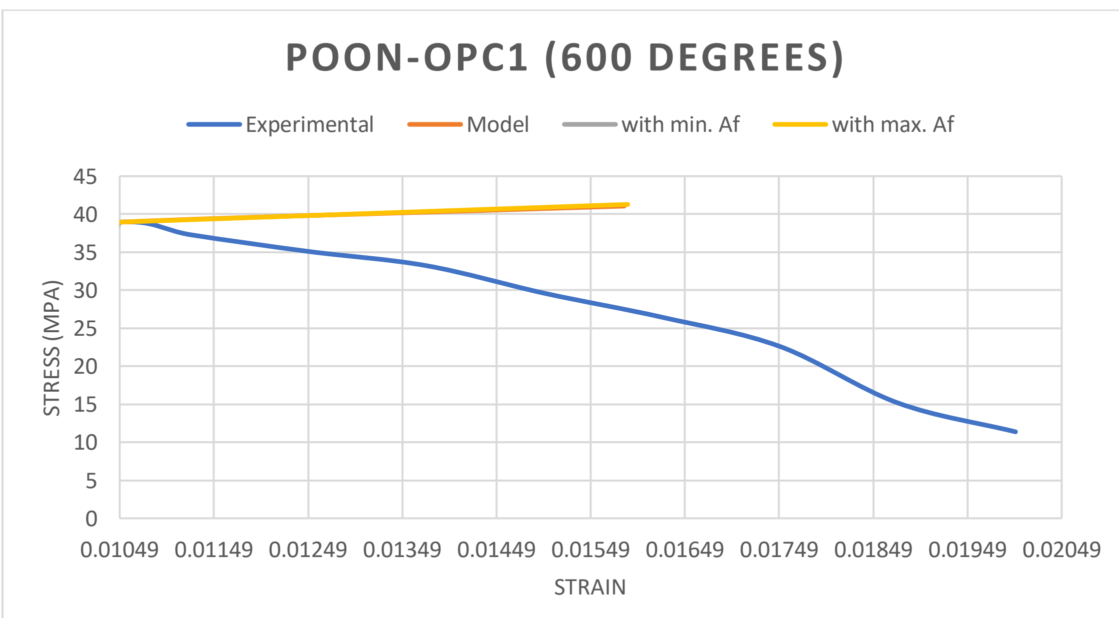

800°C (OPC1 Concrete)

Properties		
Slope/E_c	4240	Mpa
f_c'	23.8	Mpa
ε_{c1}	0.012340	
H	200	mm

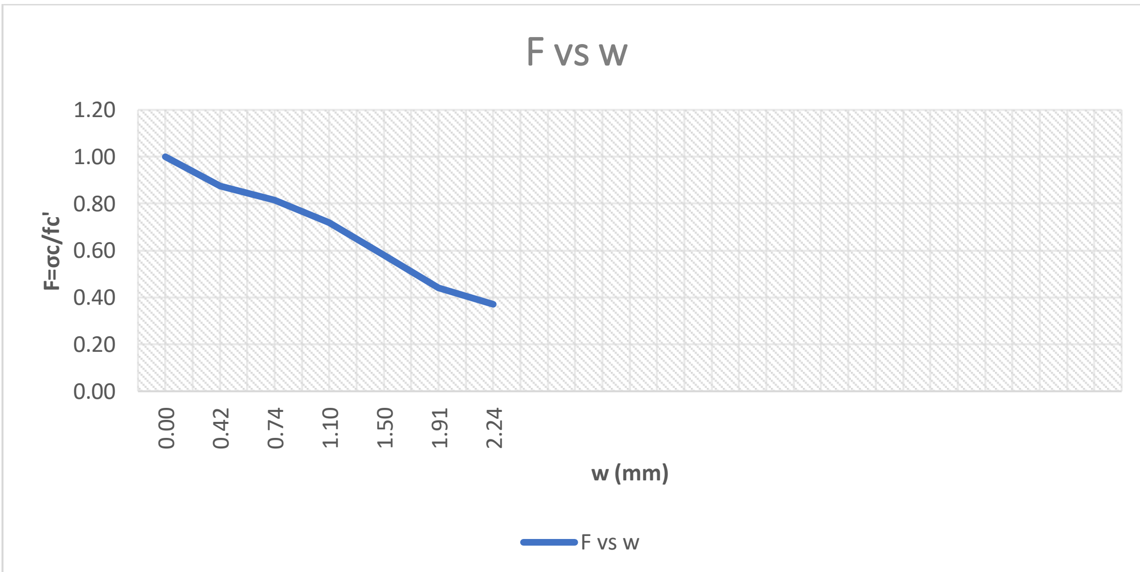

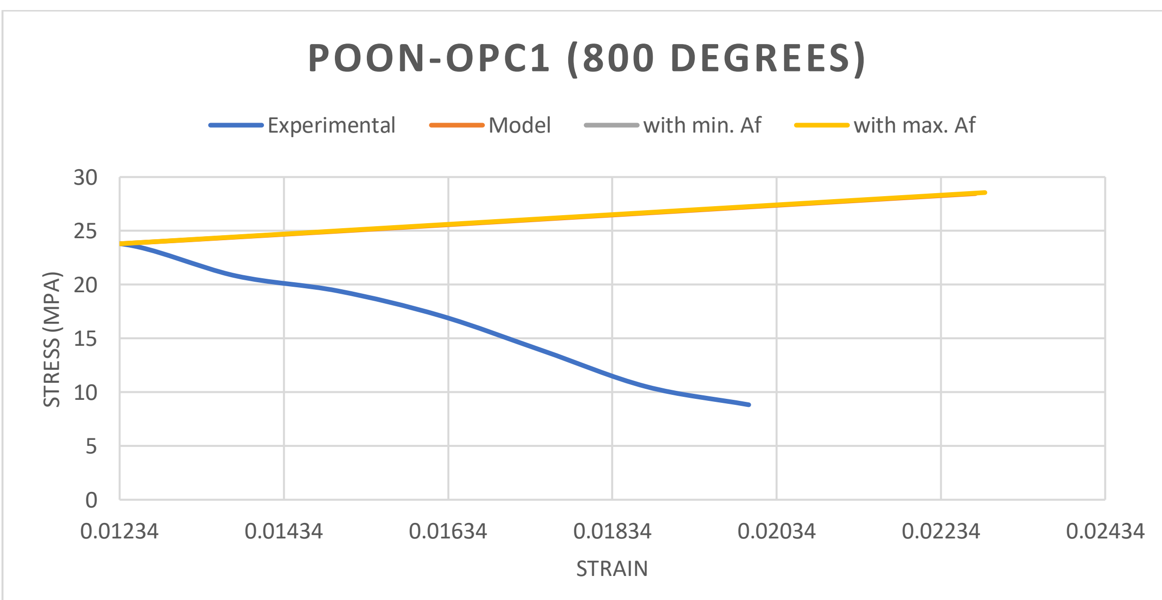

20°C (MK1 Concrete)

Properties		
E_c	23280	Mpa
f_c'	87.5	Mpa
ε_{c1}	0.004200	
H	200	mm

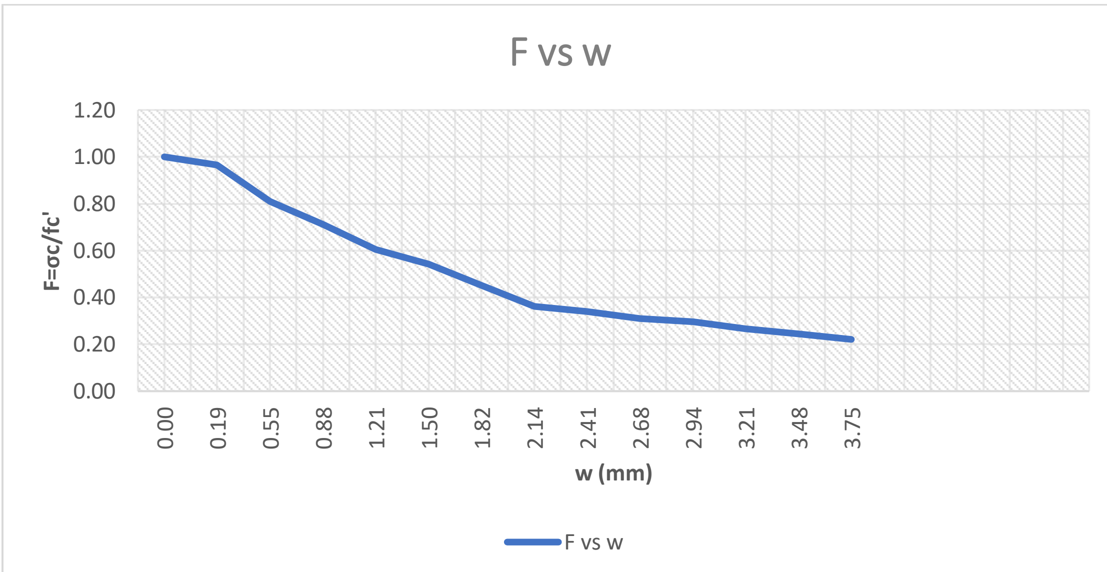

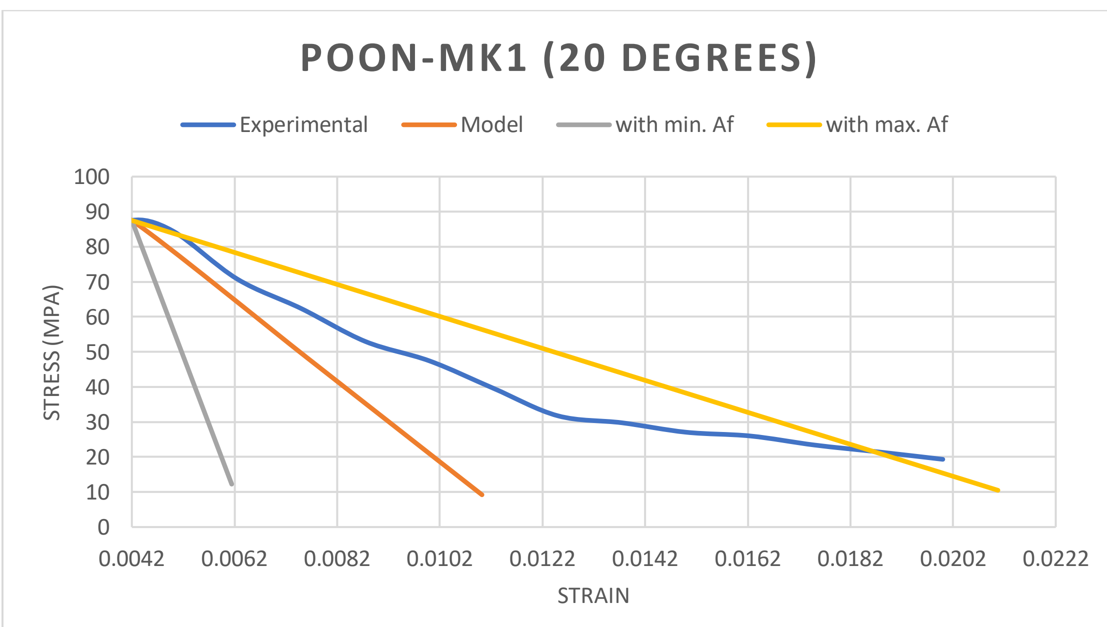

600°C (MK1 Concrete)

Properties		
E_c	4456	Mpa
f_c'	38.72	Mpa
ε_{c1}	0.010270	
H	200	mm

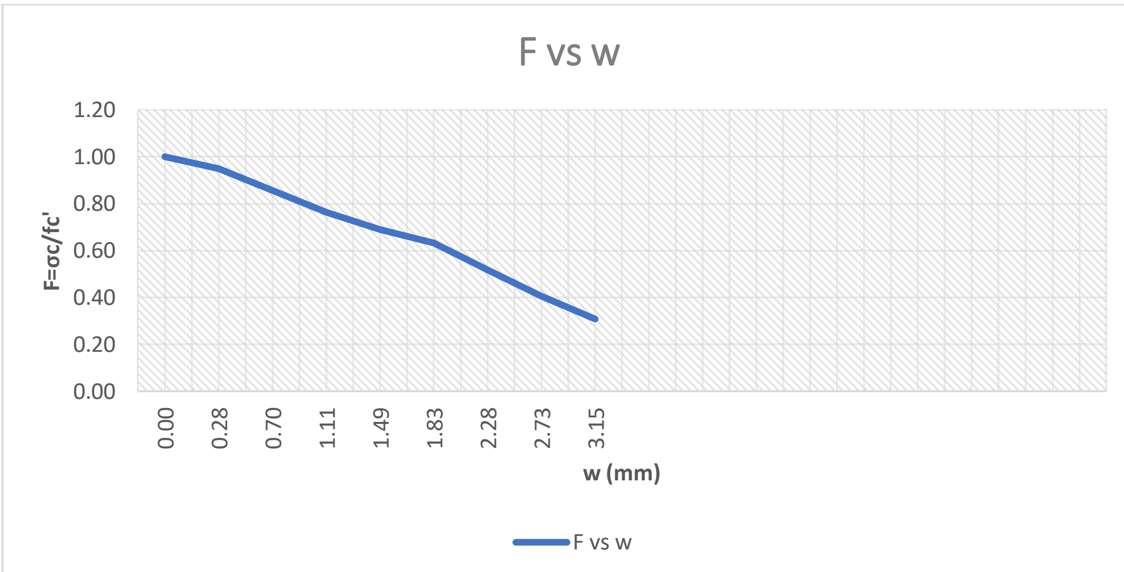

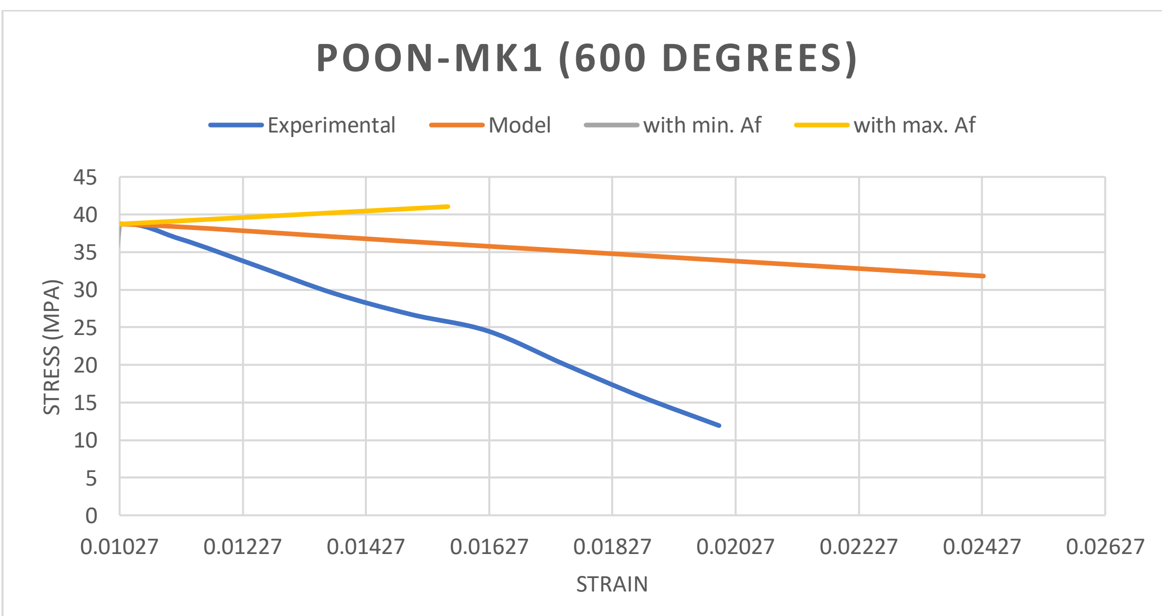

800°C (MK1 Concrete)

Properties		
E_c	3520	Mpa
f_c'	21.41	Mpa
ε_{c1}	0.013340	
H	200	mm

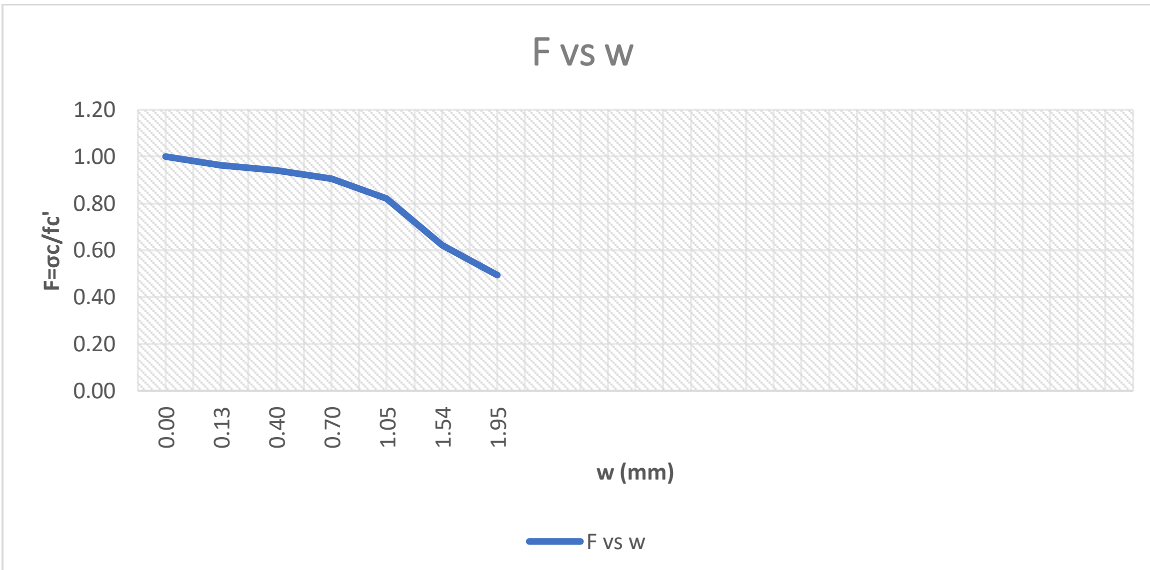

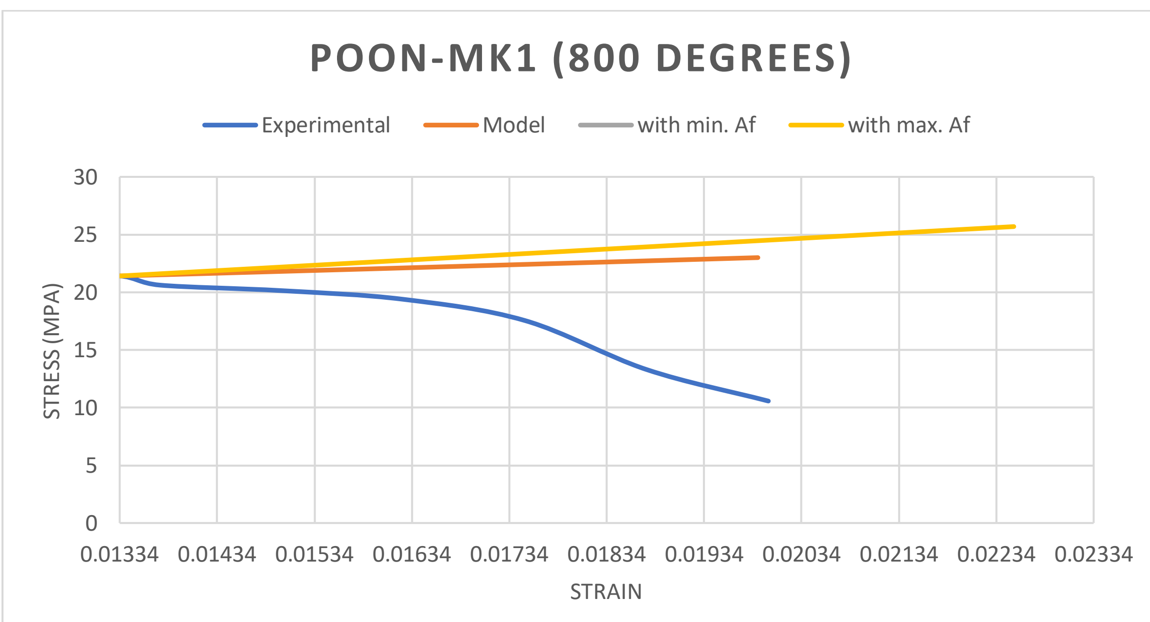

20°C (SF1 Concrete)

Properties		
E_c	23152	Mpa
f_c'	83.7	Mpa
ε_{c1}	0.003900	
H	200	mm

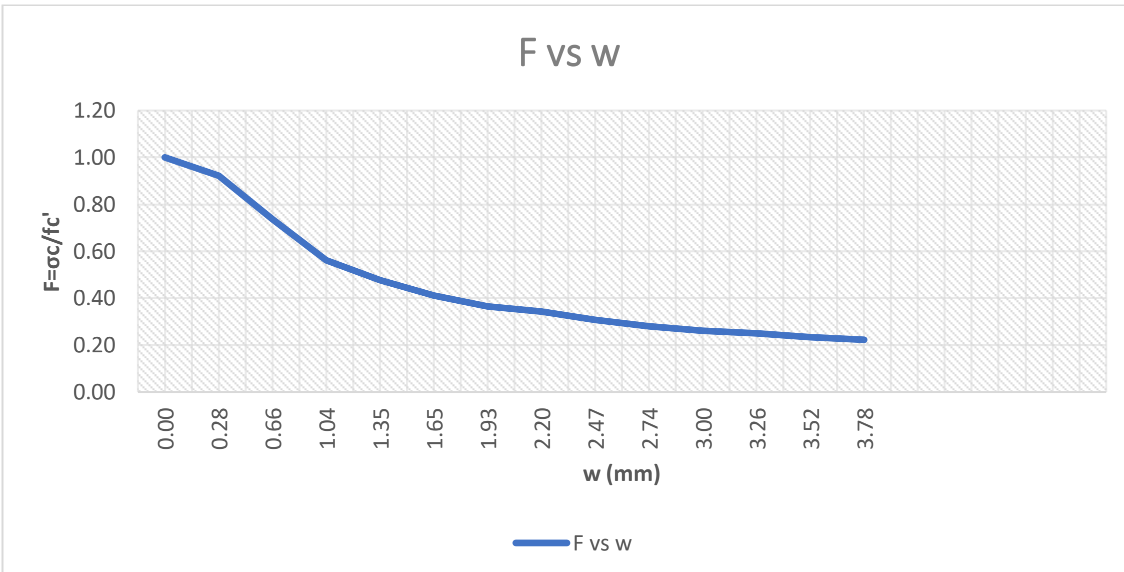

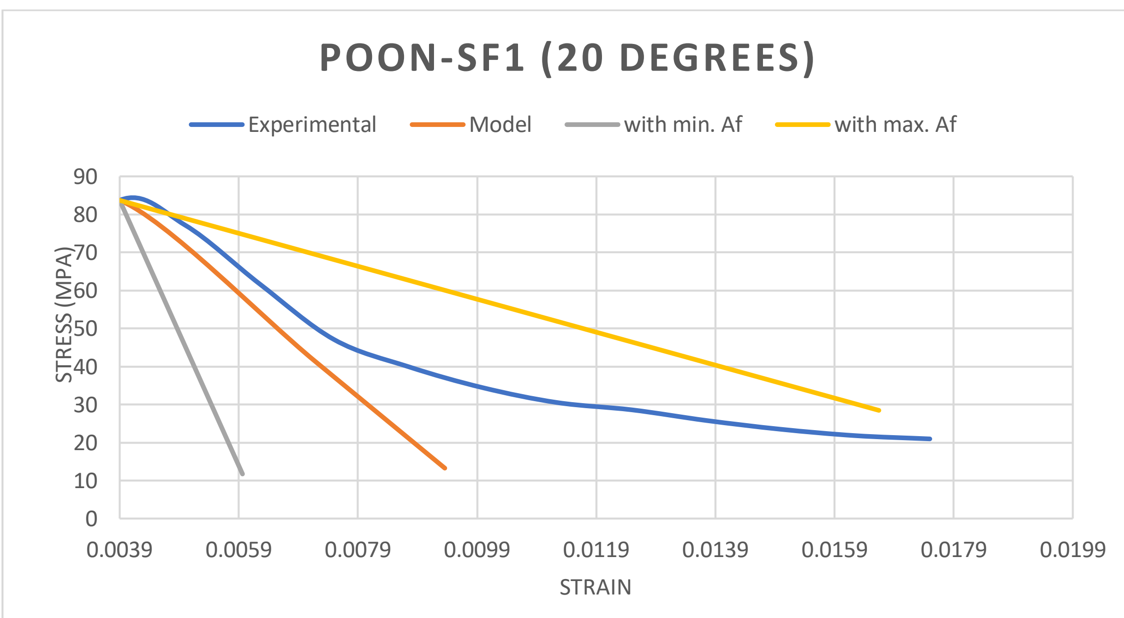

600°C (SF1 Concrete)

Properties		
E_c	5558.4	Mpa
f_c'	39.19	Mpa
ε_{c1}	0.008380	
H	200	mm

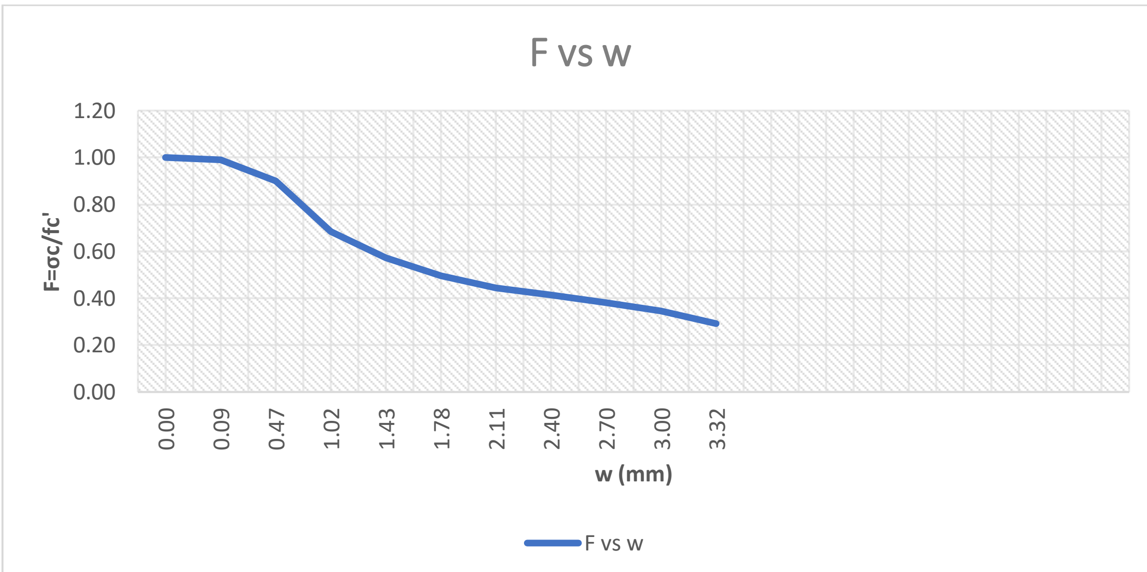

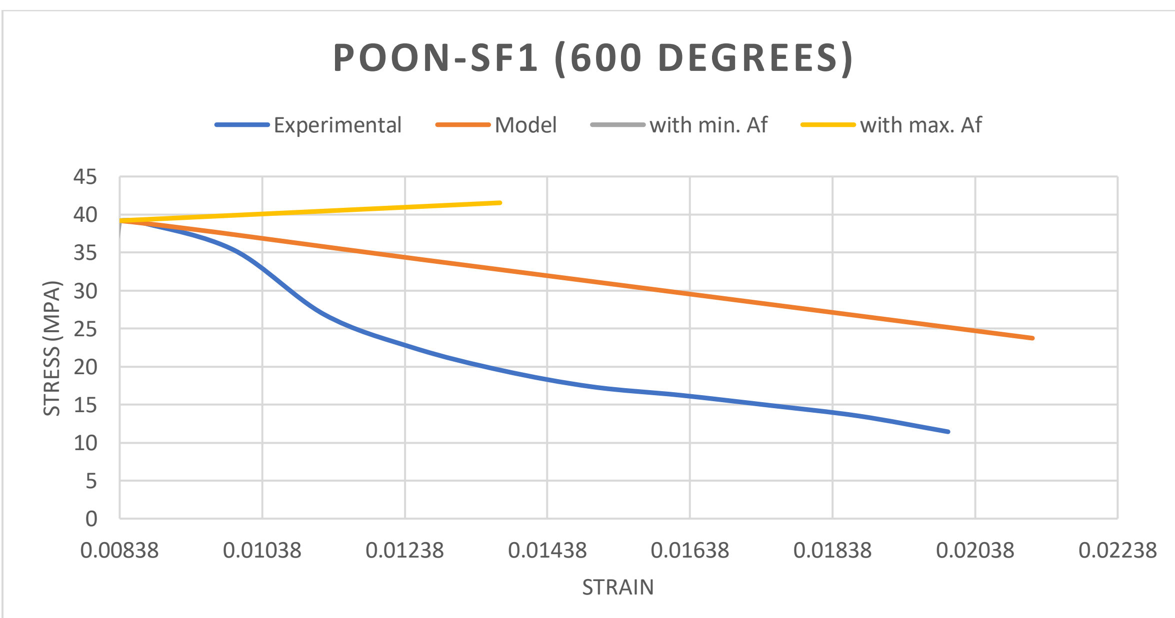

800°C (SF1 Concrete)

Properties		
E_c	3955.2	Mpa
f_c'	23.46	Mpa
ε_{c1}	0.011700	
H	200	mm